



# Identification of novel therapeutic targets and evaluation of pharmacological treatments in epigenetic and chromatin diseases- the case of Rett syndrome

Karolina Szczesna

**ADVERTIMENT.** La consulta d'aquesta tesi queda condicionada a l'acceptació de les següents condicions d'ús: La difusió d'aquesta tesi per mitjà del servei TDX ([www.tdx.cat](http://www.tdx.cat)) i a través del Dipòsit Digital de la UB ([diposit.ub.edu](http://diposit.ub.edu)) ha estat autoritzada pels titulars dels drets de propietat intel·lectual únicament per a usos privats emmarcats en activitats d'investigació i docència. No s'autoritza la seva reproducció amb finalitats de lucre ni la seva difusió i posada a disposició des d'un lloc aliè al servei TDX ni al Dipòsit Digital de la UB. No s'autoritza la presentació del seu contingut en una finestra o marc aliè a TDX o al Dipòsit Digital de la UB (framing). Aquesta reserva de drets afecta tant al resum de presentació de la tesi com als seus continguts. En la utilització o cita de parts de la tesi és obligat indicar el nom de la persona autora.

**ADVERTENCIA.** La consulta de esta tesis queda condicionada a la aceptación de las siguientes condiciones de uso: La difusión de esta tesis por medio del servicio TDR ([www.tdx.cat](http://www.tdx.cat)) y a través del Repositorio Digital de la UB ([diposit.ub.edu](http://diposit.ub.edu)) ha sido autorizada por los titulares de los derechos de propiedad intelectual únicamente para usos privados enmarcados en actividades de investigación y docencia. No se autoriza su reproducción con finalidades de lucro ni su difusión y puesta a disposición desde un sitio ajeno al servicio TDR o al Repositorio Digital de la UB. No se autoriza la presentación de su contenido en una ventana o marco ajeno a TDR o al Repositorio Digital de la UB (framing). Esta reserva de derechos afecta tanto al resumen de presentación de la tesis como a sus contenidos. En la utilización o cita de partes de la tesis es obligado indicar el nombre de la persona autora.

**WARNING.** On having consulted this thesis you're accepting the following use conditions: Spreading this thesis by the TDX ([www.tdx.cat](http://www.tdx.cat)) service and by the UB Digital Repository ([diposit.ub.edu](http://diposit.ub.edu)) has been authorized by the titular of the intellectual property rights only for private uses placed in investigation and teaching activities. Reproduction with lucrative aims is not authorized nor its spreading and availability from a site foreign to the TDX service or to the UB Digital Repository. Introducing its content in a window or frame foreign to the TDX service or to the UB Digital Repository is not authorized (framing). Those rights affect to the presentation summary of the thesis as well as to its contents. In the using or citation of parts of the thesis it's obliged to indicate the name of the author.

PhD thesis  
Karolina Szczesna

Karolina Szczesna

Identification of novel therapeutic targets and evaluation of pharmacological treatments in  
epigenetic and chromatin diseases- the case of Rett syndrome.

2014

Identification of novel therapeutic targets and  
evaluation of pharmacological treatments in  
epigenetic and chromatin diseases-  
the case of Rett syndrome.



# Identification of novel therapeutic targets and evaluation of pharmacological treatments in epigenetic and chromatin diseases- the case of Rett syndrome.

Memoria Tesis Doctoral

Karolina Szczesna

Barcelona, 2014



INSTITUT  
D'INVESTIGACIÓ  
BIOMÈDICA  
DE BELLVITGE





Cover done by Olga de la Caridad Jorge and Karolina Szczesna



**IDENTIFICATION OF NOVEL THERAPEUTIC TARGETS AND EVALUATION  
OF PHARMACOLOGICAL TREATMENTS IN EPIGENETIC AND  
CHROMATIN DISEASES  
- THE CASE OF RETT SYNDROME.**

Memoria presentada por Karolina Szczesna  
para optar al grado de Doctor por la Universidad de Barcelona

UNIVERSITAT DE BARCELONA - FACULTAT DE MEDICINA  
PROGRAMA DE DOCTORAT EN BIOMEDICINA 2014

Este trabajo ha sido realizado en el Grupo de Epigenética del Cáncer, dentro del Programa de Epigenética y Biología de Cáncer (PEBC) del Instituto de Investigación Biomèdica de Bellvitge (IDIBELL)

**Dr. Manel Esteller**

Director y Tutor

**Karolina Szczesna**

Doctorando



Not everything that counts can be counted,  
and not everything that can be counted counts.

**Albert Einstein**



## **Contents**



CONTENTS.....	9
ACKNOWLEDGMENTS .....	15
ABBREVIATIONS.....	21
INTRODUCTION .....	27
1. EPIGENETICS.....	29
1.1. Epigenetic mechanisms .....	29
1.1.1. DNA methylation.....	30
1.1.2. Histone modifications.....	32
1.2. Epigenetic implications in brain functions .....	33
2. RETT SYNDROME.....	35
2.1. Classical clinical features of Rett syndrome .....	35
2.2. Genetic basis of Rett syndrome: MeCP2 .....	37
2.2.1. MeCP2 structure.....	38
2.2.2. MeCP2 mutations .....	39
2.2.3. MeCP2 mechanism of action.....	40
2.3. EPIGENETIC ALTERATIONS IN RETT SYNDROME.....	44
2.4. ATYPICAL FORMS OF RETT SYNDROME .....	47
2.4.1. Preserved speech variant (PSV).....	47
2.4.2. Early-onset seizure variant (ESV) – CDKL5 mutations .....	48
2.4.3. Congenital variant – FOXP1 mutations .....	49
2.5. ABNORMALITIES AND NEUROPATHOLOGY IN RETT SYNDROME PATIENTS.....	50
2.5.1. BDNF as a gene regulated by MeCP2 .....	50
2.5.2. The glucocorticoid hormone system in Rett syndrome.....	51
2.5.3. The role of oxidative damage in Rett syndrome .....	53
2.5.4. Neurotransmitter system in Rett syndrome – GABA and glutamate.....	53
2.5.5. Neurotransmitter system in Rett syndrome – monoamines .....	54
2.6. ANIMAL MODELS OF RETT SYNDROME .....	55
2.7. THERAPEUTIC APPROACHES AND PRECLINICAL STUDIES TOWARD RETT SYNDROME.....	61
2.7.1. Pharmacological intervention.....	62
2.7.2. Environmental factors .....	65
2.7.3. Gene therapy.....	66
2.7.4. Bone marrow transplantation.....	66
2.8. CLINICAL TRIALS IN PATIENTS WITH RETT SYNDROME .....	68
AIM OF THE STUDY.....	71
3. AIMS .....	73
MATERIALS AND METHODS.....	75
4.1. PRIMARY AND SECONDARY ANTIBODIES .....	77
4.2. OLIGONUCLEOTIDE PRIMERS .....	77
4.3. EXPERIMENTAL MOUSE MODEL .....	78
4.4. DNA ISOLATION AND GENOTYPING OF MECP2 MICE - PCR PROCEDURE .....	79
4.5. PHENOTYPING OF MECP2 MICE - DETAILED NEUROLOGICAL SCORE TEST.....	81
4.6. PHARMACOLOGICAL TREATMENTS.....	82
4.7. TISSUE FIXATION .....	83
4.8. HEMATOXYLIN-EOSIN STAINING .....	83
4.9. DOPAMINE ASSAY .....	84
4.10. RNA ISOLATION, CDNA SYNTHESIS AND QPCR ANALYSIS .....	84
4.11. IMMUNOFLUORESCENCE ANALYSIS.....	85

4.12. WESTERN BLOT ANALYSIS .....	85
4.13. GOLGI STAINING .....	86
4.14. GLUTATHIONE ASSAY .....	86
4.15. BEHAVIOURAL TESTS .....	87
4.15.1. The horizontal bar cross test.....	87
4.15.2. Open field testing.....	88
4.15.3. Neophobia test.....	88
4.15.4. Wire Grip test.....	89
4.15.5. Y-Maze Spontaneous Alternation test .....	89
4.16. STATISTICAL ANALYSIS.....	90
RESULTS .....	91
5.1. PART 1 EVALUATION OF MOLECULAR AND BEHAVIOURAL TESTS TO ESTIMATE THERAPEUTIC EFFECTS OF PHARMACOLOGICAL TREATMENTS IN MECP2 KO MICE .....	93
5.1.1. Analysis of genotypes in Mecp2 KO mice colony by PCR.....	93
5.1.2. Pharmacological approaches for RTT mice model assessed in this thesis .....	94
5.1.3. Treatment strategies and standard treatment protocol of used drugs in this thesis ..	95
5.1.4. Phenotypic scoring of Mecp2 KO mice.....	97
5.1.5. Weight of Mecp2 KO mice and average life span.....	98
5.1.6. Evaluation of behavioural symptoms and difference between WT and Mecp2 KO animals with the focus on cognitive and motor functions.....	99
5.1.6.1. The Horizontal bar cross test.....	100
5.1.6.2. Open field testing.....	101
5.1.6.3. Neophobia test.....	102
5.1.6.4. Wire grip test .....	103
5.1.6.5. Y Maze Spontaneous Alternation test.....	104
5.1.7. Immunostaining of Th and pTh-positive neurons number in WT and Mecp2 KO mice .....	106
5.1.8. Immunostaining for the post- and presynaptic proteins, level of PSD-95 and VGLUT1 in WT and Mecp2 KO mice.....	108
5.1.9. The level of glutathione in WT and Mecp2 KO animals .....	109
5.1.10. Determination of numbers and types of dendritic spines in WT and Mecp2 KO mice .....	111
5.2. PART 2. IMPROVEMENT OF THE RETT SYNDROME PHENOTYPE IN A MECP2 MOUSE MODEL UPON TREATMENT WITH LEVODOPA AND A DOPA DECARBOXYLASE INHIBITOR (SZCZESNA ET AL., 2014) .....	114
5.2.1. Dopamine and norepinephrine are crucial in the biosynthetic pathway for the catecholamine neurotransmitters in RTT .....	114
5.2.2. Studies on potential toxic effect on Mecp2 KO mice during L-Dopa / Ddci treatment .....	115
5.2.3. Single and total symptoms score after L-Dopa / Ddci treatment .....	117
5.2.4. Life span of Mecp2 KO mice after L-Dopa / Ddci treatment.....	119
5.2.5. Partial rescue of locomotor deficits in Mecp2 KO Mice after L-Dopa / Ddci therapy .....	120
5.2.6. Level of dopamine after administration of L-DOPA with Ddci in MeCP2 mice .....	121
5.2.7. Dendritic spine density in Mecp2 KO mice after L-Dopa/Ddci treatment.....	122
5.2.8. Changes in levels of DRD2 dopamine receptor after L-Dopa/Ddci treatment.....	125
5.2.9. pTh and Th-positive neuron numbers in Mecp2 KO mice after L-Dopa / Ddci treatment .....	125
5.3. PART 3 GLYCOGEN SYNTHASE KINASE-3 INHIBITOR, SB216763, DISPLAYS THERAPEUTIC POTENTIAL IN A MOUSE MODEL OF RETT SYNDROME (SZCZESNA ET AL., IN PREPARATION) .....	129

5.3.1. Determination of possible toxic effect on Mecp2 KO mice during SB216763 treatment .....	130
5.3.2. Single and total symptoms score after SB216763 treatment .....	131
5.3.3. Evaluation of the life span in Mecp2 KO mice treated with SB216763.....	133
5.3.4. Assessment of mobility deficits in Mecp2 KO mice after SB216763 treatment .....	134
5.3.4.1. Bar cross test .....	134
5.3.4.2. Open field test.....	136
5.3.4.3. Neophobia test.....	136
5.3.4.4. Wire grip test .....	137
5.3.4.5. Y-maze test .....	138
5.3.5. Levels of total and phosphorylated GSK-3 $\alpha$ and $\beta$ , $\beta$ -catenin before and after SB216763 treatment.....	139
5.3.6. Analysis of anti-inflammatory markers before and after SB216763 treatment - measurement of NF-kappaB activity .....	141
5.3.7. Level of Glutathione in MeCP2 mice after administration of SB216763.....	142
5.3.8. Dendritic spine density in Mecp2 KO mice after SB216763 treatment .....	144
5.3.9. Changes in levels of DRD2 receptor after SB216763 treatment .....	145
5.3.10. Preliminary studies on expression of PSD-95 and VGLUT1 in Mecp2 KO mice after SB216763 treatment.....	146
5.4. PART4 EVALUATION OF SELECTED CLASSES OF DRUGS TARGETING PATHWAYS AND PROCESSES DEREGULATED IN RETT SYNDROME. ....	148
DISCUSSION .....	153
5.1. PART 1 .....	155
5.2. PART 2.....	159
5.3. PART3.....	162
5.4. PART 4.....	164
CONCLUSIONS.....	167
REFERENCES.....	171
PUBLICATION LIST .....	193
ANNEX 1 .....	197



## **Acknowledgements**



## Acknowledgements

As I look back at my stay in Barcelona, I am surprised at the way time has flown by and at the same time, I am very grateful for all that I have achieved throughout these years. The completion of this thesis would not have been possible without help from many people.

At this moment, I would like to take the opportunity to thank everyone who has supported me along the way.

First of all, I would like to thank the director of my PhD thesis. Manel, thank you for giving me a chance to work in your department during my PhD project. Without your initiative and management, this work would not have been possible. I am very grateful for your guidance and understanding during all these years - it was a fantastic learning experience and I have learned a lot from you. You provided me with the perfect balance of supervision and freedom - the combination which, I believe, was the key to the success of our projects. I hope we will have a chance to work together again in the future.

I would like to thank the whole RETT team. Dori, despite my tendency to focus on negative aspects of my work, you were always able to force me to notice the bright sides of it as well. Thank you for guiding me through it all.

Olga, thank you for your faith in my scientific skills - I would not have developed them without your continuous support and patience. I am thankful for your constant encouragement, support and suggestions at various phases of my PhD journey.

Paolo, working with you in the lab was a great experience and I learned a lot from it. Thank you for all the fun times we spent together outside of the lab, and for your help with many scientific and non-scientific issues.

Mauricio, your deep scientific insights, critical suggestions and constructive criticism have always inspired me and enriched my growth as a researcher.

Laura, your drive to work with the highest possible efficiency was always very motivating for me. Not only me, but also our beloved mice, enjoyed the time we spent together.

Mario, being your neighbour in the office for the last couple of months was a lot of fun.

This work would not be possible without help from my colleagues in the group. Alexia, Carmen, Laia, Julia, Vanessa, Rute, Anna P, Anna MC, Javi, Jose, Humberto, Miguel V, Angel, Tony, Sebas, Eli, Maria B, Yutaka, Cristina, Holger, Luca, Enrique, Sonia G,

## **Acknowledgements**

Marta S thank you for your help in the lab and critical approach during work and non-work discussions. I learned a lot from all of you! It was both pleasure and privilege to work together!

I am grateful to all PEBC members for being great co-workers and friends. I enjoyed a lot the journey between PEBC 1 and PEBC 7.

Paula, your everlasting enthusiasm and positive energy made late evenings in the lab a lot nicer. Thank you for all the fun time we spent together outside of the lab, and see you soon wherever it may be.

Catia, Fer, Jessica, Miguel L thank you for all your support and finally your smiles, which make the whole PEBC corridor a much better place! "Chiki" forever!

Maria I, even though we worked only for a couple of months, it was an extremely efficient period and I truly regret that we didn't have a chance to work together a bit longer.

Juan, your expertise in ChIP analyses was very helpful - thanks for sharing your knowledge and data with me. Looking forward for our final results!

Geert, I really enjoyed our long discussions during and after work over a Dutch treats.

Carmen C, I would like to say thank you for all your help and advice with regards to the microscope world.

I would like to express my gratitude to whole IDIBELL animal facility. Dr. Joana Visa, Dr. Rosa Bonavia, Charo, Gloria, Pablo thank you for helping and supporting me during daily mice work - without your continuous support this work would not be possible.

I am very thankful to Prof. Maurizio D'Esposito, IGB, CNR, Italy, and all the ITN7-Marie Curie Organization, Dischrom Group who organized several conferences and workshops to direct us with latest research activities.

I am very glad that I could be a part of Asociación Catalana del Síndrome de Rett. Meeting with all members and Rett families always stimulate me to further investigate Rett syndrome disease.

I would also like to acknowledge our external collaborators for fruitful collaboration and inspiring discussions about studying new drugs and techniques for scientific approach.

## Acknowledgements

This work would not be possible without long-term collaboration with Hospital Sant Joan de Deu. I would like to thank Dr. Mercé Pineda and Dr. Judith Armstrong Moron.

My Barcelona's angels thank you for all the nice moments - I truly enjoyed them! I am looking forward for next ones! Thank you for being always by my side even though sometimes it was difficult to put up with me.

Wielkie dzięki dla TYCH, którzy zawsze we mnie wierzyli. Dla moich kochanych! Dzięki Waszemu ogromnemu wsparciu ostatnie miesiące były zdecydowanie mniej stresującymi. YOU are simply the best. Liczne wspólnie wyjazdy były prawdziwą odskocznią od wszelkich frustracji związanych z pracą. Już nie mogę się doczekać następnych.

Alek, dziękuję że ze mną wytrzymałeś.

Na koniec, najważniejsze podziękowania kieruję do moich ukochanych dziadków, rodziców i brata. Dziękuję Wam za cierpliwość i wyrozumiałość - wiem, że niekiedy wysłuchiwanie moich ciągłych narzekań bywa męczące. Ta praca nie byłaby możliwa bez Waszej wiary we mnie, która towarzyszyła mi na każdym kroku.

Moltes gràcies! ¡muchas gracias! Thank you! Dziękuję!

Karolina



## **Abbreviations**



## Abbreviations

ASD	Autism spectrum disorder
BBB	Blood brain barrier
BDNF	Brain-derived neurotrophic factor
CDKL5	Cyclin dependent kinase like 5
CNS	Central nervous system
CpG	Cytosine-guanine dinucleotide
DAPI	4',6-diamidino-2-phenylindole
Ddci	Dopa Decarboxylase Inhibitor
DMSO	dimethylsulfoxide/saline
DNA	Deoxyribonucleic acid
DNMT	DNA methyl transferase
DRD2/Drd2	dopamine receptor 2
EE	Environmental enrichment
FOXP1	Forkhead box G1
GABA	Gamma-aminobutyric acid
GSH	reduced glutathione
GSK-3- $\alpha$	Glycogen synthase 3- $\alpha$
GSK-3- $\beta$	Glycogen synthase 3- $\beta$
GSSG	Oxidized glutathione
GSx	total glutathione
HDAC	Histone deacetylases
HZ	heterozygous
IGF	Insulin-like growth factor
IP	intraperitoneal
KO	Knock Out

## Abbreviations

L-Dopa - L-3,4-dihydroxyphenylalanine

MB Midbrain

MBD Methyl-CpG-binding domain

MECP2 Human Methyl-CpG-binding protein 2 gene

MeCP2 Human Methyl-CpG-binding protein 2 protein

Mecp2 KO male KO mice, no MeCP2

Mecp2 null male KO mice, no MeCP2

Mecp2 <sup>-y</sup> male KO mice, no MeCP2

Mecp2 Mouse Methyl-CpG-binding protein 2 gene

Mecp2 Mouse Methyl-CpG-binding protein 2 protein

OPT open field test

OS oxidative stress

PCR Polymerase chain reaction

PSD-95 Postsynaptic density protein 95

pTh phospo Tyrosine Hyrdoxylase

qPCR quantitative PCR

RNA Ribonucleic acid

ROS Reactive oxygen species

RTT Rett syndrome

SNpc substantia nigra pars compacta

Th Tyrosine Hyrdoxylase

TRD Transcriptional repression domain

VGLUT1 Vescicular glutamate transporter 1

WT/wt Wild-type

## Abbreviations

$\alpha$  Alpha

ANOVA Analysis of variance

Bp Base pair

$\beta$  Beta

C Celsius

$^{\circ}$  Degree

g Gram

$\geq$  Greater than or equal to

H Hour

Kda Kilo Dalton

m Milli

Min minute

M Molar

nt Nucleotide

ON Overnight

% Percentage

pH Hydrogen ion concentration

$\pm$  Plus/minus

RT Room Temperature

Sec second

SD Standard deviation

SEM Standard error of mean

$\mu$  Micro



## **Introduction**



# 1. Epigenetics

The term epigenetics refers to heritable traits resulting from changes in chromosome without altering DNA sequence (1). In 1942 epigenetics was first described by Conrad Hal Waddington (2) as “the causal interactions between genes and their products, which bring the phenotype into being”. However today it is described more as the study of heritable changes in chromatin that appear independent of changes in the primary DNA sequence. It is environmental changes in phenotype, but not in genotype, being influenced by diet (3), lifestyle, social behaviour or aging (4).

Epigenetics, from greek epi: “above”, and genetikos: “genesis, origin”, is very important for genomic regulation. It controls the whole genome and transcriptome by modifying chromatin structure. It is also responsible for development regulation (5), gene expression tissue specific pattern, X-chromosome inactivation and genomic imprinting (6).

The DNA molecule inside the nucleus is packed into chromatin that consists of nucleosomes wrapping 146 base pairs (bp) of DNA around an octamer of four core histones (H2A, H2B, H3 and H4) (7). There are two types of chromatin, euchromatin and heterochromatin. The euchromatin is a not condensed permissive chromatin, which may be transcriptionally active or inactive. Heterochromatin is condensed and transcriptionally silent. It can be in a permanent state of silence, known as constitutive heterochromatin, or potentially dynamic, known as facultative heterochromatin. Because of that, we have a spectrum of chromatin states, what suggests chromatin being a highly plastic DNA-protein structure.

The organization of the chromatin can be modified by epigenetic mechanisms to create the “epigenetic landscape”, which allows that genome displays unique properties and distribution patterns in different cell types for its cellular identity and function (8).

## 1.1. Epigenetic mechanisms

The chromatin structure can be modified by epigenetic mechanisms, which can be divided into few categories: DNA methylation, covalent histone modifications, non-covalent mechanisms (histone variants and nucleosome remodelling) and non-coding RNAs (ncRNAs). The epigenetics mechanisms are going to be included in this section.

## Introduction

### 1.1.1. DNA methylation

DNA methylation is the most widely studied epigenetic mechanism correlated with gene expression. In eucaryotes, DNA methylation consists of the addition of a methyl group at cytosines followed by guanines (CpG dinucleotides). CpGs are underrepresented in the genome and show tendency to concentrate at specific clusters, called CpG islands. DNA methylation has been classically considered as a repressive mark like in the tissue - specific gene silencing and allele - specific inactivation of the X-chromosome, which are associated with hypermethylation of CpG islands, (9). However, lately it looks like much more complex process. Generally, most of the CpG islands are unmethylated and non- CpG islands CpG sites are methylated. Usually, only very small amount of CpG islands promoters are methylated in normal cells. When they are hypermethylated it relates to tumorigenesis or not normal development. About 70% of annotated genes, as well as housekeeping genes, tissue specific and regulatory genes are related to CpG islands in their promoter regions (10), emphasizing the role of CpG islands in the gene regulation.

Regulation of CpG islands in promoter regions cannot be related only to regulation by DNA methylation. CpG islands promoters are associated with genes expressed with a low evolutionary rate and relaxed TSS (Transcription start sites) firing. Contrariwise non CpG islands promoters are mostly connected with weaker and more restricted gene expression with TSS firing, exhibiting higher evolutionary rates (6).

The large part of the CpG dinucleotides are associated with repetitive elements such as centromeres, retroelement repeats, microsatellite sequences and promoter regions. As mentioned, approximately 60-70% of human genes have CpG island promoters. There are two ways in which DNA methylation could controls transcription by inhibition. One of them is about that methylation can interfere with the interaction of transcription factors and other DNA binding proteins (11). Second control, methylation can inhibit gene expression by recruiting methyl-CpG binding protein (MBD) (12, 13).

Besides to regulate transcription process, DNA methylation has many other important biological functions. DNA methylation represses the expression of parasitic sequences, endogenous retrovirus and transposable elements, such as  $\alpha$ -satellites, a short stretch of DNA characterised by the action of the ALU restriction endonuclease - ALU-Yb8 and a long interspersed nuclear elements-1 (LINE-1).

The enzymes that are involved in DNA methylation are called DNA methyltransferases (DNMTs). They fetch the process of transfer a methyl group from an S-adenosyl-L-methionine to the cytosine. The mammals DNMTs family consist of five members: DNMT1, DNMT2, DNMT3A, DNMT3B, and DNMT3-like (DNMT3L) (14).

Only DNMT1, DNMT3A and DNMT3B are possessing methyltransferase activity. The catalytic members of the DNMT family are classified into either *de novo* DNMT (DNMT3A and DNMT3B) or maintenance DNMT (DNMT1) group. *De novo* DNMTs are highly expressed in stem cells and are downregulated after process of differentiation.

The DNMT3L protein is expressed during gametogenesis and is essential for establishing maternal genomic imprinting despite being catalytically inactive. The role of DNMT1 is to maintain DNA methylation through cell division. It is most active during the S phase of the cell cycle, when the DNA is hemimethylated after semi conservative DNA replication.

DNA methylation profile is copied from the parental to the new DNA strand through interaction with Ubiquitin-like, with PHD and RING finger domain 1 (UHRF1) (15). This way, methylation patterns are efficiently preserved throughout division. Lately, it has been shown, that in absence of both DNMT3A and DNMT3B, DNMT1 cannot maintain methylation by itself as these show gradual loss of methylation, suggesting that the *de novo* DNMTs also possess limited maintenance function (16).

DNA methylation is the oldest epigenetic mechanism known to correlate with gene expression (17). This modification consists of the addition of a methyl group at cytosine residues of the DNA template. DNMTs enzymes catalyze either the *de novo* or maintenance methylation of hemimethylated DNA following DNA replication. They transfer a methyl group from the methyl donor S-adenosylmethionine (SAM) resulting in 5-methylcytosine (Figure 1).

The 5-methylcytosine is recognized by the methyl-CpG binding domain (MBD), which is present in the proteins called MBDs. In mammals are five members: MeCP2, MBD1, MBD2, MBD3 and MBD4. MeCP2 was among all of them characterized as a first one (18). Most of the MBD proteins are located in highly methylated chromatin regions, which are participating in silencing of imprinting genes and in endoparasitic sequences, (19) promoting transcriptional repression and genomic stability.

## Introduction

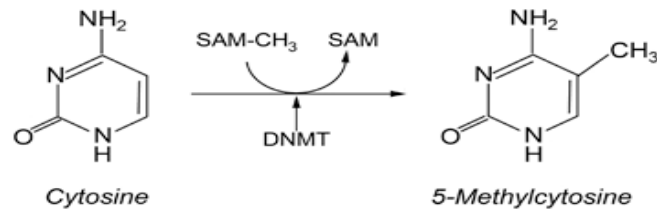


Figure1. Mechanism of DNA methylation and its conversion of cytosine to 5-methylcytosine by DNMTs. DNMT transfers a methyl group (CH<sub>3</sub>) from SAM to the 5'-carbon position of a cytosine.

### 1.1.2. Histone modifications

Next, very important epigenetic marks are histone modifications. Eukaryotic DNA is packaged into chromatin consisting of nucleosomes (7). As mentioned before, the nucleosome, is the basic unit of chromatin structure wrapped around the octamer of histones consist of two copies of each: H2A, H2B, H3 and H4 (20). Histone H1 is a linker histone that does not form part of the core nucleosome but binds to the linker DNA. The nucleosome is associated with 146bp of DNA which is wrapped 1.65 turns around the histone octamer, with the neighboring nucleosome separated by approximately 50bp of free linker-DNA. These histones contain a globular C-terminal and an unstructured N-terminal tail that can be subjected to a variety of posttranslational covalent modifications. There are about 50 known modifications that affect these amino-terminal tails. Besides doing the solid structure, N-terminal regions of histones bulge from the nucleosome and are receptive for interactions with other proteins. Common posttranslational modifications of histone tails are methylation of lysines and arginines, acetylation, phosphorylation, ubiquitination, ADP-ribosylation or SUMO-ylation. Most of the post translational histone modifications even dynamic are reversible mediated by two antagonistic enzymatic complexes. In site specific manner these complexes remove or attach the corresponding chemical group. One of the most known histone tail modifications is acetylation at lysine residues, which is related to transcriptional activation (20). Histone acetyltransferases called HATs, carry out these types of modifications, and histone deacetylases, HDACs, can invert these changes.

Another well known histone modification also takes place on lysines and their tails. It can be mono-, di- or trimethylation. Inversely to acetylation, the function of each modification depends on which amino acid is modified and on the methyl group number added. Taking one of many examples, methylation of H3 on lysines 4 and 36 (H3K4 and H3k36) is usually tied with an open euchromatin structure and activation, while

H3 methylation on lysines 9 and 27 (H3K9 and H3K27) is related to closed heterochromatin structure and gene silencing (20, 21).

Methylation of histones is performed by histone methyltransferases and demethylation by histone demethylases so called jumonji protein group (22). More specific process, including higher order chromatin mechanisms like nucleosome repositioning or genome-wide chromatin remodeling factors, with long non-coding RNA and RNA editing, can be also involved in histone modifications (23-25).

### 1.2. Epigenetic implications in brain functions

Gene mutations can be the reason of epigenetic dysfunctions. It often occurs in neurodevelopmental disorders. Human brain is a specific unit composed of hundreds billions cells (26). Plenty of different cell types, with specific epigenetic partners compose individual brain structures, which play characteristic transcriptome and profile of DNA methylation (27). In nervous system we have a boundlessly complex structure, where transcriptome machinery plays a major role. Three out of four genes are expressed in brain (28) and it expresses more alternatively spliced transcripts (29) or miRNAs (30) compared to other tissue. Epigenetics is a very important participant in controlling the gene transcription and splicing. That is one of the main reasons why mechanisms that regulate epigenetics are also important in the brain functions.

Brain functions such as synaptic plasticity, memory or learning, related to neurodevelopment of the organ, are associated with DNA methylation and histone modifications. Neurons express high levels of DNMT1 and DNMT3a (31). Neurons are considered a differentiated state of postmitotic cells for which further differentiations or maintain DNA methylation would not be necessary (32).

DNA methylation is suggested to have a role in neurons function, because of the presence of DNMTs, together with high levels of MBD1 and MeCP2. Moreover, TET proteins convert 5-methyl-cytosine (5mC) to 5-hydroxymethyl- cytosine (5hmC). Then, cytidine deaminases process the 5hmC to 5-hydroxymethyluracil (5hmU), and finally, 5hmU is turned to cytosine by the base excision repair system (33). Tet 1 is also highly expressed in brain (34) and it was mentioned that the level of 5hmc levels in frontal cortex is four times higher compared to stem cells (35). Moreover, the ablation of DNMT1 and DNMT3a in post mitotic neurons perturbs learning and memory (36). Also

## Introduction

MeCP2 mutations are the main reasons of mental retardation for example in case of Rett syndrome disease.

Besides, DNMT1 mutations provoke hereditary sensory neuropathy with dementia (37). In turn the ablation of DNMT3a impairs neurogenesis in adult brain (38).

However, the most intriguing finding in neuroscience was the fact that neuronal activity induces active DNA demethylation at specific loci (39). This DNA methylation as it was predicted depends on Tet1 and cytidine deaminase Apobec1 (33). Changes in DNA methylation associated to learning could persist more than one month (40). A parallelism between epigenetics and memory rises with the idea that epigenetics could constitute a scaffold for memory. Neuronal activity modifies gene expression, what is essential for long term memory, and also requisite associate to epigenetic chromatin changes (32). These changes are not confident with DNA methylation, also include histone modifications, that is why neuronal activity increases also histone acetylation (41). Overexpression of HDAC2 provokes decrease in dendritic spine density, or synapse number, synaptic plasticity and memory formation. Inhibition of HDAC2 increases number of synapses and memory facilitation, confirming the role of histone acetylation in learning and memory (42). CREB-binding protein regulates function of CREB/p300 HAT, and its mutation causes mental retardation, which can be ameliorated by HDACs inhibitors (43).

Presented above examples suggest that epigenetic plays important role in nervous system, even though its intervention is still not fully understandable. It seems that epigenetics participates in a framework of pathways and mechanisms that displays irrefutable function. High complexity of the nervous system entails it as a very sensitive to epigenetic disturbances, where the consequence could be reflected in mental disorders, in their mutations in epigenetic system, imbalance machinery like it is in case of Rett syndrome (44).

## 2. Rett syndrome

In 1966, Rett syndrome (RTT, OMIM#312750) was for the first time described as a clinical issue by Dr. Andreas Rett, an Austrian pediatrician (45). He has observed in 22 patients similar unique symptoms. A few years later Hagberg and colleagues described further the syndrome in 35 girls (46).

Rett syndrome is the cause of mental retardation that affects 1 in 10.000 female births, which makes it the second cause of mental retardation in girls (47). In 1999 Zoghbi lab found out the genetic basis of Rett disease. Mutation in MeCP2 is in 95% cases the reason of classical Rett (47).

MeCP2 is a nuclear protein, expressed widely in different tissues, but is most abundant in neurons of the mature nervous system (47). In 1992 Bird and coworkers identified MeCP2 as a new protein that binds to the methylated CpG dinucleotides (48). MeCP2 is located on the X chromosome, Xq28 (49).

Although the function of the MeCP2 is still unknown, it is considered likely to regulate gene expression, either through the silencing or activation of the specific genes or by more global regulation of transcriptional processes (50-52). RTT was the first neurodevelopmental disorder related to epigenetics. Later, the CDKL5 and FOXP1 genes have been associated with variant forms of Rett syndrome (53).

### 2.1. Classical clinical features of Rett syndrome

RTT is related to X-chromosome, being mainly effected in female patients. It is a postnatal progressive disease with a normal prenatal and perinatal period. Rett patients have also proper brain development during the first 6-18 months of age, called the stagnation stage. The girls achieve normal neurodevelopment, motor function and communication skills. However, then developmental regression appears (54, 55). Some changes in interactive behaviour of the girls can be also observed but since the overall developmental pattern of the child is still normal, the behavioural deviation is not always significant enough to warrant the concern of the doctors.

During the active regression stage of the disease, between 1-4 years the girls are losing the ability to speak and the purposeful use of the hands. It is a classic phenotype

## Introduction

of the syndrome. Very often they also show autistic features, related mostly to reduction in interpersonal contact. The head growth undergoes deceleration that usually causes to microcephaly. Neurological evaluations show cortical hyperexcitability on the electroencephalogram, which indicates loss of developmental features.

In the third pseudostationary phase of the disease, between 4 and 7 years, girls become more alert but with more abnormalities including the teeth grinding, screaming fits, severe scoliosis, reduced somatic growth, low mood or night crying and laughing. The epilepsy at that time becomes briefly evident. The hand stereotypes are classically described as hand wringing and washing but also hand tapping/clapping or claspings may be noticed. The eye-contact is reduced, however the visual contact somehow returns and the child may look more alert and joyful with typical eye-pointing behaviour to express needs and wishes. In this period of time, the patients are still able to learn some new skills.

Next, in late motor deterioration stage, when the girls are between 5-15 years and older, they start to have cardiac abnormalities (bradycardia and tachycardia) what gives a high risk of sudden death due to respiratory dysfunction. In many cases, the lack of mobility leads to a state called frozen rigidity. However, some girls never lose the ability to walk and remain in stage 3 throughout their lives (Summary in Figure 2).

RTT patients suffer from growth failure, gastrointestinal problems, seizures and many cardiac abnormalities. Another classic symptom of this disorder is increased incidence of long Q-T intervals (the measurement of the time between the start of the Q and the end of the T wave in the heart's electrical cycle) during electrocardiographic recordings inducing to the higher incidence of sudden unexpected death in RTT patients.

As already mentioned above, epilepsy is very often one of the main problems in Rett patients, with the frequency between 50 up to 90% of all cases (56, 57). The severity of epilepsy often tends to decrease after adolescence, with lower seizure frequency and less secondary generalized seizures even in those patients who were previously considered quite unsusceptible (58).

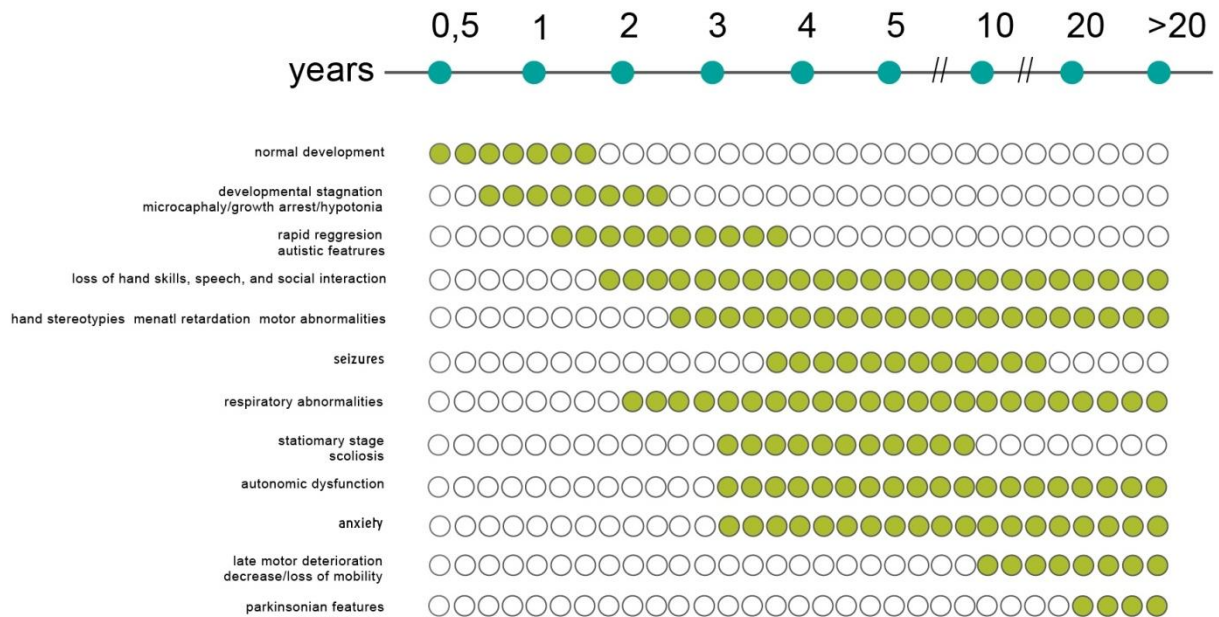


Figure 2. The illustration presents onset and progression of RTT Clinical Phenotypes (based on (53)).

## 2.2. Genetic basis of Rett syndrome: MeCP2

The proteins that have a potential to bind to methylated DNA are the methyl-CpG binding domain (MBD) proteins. The mammalian MBD family consists of 5 nuclear proteins, MBD 1–4 and Methyl-CpG binding protein 2 (MeCP2) (59). MECP2 is an X-linked gene, discovered as the prototype member of the DNA methyl binding proteins (48). Mutations in the X-linked MeCP2 gene precisely are the primary cause of RTT (47). The discovery that mutations in MeCP2 cause RTT and other neurodevelopmental disorders has called attention to the importance of epigenetic modifications in neuronal function. The MECP2 gene is expressed throughout human and mouse tissues but is particularly abundant in the central nervous system, meaning an important role of the protein in this organ (47). The onset of MeCP2 expression occurs in a defined pattern during perinatal development. That becomes apparent in the most ontogenetically ancient part of the brain, such as the brainstem and thalamic regions (60-63). The transcript levels are high during embryogenesis with a post-natal decrease, but increase again towards adulthood. On the other hand, the protein levels are low during embryogenesis and increase post-natally upon neuronal maturation (62, 63).

## Introduction

MeCP2 binds preferably to methylated cytosines inside the CpG nucleotide (64). The majority of pathogenic mutations in MeCP2 cause RTT in females. MeCP2 mutations in males are much more severe, and usually not surviving infancy. The gene is located on X chromosome causing that in each heterozygous female not only the mutant allele is expressed but also the normal one ends up theoretically in a 50:50 phenotypic mixture of the cells. However many studies showed that the ratio is quite far from 50:50 (65, 66). Brain cells express both alleles that are mixed and create a mosaic (67).

MeCP2 was considered as a methylation dependent transcriptional repressor (13), later as an enhancer of transcription (50), even as a global regulator of chromatin structure (68) or as a global dampener of transcriptional noise (52). Lately, it was demonstrated that MeCP2 work as a global activator in neurons, but not in neural precursors. Decreased transcription in neurons, in combination with a reduction in nascent protein synthesis and lack of MeCP2 was manifested as a severe defect in activity of the AKT/mTOR pathway. Additionally the lack of MeCP2 was also related to impaired mitochondrial function in mutated neurons (69). Moreover identification of new interacting partners of MeCP2 may have important and unrecognized yet implications. For instance miRNA-132, which involves MeCP2 in the regulation of the circadian cycle, is suggested as being responsible for the sleeping disorders observed in Rett girls (70).

### 2.2.1. MeCP2 structure

MeCP2 protein has 50 kDa and is encoded by four-exon gene located at q28 on the X chromosome (71). There are two isoforms of MeCP2 that differ in the N-terminus within exon2, as an outcome of alternative splicing. MeCP2 has six domains encoded by exons 3 and 4; MBD, two high mobility group protein-like domains (HMGD), a transcriptional repression domain (TRD), and two C-terminal domains (CTD).

MBD domain is related with the binding to the symmetrically methylated-CpG islands. MeCP2 binds methylated DNA *in vitro* and *in vivo*, and it is able to bind DNA in a nucleosomal context without disruption of the nucleosome (13, 72). The second, TRD is responsible to recruit a co-repressor complex that silences the gene through deacetylation of core histones (73). Moreover TRD domain represses transcription *in vitro* and *in vivo* by overlapping with nuclear localization signal (13). The C-terminal domain (CTD) could be divided into CTD $\alpha$  and CTD $\beta$ . The CTD $\beta$  contains the WW

binding domain, which is involved in splicing factor interactions (74, 75) (representative figure 3).

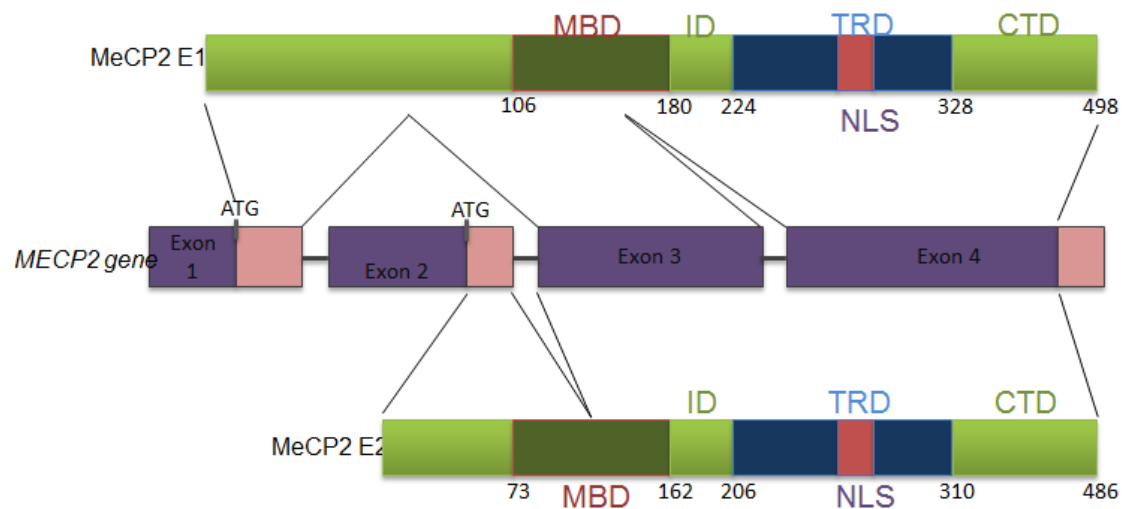


Figure 3. The MECP2 gene and its splicing isoforms. Schematic structure of the MECP2 and its different domains of two isoforms, MeCP2 E1 and E2. The primary amino acid of the N-terminus of MeCP2E1 and MeCP2E2 is depicted. (Based on (76)).

### 2.2.2. MeCP2 mutations

Rett syndrome is caused mostly by sporadic mutations in MECP2. Most mutations occur *de novo*. Some of them affecting residues of the MeCP2 protein involved in DNA binding, some of them can change the structure of the protein, alter its function, or modify the way that MeCP2 interacts with other proteins. Among over 200 different mutations, there are eight most common point mutations in RTT patients (Table 1). The deamination of methylated cytosines generate C>T transitions, which are responsible for the “hotspot” mutations. Usually, missense mutations tend to cluster in the MBD while, large multinucleotide deletions occur in the C-terminal domain (CTD). Nonsense mutations are with the distant to the MBD (77).

## Introduction

Nucleotide change	Amino acid change	Percentage
316C > T	R106W	4,8%
397C > T	R133C	5,4%
473C > T	T158M	12,2%
502C > T	R168X	11,9%
763C > T	R255X	10,7%
808C > T	R270X	9,6%
880C > T	R294X	8,2%
916C > T	R306C	6,4%
20-100bp deletion		9,7%
<b>total</b>		<b>78,9%</b>

Table 1. The table presents eight most common MECP2 mutations in RTT patients and their frequency.

### 2.2.3. MeCP2 mechanism of action

The main characterized function of MeCP2 is related to the transcriptional silencing mediated by chromatin compaction. In particular, it is known the MeCP2 ability to bind methylated CpG sites and to recruit histone deacetylases and corepressors such as Sin3A; this complex induces chromatin condensation, causing gene silencing.

From several years, the gene-specific or global regulatory role of MeCP2 has been argued. Initially Mecip2 was indentified in rat cells based on its ability to bind methylated DNA, and also found to bind a single symmetrically methylated CpG independent of sequence context (48). In the adult mouse, Mecip2 is highly abundant in the brain, lung and spleen, but less abundant in kidney and heart, and almost negligible in the liver, stomach or small intestine (62). Interestingly enough is the fact that in mouse´s brain nearly 16 million molecules of Mecip2 via nucleus neurons were found, with almost an order of magnitude less in glial cells and 30-fold less in liver cells (52).

Expression profiling of specific brain regions, such as hypothalamus and cerebellum of Mecip2 KO and overexpressing animals, revealed changes in the expression of thousands of genes (78). Interestingly, the expression level of deregulated genes in Mecip2 KO and overexpressing animals showed an opposite trend. These studies

support a role of MeCP2 as transcriptional activator of several genes, through the binding of the transcriptional activator CREB1 (50, 79). The main MeCP2 target gene is Brain-derived neurotrophic factor (BDNF), a signalling molecule with a crucial role in brain development and neuronal plasticity. It was shown that in resting neurons MeCP2 is bound to methylated promoter of BDNF, while in depolarized neurons, which cause BDNF activation, MeCP2 dissociates from the promoter (16, 80). Additional MeCP2 targets are non coding RNAs (81). In particular, two different transcriptional profiling studies on null brains indicate that the lack of MeCP2 cause deregulation of hundreds of miRNAs. Furthermore, Petazzi et al. (82) found more than 700 long non-coding RNAs (lncRNAs) deregulated in *Mecp2* KO mice brains compared to Wild Type (WT) animals. One of the up-regulated lncRNAs is regulated in an opposite way with respect to its host coding protein gene, codifying the GABA receptor subunit Rho 2. These findings suggest a global role of MeCP2 in the transcriptional regulation of many classes of genes, showing the importance of its and making out the destructive effect of its mutations in RTT patients.

On the other hand, the global regulatory role of MeCP2 has been confirmed by the large scale analysis of MeCP2 distribution (52). Skene with co-workers has reported that MeCP2 abundance in neuronal nuclei is comparable to that of histone octamer. Moreover, by ChIP-sequencing is demonstrated that MeCP2 binding sites are spread throughout the genome and that this regions coincide with -CpGs sites. Moreover, the lack of MeCP2 in neurons is responsible for the de-repression of spurious transcription of repetitive elements, such as L1 retrotransposon (52). MeCP2 can influence the chromatin structure of an imprinted gene cluster on chromosome 6, including *Dlx5* and *Dlx6* genes, which are in turn up-regulated in *Mecp2* KO brain (83). In particular, the authors demonstrated a direct binding of MeCP2 to these regions, where it mediates the formation of an 11 kb chromatin loop enriched in methylated H3K9, a mark of silent chromatin. This loop disappears in *Mecp2* KO brain. MeCP2 may thus regulate imprinted loci by conformational changes in chromatin structure (48).

Lately, MeCP2 has been also proposed as a regulator of RNA splicing through its interaction with the splicing factor, Y-box-binding protein (YB1). The protein synthesis is reduced due to lower mTOR activity. It is thus clear that further analyses are required to clarify whether MeCP2 is simply a methyl-DNA binding protein involved primarily in transcriptional repression or a multi-functional protein with global or local effects on chromatin. Recent experiments demonstrates that MeCP2 in neurons binds broadly throughout the genome, suggesting that it might function more as a global regulator of transcription and chromatin remodeling, than as a sequence-specific transcription

## Introduction

factor (52, 84). The current knowledge suggests that RTT might be the reason of the misregulation of both transcription and other MeCP2 dependent processes.

Few years ago, despite the low abundance of MeCP2 in glial cells, it was suggested that the methylbinding protein may also play an important role in astrocytes and microglia (85-87). An *in vitro* co-culture system showed that the microglia or astrocytes lacking MeCP2 inhibit dendritic arborization of WT neurons by producing a toxic factor, glutamate. *In vitro* evidence also confirmed that loss of MeCP2 within astrocytes leads to a gap junction dependent failure of affected astrocytes to properly support dendritic development.

Moreover, lately, Baker and co-workers (88)(Figure 4) described an AT-hook domain as an important for MeCP2 function. It was suggested that an AT-Hook domain in MeCP2 determines the clinical course of Rett syndrome and related disorders. A highly conserved AT-hook domain for the first time was already described in 2005 but that time the role was unknown (89). In 2005 it was suggested that AT-hooks are regions of a protein that bind to AT-rich DNA. MeCP2 requires an A/T-rich motif adjacent to methylated CpG dinucleotides for efficient DNA binding (89).

Baker and colleagues showed that the localization of  $\alpha$ -thalassemia/mental retardation syndrome X-linked protein (ATRX) to pericentric heterochromatin (PCH) is a distinguishing feature between G273X and R270X. This is an intriguing finding not only because ATRX syndrome shows overlap with RTT, but also because ATRX participates in chromatin remodelling, associates with MeCP2, and disruption of that interaction is thought to contribute to intellectual disability (90).

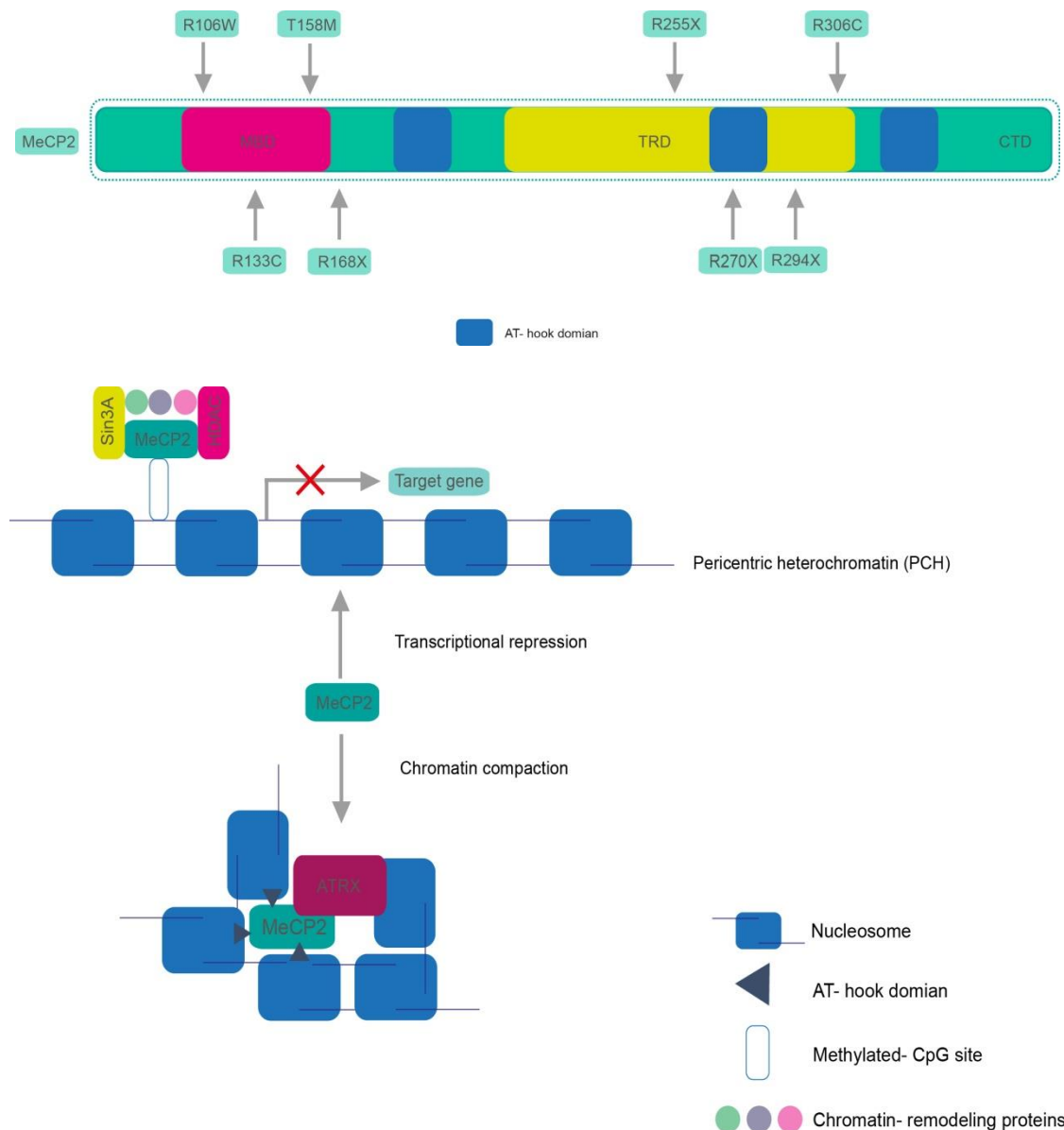


Figure 4. Mutations and functions of MeCP2 in gene silencing and chromatin compaction. The structure of MeCP2 and location of most common MeCP2 mutations in RTT patients. From the left side respectively R106W, arginine to tryptophan point mutation at residue 106; R133C, arginine to cysteine point mutation at residue 133; T158M, threonine to methionine point mutation at residue 158; R168X, arginine to stop codon at residue 168; R255X, arginine to stop codon at residue 255; R270X arginine to stop codon at residue 270, R294X, arginine to stop codon at residue 294; R306C, arginine to cysteine point mutation at residue 306. As a transcriptional repressor, MeCP2, when bound to methylated DNA, recruits Sin3A, HDACs and some chromatin remodeling proteins to silence target gene transcription. Based on (27).

## Introduction

### 2.3. Epigenetic alterations in Rett syndrome

Even though MeCP2 is widely expressed, as already noticed, the major features of RTT have been reported as a result of neuronal deficiency of MeCP2 (91). The chromatin containing MeCP2 in the brain was described as being different than in the rest of tissues (52). In nuclei of neurons, MeCP2 is very abundant, with the frequency comparable to histone H1. MeCP2 is mostly associated with methylated regions displacing histone H1 (92). MeCP2 deficiency reflects in changes in chromatin structure in neurons. It is related to the elevated acetylation and doubling of H1 (52). Even though it was proposed that MeCP2 plays as a global repressor, posterior data have suggested the protein to act as a transcriptional regulator linking DNA methylation and transcriptional modulations. It is also already known, that MeCP2 binds to the methylated DNA, HDAC SIN3A, retinoid and thyroid hormone receptors, called SMRT (93), HP1 (94), the SWI/SNF Brahma complex (95) and aforementioned ATRX (96). Lately, MeCP2 was pointed also as a gene activator that can bind directly to the gene promoter with the transcriptional activator cAMP response element binding protein 1 (CREB1) (50). That is why *inter alia* the MeCP2 cannot be considered as a classic transcriptional repressor (93, 94, 97). MeCP2 affects also gene expression by conformational chromatin changes, which are secondary to histone modifications (51). Based on that, dysregulation described in RTT could be related to different pattern of histone marks (52). Although different studies have been carried out the correlation of DNA methylation, histone modifications and the presence of MeCP2 remain unclear.

Experiments with established cell lines from RTT patients have presented an increase in the acetylation of H4 at lysine 16 (98), but no changes in H3 acetylation. Balmer and coworkers have not seen any difference in the global acetylation of H3 and H4 in RTT-patient T-cell clones (99). In 2005 Kaufmann described that untransformed cells bear difference in acetylation and methylation of H3, but no changes in H4 modifications (100). Mice with truncated MeCP2 when compared to WT littermates displayed in the brain increased acetylation of H3 but no changes in H4 were noticed (63). However in *Mecp2* full knockout (KO) mice with respect to WT littermate no H3 and H4 modifications were observed neither in cortex, nor MB or cerebellum (101).

MeCP2 could be a specific gene regulator with some restricted epigenetic changes. Recently different approaches including microarray or chromatin immunoprecipitation have been used to investigate the downstream consequences of MeCP2 mutation. The set of target genes and miRNAs have been identified (81, 101, 102). MeCP2 target

genes are summarized in Table 2. It is still not clear, if MeCP2 acts at the genome specific sites or more globally and how it is related to cell types in which MeCP2 plays major functions.

## Introduction

Gene	Function	Reference
xHairy2a	neuronal repressor	(93)
BDNF/Bdnf	neuronal development and survival	(16, 80)
IGF2	cell proliferation	(103)
MPP1	signal transduction	(103)
UBE3A/Ube3a	proteolysis, ubiquitin ligase	(104, 105)
GABRB3/Gabrb3	GABA A receptor subunit	(105)
DLX5/Dlx5	neuronal transcription factor	(68)
Dlx6	transcription factor	(68)
Fkbp5	hormone signalling	(106)
Sgk1	ion channel activation	(106)
ID1/Id1, IDRD2/IDrd2, ID3/Id3	transcriptional regulation	(107)
Uqcrc1	mitochondrial respiratory complex subunit	(74)
Crh	neuropeptide, anxiety and stress response	(108)
IGFBP3/Igfbp3	hormone signalling	(109)
FXYP1/Fxyd1	Na <sup>+</sup> /K <sup>+</sup> -ATPase activity	(110, 111)
Reln	cell signalling	(111)
Gtl2/Meg3	non-coding RNA	(111)
JUNB	early response gene, oncogene	(112)
RNASEH2A	ribonucleotide cleavage from RNA-DNA complex	(112)
Sst	hormone signalling	(112)
Oprk1	opioid receptor	(50)
Gamt	methyltransferase	(50)
Gprin1	neurite formation	(50)
Mef2c	myogenesis	(50)
A2bp1	splicing	(50)
Creb1	transcriptional co-activator	(50)
Dlk1 / Gtl2 Plagl1	imprinting	(101)
Ddc	neurotransmission, metabolism	(101)
Mobp	myelin component	(101)
Eya2	inflammatory response	(101)
S100A9	transcriptional co-activator	(101)

Table 2. MeCP2 target genes.

### **2.4. Atypical forms of Rett syndrome**

Since RTT was internationally characterized by Hagberg in 1983 (46), clinical criteria have remained the predominant tool for the diagnosis. It became evident that a number of patients did not completely follow the diagnostic criteria for RTT. A variety of specifically defined variant forms of RTT have been recognized that have distinct clinical features. Some of these forms have been recognized in only a small number of cases, making it difficult to have any clear statement concerning the defining clinical features. About 25% of RTT patients are characterized as not having a typical but variant form of Rett disease. The fact that those girls show only some severe features force to create a further subdivision of atypical RTT into several groups, from milder to more severe forms with respect to disease onset and progression. In these forms, the preserved speech variant, the congenital form, and the early-onset seizure variant are the most typical and standards for their diagnosis. They were included in the latest revised criteria described by Neul et al. (113). A varied range of mutations has been found in different loci associated with these variant forms such as mutations in CDKL5 in the early seizure variant (114) and mutations in FOXP1 in patients with the congenital variant (115).

#### **2.4.1. Preserved speech variant (PSV)**

As opposed to the more severe RTT variants, the preserved speech variant (PSV), also called the Zappella variant, constitutes a significant part of atypical RTT cases. It is characterized by a milder clinical picture including, in particular, a better conservation of language abilities. In fact, patients with the PSV may be able to make sentences even if the speech cannot be admitted as a completely normal. Usually, the regression stage is delayed compared to typical RTT. Besides, other RTT features such as deceleration of head growth, epilepsy, breathing abnormalities and scoliosis are less frequent in patients with PSV. The ability of hand use may also improve with time and the intellectual disability can be less severe while autistic traits are rather evident. The majority of girls with the PSV have missense mutations in MECP2. In particular the R133C or late truncating mutations can be identified in those girls in accordance with

## Introduction

genotype-phenotype correlations indicating that these mutations are predictive of a milder clinical picture.

### 2.4.2. Early-onset seizure variant (ESV) – CDKL5 mutations

In 1985, the early-onset seizure variant (ESV) was first described by Dr. Hanefeld, and therefore is also named the Hanefeld variant. Patients with the ESV are characterized as the name implies by the appearance of often drug resistant seizures in the first months after birth (116). Severe developmental delay, impaired communication, and the occurrence of some RTT-like features such as hand stereotypies, which often get more noticeable with age are characteristic for patients with the ESV variant. A recent study showed that more than 20% of these patients implement the diagnostic criteria for the ESV RTT, which is mainly ensuing to the absence of a clear period of regression that is needed for the diagnosis of RTT (117).

Mutations in the cyclin-dependent kinase-like 5 gene (CDKL5, OMIM 300203), located at Xp22 is a reason of ESV. In 2004 CDKL5 mutations were found in two RTT patients with early-onset infantile spasms (118). 10 years later alterations in CDKL5 have been reported in approximately 150 patients, 10% of which were males. The CDKL5 gene, which was cloned in a transcriptional mapping project of human Xp22 in 1998, encodes a serine-threonine kinase with an amino-terminal catalytic domain sharing strong homology with the mitogen-activated protein kinase (MAPK) and the cyclin-dependent kinase (CDK) families. A long C-terminal region of about 700 amino acids distinguishes CDKL5. This region, which is without homology with other proteins, exerts regulatory functions on CDKL5 controlling its catalytic activity, subcellular localization and stability (116). CDKL5 is ubiquitously expressed but has a prominent expression in brain where highest levels are present in the cortex and hippocampus. The gene, although already transcribed during late embryogenesis, gets strongly induced in the early post-natal period and remains expressed throughout adult stages. CDKL5 is present in both the cytoplasm and the nucleus of expressing cells. Interestingly though, in neurons, CDKL5 is not dynamically cycling between these two compartments. In fact the nuclear accumulation of the kinase occurs only in some brain areas and only at post-natal stages. Moreover, certain neuronal stimuli, such as the activation of extrasynaptic NMDA receptors, cause a significant exclusion of the protein from the nuclear compartment and the prolonged activation induces CDKL5 degradation. It thus appears

that CDKL5 activities are subject to a tight control allowing the kinase to respond quickly to neuronal activity.

Generally, patients with mutations in CDKL5 have a severe developmental delay appearing soon after birth. They have severely impaired motor, language and hand function skills. Seizures are in general highly polymorphic with different seizure types occurring in the same patient and changing during the time. Complex partial seizures, infantile spasms, myoclonic generalized tonic-clonic, and tonic seizures were all reported. Patients may experience a seizure-free period, which is unluckily often followed by backslides. Dysmorphic features, such as prominent forehead, deep-set but large-appearing eyes, full lips and tapered fingers describe some females with CDKL5 mutations. The intense eye glance, the cold extremities, breathing anomalies, and microcephaly, in general common in RTT patients, may be absent in individuals with CDKL5 defects. Altogether, it has recently been proposed that CDKL5 associated disorder could be an independent clinical unit in accordance with the genetic heterogeneity underlying RTT and the early onset encephalopathy (117).

### **2.4.3. Congenital variant – FOXP1 mutations**

Mutations in MECP2 are rarely found in patients with the congenital variant. In 2008 mutations were identified in the Forkhead box G1 (FOXP1, OMIM 164874) gene, located on chromosome 14q2. It was found in two patients with congenital RTT and soon after in other patients (115). Presently, mutations in 26 patients have been identified. Initially, there was a bias towards screening for FOXP1 mutations mainly in females but mutations have been identified so far in 7 males. Based on the overall clinical picture of individuals with FOXP1 mutations, it has recently been suggested that is a distinct disorder, the FOXP1 syndrome can be recognized (119). This is further supported by the autosomal location of FOXP1, which contrasts the strong X-chromosome linkage of Rett syndrome. The characteristic features of the FOXP1 syndrome include post-natal growth deficiency and microcephaly. The patients suffer severe intellectual disability, deficient social interactions and communication, combined stereotypies and dyskinesias, epilepsy, and, often, repetitive protusive tongue movements. Seizures in individuals with FOXP1 deficiency appear to be complex partial, generalized tonic-clonic, or myoclonic and, differently from those associated with CDKL5 that can often be treated with anti-epileptic drugs. Importantly, brain

## **Introduction**

imaging studies have revealed simplified gyral pattern and reduced white matter volume in the frontal lobes, corpus callosum hypogenesis, and mild frontal pachyria. Patients with 14q2 duplications including FOXP1 have also been reported. The phenotype of these patients generally resembles that of patients with FOXP1 haploinsufficiency, but they are characterized by more severe seizures and normal head circumference compared to FOXP1 haploinsufficient patients.

### **2.5. Abnormalities and neuropathology in Rett syndrome patients**

The weight of the brain of RTT affected patient is significantly lower, when compared to the brain of age-matched healthy controls however the weight does not decrease significantly with age (120). The neurons are smaller and more densely packed resulting in a reduced brain volume. Moreover, decreased axonal and dendritic arborization and dendritic spine density are observed in hippocampal pyramidal neurons from *Mecp2*-null mice, demonstrating that the protein plays a significant role in regulating neuronal morphology.

The main alterations are related with prefrontal, posterior temporal and posterior occipital regions (121). Neuropathology was also observed in cerebrospinal fluid, included acetylcholine (122, 123), dopamine (124-126), serotonin (127, 128), glutamate (129, 130) or nerve growth factor (131, 132). Age of a patient and the severity of the symptoms influence the results. That is why reduced level of acetylcholine and cholinergic markers (120) are not the most consistent findings (122).

The levels of microtubule-associated protein 2 (MAP2) were also found to be reduced upon loss and gain of MeCP2 expression in accordance with the involvement of MeCP2 in shaping dendritic morphology. The imbalanced level of MeCP2 also affects synaptic connectivity since its loss tends to decrease the excitatory synapse number (133, 134).

#### **2.5.1. BDNF as a gene regulated by MeCP2**

BDNF is a large gene, containing a functional promoter with different activity preceding each of the identified four short 5' exons and one 3' exon encoding the mature BDNF protein (135). That produces a variety of mature mRNA. One of these, the promoter III

(135) (the analogous promoter in the mouse is the BDNF exon IV promoter, (136) is activated by calcium influx through L-type voltage-sensitive calcium channels. In the absence of calcium, the promoter is largely inactive. In particular, Tao and colleagues (137) demonstrated that CREB or a closely related protein mediates Ca<sup>2+</sup>-dependent regulation of BDNF. In cortical neurons, Ca<sup>2+</sup> influx triggers phosphorylation of CREB, which by binding to a critical Ca<sup>2+</sup> response element (CRE) within the BDNF gene activates BDNF transcription. In 2003 it was reported that BDNF regulates MeCP2 (16, 80). The result suggested that DNA methylation might be involved in repression of the promoter *in vivo*. It was confirmed by a direct analysis of CpG methylation in situ of exon IV promoter (136). Moreover chromatin immunoprecipitation experiments with cultured neurons revealed that MeCP2 was associated with the promoter IV (136) locus in the absence of stimulation. Histone modifications at BDNF locus were accompanied also by a loss of association with MeCP2. The model proposed by Chen and coworkers was saying that in absence of neuronal activity in WT cultured neurons, MeCP2 binds to the BDNF promoter and mediates its transcriptional repression. Membrane depolarization triggers the phosphorylation of MeCP2 at serine 421 (S421) through a CaMKII-dependent mechanism. It releases from the promoter, thus allowing transcription. It is important to note that the reduced cortical activity may lead to lack of activation of BDNF upregulation in the *Mecp2* mutant brain. However, it can be reverted by application of exogenous BDNF (138).

In 2007, it was further defined the role of MeCP2 in regulation of BDNF expression and neural function. In particular Deng et al., reported reduced BDNF gene expression in the frontal cortex of RTT patients (110). Next, Ogier and colleagues reported that under both depolarizing and nondepolarizing conditions, deficits in BDNF expression are particularly significant in the brainstem. That terse cranial sensory ganglia (NGs), which contains critical structures for cardiorespiratory homeostasis, and may be linked to the severe respiratory abnormalities characteristic for RTT (139).

### 2.5.2. The glucocorticoid hormone system in Rett syndrome

The mammalian response to stress is related to the interaction of the hypothalamus, pituitary and adrenal cortex, the hypothalamic-pituitary-adrenal axis (HPA) (140). Upon stress condition, parvocellular neurons of the hypothalamus exude the neuropeptide corticotropin-releasing hormone (CRH) to the portal vessel system. CRH binds to the

## Introduction

CRH1 receptor (CRHR1) in the anterior pituitary gland and induces the synthesis of pro-opiomelanocortin (POMC). POMC is a precursor polypeptide that undergoes post translational processing via cleavage through tissue-specific prohormone convertases and is converted into different bioactive peptides. In the pituitary gland, POMC is processed to melanotropin, involved in the production regulation of melanin, by melanotropic cells of the intermediate lobe while in the anterior part it is processed to adrenocorticotrophic hormone (ACTH). ACTH finally stimulates the adrenal cortex to secrete glucocorticoids (cortisol in humans, corticosterone in rodents) into the blood. Glucocorticoids can function in a fast, non genomic pathway, directly affecting excitability of cells in subfields of the hippocampus and via a genomic pathway that is slower and longer permanent (141). The genomic pathway of glucocorticoid hormones is mediated by receptor system make up of the glucocorticoid receptor (GR) and mineralocorticoid receptor (MR) which are co-expressed in the limbic system in brain. While MRs bind glucocorticoids with high affinity and are already occupied at low glucocorticoid levels, GRs, that are expressed ubiquitously in neurons and glia, have only one tenth of the affinity of MRs and become fully activated when glucocorticoid levels rise significantly (140).

Using microarray analysis of total RNA from symptomatic *Mecp2*<sup>-y</sup> and WT littermate control brains, eleven differentially expressed genes were found (106). Five of them are known to be regulated by glucocorticoids. Two of them, *Fkbp5* and *Sgk1* were studied in more details. Importantly, subsequent analysis of total brain RNA from pre symptomatic, early symptomatic and late symptomatic mice revealed that these genes are misregulated already before symptoms appear, thereby ruling out that the deregulation as a secondary symptom-regulated changes. Besides, no raised basal plasma glucocorticoid levels can provoke *Fkbp5* and *Sgk1* over-expression, detected in *Mecp2*<sup>-y</sup> mice. It could be that MeCP2 directly binds to GR independent sites of the *Fkbp5* and *Sgk1* promoters. Sum up, we have the evidence that MeCP2 works as a modulator of glucocorticoid inducible gene expression. The noxious effect of an excessive glucocorticoid-exposure lifted the possibility that disrupt MeCP2-dependent regulation of stress-responsive genes is contributing to the symptoms of RTT.

### 2.5.3. The role of oxidative damage in Rett syndrome

Reactive oxygen species (ROS) are the physiologic by-products of several biological processes. They are known as a being potentially damaging for the cells. Eukaryote evolved a comprehensive range of proteins to detoxify ROS and also repair oxidative damage related to DNA, lipids or proteins.

Already Dr. Rett indicated reduced ascorbic acid and glutathione in postmortem brain in RTT patient (142). It is also described that MeCP2 is implicated in cell commitment and maintenance in neurons by triggering senescence (143). Besides, neurotoxic activity is consequent to an excessive release of glutamate, what was reported in MeCP2-deficient microglia. Nevertheless, the direct link between MeCP2 and ROS was reported in 2004. Valinluck and colleagues have presented that oxidative damage is able to diminish the binding affinity of MBD of MeCP2 (144). This could suggest that oxidative damage to DNA can provoke epigenetic changes in chromatin organization. MeCP2 could be one of the end targets of a chain reaction process triggered by free radical species (145).

Additionally, several receptors and ion-channels are known to be redox-modulated (146). It is possible that described before mitochondrial (147) and redox changes (147, 148) in patients and animal models could link to the hyperactivity and diminished synaptic plasticity.

Moreover, the occurrence of biochemical signs of oxidative damage in brain antecedent the neurological symptoms may clarify the inconsistency of the apparently normal developmental phase (in latency period) before clinical onset in the RTT patients. Pharmacological therapies targeting antioxidants could create an opportunity for an early oxidative stress-modulating intervention during the preclinical window in RTT.

### 2.5.4. Neurotransmitter system in Rett syndrome – GABA and glutamate

The brain need to have a balance between excitatory and inhibitory neurotransmission to sustain proper neuronal function. Among the many central nervous system (CNS) neurotransmitters, biogenic amines and amino-acids are particularly important.

## Introduction

Two classes of neurons play the important role: the excitatory projecting neurons and their local inhibitory neighbours. In adulthood, excitation is mediated by the neurotransmitter glutamate while  $\gamma$ -aminobutyric acid (GABA) has an inhibitory effect. Dysfunctions in GABA neurons and GABA-regulated circuits have been implicated in several psychiatric and neurological diseases (149, 150), also in Rett syndrome (RTT).

Glutamate is the primary excitatory transmitter in the CNS. The lack of MeCP2 is related to structural and functional changes in the glutamatergic synapses. As a consequence is the reduction in various forms of short and long-term synaptic plasticity in *Mecp2* KO mice brains. The signaling between neurons and neurotoxic actions of glutamate emitted from glia are pointed to be one of the main reasons for onset and progression of the disease (86). Maliszewska-Cyna showed that mice lacking *Mecp2* display altered NMDA subunit distribution within glutamatergic synapses (151). NMDA receptors are key players of many forms of synaptic plasticity and are important in excitotoxic processes.

GABA is the major inhibitory neurotransmitter in the brain. Selective silencing of *Mecp2* in the GABA neurons was showing that *Mecp2* is crucial for their normal function (152, 153). Dysfunction of GABA signaling mediate some of the autism-like behaviours presented in RTT and also other RTT-like phenotypes including deficits in locomotor activity, or motor function and breathing patterns (Chao et al., 2010). Moreover, *Mecp2* differentially regulates the maturation of GABAergic synapses in excitatory and inhibitory neurons in the thalamus (153). In 2010 glutamatergic and GABAergic unbalanced neurons have been reported as a directly effect that develop Rett disease (154).

### 2.5.5. Neurotransmitter system in Rett syndrome – monoamines

Monoamines are another transmitter system that is affected in RTT disease. All of the amines: dopamine, noradrenaline and serotonin play important role in regulation of brainstem function. Also all of them in RTT patients were reported to be decreased (124, 125). One of the main function of biogenic amines is to facilitate the formation and maintenance of synapses in diverse regions of the central nervous system during development and also in adulthood (155). Dendrites are severely affected in different regions of the RTT brain. This reduction was also observed in *Mecp2* KO mice in

conjunction with reduced levels of the primary synthesizing enzyme tyrosine hydroxylase (Th) in the brain, peripheral neurons and the adrenal medulla (156-158).

Similarly abnormal levels of monoamine metabolites were found in the Cerebrospinal fluid (CSF) of RTT patients (126, 159).

Biogenic amines modulate a large number of autonomic and cognitive functions. Likewise, many of these functions are affected in RTT patients. Biogenic amines are the only neurotransmitters that have been frequently found to be altered in RTT patients. That is why it is so important to find pharmacological interventions with authorized drugs to compensate RTT patients for the discovered deficits (157).

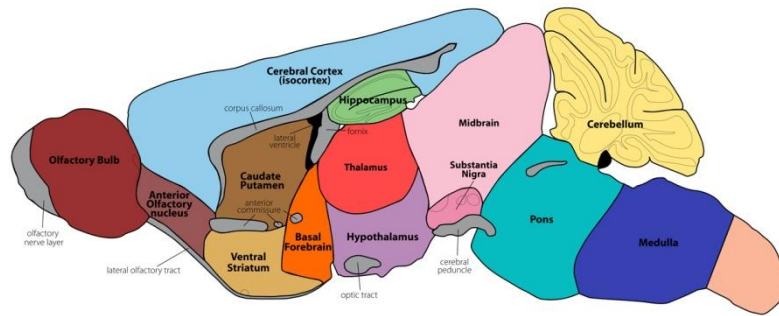
### **2.6. Animal models of Rett syndrome**

To advance the current knowledge of MECP2 role in brain development and to understand the molecular bases of RTT pathophysiology we use mice models. Mice models are helping to understand the mechanisms and pathology of many diseases by having similar structure to human brain (Figure 5). Several mouse model of Rett syndrome disease are developed (summary in table 3 in chronological order).

Among of many Rett mice models, three of them are widely used. Jaenisch model (91) utilized the cre-lox recombination system to delete the *Mecp2* exon 3. During first five weeks of age the mice have a normal development. After this period of time mice develop body trembling, breathing abnormalities, weight loss and most die at 10 weeks of age. They normally have smaller cortical neurons packed at a higher density and show reduced dendritic complexity in pyramidal neurons in the cortex (64), in the hippocampal CA3 region, and granule cells of the dentate gyrus (85).

# Introduction

A)



B)

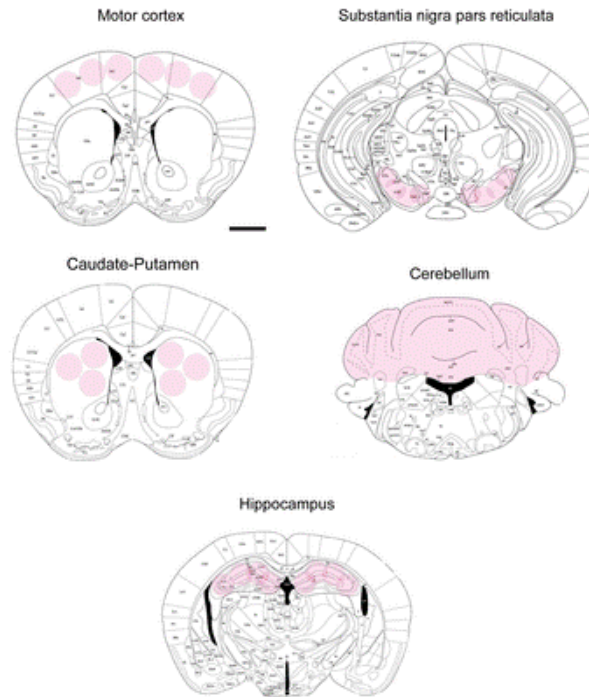


Figure 5. Schemes present detailed structure of the mouse brain. The scheme of mouse brain (A) and the drawings are adapted from GENSAT brain atlas and Mouse Brain in Stereotaxic Coordinates atlas. B) The pink areas mark sites where the brain tissue was dissected out for further analysis. The motor cortex (Distance from the Bregma, +1.18), caudate-putamen (+0.98), hippocampus (-1.94), substantia nigra pars reticulata (compacta) (-3.28), Cerebellum (-6.96) were micropunched. The selected regions were dissected. With Rodent Brain Slicer matrix, Zivic Instruments Scale bar, 2 mm.

Bird model, is related to deletion of exons 3 and 4 in embryonic stem cells to gain a complete null in terms of the Mecp2 protein (160). The males are without any symptoms till 3 to 4-5 weeks of age, but later develop uncoordinated gait, hindlimb claspings, irregular breathing and tremor. The progress of the symptoms is very fast, within weight loss and death at around 10-11 weeks of age. In comparison with males, female mouse live even 10 months, and the first symptoms appear around 3 months of age, irregular breathing pattern and decreased mobility included.

The Mecp2 308/y model (161) is a milder model generated by insertion of a truncating Mecp2 mutation. A stop codon, just after amino acid 308 produces a protein that is truncated yet retains the MBD, TRD domains and nuclear localization signal motif. Male mice have healthy development till 6 weeks of age, and after occur tremor, motor dysfunction, anxiety behaviour and stereotypic forelimb motions. This model has the longest life span, up to 10 months, and female have milder symptoms than seen in the null models. Mecp2 308/y mice displays milder symptoms and show impairments in hippocampal-dependent spatial memory (162). Moreover, these mice show hyperacetylation of histone H3, suggesting that MeCP2 dysfunction has an effect on the chromatin architecture.

Additionally, Collins and colleagues developed a mouse model (Mecp2Tg1) expressing MeCP2 at approximately 2 fold levels (163). At the same time Luikenhuis developed another mouse line overexpressing a Tau-MeCP2 fusion protein selectively in post-mitotic neurons from the Tau locus in homozygous - Tau knockout mice (164). Both transgenic models overexpressing MeCP2 show neurological phenotypes that are largely overlapping. The Mecp2Tg1 mice appear clinically normal until 10–12 weeks of age. After that period of time they start exhibiting symptoms such as motor dysfunctions and contextual learning and enhanced synaptic plasticity in the hippocampus. Later on, these mice develop seizures and become hypoactive and approximately 30% die by the age of 1 year (163). The phenotype associated with increased Mecp2 levels implies that Mecp2 is a dosage sensitive gene. Slight perturbations in its levels are deleterious for brain functioning in mice. Accordingly, in the last years in humans the MECP2 duplication syndrome has been recognized as a distinct clinical phenotype in males (165).

There is also a mouse model that has a 50 % of reduction of Mecp2 RNA and protein expression, Mecp2 Flox/y (166). Another described model has a deletion of MBD domain named Mecp2Tam (167). Next mouse model is missing Mecp2 in neurons of hypothalamus, called Sim1-cKO (168), or display a lack of Mecp2 in serotonergic

## Introduction

neurons (Pet-cKO; (169)). One more model displays no Mecp2 in catecholaminergic and noradrenergic neurons, named Th-cKO (169). Nestin-cKO do not have any Mecp2 in neurons and glia (91, 160), where CamKII-cKO mice present postnatal loss of Mecp2 in the forebrain (170). Researchers also bred two strains of genetically engineered mice in which GABA-releasing neurons lack MeCP2. In control mice, neurons that release GABA contain roughly twice as much MeCP2 as do neighboring cells. Binding to DNA, MeCP2 promotes the expression of two closely related enzymes, GAD1 and GAD67 that produce GABA. In the mutant mice, by contrast, these enzymes are expressed at lower levels, and their neurons produce about 30 to 40 percent less GABA than do control mice (154).

Most Rtt models are focused on global deletion or truncation of Mecp2 (91, 160, 161, 167, 171). Many behavioural studies in these models have revealed altered defects including motor dysfunctions, gait, paw stereotypies and swimming impairments. Majority of RTT mice models are also showing reduced exploration and altered plus and zero maze behaviour. The mice are showing fear conditioning and problems with object recognition (167, 171).

Besides, generally MECP2-deficient mice have smaller brain and impaired synaptic plasticity (163). Therefore RTT mice morphologically are similar to human patients. Mice have smaller cortical neurons packed at higher density than the WT littermates (64, 91, 171). Additionally pyramidal neurons in the cortex (64) and hippocampal CA3 region, and granule cells of the dentate gyrus show reduced dendritic complexity (85). Moreover, a disorganized olfactory neuropithreium indicates delayed terminal differentiation in Jaenisch mouse model (172). However, dendritic branching in layer III and IV pyramidal neurons of the frontal cortex mice were comparable to the control group (162). In the Bird model, 6 weeks old animals showed lower cortex spine density in pyramidal neurons compared to WT control (134). Generated granule cells in the dentate gyrus of 8 weeks old Jaenisch model showed impaired dendritic spine density and distribution (173). In heterozygous female mice, the onset of dendritic spine phenotype is delayed and more severe in Mecp2-lacking neurons than in Mecp2-expressing neurons. That is suggesting both cell autonomous and non-cell autonomous effects (174). The intensity of an abundant postsynaptic protein, PSD-95, was also reported to be lower in layer V pyramidal neurons of the motor cortex of Mecp2 -null mice (175). Because the pre-synaptic terminals are concerned, the motor cortex of Bird model mice displays defects in axonal fasciculation (174). On the top of that, the intensity of VGLUT1, a pre-synaptic marker, is lower in the dendritic region of the hippocampal CA1 region from Mecp2 KO mice, but the post-synaptic dendritic

marker MAP-2 did not show any difference between WT and Mecp2 KO groups. One of the reasons might be that Mecp2 deletion caused the reduction in the number of mature synapses in CA1 area, consistent with results from dissociated neuronal cultures (152). Mice lacking Mecp2 in neurons show overt RTT-like symptoms, whereas mice in which the expression of Mecp2 is driven in neurons alone are reported to show normal phenotype (164).

## Introduction

Mouse model	Genetic modifications	Phenotype	References
Mecp2 Jae	Deletion of exon 3 and partial of exon 4 – truncated Mecp2 protein	Neurological symptoms occur at 4 weeks of age, and death at 6-12 weeks	(91)
Mecp2 Bird	Deletion of exon 3 and 4 – Mecp2 KO mice	Neurological and behavioural symptoms at 5-6 weeks of age, short life span till +/- 10 weeks	(160)
Nestin-cKO	Mecp2 absent from neurons and glia (from embryonic stage)	Similar to null mice	(91, 160)
Mecp2 308/y	Truncation of Mecp2 protein at amino acid 308, maintenance of MBD and TRD	Progressive neurological symptoms, but with longer survival time, till 1 year	(161)
Mecp2 2Tg1	Human WT Mecp2 gene overexpressed in transgenic mice; the consequence of which Mecp2 is expressed two fold WT levels	Phenotype occurs at about 10 weeks of age. Enhanced motor skills and synaptic plasticity, at 20 weeks seizures develop and about 30% of mice die at 1 year	(163)
Tau-MeCP2	Overexpression microtubule-binding protein, Tau in postmitotic neurons, by introducing the cDNA into exon 1 of the tau gene in-frame with the endogenous start codon	Mice present decreased body weight, motor coordination deficits, heightened anxiety, and impairments in learning and memory that are accompanied by deficits in long-term potentiation and short-term synaptic plasticity	(164)
camKII-cKO	Mecp2 absent from forebrain (from postnatal stage)	Normal life span, but increased anxiety and abnormal social behaviour	(91, 170)
Mecp2 Tam	Deletion of MBD, Mecp2 KO mice	Very similar to Bird mouse model	(167)
Mecp2 Flox/y	Conditional “floxed” Mecp2 allele which mimics loss of function, 50% reduction of Mecp2 RNA and protein expression	Learning and motor deficits with respiratory problems	(166)
Sim1-cKO	Mecp2 absent from neurons of the hypothalamus	Normal life span, but increased aggression, heightened stress response and hyperphagia	(168)
Pet- cKO	Mecp2 absent from serotonergic neurons	Normal life span, increased aggression, reduced 5-HT expression	(169)
Th -cKO	Mecp2 absent in catecholaminergic and noradrenergic neurons	Normal life span, mild phenotype, but reduced ND/DA content as a measure by reduced of TH expression	(169)
GABA-KO	Mecp2 absent in GABA releasing neurons	Rett syndrome repetitive behaviours; reduction in glutamic acid decarboxylase 1 (Gad1) and 2 (Gad2) levels, and GABA immunoreactivity.	(154)

Table 3. Rett syndrome mouse models of Mecp2 deficiency and overexpression.

### **2.7. Therapeutic approaches and preclinical studies toward Rett syndrome**

The viability of neurons is not affected by MeCP2 mutations. Therefore, Rett is rather a neurodevelopmental than neurodegenerative disorder. This led the Bird lab to test whether re expression of *Mecp2* in symptomatic mice lacking *Mecp2* might be sufficient to rescue the RTT-like symptoms. Interestingly, several features of the disease such as general health condition, long-term potentiation (LTP) defects, and viability were restored (67), raising the possibility of a beneficial effect of gene therapy to increase MeCP2 levels in RTT individuals.

Two other studies demonstrated that restoring *Mecp2* in postmitotic neurons rescues the RTT-like phenotypes observed in *Mecp2*-deficient mice (67, 164). Even if these studies have provided evidence that RTT is a reversible condition, at least in mice, it is important to recall that neuronal functions are highly sensitive to MeCP2 levels and a gene therapy approach in humans must be well controlled to express MeCP2 at physiological level.

To understand whether the loss of MeCP2 in fully mature mice generate the same symptoms as the loss of the protein in early post-natal life, McGraw and colleagues developed an adult onset model of RTT by crossing mice harboring a floxed MeCP2 allele with mice carrying a tamoxifen-inducible CreER allele (176). These adult knockout mice after tamoxifen administration displayed hypoactivity, abnormal gait and hind-limb clasping, motor abnormalities, impaired nesting ability as well as impairment in learning and/or memory and finally they die. These studies suggest that the MeCP2 functions must be continuously maintained throughout the life for proper functioning of the brain (176).

Despite the complex physiopathology of Rett syndrome, RTT mice model have revealed essential information for the knowledge of the disease, being the most important the reversibility of symptoms. This key finding, although so far restricted to RTT animal models, when joined with the absence of neuronal degeneration, emphasizes the reversibility of the disease. This fact has stimulated the activity in exploring therapeutic approaches and importantly has given hope to RTT families. RTT therapeutic strategies are based in pharmacological intervention, environmental factors, gene therapy, and bone marrow transplantation.

## Introduction

### 2.7.1. Pharmacological intervention

According to the pharmacological intervention, RTT mice models have been treated with a range of drugs that impact over different neurological targets that are deregulated in RTT brain. These targets are related to BDNF, IGF1, neurotransmitters, corticosteroids, rho GTPases, antioxidants, and the readthrough of nonsense RTT mutations (Chronological summary in table 4).

As it was already mentioned, BDNF was one of the first described targets of MeCP2. It was found that *Mecp2* selectively binds to the BDNF promoter and directly regulates its expression. It is a neurotrophic factor, which plays a major role in neuronal survival, neurogenesis and plasticity. Mature BDNF is a 14 kDa protein unable to cross the Blood brain barrier (BBB). To overcome this problem it has been used BDNF-receptor agonists, such as TrkB agonists: 7,8-dihydroxyflavone (7,8-DHF) and LM22A-4, which rescues TrkB phosphorylation in the medulla and pons improving breathing abnormalities (177). Other drugs that increase BDNF levels are ampakines, the sphingosine-1 phosphate receptor modulator (fingolimod), and inhibitor of transglutaminase, such as Cysteamine. Ampakines, such as CX546 modulates neurotransmission in the brain by acting on glutamate AMPA receptors, ameliorating breathing patterns in *Mecp2* mutant mice (178). Fingolimod significantly improve motor behavioural tests and life span in a mouse model of RTT through activation of the MAPK downstream signaling pathways triggered by BDNF (178). Cysteamine shows improvement in life span and reduction of motor defects in *Mecp2* mutant mice (179).

The level of insulin-like growth factor 1 (IGF1) is low in the hippocampus of *Mecp2* mutant mice. Both, BDNF and IGF1 can directly activate PI3Akt pathway, but only IGF1 is able to cross the BBB. Based on this data, it has been shown that daily treatment with IGF1 three-peptide form, prolonged life span and improved motor functions in *Mecp2* mutant mice. Even breathing and heart rate were normalized in mutant mice (175).

At the morphological level, the lack of BDNF impacts upon the development of GABAergic neurons. Then, augmenting GABA levels with a selective GABA uptake inhibitor (N0-711) improves respiratory disorders. Moreover, chronic treatment of heterozygous female mice with N0-711 and serotonin 1a agonist completely correct breathing defects in this model (180). In the last months it was described that treatment with LP-211, a brain-penetrant selective 5-HT<sub>7</sub>R agonist, was able to rescue RTT-related defective performance related to anxiety-related profiles in a Light/Dark test, or memory in the Novelty Preference task (181).

The levels of biogenic amines, such as dopamine and norepinephrine are reduced in RTT. Norepinephrine plays a key role in maturation and modulation of the respiratory network. Besides, biogenic amines facilitate the formation and maintenance of synapses of the central nervous system in developing (155). Chiron and colleagues found also a low DRD2-receptor number in the brain of RTT girl (1993) what was described as a potential consequence of decreased number of spines (182).

Neuropathology was also found in the reduction neurons number in substantia nigra (SN) (183) and the Th immunoreactivity was also detected to be reduced (184). In 2003 an abnormal thinning of dendrites within the SN in RTT girls have also been described (185). An alteration of the dopaminergic metabolism is also involved in the abnormal motor movements, as well as the late motor deterioration that are observed in the classic form of RTT disease. In mouse models, neurological symptoms resulting from global MeCP2 deficiency are largely recapitulated by MeCP2 deficiencies in brain, or in neurons, indicating a neuronal basis for the development of RTT (164). As it was previously described not only in the RTT patients, also in the RTT model mice the levels of norepinephrine and dopamine are reduced (231) and deficiency of Th-expressing neurons was observed (158). A recent paper described a deficit in the MB (MB) catecholaminergic metabolism in *Mecp2* KO mice (169). The MB dopaminergic (mDA) area substantia nigra pars compacta (SNpc) regulates the elaboration of motor strategies (186) and dopaminergic deficit is also the reason of motor disabilities in Parkinson disease (187). Chuong Nguyen MV and colleague are showing that mature dendritic arbors of pyramidal neurons are severely retracted and dendritic spine density is dramatically reduced in the *Mecp2* KO mice (188).

It is already shown that a conditional loss of *Mecp2* in brain areas induce also motor impairments and dopaminergic deficits in SNpc of *Mecp2* KO mice. One of the pharmacological interventions was a chronic treatment with L-Dopa in *Mecp2* mutant mice, which has improved the motor deficits of these animals (189). Another study aimed at restoring proper synaptic function by treatment the mice with desipramine, a serotonin and a norepinephrine reuptake inhibitor. Injections of desipramine improved the respiratory rhythm over several weeks, and the life span of *Mecp2* mutant animals was prolonged (156, 190).

The CSF analysis performed in RTT patients showed reduced levels of homovanilic acid (HVA) and serotonin level (125, 191, 192). By targeting the pathway of acetylcholine some improvements can be shown. Using cerebrolysin in *Mecp2*-308 mice we have observed a recovery of dendritic arborization and neuronal damages,

## Introduction

and also some behavioural improvements were observed (193). Likewise, acetyl-L-carnitine improved grip strength, locomotor activity and cognitive function in *Mecp2* mutant Jaenisch mice (194-196).

Significant changes in specific glutamate receptors, including NMDA, have also been reported. One of the hypothesis was that neurotransmission is enhanced in the early stage of disease. Memantine, a NMDA receptor blocker partially reversed plasticity and synaptic transmission deficits in symptomatic *Mecp2* mutant mice (197).

Treatment with corticoids modulators is based in the finding that glucocorticoid hormone-induced genes *Sgk1* and *Fkbp5* are up-regulated in brain tissue of RTT mouse models, as well as the increased corticotropin-releasing hormone (*Crh*) gene expression. Corticoids have been tested in two studies in RTT mice with controversial results. Braun and colleagues (198) found that inhibition of the glucocorticoid system by the RU486 drug led to a significantly later onset of symptoms in male *Mecp2*-null mice. However, low and high-dose of corticosterone treatment at 3 weeks of age resulted in a significantly shorter lifespan of male *Mecp2*. On the contrary, when low doses of corticosterone are administrated in drinking water to the mother, so impacting very early in development, such as 1 week of age, RTT mice improve locomotor and exploratory behaviour (199).

Rho GTPases signaling has been also shown to be involved in the pathophysiology of Rett syndrome. RhoGTPases are central molecules in neuronal plasticity and cognition. It has been demonstrated that their activation by the bacterial cytotoxic necrotizing factor 1 (CNF1) enhances neurotransmission and synaptic plasticity in mouse brains. With the aim of evaluate the effects of CNF1 in RTT mice model, De Filippis (200) inoculated a single administration of intracerebroventricular CNF1 in the *MeCP2-308* hemizygous male mice. The results show that RTT mice improved all the behavioural tests and reversed astrocytic deficits.

Interestingly enough is also the link between ROS and RTT, Rett among of many authors indicated reduced ascorbic acid, and glutathione level in a postmortem brain tissue (142). The body of evidences that oxidative stress is a feature of Rett syndrome is been even increased recently. The current knowledge about OS and RTT has been accumulated with evidences in the deficits of the antioxidant defense system and excesses in ROS generation. It has been proved recently that vessels from heterozygous female mice show reduced endothelium-dependent relaxation due to a reduced NO and an increase ROS production. In the same study, treatment with curcumin reversed such as alteration restoring endothelial NO availability and

decreasing intravascular ROS generation (201). In 2013 the treatment with statins was also proposed, like the one that control the cholesterol homeostasis and improve life span and motor functions (202).

Since MECP2 has complex functions and mechanisms of action, different approaches have been already tested in mouse models. Pre-clinical evaluation of therapeutic approaches in RTT mouse models depends on many factors such a like timing, features, length of the treatment and next, effects of phenotype.

Nonsense mutations in MECP2 comprise a significant proportion of total mutations in Rett syndrome. Aminoglycosides, such as gentamicin, have been shown to readthrough nonsense mutations in several human genetic disorders. However its toxicity has compromised its clinical applicability. To overcome its toxicity, synthetic NB aminoglycosides has been developed, with better efficiency and reduced acute toxicity. These synthetic aminoglycosides has been tested in fibroblasts from RTT patients and *Mecp2*<sup>R168X</sup> mouse model with recovery of MECP2 full length expression (203). Although aminoglycosides have not been tested *in vivo* in model mice, they could be promising candidates for readthrough therapy for Rett syndrome patients.

### 2.7.2. Environmental factors

Another important factor is environment. It is known that exposure to an enriched and stimulating environment can delay the onset and progression of neurological signs in different disease models, such as Huntington, or Alzheimer diseases. The effect of environmental enrichment (EE) in RTT mice has been tested in three different studies finding that post-weaning EE improves motor coordination deficit in heterozygous females and BDNF protein levels (204). In this study, no effect was shown in *Mecp2*<sup>-/-</sup> males. In a subsequent study EE ameliorated motor coordination and motor learning by modifying excitatory and inhibitory synaptic density in cerebellum and cortex, reversing the cortical long-term potentiation deficit and augmenting cortical BDNF levels in males and females (205). EE provided subtle improvements in locomotor activity and contextual fear conditioning in the *Mecp2*(1lox) male mice (206). Overall, these results suggest that post-weaning EE may provide a non-invasive palliative treatment for RTT.

## **Introduction**

### **2.7.3. Gene therapy**

Already mentioned, the tamoxifen induction of MeCP2 gene expression reversed the phenotype in RTT model mice even when the onset of symptoms has been initiated (67). The demonstration of this reversibility in mice suggested that MECP2 gene replacement could be a potential therapy for patients. With this aim, it was achieved the administration of a neonatal intracranial injection of a single-stranded adeno-associated virus driving MeCP2 expression. The mice ameliorated life span, improved locomotor function, and exploratory activity, as well as the normalization of neuronal nuclear volume in transduced cells (207). However, when the vector was injected intravenously into 4–5 weeks old *Mecp2*-null mice, the brain transduction efficiency was low. 2–4% of neurons and modest improvements in survival were observed (208). These results suggest that MECP2 gene therapy could be possible but the delivery of virus vector should be improved intensively.

### **2.7.4. Bone marrow transplantation**

It has already been discussed in previous section that MeCP2 plays an important role in glia. Microglia, the brain-resident macrophages are of hematopoietic origin and have received increasing attention in the pathophysiology of several neurodegenerative and neuropsychiatric diseases. Derecki and colleagues analysed the role of the microglia in RTT by transplanting WT bone marrow into irradiation conditioned *Mecp2*-null mice resulting in the engraftment of brain parenchyma by bone marrow derived myeloid cells of microglial phenotype. Interestingly, the transplantation of WT MeCP2-expressing microglia attenuates numerous facets of disease pathology in *Mecp2*-null male and heterozygous female mice. Indeed, the targeted expression of MeCP2 in myeloid cells in an otherwise *Mecp2*-null background increased the lifespan, normalized the breathing patterns and improved locomotor activity. It restores the normal body weight whereas neurological symptoms remained unaltered (209). This effect was found to depend on the phagocytic capacity of the microglia. Based on these results it has been proposed that apoptotic debris accumulates over time in the *Mecp2*-null brain, contributing to neuronal malfunction and accelerating disease progression. Therefore, these observations suggest the importance of microglial phagocytic activity in Rett syndrome and finally it can be speculated that bone marrow transplantation might offer a feasible therapeutic approach for this disorder.

Name of the drug	Involved pathway	Effects on phenotype	RTT mouse model	References
Ampakine CX546	BDNF	increase in BDNF protein content, decrease of high breathing frequency episodes	Mecp2 mutant Jaenisch mice	(139)
Desipramine	BDNF	improves breathing and life span	Mecp2-null Bird mice	(156, 190)
Cerebrolysin	acetyl-choline	recovery of dendritic arborization and neuronal damages, behavioural improvements, neurotrophic effects	Mecp2-308 mice	(193)
IGF-1	growth hormone	prolongation of lifespan; amelioration of motor, breathing and cardiac function	Mecp2 mutant Jaenisch mice	(175)
NO-711	GABA	improves breathing	Mecp2-null Bird mice	(180)
Postnatal dietary choline supplementation	Acetylcholine	improved locomotor coordination, normalization of ChAT activity values in striatum	Mecp2 mutant Jaenisch and Mecp2-308 mice	(194, 195)
Acetyl-L-carnitine	Acetyl-choline	improves motors and cognitive functions	Mecp2 mutant Jaenisch mice	(196)
L-dopa	Dopamine	improvements of motor deficits	Mecp2-null Bird mice	(189)
Memantine	NMDA-receptors	Improvement of synaptic transmission	Mecp2-null Bird mice	(197)
Fingolimod	BDNF	Increase locomotor activity, reduction of hind-limb claspings and extension of lifespan	Mecp2-null Bird mice	(178)
LM22A-4	BDNF	improves breathing	Mecp2 mutant Jaenisch mice	(177)
7,8-DHF	BDNF	extension of lifespan, delayed weight loss, increase of voluntary locomotor activity and improvement of breathing pattern	Mecp2 mutant Jaenisch mice	(210)
Cysteamine	BDNF	improvement of lifespan and reduction of locomotor deficits	Mecp2-null Bird mice	(179)
RU-486	Glucocorticoids	improves life span and motor functions	Mecp2-null Bird Mecp2-mutant Jaenisch mice	(198)
Postnatal low doses of corticosterone	Glucocorticoids	restoration close to WT levels of locomotor/exploratory activity	Mecp2-308 mice	(199)
CNF-1	Rho GTPase	Improvement of locomotor activity	Mecp2-308 mice	(200)
Statins	Cholesterol homeostasis	improve life span and motor functions	Mecp2-null Bird mice	(202)
curcumin	Oxidative stress	normalization of vascular eNOS gene expression and endothelial NO availability, decrease of intravascular ROS production	Mecp2 mutant Jaenisch mice	(201)
LP-211	Serotonin	improves specific behavioural and molecular manifestations of RTT	Mecp2-308 mice	(181)

Table 4. *In vivo* preclinical drugs treatments in RTT mice models.

## Introduction

### 2.8. Clinical trials in patients with Rett syndrome

It should be high emphasized the value of pre clinical tests. Many clinical trials based on data obtained first in mice models. Previous and current clinical trials are summarized in table 5. One of the first clinical studies were already in 1990. That time Bromocriptine and Tyrosine/Tryptophan were tested in RTT girls, targeting the bioamine pathway. Bromocriptine acts as an agonist of dopamine receptor DRD2 and Tyrosine/Tryptophan as precursor of neuroreceptors. A few years later the acetylcholine pathway was touched by using L-Carnitine and cerebrolysin (211, 212). Creatine, Folinic acid alone or in combination with Betaine were the drugs that were targeting DNA methylation in RTT patients.

Following good results of the preclinical studies with mice, currently there are also two clinical trials related to the IGF1 treatment. IGF1 treatment is now in clinical phase II.

Some pharmaceutical companies are also performing clinical trials with RTT patients. Two anti- inflammation and anit-oxidant drugs called NNZ-2566 and EPI-743 are in clinical phase II.

Lately, it was shown that treatment with  $\omega$ -3 polyunsaturated fatty acids ( $\omega$ -3 PUFAs), well described antioxidant, could be promising for the patients (213). Authors showed a significant reduction in the clinical severity, such as motor-related signs, nonverbal communication deficits, and breathing abnormalities in the  $\omega$ -3 PUFAs supplemented patients. As well a significant decrease in OS markers was observed with no significant changes in the untreated group.

However, much work is required to find a good treatment for RTT syndrome disease. We should take into account the benefit of the many following and already described preclinical treatments with RTT mice models. Importantly there is much to be done in terms of indentifying and next validating the treatments in mouse model, as much similar to the patients as possible. Different mice models are giving us hope for dramatic change the therapeutic landscape for RTT disease, discovering new pathways and creating new drugs that will improve the lives of RTT patients.

Treatment	Target	Clinical phase	Treatment duration	Results	Reference
Bromocriptine	dopamine	6 girls	6 moths	some improvement in apneas and more regular sleep pattern	(214)
Tyrosine/tryptophan	neurotransmitters	11 girls, double blind	8-10 weeks	no improvement	(215)
L-carnitine	Acetyl-choline	35 girls, double-blind randomized, placebo	8 weeks	A few clinical improvements	(211)
L-carnitine	Acetyl-choline	21 girls, open label trial	6 moths	improves sleep efficiency, energy level and communication skills	(212)
Cerebrolysin	neurotrophic factor	9 girls	20-40 days	some motor and cortical improvement	(216)
Folate-betaine	DNA methylation	73 girls, double-blind randomized, placebo	1 year	no clinical improvement	(217)
Creatine	DNA methylation	21 girls, double-blind, randomized, placebo	6 months	not significant improvement	(218)
Folinic acid	DNA methylation	12 girls, double-blind randomized, placebo	1 year	did not ameliorate epilepsy	(219)
Folinic acid	DNA methylation	8 girls, double-blind randomized, placebo	1 year	not significant difference	(220)
PUFAs w-3	antioxidants	20 girls, single randomized, single blind	6 months	improve 50% the clinic score (CSS)	(213)
Fluoxetine	serotonine	6 girls		no improvements	Dr. Nadia Bahi-Buisson
Dextromethorphan	NMDA receptors	phase II	recruiting more RTT patients		Dr. Sakkubai Naidu
EPI-743	Oxidative stress	phase II		finished December 2013	Edison Pharmaceuticals Inc.
NNZ-2566	inflammation	phase II		finished in May 2014	Neuren Pharmaceuticals
IGF1	Growth hormone	phase I (12 girls)		cross BBB, tolerable, finished 2012	Dr. Omar Khawaja
IGF1	Growth hormone	phase II (12 girls)		recruiting more RTT patients, finished in July 2014	Dr. Walter Kaufmann

Table 5. Previous and current clinical trials with RTT patients.



## **Aim of the study**



### 3. Aims

No effective treatment of Rett syndrome is available. Mecp2 knockout mice have a range of physiological and neurological abnormalities that resemble the human syndrome and can be used as a model to evaluate new therapies. Studies of behavioural and molecular mechanisms leading to Rett syndrome phenotype in mice may impact on how therapeutics are designed and used. Then, it would allow us to select the most suitable Rett – preclinical drug therapy.

Furthermore, a difficulty in the analysis of mouse model occurs, because frequently different tests are used to verify the severity of specific phenotypes, rendering it difficult to compare different studies. That is why proper severity score and tests evaluation between WT and Mecp2 KO mice may facilitate a formal comparison of preclinical treatments with different drug classes.

Pathways which are altered in Rett syndrome, such as the neurotrophic factor BDNF, bioamines, acetylcholine, glutamate receptors NMDA and AMPA types, the neurotransmitter GABA and oxidative stress, could be therapeutic targets for preclinical assays first evaluated in Mecp2 KO mice.

The possibility to find new pathways involved in Rett syndrome is particularly important and may have relevant preclinical implications.

Hypotesis:

The main aim of this thesis is to perform preclinical evaluation of drugs that are known to target pathways which are altered in Rett syndrome. In our approach we use the Bird mouse model for Rett syndrome. It is also necessary to investigate new mechanisms associated with the development of Rett syndrome, aiming to find new pathways related to Rett phenotype that can be manipulated through the pharmacological approach.

## **Aim of the study**

Goals:

Determine tests that can reflect the difference at the behavioural and molecular levels between the Mecp2 KO and WT littermate mice.

Optimize study design protocol for evaluation of in vivo drug treatments.

Identify candidate drugs against selected targets in order to improve Rett disease, with the goal to reverse the symptoms, prolong the life span or ameliorate dysfunctions based on inflammation and neural mechanisms.

Determine the potential effects of novel therapeutic approaches for newly discovered pathways dysregulated in Rett syndrome.

## **Materials and methods**



#### 4.1. Primary and secondary antibodies

Antibody (dilution)	Company	Reference
Phospho-GSK-3 B (Ser9) (5B3) 1:1000	Cell signaling	9323
Phospho-GSK-3 (Tyr279/Tyr216) 1:500	Milipore	05-413
Phospho-NF-κB p65 (Ser468) 1:1000	Cell signaling	3039
Anti-GSK-3 beta antibody (M131) 1:1000	Abcam	ab31826
Anti-beta Catenin antibody (E247) 1:3000	Abcam	ab32572
PSD95 1:200	Cell signaling	2507
VGLUT1 1:500	Cell signaling	12331
Tyrosine Hydroxylase 1:1000	Cell signaling	2792
Phospho-Tyrosine Hydroxylase (Ser40) 1:1000	Cell signaling	2791

Table 6. Primary antibodies.

For immunofluorescence studies Anti-mouse Alexa 488/anti-rabbit Alexa 555 were used as secondary antibodies (BD Pharmingen).

For western blot analysis membranes were incubated with secondary antibody peroxidase-conjugated (Milipore).

#### 4.2 Oligonucleotide primers

	Forward	Reverse
<i>Drd2</i>	TGG ATC CAC TGA ACC TGT CC	TTG TAG TGG GGC CTG TCT G
<i>PPIA</i>	CAA ATG CTG GAC CAA ACA CAA	GTT CAT GCC TTC TTT CAC CTT
<i>RPL38</i>	AGG ATG CCA AGT CTG TCA AGA	CC TTG TCT GTG ATAACC AGG G

Table 7. Olinucleotide primers.

## Materials and methods

### 4.3 Experimental mouse model

Mecp2 KO animals are a well-established murine model that mimics RTT human disease (160). This model is an excellent tool for the study of the consequences of the loss of MeCP2 in neuronal and epigenetic functions. In order to perform *in vivo* studies we work on the B6.129P2(c)-Mecp2<sup>tm1.1Bird</sup> mouse model for RTT syndrome (160). All experiments were performed in the animal facility at IDIBELL biomedical centre (B9900010 registered by the Government and accredited by the AAALAC # 1155).

Males' homozygous KO for the MeCP2 gene derived from heterozygous female B6.129P2(C)-MeCP2<sup>tm1.1Bird</sup>/J mice purchase from the Jackson Laboratory is the final model that we use (MeCP2 + / -) B6.129P2 (C) MeCP2<sup>tm1.1Bird</sup> / J (Ref: 003890) (160) (<http://jaxmice.jax.org/strain/003890.html>).

The mutant strain was generated by replacing exons 3 and 4 of Mecp2 in embryonic stem cells with the same exons flanked by loxP sites. Homozygous Mecp2 lox/lox females were mated with WT males mice with ubiquitous Cre expression to bring about gene disruption. The offspring from the crosses of Mecp2<sup>+/-</sup> females with C57BL/6J males were genotyped by PCR. Mice were kept under specific pathogen-free conditions in accordance with the recommendations of the Federation of European Laboratory Animal Science Associations. Lighting conditions (lights on from 06:00 am to 6 pm) and temperature (22°C) were kept constant. Animals were allowed *ad libitum* access to food and water and were inspected every day.

In order to start preclinical drug evaluation, we establish the Mecp2 mice colony making 70 crosses, to get approximately 12 Mecp2 KO males weekly. Both pre-symptomatic and symptomatic mice were analysed at different developmental stages. Animals ranged in age from 4 to 10 weeks. For the pharmacological treatment, treated and untreated (vehicle) mice were studied. Moreover Mecp2-deficient treated and untreated mice were compared to their respective WT littermates. The Mecp2<sup>-/-</sup> (null male, called Mecp2 KO) and WT male mice were studied at 24, 55 and 70 postnatal days for molecular studies.

The KO male are normal at birth, seem to be like WT mice. They do not express MeCP2 gene product. The typical syndromes appear after 4 or 5 weeks. It can be observed some problems with mobility, breathing or even continuous trembling. Around 50% have problems with hunched posture or ungroomed coat. Even the adult males

## Materials and methods

have sperm in the caudal epididymis, they are rather alone, not internal and not too close to each other.

During the period of time the symptoms are more recognizable. The *Mecp2* KO mice also suffer weight loss and problems with spontaneous movement. An average lifetime is between 10 and 11 weeks. One of the typical symptoms of the phenotype is hind limb clasp in *Mecp2* KO male (representative pictures for *Mecp2* KO and WT animals in Figure 6). Tissue samples were obtained from *Mecp2*-null males (*Mecp2*<sup>-/-</sup>, KO) and their WT littermates. All mice procedures and experiments were approved by the Ethics Committee for Animal Experiments at IDIBELL Centre, under the guidelines of the Spanish law concerning animal welfare. Mice were euthanized in accordance with the Guidelines for Humane Endpoints for Animals Used in Biomedical Research. Tissues were frozen on dry ice immediately after removal and stored at -80°C until use.



Figure 6. Onset of hind limb clasp in *Mecp2* KO males. The left panel shows normal spreading of hindlimbs in WT at 7 weeks of age. Right panel represents hind limb-clasp phenotype in a mutant male aged 7 weeks.

### 4.4 DNA isolation and genotyping of MeCP2 mice - PCR procedure

DNA for Polymerase Chain Reaction (PCR) was isolated from mouse tails. Tails were put into eppendorf tubes containing 200  $\mu$ l of 100mM NaOH and incubated 10 min at 96°C. After incubation tubes were spun down at 3000g for 30 min at RT. Supernatants were transferred to new eppendorf tubes and 500  $\mu$ l of isopropanol was added to each

## Materials and methods

tube for DNA precipitation. Tubes were vortexed and centrifuged for 15 min at 3000g, RT. Supernatants were discarded, 100 µl of TE buffer was added to each tube and dry DNA pellets were dissolved at 37°C. PCR products were visualized in 2% agarose gels. 0.5X TAE was used as a gel electrophoresis buffer. Gel electrophoresis was carried out at 100-120V using a PowerPac basic power supply (Bio-Rad). Samples were visualized using the Q-Box equipment and GeneSys automatic software.

### Screening of Mecp2 KO mice by PCR

Females MeCP2 + / - are paired with C57BL/6J males and their offspring is genotyped by chain reaction PCR with the following primers:

Mecp2\_WT\_F GACCCCTTGGGACTGAAGTT

Mecp2\_KO\_F CCATGCGATAAGCTTGATGA

Mecp2\_Rev CCACCCTCCAGTTTGGTTTA

(primers adapted from (221)).

Each PCR screening contains 4 control samples (negative control: H<sub>2</sub>O and 3 positive controls: DNA from WT, KO and HZ mice). 1 ul of DNA sample was added to 19 ul of PCR mix and 35 cycles of PCR were performed as described in tables 8 and 9.

PCR step	temp	time
preheating	95°C	10min
35 cycles		
denaturation	95°C	30s
annealing	72°C	40s
amplification	72°C	7min

Table 8. PCR procedure

19 µl PCR mix:	
H <sub>2</sub> O	13.54 µl
10 x PCR buffer	2 µl
Primer_WT_F (10 uM)	0.4 µl
Primer_KO_F (10 uM )	0.8 µl
Primer_Rev (10uM)	0.8 µl
MgCL2 (50mM)	1.2 µl
D NTP (25Mm)	0.16 µl
Taq polymerase	0.1 µl

Table 9. PCR mix

### 4.5 Phenotyping of MeCP2 mice - detailed neurological score test

Progression of the RTT phenotype was monitored by scoring test. Animals were scored twice a week by a 3 point system created by Guy and co-workers (67). Score tests were performed in the same room, the same days of the week (Tuesdays and Fridays), at the same time of a day. Animals were also weighed during each score test. We focus on mobility, gait, hindlimb clasp, tremor, breathing and general condition. Each of the 6 symptoms will be scored from 0 to 2 to give semi-quantitative measurement of RTT-like phenotype.

0 - absent or the same as in the WT

1 - when the symptom is present

2 - when the symptom is severe

Criteria to perform score experiments according to:

1. Mobility: The mouse is observed when placed on the bench, then when handled gently. 0 = as WT. 1 = reduced movement when compared to wild-type: extended freezing period when first placed on the bench and longer periods spent immobile. 2 = no spontaneous movement when placed on the bench; mouse can move in response to a gentle prod or a food pellet placed nearby. (Note: mice may become more active when in their own cage environment).

2. Gait: 0 = as WT. 1 = hind legs are spread wider than WT when walking or running with reduced pelvic elevation, resulting in a "waddling" gait. 2 = more severe abnormalities: tremor when feet are lifted, walks backwards or 'bunny hops' by lifting both rear feet at once.

3. Hindlimb clasp: Mouse observed when suspended by holding the base of the tail. 0 = legs splayed outwards. 1 = hindlimbs are drawn towards each other (without touching) or one leg is drawn in to the body. 2 = both legs are pulled in tightly, either touching each other or touching the body.

4. Tremor: Mouse observed while standing on the flat palm of the hand. 0 = no tremor. 1 = intermittent mild tremor. 2 = continuous tremor or intermittent violent tremor.

## Materials and methods

5. Breathing: Movement of flanks observed while the animal is still standing. 0 = normal breathing. 1 = periods of regular breathing interspersed with short periods of more rapid breathing or with pauses in breathing. 2 = very irregular breathing - gasping or panting.

6. General condition: Mouse observed for indicators of general well-being such as coat condition, eyes, body stance. 0 = clean shiny coat, clear eyes, normal stance. 1 = eyes dull, coat dull/ungroomed, somewhat hunched stance. 2 = eyes crusted or narrowed, piloerection, hunched posture.

Each category was scored and the digits totalled to give an aggregate number that could be displayed graphically (e.g., 112010 = 5) and used to express overall phenotype.

When an animal score is 2 for two from the last three criteria, the animal is killed. Moreover, if a mouse loses 20% of its body weight during the experiment, it is sacrificed. The maximum score is 12.

### 4.6. Pharmacological treatments

L-Dopa and Ddc1 treatment:

Mecp2 KO mice received either L-Dopa alone at a concentration of 30 mg/kg/day, Ddc1 alone at a concentration of 12 mg/kg/day, or a combination of a chronic intraperitoneal (i.p.) injection of Ddc1 at a concentration of 12mg/kg/day (Benserazide, B7283) followed by an L-Dopa injection after 15 minutes (Sigma-Aldrich; D1507) at a concentration of 30 mg/kg/day, all diluted in saline. The dosage was selected on the basis of its ability to induce a major effect on DA metabolism.

SB216763 treatment:

Mecp2 KO mice received daily either an intraperitoneal (i.p.) injection of vehicle (20% dimethylsulfoxide (DMSO) /saline) or SB216763 treatment at a concentration of 0.5 mg/kg (Selleckchem; Catalog No.S1075, diluted in DMSO 20%).

### 4.7. Tissue fixation

After the mouse anesthesia, the incision was made just below the sternum to reveal the rib cage and abdominal muscles. The muscle layer is cut to expose the diaphragm, which was cut away from the ribs cage, and the ribs themselves were cut through laterally in order to allow the ventral portion of the rib cage to be folded back, revealing the heart. A G21 needle (medicor neomed) was connected with peristaltic pump, and next inserted into the apex of the heart and fed into the left ventricle. Once the needle was secured in place, the right atrium was punctured and mouse was perfused at a constant pressure (speed between 42 and 48) with PBS solution. PBS wash lasts until the liver has been cleaned of blood and it is lighten in colour. Next step was perfusion with 4% paraformaldehyde until the animal was rigid and tissues were drained in colour.

Next step was to remove the fur and the skin from the head. The skull was removed to expose the brain. The upper few vertebrae were cut open to expose a small amount of the spinal cord and cutting continued toward the head until junction where the brain stem met the spinal cord. Brain tissue was put into the post-fix solution, 4% paraformaldehyde overnight (ON). The following day, tissues were put in 30% sucrose, to remove any excess of water and prevent ice crystals of artefacts forming when frozen sections were cut from the brain. After dehydration step the tissue is placed into the OCT solution, and then cut in coronal sections (by Rodent Brain Slicer matrix, Zivic instruments, based on <http://mouse.brain-map.org/agea>). Tissue slides were cut at 25 microns thick at -22 °C using the cryostat. Sections were collected into 24 well plates with 1ml PBS/well, next divided into proper groups of free floating sections in small glass vials.

### 4.8. Hematoxylin-eosin staining

Liver histological sections were stained with hematoxylin-eosin (HE) in order to study the toxicity aspects. Liver samples fixed in buffered 4% formaldehyde were embedded in paraffin, cut in 5µm sections and stained with HE. The slides were placed in hematoxylin dye for five minutes. Next they were dipped in acid alcohol for three times, each time taking approximately one second. All the slides were placed in eosin and left there for one minute. Next, the washing was done for a short period since eosin is a water soluble dye which can easily be carried away. After the rinsing with tap water, the

## **Materials and methods**

slides were quickly rinsed again with 70% ethanol and finally with 100% of ethanol. The slides were then placed in Xylene. Finally the mounting medium was added and a cover slip was placed on the slide.

### **4.9. Dopamine assay**

For the determination of Dopamine levels in brain regions, the Mouse Dopamine Elisa Kit was used (Blue Gene, Cat. E03D0043, Shanghai, China). Briefly, mice were sacrificed at 8 weeks of age and brain regions were dissected and snap-frozen. Samples were weighed and homogenized in presence of saline solution (20 ul/mg tissue). The resulting suspension was then sonicated and centrifuged to remove insoluble material. The samples were diluted and assayed according to the manufacturer protocol. The final dopamine concentration for each sample was normalized with the respective total protein amount.

### **4.10. RNA isolation, cDNA synthesis and qPCR analysis**

Frozen tissue brain was ground into powder with mortar and pestle, and resuspended in Trizol reagent (Life technologies, CA). The RNA purification was performed from the RNA-containing aqueous phase with RNeasy mini kit (Qiagen). DNA was removed with Turbo DNase (Ambion). cDNA synthesis was performed with 2 µg total RNA and random hexamers primers using the ThermoScript reverse-transcriptase (Life technologies). A negative sample (no ThermoScript enzyme) was performed to exclude DNA contamination. Primers for the reaction were designed according to Primer3 software and tested with a cDNA serial dilution to check amplification linearity and unique amplification product. PPIA and RPL38 were used as house-keeping genes for normalization. 50 ng cDNA were used for each PCR reaction together with 5 ul 2X SYBR green PCR master mix (Life technologies), 250 nM of each primer and water up to 10 ul. Data were analysed using Qbase (Biogazelle). Primers are summarized in Table 7.

### 4.11. Immunofluorescence analysis

The brain's regions were identified using AGEA Allen Brain Atlas Mouse. All the steps of the immunostaining were realized in free-floating solution. All tissues were permeabilized and blocked with 0,2% Triton X-100, 20 % goat serum /PBS for 1 hour at RT, and incubated with the appropriate primary antibodies in 0,2% Triton X-100, 2 % goat serum /PBS ON at 4°C (Table 6). Anti mouse Alexa 488/ anti rabbit Alexa 555 were used as secondary antibodies. DAPI (4,6-diamino-2-phenolindol dihydrochloride) counterstaining was performed in all experiments in order to visualize the nucleus, after staining coverslips were mounted in Mowiol (Callbiochem).

The single and double-labeled images were acquired using a Leica TCS SP5 Spectral Confocal microscope (Leica, Milton Keynes, UK; Magnification: HCX PL APO lambda blue 63X oil -numerical aperture-NA:1.4 and resolution of 1024x1024; Acquisition Software: Leica Application suite Advanced Fluorescence – LAS AF, version 2.6.0.7266). Z project and Tile were realized in order to get all staining with both antibodies. Densitometric analysis of the staining level was performed on 8-bit images using ImageJ Fiji vs 1.47 software (<http://rsb.info.nih.gov>). The integrated density was calculated as the sum of the pixels values in the region of interest. We realized pictures from different slices in the same region and then calculated the average of the successive impaired sections for each animal in each experimental group (total five).

### 4.12. Western blot analysis

For western blotting, animals were killed 4 weeks after the first treatment (at 8 weeks of age) and the selected area of the brain region was rapidly removed and cut with a Rodent Brain Slicer matrix (Zivic Instruments; 2 mm sections). Total protein extract was obtained with lysis buffer (20 mM Tris-HCl, pH 7.5, 150 mM NaCl, 2 mM EGTA, 0.1% Triton X-100 and complete protease inhibitor and phosphatase inhibitor cocktail tablet from Sigma and Roche respectively) sonicated and denatured for 10 minutes at 95°C. Protein concentrations were determined using the BCA (Pierce BCA Protein Assay kit). 25 µg of each protein sample was separated on a 10% SDS-polyacrylamide gel, by sodium dodecyl sulfate electrophoresis, and transferred onto a PVDF membrane (Immobilon-P, Millipore) by liquid electroblotting (Mini Trans-Blot Cell, Bio-Rad) for 1 h at 100 V (222). The membrane was blocked in 5% nonfat dry milk in TBS-0.1% Tween

## Materials and methods

20, for 1 h at RT. Membranes with selected antibodies were incubated ON at 4°C (Table 6). Appropriate secondary antibody conjugated to peroxidase was incubated for 1 hour at RT. Finally, the specific reaction was detected with a chemiluminescence reagent kit (Supersignal West Pico chemiluminiscent, Thermo Scientific). Digital images were processed with a GS-800 Calibrated Densitometer (BIORAD). Bands were quantified with BIORAD Quantity One software. In all cases, images correspond to the results of one representative experiment out of three.  $\beta$ -Actin was used as loading control.

### 4.13. Golgi staining

Golgi staining was used to study the neuronal morphologies (FD Rapid GolgiStain™ Kit, FD Neurotechnologies; INC). The animals were anesthetized as described above. The brains were extracted and the protocol was performed according to the manufacturer instructions. Three brains from each group were dissected into coronal pieces of 2mm (Rodent Brain Slicer matrix, Zivic instruments), mounted in freezing medium (TFM, TRIANGLE BIOMEDICAL) and stored at -80 °C. Sections between 80-100  $\mu$ m were cut using a cryostat and mounted on gelatin-coated microscope slides with solution C. We proceeded with the staining protocols by following the instructions included in the manual. Between 10 and 15 neurons of the hippocampus zone were analysed from 2 or 3 different animals of each of the group. Images of dendritic spines were acquired with Zeiss Axio Observer Z1 with Apotome microscope (magnification: Plan-APOCHROMAT; 63X oil Dic NA. 1.4; Acquisition Software: ZEN 2011). Three-dimensional reconstructions were done by using the NeuronStudio software for image processing in order to enable higher identification and to improve the quality of spine analysis (223, 224). Dendritic Spines were counted with Sholl analysis along 20  $\mu$ m with centric circles of 10  $\mu$ m (225).

### 4.14. Glutathione (GSH) Assay

Glutathione Assay Kit (Bio Vision, Catalog #K264-100 kit; Milpitas, California, USA) was used for the determination of total glutathione (GSx), reduced (GSH), and oxidized (GSSG). At eight and ten weeks of age, the mice were killed, and the MidBrain (MB) area with the weight of +/- 40 mg was rapidly removed from the brain by Rodent Brain

## Materials and methods

Slicer matrix, Zivic instruments. Brain tissues were washed in 0.9% NaCl solution and homogenized on ice with 100 µl of ice cold Glutathione Assay Buffer. 60 µl of each homogenate was placed into a tube containing 20 µl of cold Perchloric Acid (PCA) and vortexed several seconds to achieve a uniform emulsion. Next, the samples were centrifuged and the supernatant (containing glutathione) was collected. 20 µl of ice cold KOH was added to 40 µl of PCA preserved samples to precipitate the PCA and neutralize the samples. In order to detect the GSH we add assay buffer, a final volume of 90 µl. To obtain the GSx, 70 µl of assay buffer was added to 10 µl of each sample with 10 µl of Reducing Agent Mix to convert GSSG to GSH. To get the results of GSSG, to the 60 µl of assay buffer and 10 µl of sample, 10 µl of GSH Quencher was added to quench GSH. After 10 min of RT incubation 10 µl of Reducing Agent Mix was added to destroy the excess GSH Quencher and convert GSSG to GSH. Next, after 10 min of RT incubation 10 µl of o-phthalaldehyde (OPA) probe was added to all samples. All samples were incubated at RT, in the dark for at least 30 min. The fluorescence was read at Ex/Em = 340/420 nm (73).

### 4.15. Behavioural tests

We examined Mecp2 KO and WT (both groups 8-9 weeks old) in the open field, Y-maze, bar cross, grip strength, and corner tests to determine if they exhibited genotype differences in mobility and anxiety-related behaviour. Before the drug treatment evaluation, for each of the test we set up the baseline between WT and Mecp2 KO animals in order to reduce the variability and check if the test is sensitive enough to prove that our treatment is working. For the final experiments, treated, untreated Mecp2 KO mice, and control mice (WT) were tested during same sessions to minimize the variability.

#### 4.15.1. The horizontal bar cross test

The bar cross test was carried out using a wooden bar of 100 cm in length and 2 cm in width (diameter). This bar was wide enough for mice to stand on with their hind feet hanging over the edge such that any slight lateral misstep will result in a slip. The bar was elevated 50 cm from the bench surface, so that animals did not jump off, and were not injured upon falling from the bar. The mice were put on one end of the bar and

## **Materials and methods**

expected to cross to the other end. To eliminate the novelty of the task as a source of slips, all animals were given 4 trials on the bar the day before and 2 trials at the beginning of the testing session. In an experimental session, the number of hind limb lateral slips and falls from the bar was counted on 3 consecutive trials. If an animal felt, it was placed back on the bar at the point at which it felt and was allowed to complete the task.

### **4.15.2. Open field testing**

The Open field testing (OFT) is one of the most common test to measure exploratory, behaviour and global activity in mice and rats (226). Distance moved, time spent moving, rearings, change in activity over time are among of others many parameters that can be evaluated by OFT. Some outcomes, particularly defecation, center time and activity, within the first 5 minutes, likely gauge some aspects of anxiety-like and fear-related behaviour. Additionally, OFT is also commonly used for toxicity measurement after compound's treatments.

Mecp2 KO mice were tested for novelty-induced exploratory activities and mobility in general using an OFT. The OFT consisted of a white woodwork 40 cmx40 cm square arena surrounded by 50 cm high wall. The floor of the OFT was divided into 16 equal squares, considering the 4 squares at the centre as the central area and the rest as the periphery. Mice were individually tested during 5minutes session. Animals were placed at the centre of the OFT and the latency to the first exit from the central area was measured. Also the square crossings, rearing frequency, freezing episodes, visited corners and defecation boluses were quantified. The apparatus was cleaned with ethanol after each animal and the test was carried out under 340 lux.

### **4.15.3. Test of neophobia to a new home cage**

The corner test is a sensor motor functional assessment. Animals were gently placed in the center of the standard cage (measures, 20 lux) containing bedding. The number of visited corners and rearings were recorded during 30s. New bedding was used for each animal.

### 4.15.4. Wire Grip test

Wire grip test is an easy way to objectively quantify the muscular strength of mice, and to assess the effect of drugs. It is a very common test used for evaluation of neurodegenerative diseases on muscular degeneration. It is based on the natural tendency of the mouse to grasp a bar or grid when it is suspended by the tail. During this test the mouse grips with both forelimbs (or hind-limbs) a single bar or a mesh. The model of *Mecp2* KO mice has a problem with hind limb clasping.

The wire grip test was used to assess whole body force, grip strength and limb coordination. The mice were allowed to grasp by the two front paws a 2 mm diameter metal wire maintained horizontally 40 cm above a thick layer of soft bedding. The wire was 40 cm in length and divided into 8 segments of 5 cm. The animal was placed in the centre of the wire and the latency to fall from the wire and the segments crossed were recorded. Animals performed 3 trials: two first trials of 5 seconds (adaptation) and a third trial of 1 min (final score). After each fall, the mice were allowed to recover for 1 min.

### 4.15.5. Y-Maze Spontaneous Alternation test

The apparatus is consisted in a Y-shaped maze made of plastic, with three light-gray and opaque arms, at 120° angle from each other (Figure 7). We performed the spontaneous alternation version of the Y-maze. The animal was introduced in the centre of the maze and it was allowed to freely explore the three arms during 5 min. During the experiment we count the number of rearings, arms entered, as well as the sequence of entries, to determine the alternation rate (degree of arm entries without repetitions). The number of arms entries and triads are recorded in order to calculate the percentage of alternation, which is used to quantify cognitive deficits in rodents. An entry occurs when all four limbs are within the arm. Rodents typically prefer to explore a new arm of the maze rather than returning to one that was previously visited. However, since it is already described *Mecp2* KO mice are presenting rather heightened anxiety like behaviour (108, 227). The Y-maze was cleaned with ethanol after each animal tested.

## Materials and methods

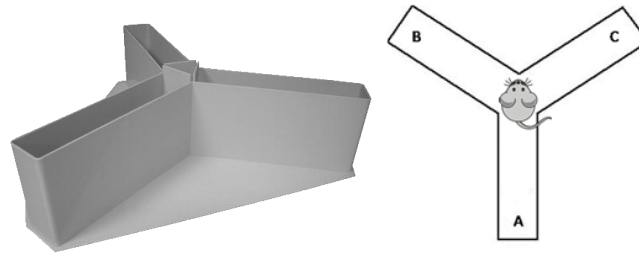


Figure 7. Y maze instrument (BioSeb)

### 4.16. Statistical analysis

The data obtained between WT and KO animals in the initial experiments were performed using unpaired Student t test. Comparisons between different treatments groups, including Score data, bar cross, Glutathione Assay, Immunofluorescence, qPCR analysis, Golgi staining and Western blots experiments were performed using one-way ANOVA with Bonferroni's Multiple Comparison post hoc test for intergroup comparisons. All results were analysed by the GraphPad 5.04 prism software. For the life span data we plotted Kaplan-Meier survival curves. Results were considered significant if the p-value was  $< 0.05$  (\*),  $< 0.01$  (\*\*) or  $< 0.001$  (\*\*\*). Data are presented as the mean  $\pm$  SEM (standard error of the mean).

## Results



## 5.1. Part 1 Evaluation of molecular and behavioural tests to estimate therapeutic effects of pharmacological treatments in *Mecp2* KO mice

### 5.1.1. Analysis of genotypes in *Mecp2* KO mice colony by PCR

In order to investigate the pharmacological treatment for RTT, we used *Mecp2* KO mice. The PCR was performed to discriminate mice between *Mecp2* KO, WT and HZ.

Tail samples from all mice were collected. Genomic DNA was extracted and subjected to the previously described protocol in material and methods section. 3 set of primers were used to amplify a 415 bp kb WT - product and a 450 bp kb KO - product. In HZ mice both bands were present. Agarose gel electrophoreses was used to identify each mouse genotype (Figure 8).

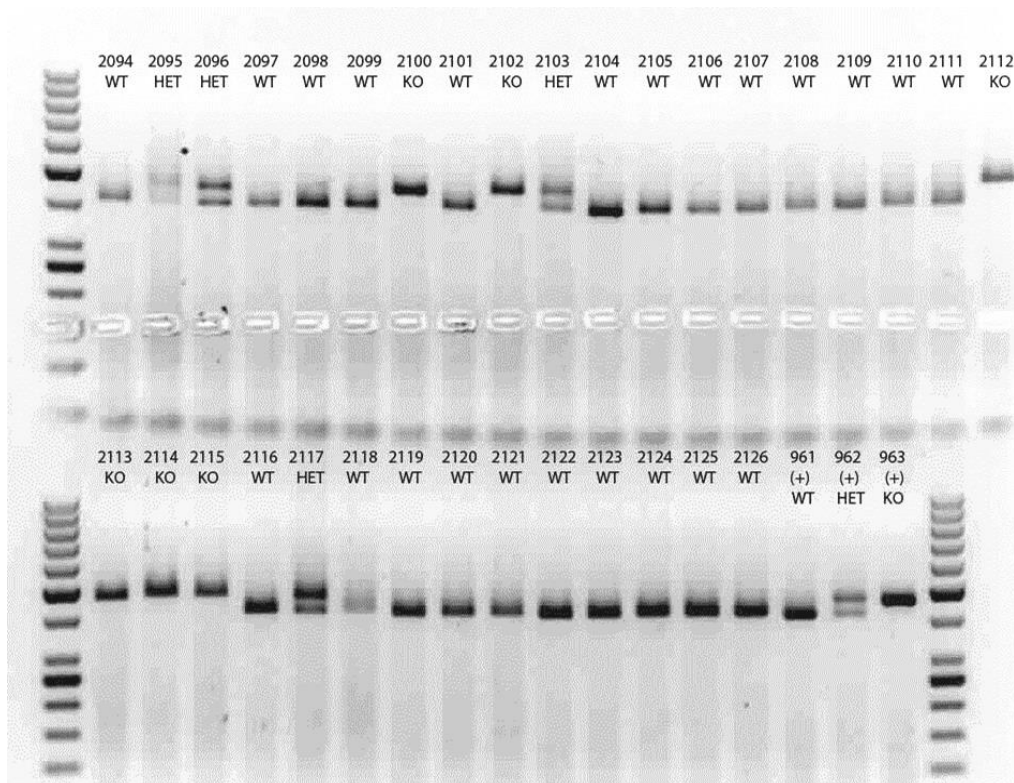


Figure 8. PCR identification of mice genotype. Representative image of agarose gel showing the PCR verification of mouse genotype. Numbers from 2094 to 2126 represented mice from littermate colonies. Last 3 samples (from the left: WT, HZ and *Mecp2* KO) were used as controls.

## Results Part 1

Based on this analysis it was possible to divide mice into 3 groups. One of the group consisted of WT mice (numbers: 2094, 2097-2099, 2101, 2104-2111, 2116, 2118-2126), the second one of Mecp2 KO mice (numbers: 2100, 2102, 2112-2115), and all the remaining mice were classified as HZ.

### 5.1.2. Pharmacological approaches for RTT mice model assessed in this thesis

During the thesis I was trying to identify potential new therapies for Rett syndrome, with the main focus on preclinical studies in an animal model of Rett disease.

We have focused on the main targets that are known to be altered in Rett syndrome, including BDNF, glucocorticoids, the bioamines Dopamine, Serotonin, glutamate receptors NMDA, AMPA types, and the neurotransmitter GABA. I have also tried epigenetic and oxidative stress drugs. Lately, it was proposed a new target for Rett treatment, glycogen synthase kinase 3 (GSK-3).

Following the Drug Bank and data retrieved from the Spanish Agency for Medicine and Health Product, we selected classes of drugs targeting pathways and processes which are deregulated in Rett syndrome. At least one compound from each group of drugs was used for *in vivo* experiments. Some of the tested drugs have already been used clinically in human diseases. The availability of pharmacokinetic information allowed us to better control the drug safety and facilitated monitoring of possible side effects. The list of selected drugs evaluated in the course of this thesis is presented in Table below (Table 10).

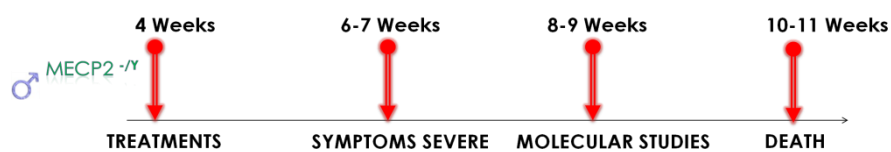
pathway	name of the drug
BDNF	Copaxone Cysteamine
Glucocorticoids	Dexamethasone
Dopamine	L-Dopa/Ddci Ropinirole L-DOPA
Serotonin	Bromperidol
GABA	Gabapentin
GSK-3	SB-216763 TDZD-8
Oxidative stress	Vitamins C+E Coenzyme Q10 Resveratrol DIDS
Epigenetics drugs	AZA (VIDAZA) SAHA (Vorinostat) Sodium phenylbutyrate (NaPB) Trichostatin A (TSA) Entinostat (MS-275)

Table 10. Pharmacological approaches in RTT in preclinical studies with Mecp2 KO mice

### 5.1.3. Treatment strategies and standard treatment protocol of used drugs in this thesis

Following the guidelines proposed by the National Centre for the Replacement, Refinement and Reduction of Animals, and guide related to preclinical research in Rett disease (228, 229), we tried to use only necessary number of animals. All selected treatments started when the animals were 4 weeks of age. At that time it was still not possible to observe characteristic symptoms of this model. All studies were performed on the B6.129P2(c)-Mecp2<sup>tm1+1</sup>Bird mice (160). For each pharmacological treatment, treated and untreated (vehicle) mice were studied. Treated and untreated Mecp2 KO mice were compared to their respective WT littermates. In order to evaluate the treatment an optimized timeline and standard procedure were obtained in the lab and next followed for all tested drugs (Table 11).

## Results Part 1



### Study protocol

1. Genotyping the mice
2. Distribution in three groups; WT, vehicle and treated group
3. Gender and litter matching
4. Dose optimization
5. Randomized and phenotypically blind studies
6. Survival curve
7. Selection of the most responding dose
8. Phenotypic score
9. Behavioural test:
  - a) bar cross
  - b) grip strength
  - c) open field
  - d) neophobia test
  - e) Y-maze
10. Neuronal phenotype:
  - a) sholl analysis
  - b) pre- and postsynaptic markers
  - c) oxidative stress measurements
11. Target-specific test for determination of drug activity

Table 11. Standardized time line and procedure obtained for all tested drug *in vivo*.

#### 5.1.4. Phenotypic scoring of Mecp2 KO mice

During the time the progression of typical symptoms for Rett disease is clear. The weight, total symptom score and average life span of Mecp2 KO mice were verified during progression of the disease in IDIBELL animal's facility. Mecp2 KO mice have an onset of disease at about 5 weeks of age. Before, it is not possible to differentiate KO mice from the WT littermate. The scoring system published by Guy et al in 2007 was adopted for the phenotype Mecp2 KO mice (67).

12 Mecp2 KO and 12 WT mice were used for preliminary studies in order to monitor the progression symptom scores during the time (based on 6 categories of symptoms mobility, gait, hindlimb claspings, tremor, breathing and general condition). All animals were monitored from 4 till 10 weeks of age. After the 10th postnatal week, symptoms progressed rapidly and reach a score 10 or more. All the mice and their littermates were documented twice a week for symptom scoring. When Mecp2 KO animal was scored two in two out of the mentioned criteria (tremor, breathing and general condition) was humanely culled and reported as a death. Figure 9 presents the progression of sum symptom score in Mecp2 KO mice and their WT littermate. WT mice invariably score 0.

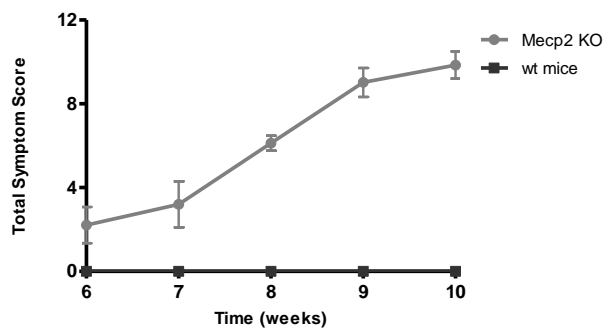


Figure 9. Symptoms score progression in Mecp2 KO mice. Time plot showing onset and progression of phenotypic signs in Mecp2 KO mice (n=12). Scores for WT littermates (n=12) were plotted for comparison. The curve of average symptom scores is showing phenotypic severity progression in Mecp2 KO mice and WT mice invariably score 0.

## Results Part 1

### 5.1.5. Weight of Mecp2 KO mice and average life span

The progression of symptoms in the Mecp2 KO male mice leads to rapid weight loss and death at approximately 10 weeks of age. In comparison WT animals can survive even till 2 years. We further analyse the weight of KO animals. From the previous studies it is known, that a distinct feature of the phenotype was varying body weight depending on genetic background (160). Body weight from the birth of individual males from a single litter are similar, however Mecp2 KO males are significantly smaller than WT from around weaning 4 weeks of age. To test the Mecp2 KO phenotype we determined the weight of animals by daily measurement of each animal.

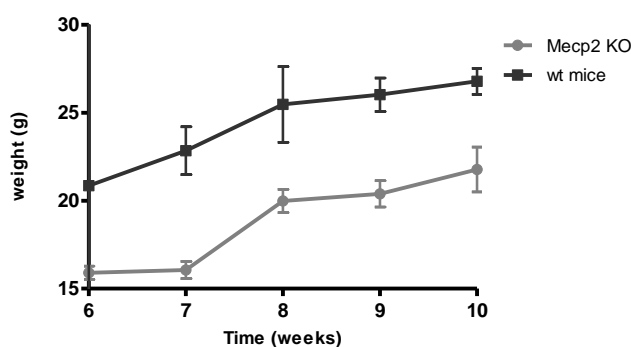


Figure 10. Mecp2 KO mice display reduced body weight compared with the C57BL/6 WT animals (WT n=12, Mecp2 KO n=12).

Both, progression of symptoms and the shortened survival were characteristic of phenotype in Mecp2 functional KO mice. Previous study demonstrated that Mecp2 KO had a shorter life span compared to WT (160). Mecp2 KO (n=12) and their WT littermates (n=12) were caged under identical conditions in the IDIBELL animal facility and complied with protocols approved by the IDIBELL Committee on Animal Care. The incidence of sudden or unexpected death in Mecp2 KO group before 2 month of age was rather low (2 out of 12 mice) under the care of experienced animal unit staff. Animal were monitored daily. The distribution of Mecp2 KO mice survival ranged from 55 (8 weeks) to 77 (11 weeks) with the average life span of 67 days (Figure 11).

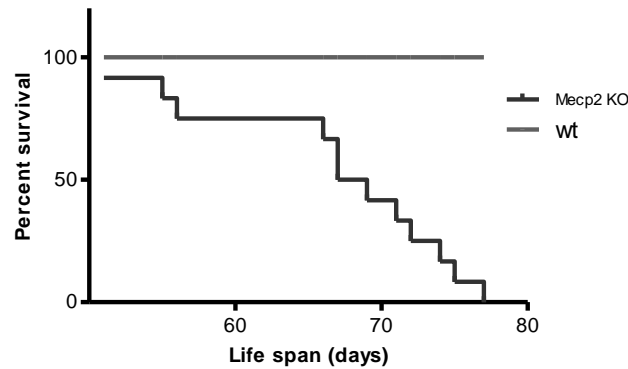


Figure 11. Survival of Mecp2 KO mice. Mecp2 KO mice and their WT littermates were assessed for the normal life span. Average survival in Mecp2 KO mice is about 10 weeks (Mecp2 KO n=12 with an average life span = 67 days), while WT animals can survive 24 months (n=12).

#### 5.1.6. Evaluation of behavioural symptoms and difference between WT and Mecp2 KO animals with the focus on cognitive and motor functions

As it was already mentioned, Mecp2 KO males appear normal till +/- 5 weeks of age. Then they are starting develop tremors, motor impairment, anxiety behaviour, seizures kyphosis or typical hind limb movements. Previous studies on Bird mice model already described altered gait, motor defects or balance impairments. Mecp2 KO mice also display reduced exploration in the behavioural test. Animals move toward or away from mechanical stimulus. Their motor dysfunctions limit novel object recognition and increased fear (167, 171). Thus, to evaluate the expected improvement of new drug treatment, we require appropriate behaviour assays to check the phenotype *in vivo*. Behaviour tests are excellent indicators for evaluation RTT phenotype. In order to choose the most adequate behaviour tests, we performed panel of experiments that could reflect reduced learning, motor dysfunctions or hypoactivity in Mecp2 KO when compared to WT littermates.

All tests were performed blind to the mouse's genotype by two observers. Mice were subjected to a behavioural test battery once, at 8 weeks of age, when the difference according to the score test are most noticeable (except bar cross test, which was performed weekly, starting at 4 weeks of age). Each test was carried out during a single day, between 9 am and 5 pm. The initial experiments between WT and Mecp2 KO mice were performed in order to set up baseline between these two groups of

## Results Part 1

animals. The most sensitive tests were chosen later for evaluation selected pharmacological drug treatments.

### 5.1.6.1. The Horizontal bar cross test

Bar cross was the first test set up in the lab. We used 8 mice for each group (WT and KO mice). To eliminate first the novelty of the tasks as a source of slips, all mice were given 2 or 3 trials on the bar at the beginning of the testing session. By the 3rd trial, WT control animals ran the bar with not more than one or two slips (230). Every week, during the real experimental session the number of hind limb lateral slips and the time to reach the platform were counted on three trials for each tested mouse.

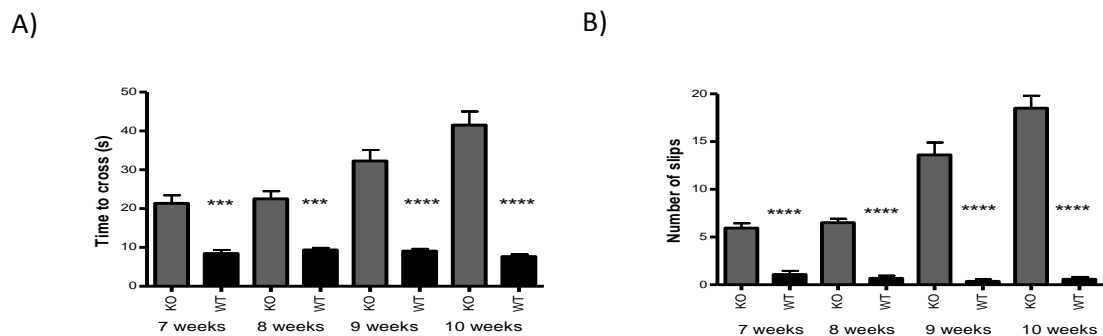


Figure 12. Changes in motor capabilities in Mecp2 KO mice versus WT littermate. Bar cross test was carried out once per week. A) The time spent to cross the bar and B) the number of slips were quantified from 7 to 10 weeks of age. Graphs represent the mean of two independent experiments  $\pm$  SEM,  $n=8$  for each group. Asterisks indicate significant difference between WT and Mecp2 KO mice: \*  $p < 0,05$ ; \*\*  $p < 0,01$ ; \*\*\*  $p < 0,001$ ; \*\*\*\*  $p < 0,0001$ .

Mecp2 KO mice have mobility abnormalities. It was also confirmed by using bar cross test. KO mice need more time to reach the platform. Moreover the symptoms during the time progression are more severe what corresponds to the longer time to complete the task during following weeks of experiment. The time required for mice to reach a platform along a balance bar was significantly increased in the Mecp2 KO mice, starting from 7 weeks of age and showing the tendency of being prolonged during the progression of the disease. WT mice presented normal scores as they required few seconds to complete the test. Mecp2 KO mice showed abnormal scores and they

required more time to reach the platform along the bar. The time is increasing with the age of animals, being around 20 sec at 7 and 8 weeks, 30 sec at 9 weeks, and 40 sec at 10 weeks. At 10 weeks of age Mecp2 KO mice need four times more to cross the bar when compared to the WT littermates (Figure 12A).

Figure 12B shows that besides delayed time to cross the bar, (Figure 12A) Mecp2 KO animals display higher number of slips respectively to WT mice. Mecp2 KO mice slipped away more often than their WT littermates, showing clear disabilities of mobility and ataxia phenotype. KO mice failed much often to maintain balance. Based on the experiment, it was observed that Mecp2 KO mice instead of walking and maintain a stable upright posture, they displayed ventral recumbence. The body flattened against the surface of the bar, and hind/fore limb wrapped laterally around the bar. At the last tracks of the experiment, when the symptoms are visible (starting from 7-8 weeks of age). KO mice use their fore limbs to drag themselves along the beam, being their hind limbs generally not used. The number of slips for WT animal is very little; but the number of slips in Mecp2 KO animals is increasing with the age of mouse. At 7 weeks of age KO mouse performed average of 5 slips while crossing the bar. At 10 weeks the number of slips is increased till average of 20. This is a sign of suffering the postnatal deterioration in their muscle strength and in the coordination of movements

Additionally at the 10 weeks of age 2 out of 8 KO mice were not able to complete the test, because they “froze” or fell repeatedly from the bar.

### 5.1.6.2. Open field testing

For studying the spontaneous locomotion and exploratory behaviour the OFT was performed. Locomotor activity was assessed by total distance moved and number of rearings. The arena was divided in a central zone (15cm x 15cm) and a peripheral zone (5cm wide area around the walls). Each mouse was individually placed in the OFT in the center of arena and was allowed to explore during 5 min. Mecp2 KO mice display decreased social approach and fears. The number of defecation bolouse was higher when compared to WT (figure 13A).

Surprisingly, in this test Mecp2 KO despite the motor deficits and their impaired performance in bar cross, in OFT display similar number of squares crossing like WT animals. There was no significant difference in the number of crossing between these two tested groups. No effect of genotype was detected on the crossed squares/ 5 min

## Results Part 1

(figure 13B). However, the number of rearings was higher in WT group. As it was expected the overall number of rearings was reduced in Mecp2 KO group. WT mice spent more time in the centric area, and in the corners. That is indicated by curiosity of the environment around. Motor dysfunction or a reduced interest of the unknown environment had a significant effect on phenotype of KO group mice. In the case of Mecp2 KO the rearing number was decreased 50% respectively to WT (figure 13C).

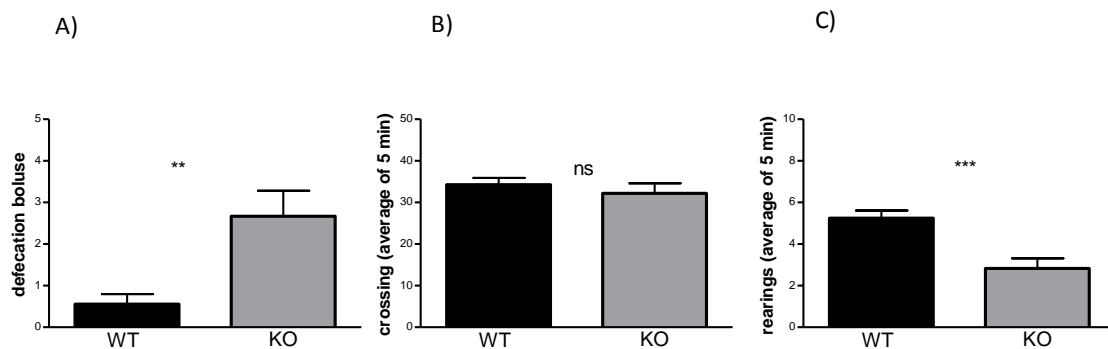


Figure 13. Mecp2 KO mice present social fears (A) and a progressive mobility dysfunction. Open field experiments show no difference between WT and Mecp2 KO mice in number of crossing (B) however number of rearings in Mecp2 KO group was significantly reduced (C). All mice were 8 weeks of age. Values represents mean +/- SEM, n=8 for each group (\* p < 0,05; \*\* p < 0,01; \*\*\* p < 0,001).

### 5.1.6.3. Test of neophobia to a new home cage

Mecp2 KO mice exhibit neophobia. Previous reports shows abnormal social interactions describe Mecp2 KO animals as spending more time in the shaded, quiet places, rather far from the other mice (162). During the test we measured the number of rearings and number of visited corners. Mecp2 KO visited significantly less corners and performed significantly less rearings during the test. WT littermates are more interested in exploring the new situation, trying to cognize the surrounding environment. They are displaying higher number of the corners with the average of 10, what corresponds to 5 visited corners in case of KO mice (Figure 14A). Presented in Figure 14B lower number of rearing in the Mecp2 KO could be an explanation that they have a lower motor balance and coordination, and also suffer body tremor. The KO mice performed average 3 times less rearing.

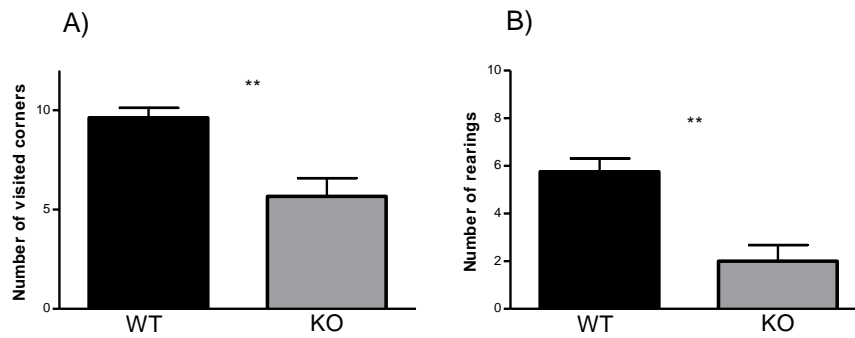


Figure 14. The neophobia was observed in *Mecn2* KO mice. A) Higher number of visited corners was counted in WT littermate when compared to *Mecn2* KO. B) The number of rearings was reduced in *Mecn2* KO mice, emphasizing the changes in motor capabilities between WT and *Mecn2* KO during progression of the disease. Values represents mean  $\pm$  SEM,  $n=8$  for each group, \*\*  $p < 0,01$ ; all mice were postnatal week 8.

#### 5.1.6.4. Wire grip test

A wire grip test was used to measure the grip strength of mice with a trial of 1 minute for each animal. During the experiment two types of measurements were performed: time to fall down (latency) and number of segments, which animal cross during the time being on wire (with a maximum duration of 1 min).

Obtained difference was significant regarding to WT - *Mecn2* KO genotype interaction on forelimb grip performance. At 8 weeks of age, WT animals do not have any problem to keep the wire during one minute, where the *Mecn2* KO can complete the test only with average of a half of the time according to the WT littermates (Figure 15A). There was also a significant effect in *Mecn2* KO group mice regarding to the number of segments. The number of crossed segments in WT group was higher than in *Mecn2* one, being 11 in the WT group mice and between 2 and 3 in KO group (Figure 15B). Additionally during the test we could observe high score of tremor and breathing's problem in *Mecn2* KO group. The KO mice suffer hypotonia and spasticity (Video 1 *Mec2* KO; Video 2 WT control).

## Results Part 1

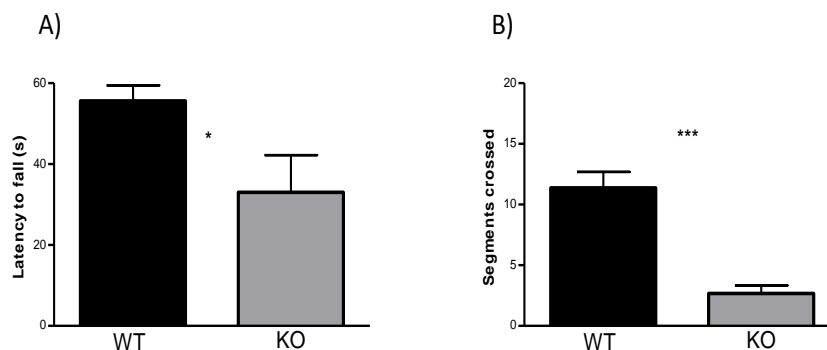


Figure 15. Changes in grip strength between WT and Mecp2 KO mice. A) Mecp2 KO spent shorter time on wire and cross less segments than WT animals (B). Values represents mean +/- SEM, n=8 for each group, all mice are postnatal week 8. Asterisks indicate significant difference between WT and Mecp2 KO mice: \*  $p < 0,005$ ; \*\*\*  $p < 0,001$ .

### 5.1.6.5. Y Maze Spontaneous Alternation test

(based on <http://www.youtube.com/watch?v=VuYWiHGxxLI>)

During the Y-Maze test the behaviour of each mouse was observed over 5 min. We count the number of rearings and then calculate the average, showing the tendency of higher number of rearings in WT group (Figure 16A). The WT group end up with 6 rearings, as an average obtained over 5 minutes of the test, and KO group with about two times less, 3 rearings, being significantly different. Mice movement were more coordinated in WT group, but we did not observe the difference in the number of repetitions between tested animals (Figure 16B, right panel) what could be the consequence that the number of entrance was lower in Mecp2 KO group (Figure 16B, left panel). The WT mice were doing more entrance when compared to KO mice, resulting with the same sequence of repetitions. Comparison of the entrance trail, WT mice present double number of entrance versus KO group. However the most important results are presented in figure 16C. The Y-Maze test has confirmed that Mecp2 KO mice have a significant motor impairment. One of the hallmarks of autism-spectrum disorders is a restriction of interest. To determinate whether these factors may have affected the apparent lack of interest or fear of the novelty we compared the level of exploration as measured by the relation of ratio between number of entrances divided by sequence of repetition. Both parameters were counting during 5min. What was expected the overall number of entrance is lower in Mecp2 KO group. This is an explanation that motor dysfunctions and reduced interest have a significant effect for

this parameter. As a consequence, the ratio between the number of entrance and repetition was also higher in WT mice suggesting that Mecp2 KO mice spent significantly less time in the novel arm of the test. They are rather repeating the same scheme going to the Y-maze arm discovered before.

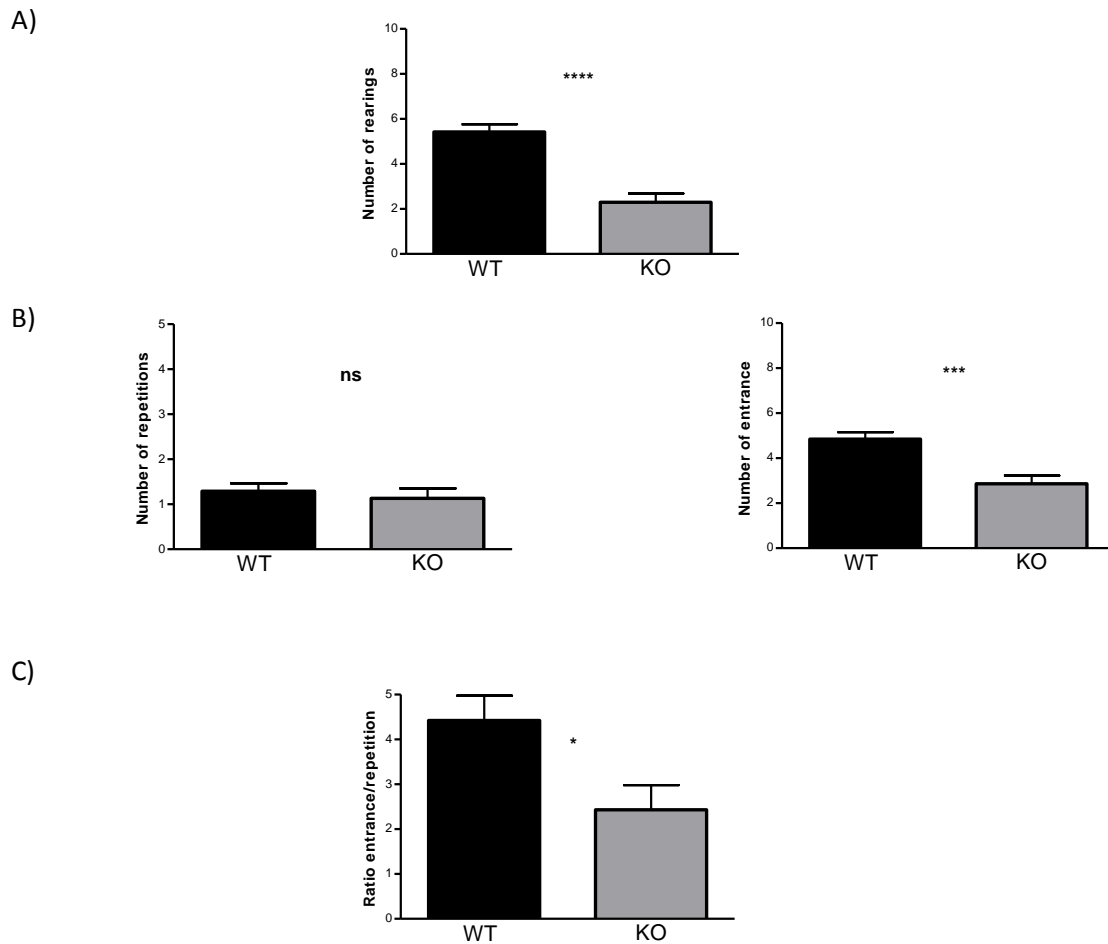


Figure 16. Y-maze performance between WT and Mecp2 KO mice at 8 postnatal weeks A) The number of rearings was significantly higher in the WT group, but B) no difference between two groups in the number of repetition was detected (right panel). The number of entrance was higher in WT group (left panel). C) The ratio of number entrances divided by number of repetitions was higher in WT animals. (Mean +/- S.E.M., n=8/ per group; \* p< 0,005; \*\* p< 0,01; \*\*\* p< 0,001).

## Results Part 1

### 5.1.7. Immunostaining of Th and pTh-positive neurons number in WT and Mecp2 KO mice

We know that Dopamine (DA) is an important neurotransmitter and hormone in the brain that controls several functions including locomotor activity, learning, memory, and endocrine regulation. Not only in RTT patients, but also in Mecp2 KO mice the level of serotonin (5-hydroxytryptamine), adrenaline, and dopamine are reduced (169, 231, 232). That is associated with defects in the expression of rate-limiting enzymes like for example Tyrosine Hyrdoxylase (Th) in the brainstem substantia nigra (158, 233). It is possible that by restoring the bioamine system we could rescue the RTT phenotype, including here the mobility deficits. Th defects is suggested as a molecular mechanism that explain mobility score in Mecp2 KO group respected to the WT. Trying to answer if after drug treatment we can rescue mobility deficits we analysed the Th staining first in WT and Mecp2 KO groups..

We measured the intensity of Th staining in neurons from SNpc (Sustantia Nigra) localized in MB from Mecp2-deficient mice at 8 weeks old. In figure 17 we can see the differences in Th immunostaining between WT and Mecp2 KO. The Mecp2 KO mice have less Th immunostaining. Obtained results suggest the higher level of Th in WT animals.

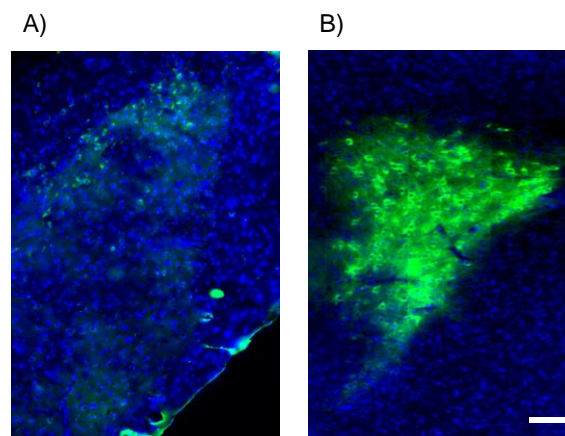


Figure 17. Representative immunostaining of coronal brain sections from Substantia nigra pars compacta (SNpc). In both groups, Mecp2 KO (A) and WT (B) mice mDA neurons were coinmunostained for Th (green), and DAPI counterstain (blue). Scale bar=20 $\mu$ m. All pictures were realized with spectral confocal microscope, magnification of 63X 1.4 NA. Animals were analysed at 8 weeks of age, n=3/ each group.

Going step further that the phosphorylation of Th at Ser40 increases the enzyme's activity *in vitro*, *in situ* and *in vivo*, we carried out also immunofluorescence to measure

the intensity of pSer-40Th staining in Th expressing neurons from SNpc localized in MB of Mecp2-deficient mice. Based on previous results (Figure 17) that the Th level is decreased in Mecp2 KO mice, we detected also lower level of pSer-40 Th (pTh) in KO mice (Figure 18).

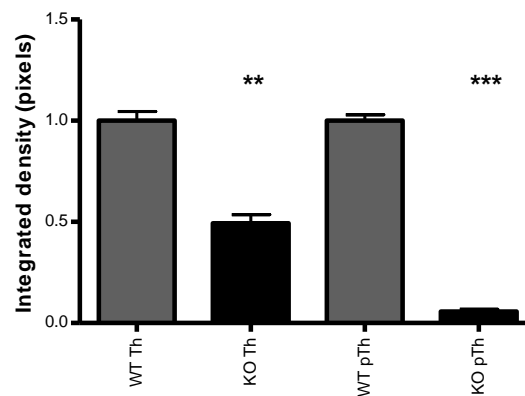
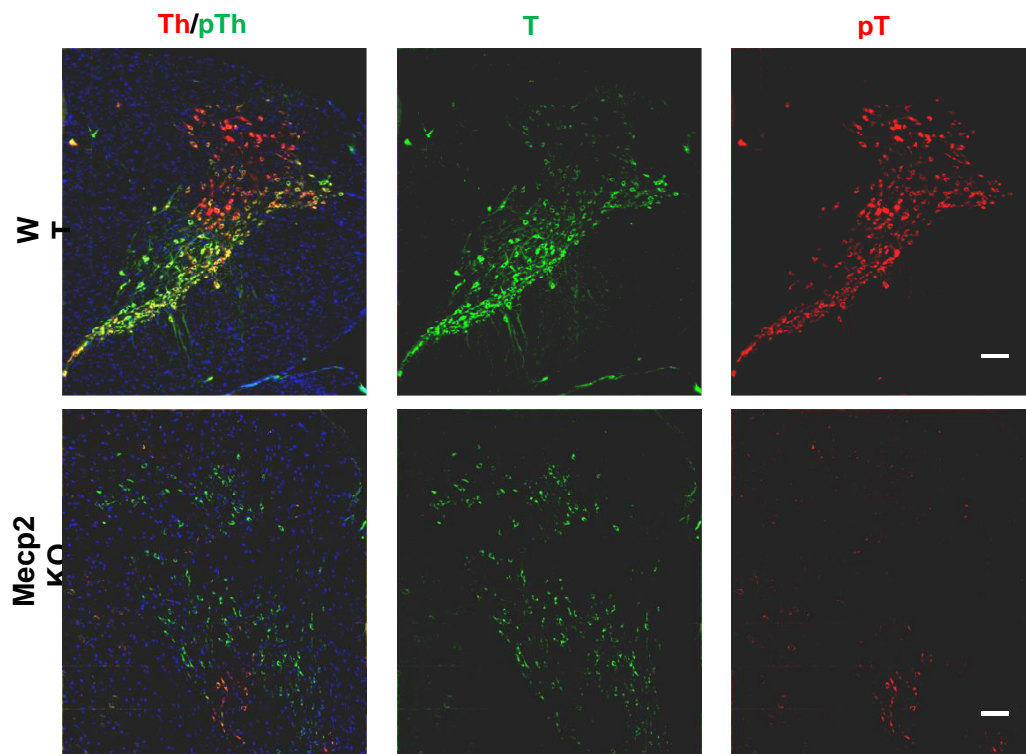


Figure 18. Lower pTh and Th levels in Mecp2 deficient mice when compared to WT littermate. Upper panel shows representative immunostaining of coronal brain sections from Substantia nigra pars compacta (SNpc). mDA neurons were coinmunostained for Th (green), pTh (pSer-red) and DAPI counterstain (blue). Scale bar=20µm. Quantification of Th and pTh positive staining in studied experimental groups mentioned above in figure. The bars represent the Integrated density (ImageJ Fiji vs 1.47) of picture realized with spectral confocal microscope, magnification of 63X 1.4 NA; \*\* p< 0,01; \*\*\* p< 0,001 (lower panel).

## Results Part 1

All immunostainings analysis of Th and pTh were performed in the region of Sustancia Nigra compacta (SNPc) based on <http://mouse.brain-map.org/agea>.

### 5.1.8. Immunostaining for the post- and presynaptic proteins, level of PSD-95 and VGLUT1 in WT and Mecp2 KO mice

Previous studies described the difference of PSD-95 and VGLUT1 levels between WT and KO mice. Coronal brain sections were obtained and brain tissues were stained for PSD-95 and VGLUT1 antibodies (1:500 mouse anti-VGLUT1 and 1: 200 rabbit anti-PSD-95). The double-labeled images were acquired using a Leica TCS SP5 Spectral Confocal microscope (Leica, Milton Keynes, UK; Magnification: HCX PL APO lambda blue 63X oil -numerical aperture-NA:1.4 and resolution of 1024x1024; Acquisition Software: Leica Application suite Advanced Fluorescence – LAS AF, version 2.6.0.7266). Z project and Tile were realized in order to get all staining with both antibodies (Figure 19 A). Densitometric analysis of the staining level was performed on 8-bit images using ImageJ Fiji vs 1.47 software (<http://rsb.info.nih.gov>). The integrated density was calculated as the sum of the pixels values in a region of interest. We realized pictures from different cover slips (for each condition 5 cover slips) of different slices from 3 animals in the same region of interest (3 WT and 3 Mecp2 KO animals). The average of the successive impaired sections for each cover slip was calculated for each animal in all experimental groups (total five, Figure 19 B).

Some of the selected drugs for *in vivo* experiments should improve the PSD-95 and VGLUT1 intensity. That would mean that the drug promotes synapse maturation and exerts a major influence on synaptic strength and plasticity (175).

Obtained here results display significant lower level of PSD-95 positive stained cells, and less VGLUT1 stained cells, however not statistically important.

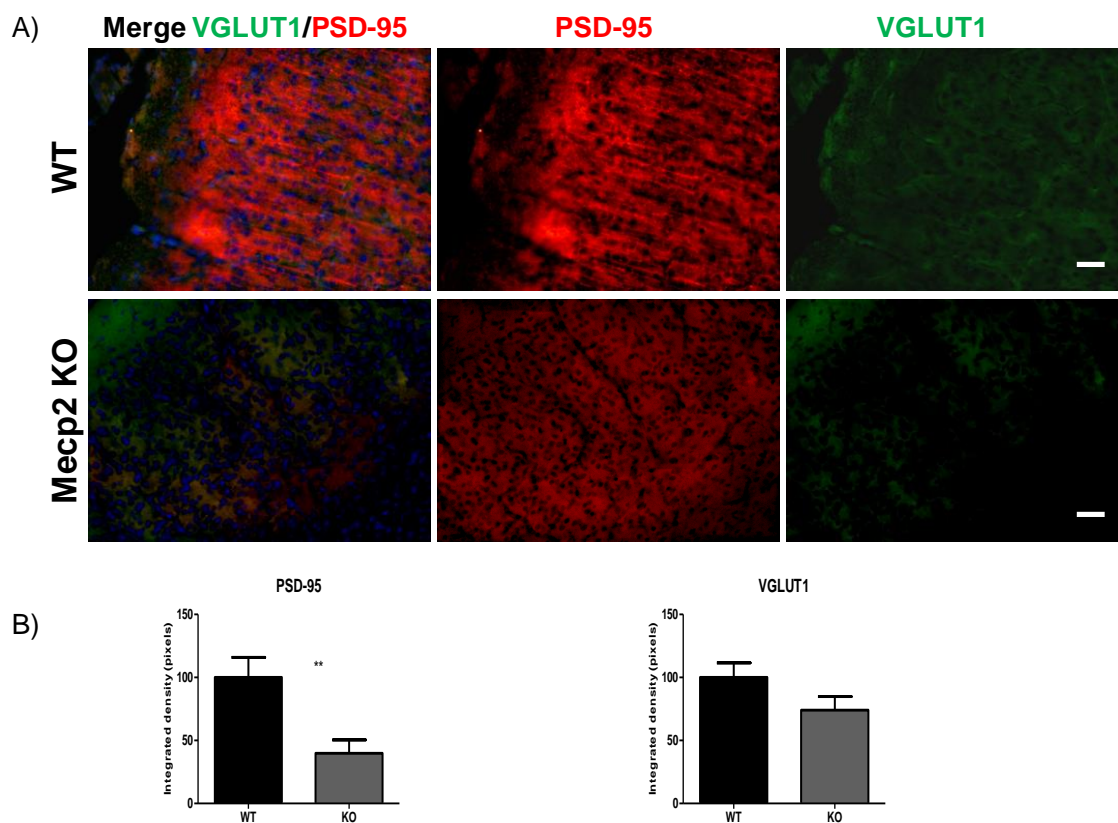


Figure 19. Quantification of PSD-95 and VGLUT1 positive staining in experimental groups, WT and Mecp2 KO animals. A) Representative Immunostaining of coronal brain sections from Substantia nigra pars compacta (SNpc). mDA neurons were coimmunostained for PSD-95 (Alexa 455), VGLUT1 (Alexa 488), and DAPI counterstain (blue). The images were taken with Zeiss microscope 20 X, Scale bar=20 $\mu$ m. B) The bars represent the Integrated density (ImageJ Fiji vs 1.47) of picture realized with Confocal microscopic SPS5, obj 20X indicating higher levels of both markers in WT group (being statistically significant in the case of PSD-95 \*\*  $p < 0,01$ ).

### 5.1.9. The level of glutathione in WT and Mecp2 KO animals

The neuroprotection is associated with increase cellular level of reduced glutathione (GSH), which acts as an antioxidant. GSH is an electron donor for the conversion of  $H_2O_2$  into  $H_2O$ , and is able to react with the ROS. Reacting with ROS, GSH is converted into glutathione disulphide (GSSG), the oxidized form.

We first analysed levels of different forms of glutathione (GSx –total glutathione, GSH and GSSG) in WT compared to Mecp2 KO animals. The levels of GSH, as well as the ratio of GSH/GSSG in WT brains is higher than in Mecp2 KO mice, being statistical significant. Obtained here levels of oxidative stress (OS) marker in RTT animals suggest a potential role of OS in pathogenesis of the disease. OS was already

## Results Part 1

indicated in other studies as having role in neurological symptom severity in RTT syndrome (145). These results also show for the first time that levels of glutathione species are altered in Rett mice, contributing to increase the OS of these mice and assist the results obtained in Parkinson disease, where GSH is decreased in the substantia nigra (234, 235). Taking into account that OS production is imbalanced in RTT, we wanted to test if our treatments have some neuroprotective properties.

The experiment was performed at 3 different time points corresponding to the age of the animal, respectively 4, 8 and 10 weeks of age. First part of the experiment was done at 4 weeks of age, where physically is not possible to distinguish the Mecp2 KO animal from WT one. Second set of the experiment was at 8 weeks of age, when the symptoms are severe. As a third point we studied 10 weeks old mice.

At 4 weeks of age no significant difference between the groups was noticed (Figure 20). At 8 and 10 weeks of age, the levels of total level of glutathione (GSx) in KO mice was decreased (Figure 20A). Oxidized glutathione (GSSG) was higher in KO mice and reduced one present similar pattern to the total one (Figure 20B). At 8 weeks of age the ratio GSH/GSSG in Mecp2 mice was decreased versus the WT animals being significant and reaching 55% of the GSH values of WT and 62% of the ratio GSH/GSSG of control group. At 10 weeks of age, when the KO animals are about to die the tendency is even stronger, reflecting the oxidative damage results in lower level of GSH (Figure 20B) and higher level of GSH/GSSG ratio (Figure 20C).

The ratio of GSH versus GSSG shows that the Mecp2 KO mice undergo a significant oxidative stress in comparison to the WT littermate mice. These results could suggest that by recovering the levels of GSH in the brain of RTT mice, oxidative stress is reduced. It might be the neuroprotective effect of GSH as it has been already described in Parkinson disease (236).

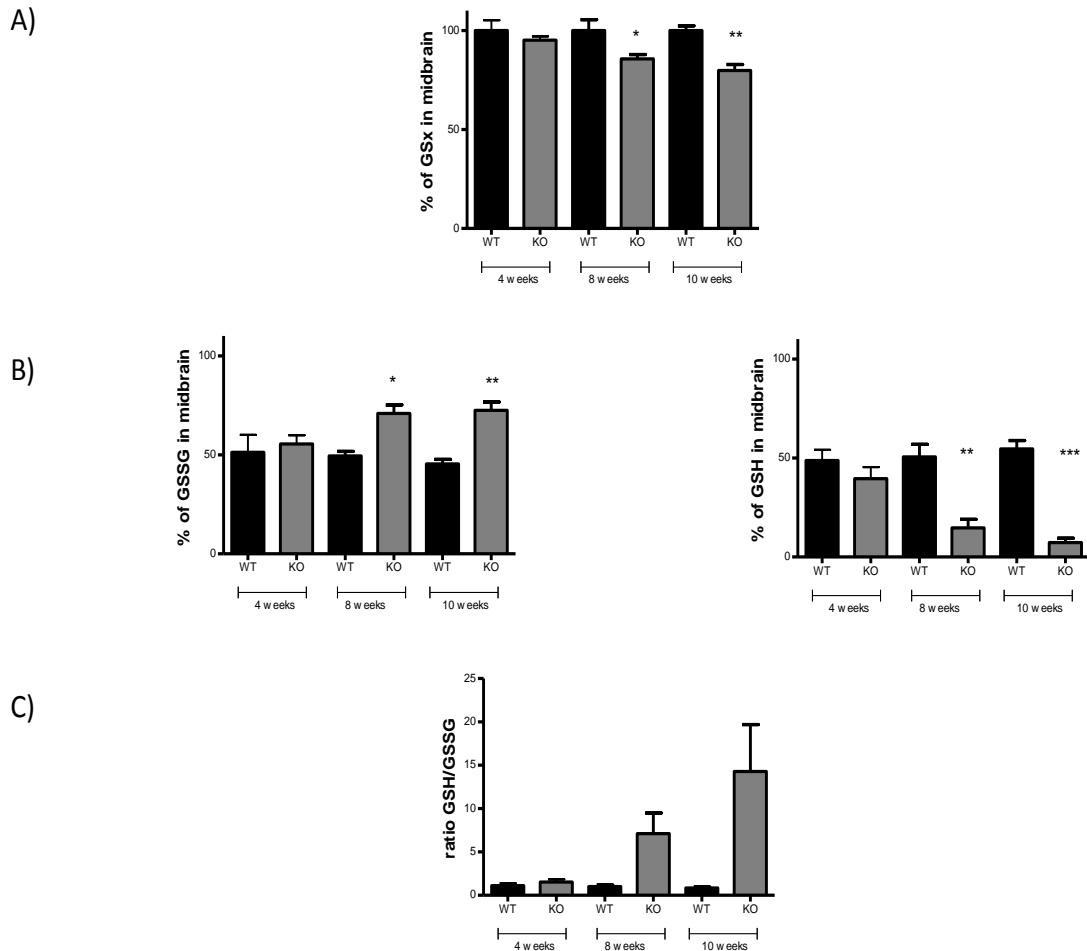


Figure 20. Levels of GSx, GSH and GSSG in WT and Mecp2 KO animals during the progression of the disease. A) The levels of GSx at 8 and 10 weeks of age in KO group were significantly decreased compared with WT animals, B) what corresponds to the higher level of GSSG and lower of GSH at 8 and 10 weeks of age in KO mice group. D). Calculated ratio of GSH vs GSSG glutathione was also increasing during the time of the experiment. At 4 weeks of age no difference were noticed. All presented graphs show the mean of three independent experiments +/- SEM (n=3 mice per group \* p< 0,05; \*\* p< 0,01; \*\*\* p< 0,001).

### 5.1.10. Determination of numbers and types of dendritic spines in WT and Mecp2 KO mice

Reduced dendritic complexity and spine density have been reported in postmortem RTT brain tissue and in Mecp2 animal models (237). We would like to study this issue in treated mice. The number of excitatory synapses in the hippocampus has been reported to be significantly reduced in the Mecp2 KO mice, (152) but some groups reports that there is no changes in spine density (162).

## Results Part 1

For the analysis of dendritic spines sections of the mouse brain were prepared and processed as described in Material and Methods (Golgi staining). Mice from both groups were transcardially perfused, and brains were processed with FD Rapid Golgi Staining Kit (FD Neurotechnologies).

The Golgi staining was used to label neurons sparsely and distinctly to visualize dendritic spine density on secondary dendritic branches of pyramidal neurons in layer 5 of motor cortex. Analysed mice were at 8 weeks of age. While low-magnification imaging clearly delineated the extent of the dendrites of these pyramidal cells (Figure 21Aa representative for WT animal and 21Bb representative for Mecp2 KO animal) higher magnifications was accomplished to identify and count the spines (figure 21A representative for WT animal and 21B representative for Mecp2 KO animal).

The density of the spines per unit branch revealed a significant decrease in total spine density in neurons from Mecp2 KO mice. The results are displayed in figure 21C where it is presented that total number of spines in Mecp2 KO mice was significantly decreased compared to WT littermates. The differences were very clear  $49 \pm 8$  in the case of WT, and  $21 \pm 3$  in Mecp2 KO mice (Figure 21C). The number of spines was calculated with Neuronstudio software and the Sholl analysis algorithm (223). As an example of the more mature type of spines, mushroom spine density was analysed (133). The obtained data show mushroom spine density as a being higher in WT mice group; WT mice  $23 \pm 5$  and respectively Mecp2 KO mice  $6 \pm 2$  (Figure 21D).

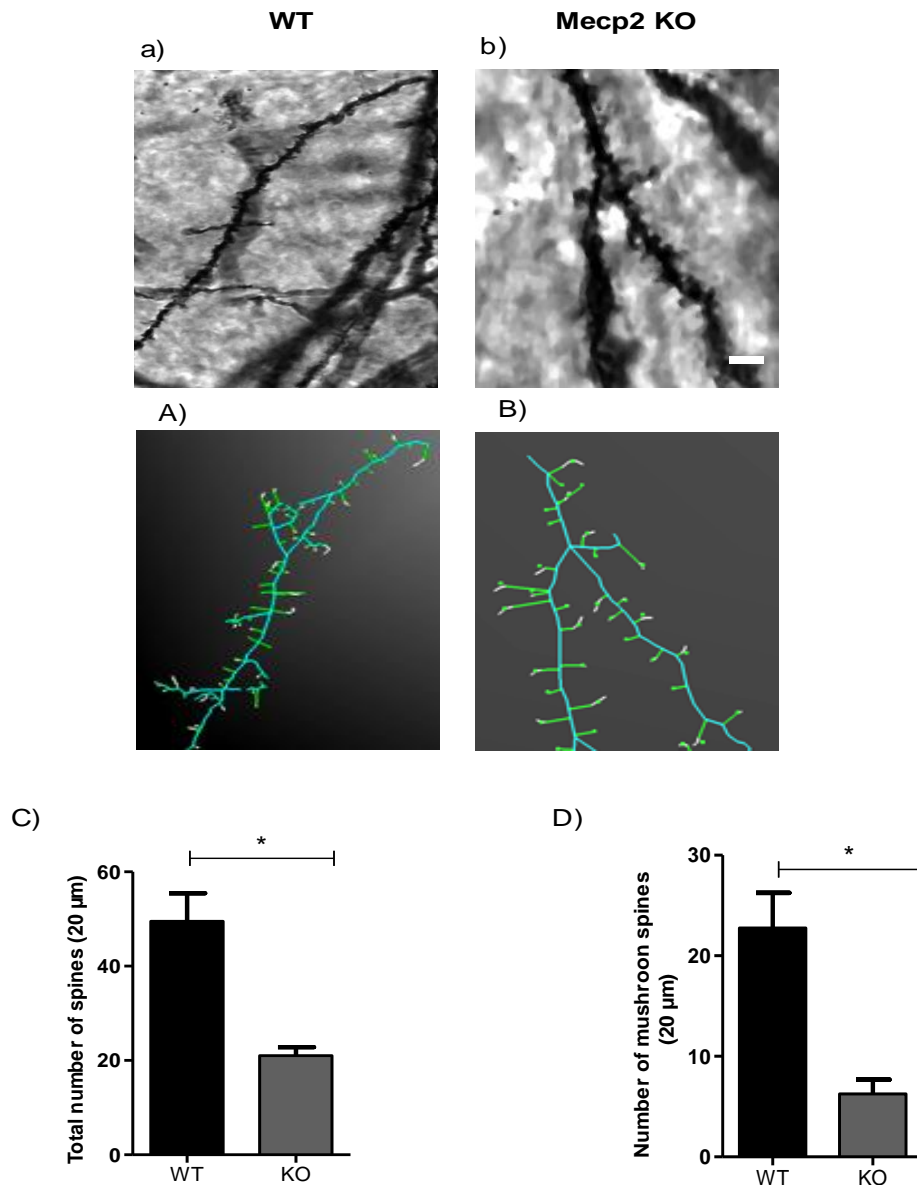


Figure 21. Changes in brain structure of *Mecp2* KO mice. a) Golgi staining of hippocampus region of pyramidal cells in 8 weeks old WT animal and b) 8 weeks old *Mecp2* KO animal, which enable specific, sparse labelling of neurons and spine morphology (scale bar 20  $\mu\text{m}$ ). A) Image at high magnification performed by Neuron Studio to enable clear identification of dendritic spines in WT (A) and *Mecp2* KO (B) animals. C) Bars showing the spine density (mean $\pm$  SEM) in hippocampus region of *Mecp2* deficient mice versus WT. Total number of spines in adult (8 weeks of age) and D) the number of mushroom type of spines are lower in *Mecp2* KO group comparing to WT littermates. Dendritic segments of 20  $\mu\text{m}$  were analysed for each group, the images were taken with Zeiss microscope 63 X and processed with Neuron studio software. The bars represent the average of total count-spine in dendritic segments in two experimental groups (the Sholl analysis). All graphs represent the mean of two independent experiments  $\pm$  SEM (n=3 mice per group; \*p<0.05, \*\*p<0.01).

## Results Part 2

### **5.2 Part 2. Improvement of the Rett Syndrome phenotype in a *Mecp2* mouse model upon treatment with Levodopa and a Dopa Decarboxylase Inhibitor**

#### **5.2.1. Dopamine and norepinephrine are crucial in the biosynthetic pathway for the catecholamine neurotransmitters in RTT**

It is hypothesized that dopaminergic dysfunction in Rett patients could play a role in the cognitive disorders, and can be responsible for chronic aberrant behaviours such as hyperactive, aggressive or self-injurious behaviour (238). As it is also known Rett patients suffer breathing irregularities (239, 240). More than 25% of deaths in girls with the Rett syndrome are related with sudden respiratory arrhythmia (240). Many clinicians think that the breathing problems are a consequence of disturbed cortical and may be behaviourally determined (239).

The key role plays here norepinephrine, which is involved in maturation and modulation of the respiratory network (241). The levels of biogenic amines, such as dopamine and norepinephrine are reduced in RTT postmortem samples (125, 192). Deficit in MB related with catecholaminergic metabolism and the decrease in size and function of neurons were also observed in adult *Mecp2* mice (169, 242).

L-Dopa itself is used for a long time as a standard for dopaminergic stimulation therapy in Parkinson disease patients (243). It had also a positive effect in *Mecp2* KO mice, reducing problems with mobility (189). Because of Dopadecarboxylase, L-Dopa is converted to Dopamine, which it is not able to cross the blood brain barrier (BBB) (Figure 22). Based on the previous work from our group that *Ddc* is upregulated in *Mecp2* KO mice (101), the rationale was to treat the *Mecp2* KO mice with L-Dopa plus an inhibitor of *Ddc*, named *Ddci*. Because *Ddci* is blocking L-Dopa to convert into the dopamine in the peripheral tissues, the level of L-Dopa that can cross the BBB is higher and the treatment could be more effective in the brain following its neurological pathway (Figure 22).

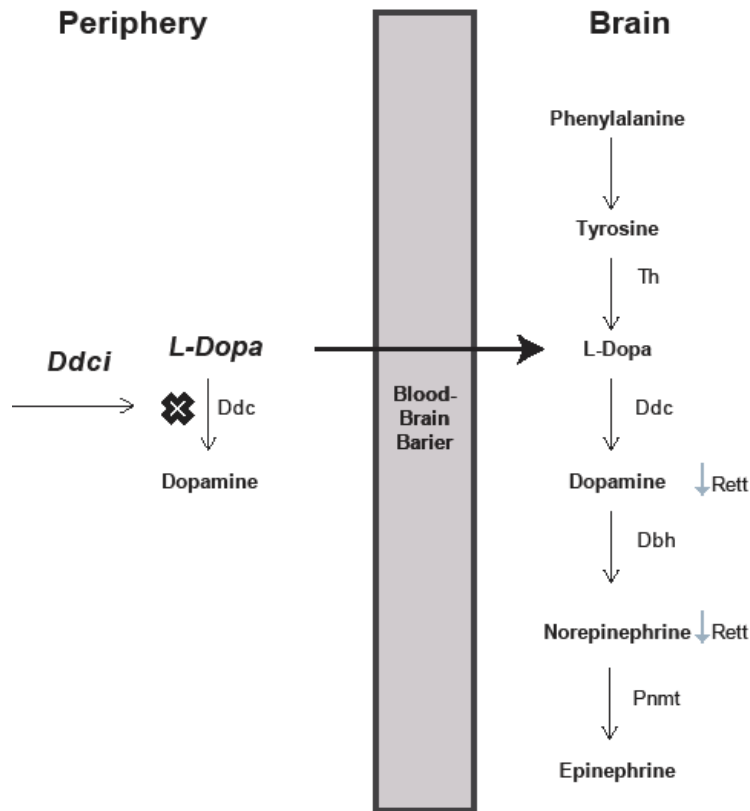


Figure 22. Metabolic pathways of biosynthesis of major biogenic amines with the focus on L-Dopa / Ddc treatment. Abbreviations: Ddci, dopa-decarboxylase inhibitor; L-Dopa, Levodopa; Ddc, dopa-decarboxylase; Tyrosine hydroxylase, Th; Dbh, dopamine beta-hydroxylase; Pnmt, phenylethanolamine.

### 5.2.2. Studies on potential toxic effect on Mecp2 KO mice during L-Dopa / Ddc treatment

Mentioned before, the progression of symptoms in the Mecp2 KO mice leads to rapid weight loss and death at approximately 10 weeks of age in comparison with WT animals (160). In order to make sure if administrations of L-Dopa; the combination L-Dopa / Ddc, or Ddc alone were not toxic for Mecp2 KO mice, we monitored every day the weight of each animal before to perform following injections. Then we made a weekly average of the weights of all animals within each group. In figure 23 representative photo of treated animals and average weights of each group are presented. All untreated and treated Mecp2 KO groups display the same weight. Notice that the group of WT animals has a higher weight than the Mecp2 KO ones. It confirms that the evaluated treatments have no effect on body weight. Injections have also no

## Results Part 2

negative effect on the life-span during the drug administration in comparison with the vehicle Mecp2 KO group. To confirm the lack of toxicity after the drug administration the histologic analysis of liver were performed. Upon killing mice liver tissues were collected to analyze endogenous toxicity by hematoxylin and eosin staining. These data show that the dose that was proposed is not toxic for the Mecp2 KO animals (Figure 24).

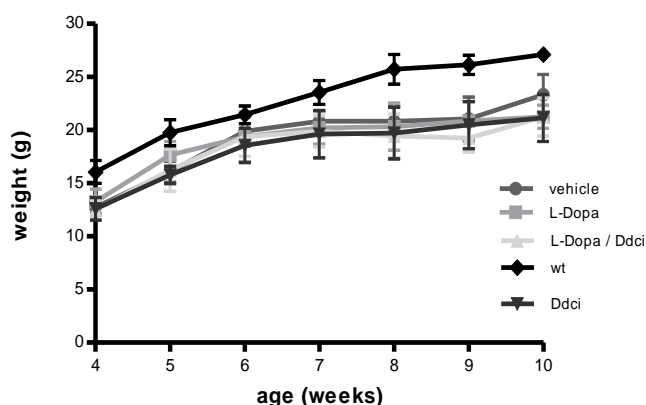


Figure 23. Mice weight during selected drugs treatment. No effect of MeCP2 deletion on body weight was observed after the drug treatment, however Mecp2 KO mice display reduced body weight compared with the C57BL/6 WT animals (vehicle n=37, mice treated with L-Dopa / Ddci n=40, mice treated with L-Dopa alone n=20, and mice treated with Ddci alone n=15). The upper panel is a representative picture showing no difference between treated groups at the end of the treatment, 10 weeks of age (from the left L-Dopa treated mouse with one black mark on the tail, L-Dopa / Ddci –treated mouse with two black marks on the tail and vehicle treated mouse with saline without any mark, mice treated with Ddci alone are not shown but no differences were found).

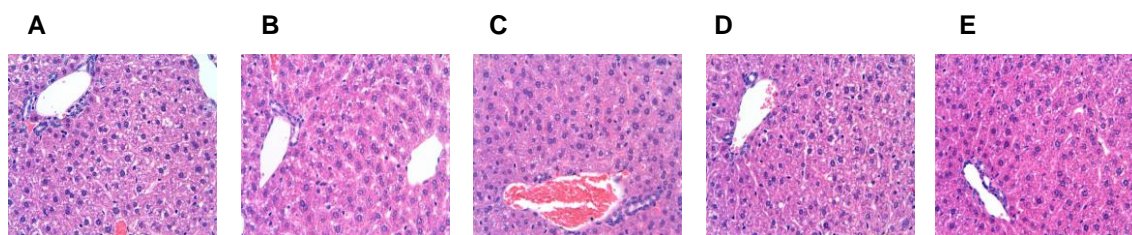


Figure 24. No evident toxicity was detected by hematoxylin and eosin (H&E) staining in any of the mice used for different drug treatments. At the time of sacrifice, liver tissues were resected for pathological analysis: Representative pictures of A) WT, B) Mecp2 KO vehicle-treated, C) Mecp2 KO Ddci-treated, D) Mecp2 KO L-Dopa treated and E) Mecp2 KO L-Dopa+Ddci treated mice (n=3 per each group).

### 5.2.3. Single and total symptoms score after L-Dopa / Ddci treatment

Rett syndrome patients and Mecp2 KO mice display a progressive, postnatal neurological phenotype (53, 160). Mecp2 KO mice are globally normal until 4 weeks of age and then begin to suffer cognitive and motor dysfunctions. In order to test the effect of the L-Dopa/Ddci combination in the symptomatology of RTT mice, the mice were treated daily during 6 weeks. Twice a week mice were scored following the recommendations of Guy et al., 2007 as specified in material and methods. The treatment was started with 4 weeks old animals. At 6 weeks of age it is already possible to observe some of the characteristic symptoms of the Mecp2 KO model. The plots show the overall distribution of symptoms at 7, 8, 9, and 10 weeks of age. They compare the score between vehicle, Ddci, L-Dopa, and L-Dopa/Ddci treated groups. During each week of treatment an average of each symptom was performed separately, and next normalized with the vehicle group (Figure 25, one-way ANOVA with post hoc Bonferroni's Multiple Comparison). We found a significant difference between vehicle versus L-Dopa / Ddci, and L-Dopa versus L-Dopa / Ddci treated groups when we score mobility, tremor and breathing from 7 to 10 weeks of age,  $p < 0,001$  (Figure 25 A). There is no difference between groups of vehicle and Ddci alone. Treatment with L-Dopa/Ddci improves the mobility, tremor and breathing phenotype in an average of 50% along the age, being less efficient in older mice. At the age of 7 weeks the improvement is even greater than 50%, reaching to 70-75% in tremor during 7, 8 or 9 weeks. The similar pattern is observed for breathing. Regarding to the phenotypes of gait, hindlimb clapping or general condition symptom scores we can found a tendency of improvement in the L-Dopa/Ddci treated mice respect to the

## Results Part 2

Mecp2 KO vehicle (Figure 25 B). The most significant improvement was observed for the symptoms controlled by the dopaminergic pathway in the nigrostratum: mobility, tremor and breathing.

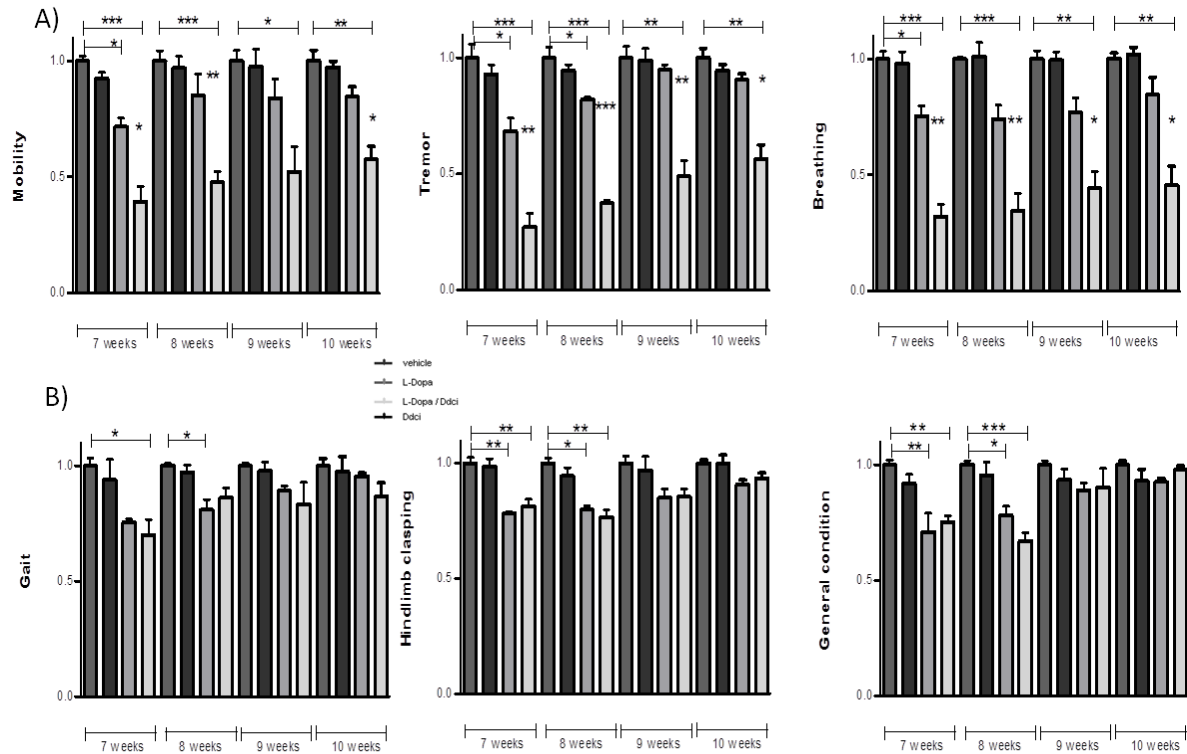


Figure 25. Treatment with L-Dopa / Ddci reduces symptoms in Mecp2 KO mice (vehicle n=37, mice treated with L-DOPA+DDCI n=40, mice treated with L-DOPA alone n=20, mice treated with Ddci alone n=15). A) Plot of average symptom scores representing mobility, tremor, breathing B) gait, hindlimb claspings and general condition normalized versus control group treated with saline (\* p < 0,05; \*\* p < 0,01; \*\*\* p < 0,001).

The average of total symptoms score was plotted in Figure 26. Mice treated with L-Dopa / Ddci showed significant enhancement in the phenotype severity score in the 2 post-treatment weeks compare with the vehicle group. In contrast, WT animals did not develop signs and most of them constantly scored 0 for the duration of the study. This average plot shows a windows enhancement at 7 and 8 weeks, where the differences in the score are more significant between the L-Dopa/Ddci and vehicle group. The symptoms improvement caused by L-Dopa treatment is less significant that the L-Dopa/Ddci, indicating that the combination is more effective. Treatment with Ddci alone does not have effect. The best results for L-Dopa treatment are also at 8 weeks, showing the possibility for a therapeutic window during the 7-8 weeks of age.

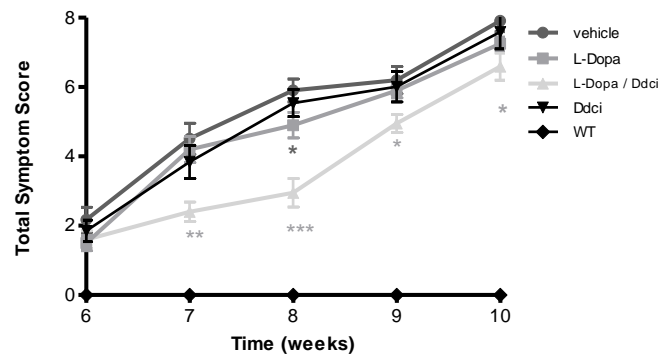


Figure 26. Treatment with L-Dopa combined with Ddci reduces symptoms in Mecp2 KO mice. Plot of average symptom scores showing phenotypic severity progression in Mecp2 KO treated mice and WT mice invariably score 0. (Vehicle group n=30, mice treated with L-Dopa / Ddci n=30, mice treated with L-DOPA alone n=20, mice treated with Ddci alone n=15; \* p< 0,05; \*\* p< 0,01; \*\*\* p< 0,001)

#### 5.2.4. Life span of Mecp2 KO mice after L-Dopa / Ddci treatment

L-Dopa / Ddci treatment significantly lengthened the life span of Mecp2 KO mice. The vehicle group lives an average of  $68,9 \pm 3,08$ ; and the L-Dopa/Ddci treated group lives  $80,5 \pm 4,4$  days; p<0,001, Kaplan–Meir log-rank test (Figure 27). This represents an increase in duration of life span of about 11 days. Taking into account that average life span of Mecp2 KO mice is about 70 days, prolongation of 11 days is already improvement at about 15-20 %.

## Results Part 2

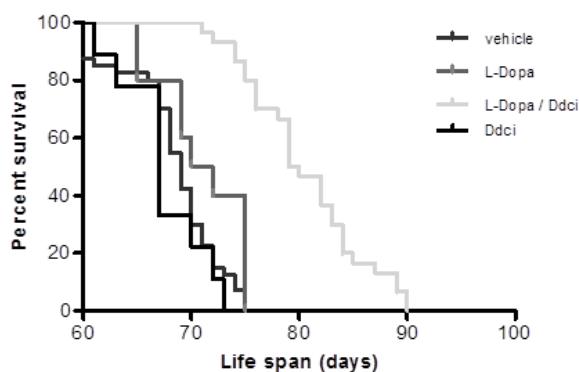


Figure 27. Treatment with L-Dopa / Ddci prolongs survival in Mecp2 KO mice (vehicle group  $68,9 \pm 3,08$  days; Ddci  $67,45 \pm 2,8$  days L-Dopa  $71 \pm 3,4$  days; L-Dopa / Ddci :  $80,5 \pm 4,4$  days;  $***p < 0.001$ ; vehicle  $n=30$ , mice treated with L-Dopa / Ddci  $n=30$ , and mice treated with L-Dopa alone with  $n=10$ ).

### 5.2.5. Partial rescue of locomotor deficits in Mecp2 KO Mice after L-Dopa / Ddci therapy

Alterations in the nigrostriatal pathway can lead to the reduction of Dopamine concentration, mostly in the CPU terminals, which are involved in motor impairments (189). Administration of L-Dopa/Ddci stimulates the DA metabolism and improves the mobility of Mecp2 KO mice. As it is mentioned, the mice were treated from 4 weeks of age. First we evaluated the impact of treatment on the locomotion using the mobility score test. We detected significant differences during the whole treatment between all treated groups, with the focus on vehicle versus L-Dopa / Ddci and L-Dopa alone versus L-Dopa / Ddci. We thus launched a preclinical trial with 3 groups of Mecp2 KO mice: L-Dopa; L-Dopa / Ddci, and vehicle. Our results detected beneficial effects of L-Dopa /Ddci treatment, representative by the shorter time used to cross the bar and the lower number of slips in comparison, not only with the vehicle group but also when compared to the L-Dopa treatment alone (one-way ANOVA with post hoc Bonferroni's Multiple Comparison, Figure 28). The time that L-Dopa/Ddci treated mice spend to cross the bar decrease respect to the time spent by vehicle control group. It is also dependent on the age of mice, being most significant at 8 and 9 weeks, when the time to cross is reduced 50% respecting to the vehicle (figure 28A). At 8 weeks the L-Dopa/ddci treated group spends around 12 sec while the vehicle group spends around 25 sec. At 9 weeks of age, the vehicle group spends around 35 sec, and the L-Dopa/ddci treated group spends 18 sec. The L-Dopa treated group always spends an intermediate time between the vehicle group and the L-Dopa/Ddci treated one.

However, reduction in the number of slips is only significant at 8 weeks. At that time the reduction is around 40%, from 10 slips in the vehicle, to 6 in the L-Dopa/Ddci treated group (Figure 28B). All presented data support the hypothesis that administration of L-Dopa/Ddci to Mecp2 KO mice has improved significantly their locomotor dysfunctions.

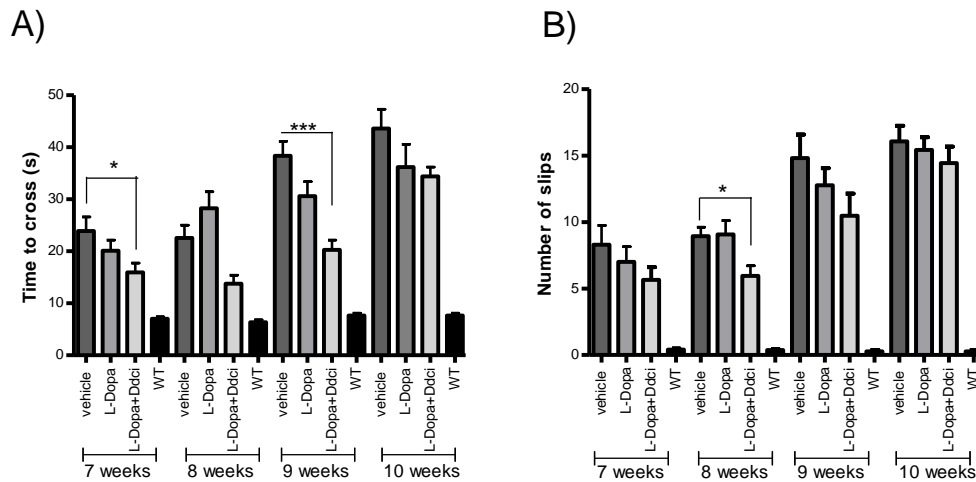


Figure 28. Changes in motor capabilities in Mecp2 KO mice with and without treatments. A) Bar cross test was carried out once per week. The time spent to cross the bar and B) the number of slips were quantified from 4 to 10 weeks of age. Representative graphs for 7,8, 9 and 10 weeks of age are shown. Combination treatment of L-Dopa / Ddci rescues locomotor deficits in Mecp2 KO mice. Graphs are representing the mean of two independent experiments +/- SEM; \* p< 0,05; \*\* p< 0,01; \*\*\* p< 0,001 with n=10 for each tested group.

### 5.2.6. Level of dopamine after administration of L-DOPA with DDCI in MeCP2 mice

It is already described that L-Dopa has a protective effect on dopaminergic neurons (236, 244) and dopaminergic neurons are believed to be particularly prone to oxidative stress due to their low levels of antioxidants (245). The levels of norepinephrine and dopamine in RTT are reduced (231). The L-Dopa/Ddci treatment could provide an efficient dopaminergic stimulation therapy as previously described in Parkinsonism and related disorders (243). In order to check and verify if by injection with Ddci the level of L-Dopa that can cross the BBB is higher, the dopamine level was measured in the brain tissue.

L-Dopa + Ddci-treated group significantly recovered dopamine levels in hippocampus and caudate putamen, but not in Frontal Cortex when compared to the vehicle-treated group (Figure 29). Thus, an activation of Dopaminergic neurons is a likely mechanism

## Results Part 2

that explains the observed improvement of the Rett syndrome phenotype upon the combined administration of L-Dopa + Ddci.

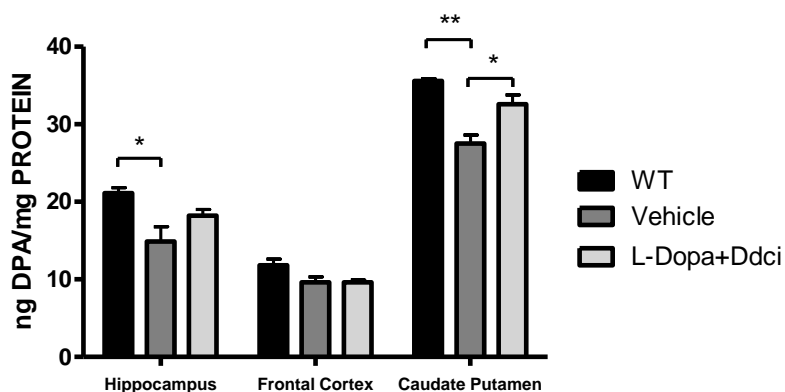


Figure 29. Dopamine concentration normalized with the respective total protein amount in hippocampus, frontal cortex and caudate putamen of WT and Mecp2 KO mice treated with vehicle or L-Dopa + Ddci. All animals were analysed 4 weeks post-treatment (8 weeks old); n = 3 per group. One-way ANOVA and a Bonferroni HSD post-hoc test were used for statistical comparison; \* p < 0,05; \*\* p < 0,01.

### 5.2.7. Dendritic spine density in Mecp2 KO mice after L-Dopa/Ddci treatment

Morphological studies in postmortem brain samples from RTT individuals described a characteristic neuropathology. Amongst many, the neuropathology included decreased neuronal size and increased neuronal density in the cerebral cortex, hypothalamus and the hippocampal formation (246). Decreased dendritic growth in pyramidal neurons of the subiculum, frontal and motor cortices was also noticed (247). We have already shown that LDopa/Ddci treatment has a positive effect in behavioural tests. The next point was to check if after L-Dopa /Ddci treatment it is possible to obtain improvement on spine pathologies described before in Mecp2 KO mice.

Based on the previous work, that abnormalities in morphology, density of dendritic spines and reduction of synaptic activity are related with the hippocampus region (138, 152, 248), the analysis of dendrites by Golgi staining were performed in this region of treated Mecp2 KO mice (Figure 30 A).

We have examined the number of spines in ten dendrites for each group of animals over a length of 20  $\mu$ m (3 animals for each treated group). The number of spines was calculated with Neuronstudio software and the Sholl analysis algorithm (223). The

results are displayed in figure 30 where it is indicated that total number of spines in Mecp2 KO mice was significantly decreased compared to WT littermates, what has confirmed also the previous obtained results. However after the treatment with L-Dopa alone or with the combination of L-Dopa/Ddci, we showed that number of spines is increased. It was considerably in Mecp2 KO mice, from 13 +/-0,8 in the Mecp2 KO mice to 17 +/- 1,8, and 24 +/- 0,9, in the presence of L-Dopa, and L-Dopa/Ddci, respectively. Important to notice that only the increase related to L-Dopa/Ddci is statistically significant (figure 30B).

We also have analysed the mushroom spine density, as more mature type of spines (133). The obtained results were similar. Mushroom spine density is also higher in WT than in KO mice, 23 +/- 3,5 versus 6 +/- 1,4, respectively and the number in KO mice treated with L-Dopa/Ddci increased to 9 +/- 0,9. No significant difference was observed in the number of spine between L-Dopa and vehicle treated mice (Figure 30C). These results suggest that when the animals are treated with L-Dopa/ Ddci, the synaptic function is activated.

## Results Part 2

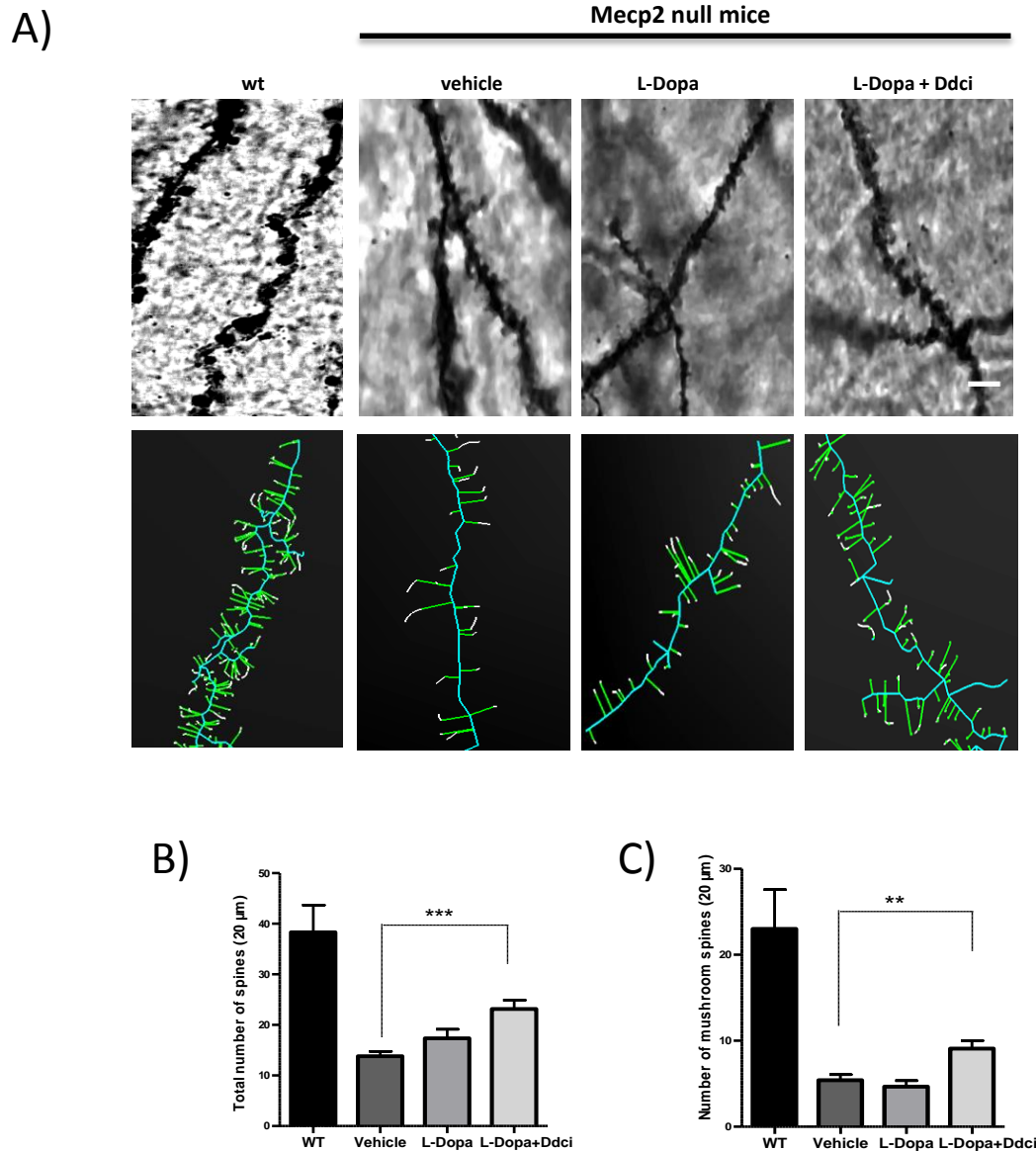


Figure 30. Spine density in Mecp2 KO and WT animals determined by Golgi staining, Sholl analysis. A) Changes in dendritic spine density in hippocampus region of WT, Mecp2 KO and Mecp2 KO treated mice. B) Total spine density and C) the number of mushroom spines in hippocampus of WT and Mecp2 KO mice with or without treatment were acquired with a Zeiss wide field microscope, magnification of 63X 1.4 NA. Bars are showing the number of spines (mean $\pm$  SEM) in hippocampus region of Mecp2 deficient mice with L-Dopa / Ddci or L-Dopa treatment, versus control KO animals and WT littermate. Dendritic segments of 20  $\mu$ m were analysed for each group. All images were taken with Zeiss microscope 63 X, and processed with Neuron studio software; \*\*  $p < 0,01$ ; \*\*\*  $p < 0,001$ .

### 5.2.8. Changes in levels of DRD2 dopamine receptors after L-Dopa/Ddci treatment

It is already described that DRD2 receptor is involved in the spinogenesis process (182). To evaluate whether DRD2 was activated after the treatment, quantitative real time-PCR with total RNA isolated from MB from WT, vehicle, L-Dopa and L-Dopa /Ddci treated mice was performed. The comparison between all experimental groups showed that the combination L-Dopa /Ddci increases the level of DRD2 receptor, confirming the synaptic activation and density results (Figure 31).

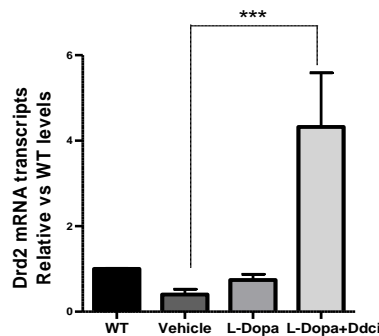


Figure 31. LDopa/Ddci treatment causes an increase in DRD2R level. All transcripts levels were determined using RT-qPCR (Applied Biosystem). The values (mean  $\pm$  SEM) are the ratio vs WT , \*\*\* $p < 0.001$ ;  $n = 3$  for each studied group.

### 5.2.9. pTh and Th-positive neuron numbers in Mecp2 KO mice after L-Dopa / Ddci treatment

As mentioned before, the catecholamine dopamine and norepinephrine, important as hormones and neurotransmitters in both the central and peripheral nervous systems, have reduced levels in RTT (192). Th is the rate-limiting enzyme of catecholamine synthesis. It catalyzes the hydroxylation of tyrosine to L-DOPA (249). In addition, the phosphorylation of Th at Ser40 increases the enzyme's activity *in vitro*, *in situ* and *in vivo*. L-Dopa/Ddci treatment improves the locomotor activity, decreases the score of tremor and breathing in RTT mouse. In order to elucidate the molecular mechanism that could be the explanation for the better score of treated mice, we analysed the protein levels of Th and pTh (pSer-40 Th). The activity of Th can be modulated by two mechanisms: medium- to long-term regulation of gene expression (enzyme stability,

## Results Part 2

transcriptional regulation, RNA stability, alternative RNA splicing and translational regulation) and short-term regulation of enzyme activity (feedback inhibition, allosteric regulation and phosphorylation (250).

We measured the intensity of staining of Th and pSer-40Th in Th expressing neurons from SNpc localized in MB from *Mecp2*-deficient mice of 4 weeks post-treatment (8 weeks age). Mice were treated with L-Dopa / Ddci, L-Dopa alone or vehicle. In figure 32 we can see the differences in Th and pTh immunostaining between WT and *Mecp2* KO. The vehicle has less than 50% of Th immunostaining. Th levels increases when the mice are treated with L-Dopa and LDopa/Ddci, being more pronounced in the combined treatment, reaching even the WT levels (Figure 33A). One regulatory mechanism of Th includes phosphorylation of Ser 40 (Dunkley et al 2004). The active form of Th is pSer-40 Th, which is reduced in *Mecp2* deficient animals when increasing severity of the symptoms (189). We have analysed the intensity of staining of pSer-40 Th in MB sections. The data are showing an increase in pSer-40 Th integrated intensity signals when L-Dopa/Ddci versus LDopa alone was administered and vehicle controls normalized versus WT. These differences were significant when we analysed with ANOVA and multiple comparison test ( $p < 0,001$ ), except for L-Dopa vs vehicle controls where we have not obtained any differences (Figure 33A, lower panel).

To corroborate the results presented above, we obtained total extract from MB region and analysed Th protein level by western blot using specific antibody. As show in figure 33B, Th expression in the L-Dopa/Ddci group was increased when compared with all others, however the quantified level showed no significant difference between LDopa and vehicle controls. Our results indicated that at 8 weeks of age L-Dopa / Ddci treatment favors that the protein content augments in the MB of the *Mecp2* KO mouse model. Several authors have described that L-Dopa have positive neurotrophic effects for dopaminergic neurons, facility the survivals and neurite outgrowth (244, 251). Here, we have shown that administration of L-Dopa/Ddci recovers the levels of Th and pTh positive neurons. It is probably by a positive allosteric regulation mechanism, where the increase amount of L-Dopa, the product of Th, increase the level of the Th enzyme. The levels of Th are recovered up to WT status but the levels of pTh are not, meaning that in *Mecp2* KO mice this step is limited for unknown yet reasons.

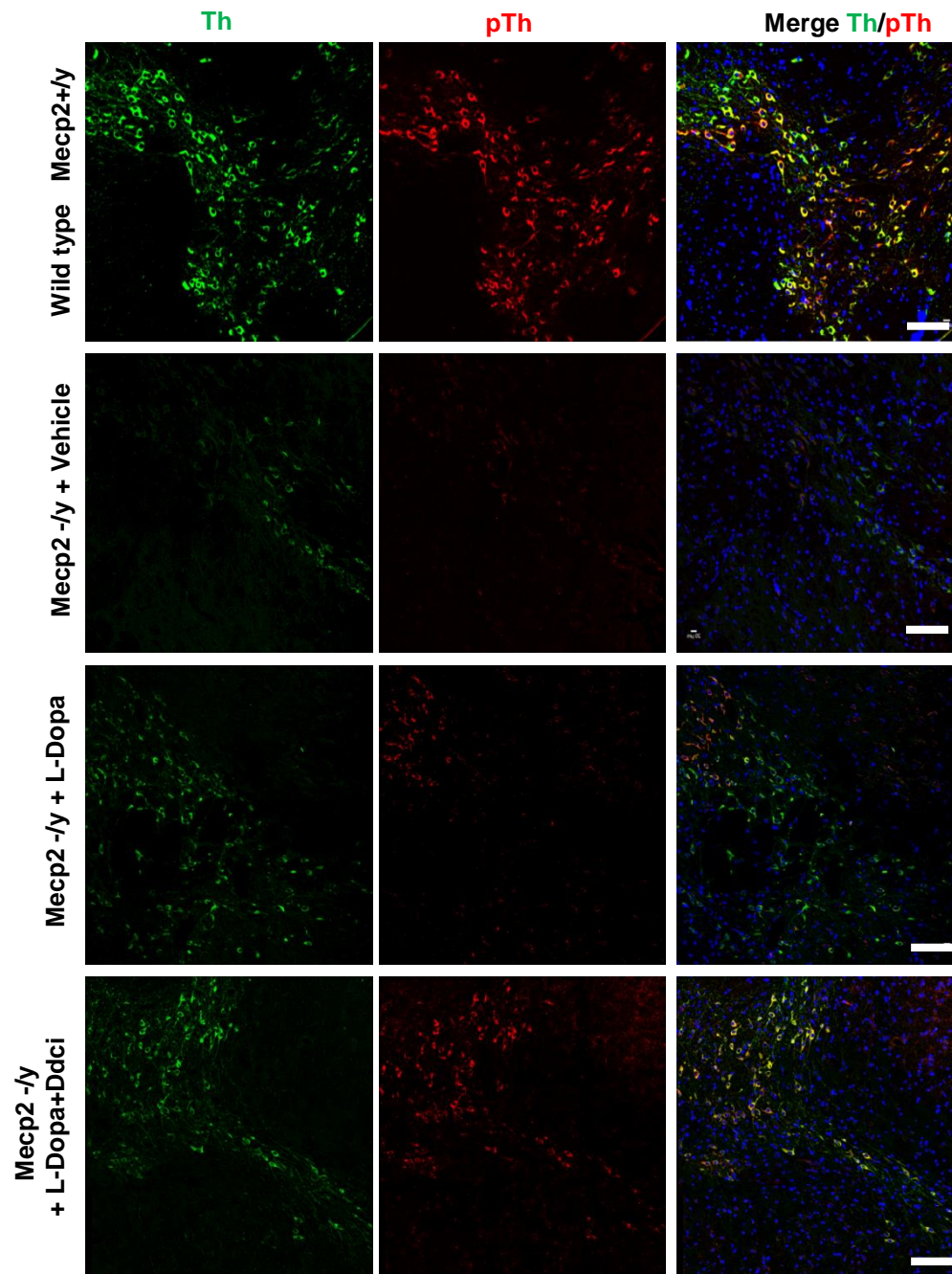
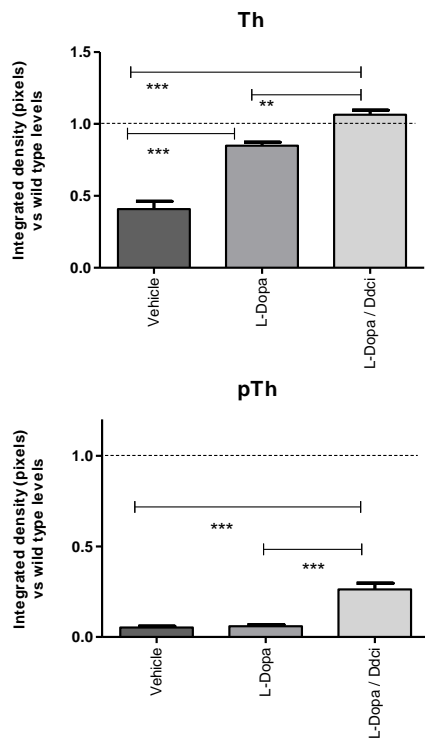


Figure 32. Increase in pTh and Th levels in Mecp2 deficient mice treated with L-Dopa Ddci vs L-Dopa alone and vehicle control. Representative immunostaining of coronal brain sections from SNpc. mDA neurons were coinmunostained for Th (green), pTh (pSer-red) and DAPI counterstain (blue). Scale bar=20 $\mu$ m.

## Results Part 2

A)



B)

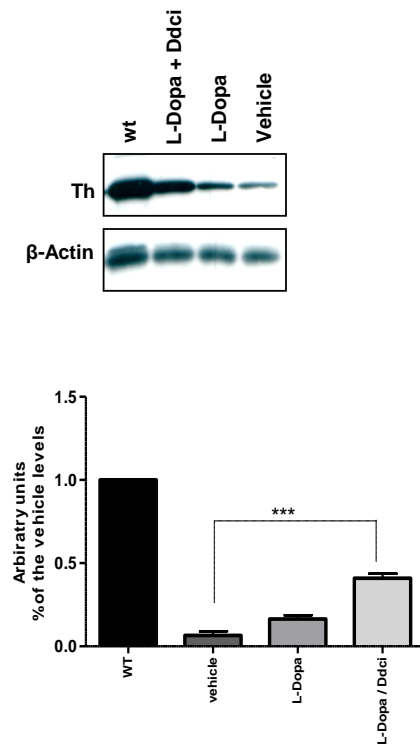


Figure 33. Increase of pTh and Th levels in Mecp2 deficient mice treated with L-Dopa Ddci. A).Quantification of Th and pTh positive staining in all experimental groups mentioned above in figure 32. The bars represent the Integrated density (ImageJ Fiji vs 1.47) of picture realized with Confocal microscopic SPS5, obj 63X. B) Representative western blot showing the levels of Th protein in MB from four experimental groups. Actin was used as loading control. All animals were analysed 4 weeks post-treatment (8 weeks age), n=3/ each groups. One-way ANOVA and Bonferoni posthoc test was use as comparative statistic, \*\*p< 0,01; \*\*\* p< 0,001.

### 5.3. Part 3 Glycogen synthase kinase-3 inhibitor, SB216763, displays therapeutic potential in a mouse model of Rett syndrome

Since GSK-3 is important in neural developmental activities, such as neurite growth and specification, or synapse development we proposed this pathway as a possible target for Rett therapy. GSK-3 consist of two members, GSK-3 $\alpha$  and GSK-3 $\beta$  that show 98% sequence indentity within their kinase domains and overall share 85% amino acid sequence identity (252). Both of the kinases are highly expressed in brain, including one of the two splice variants expressed in the developing nervous system (253). Overexpression of GSK-3 $\beta$  in the brain results in hyperactivity and mania (254). It also has an important function in downstream signalling of dopamine receptors (255), showing that GSK-3 $\beta$  regulates behavioural functions by downstream signalling of neurotransmitter receptors.

Overexpression of a constitutively active GSK-3 in cultured neurons reduces expression and clustering of a synaptic protein Synapsin I (256), while pharmacological inhibition of GSK-3 activity induces Synapsin I clustering in developing neurons (257). Activation of glycogen synthase kinase-3 inhibits expression of postsynaptic markers. In contrast, pharmacological inhibition of GSK-3 activity induces Synapsin I clustering in developing neurons (258). Moreover, GSK-3 activation reduces presynaptic glutamate release by inhibiting the synaptic vesicle exocytosis in response to membrane depolarization (259). GSK-3 $\beta$  negatively regulates synaptic vesicle fusion events via interfering with Ca<sup>2+</sup>-dependent SNARE complex formation.

A recent study has reported functional roles of GSK-3 in the regulation of N-Methyl-d-aspartic acid (NMDA) receptor dependent synaptic plasticity (260). Activation of GSK-3 mediates NMDA-dependent long term depression (LTD) induction. In contrast, inhibition of GSK-3 activity prevents LTD induction and participates in long term potentiation (LTP) induction (256).

In order to check whether targeting this pathway is possible to improve the phenotype or increase the life span of Rett mice, we decided to use SB216763 as a GSK-3 $\beta$  inhibitor for our preclinical studies. It is known, disordered neural immune system might contribute to autism, unsocial behaviour also in RTT syndrome (261). GSK-3 is involved in inflammation in the brain. Besides, microglia is extremely responsive to inflammatory signals. Inflammation and oxidative stress, which includes microglial

### Results Part 3

activation, are blocking production of new hippocampal neurons connections (Figure 34).

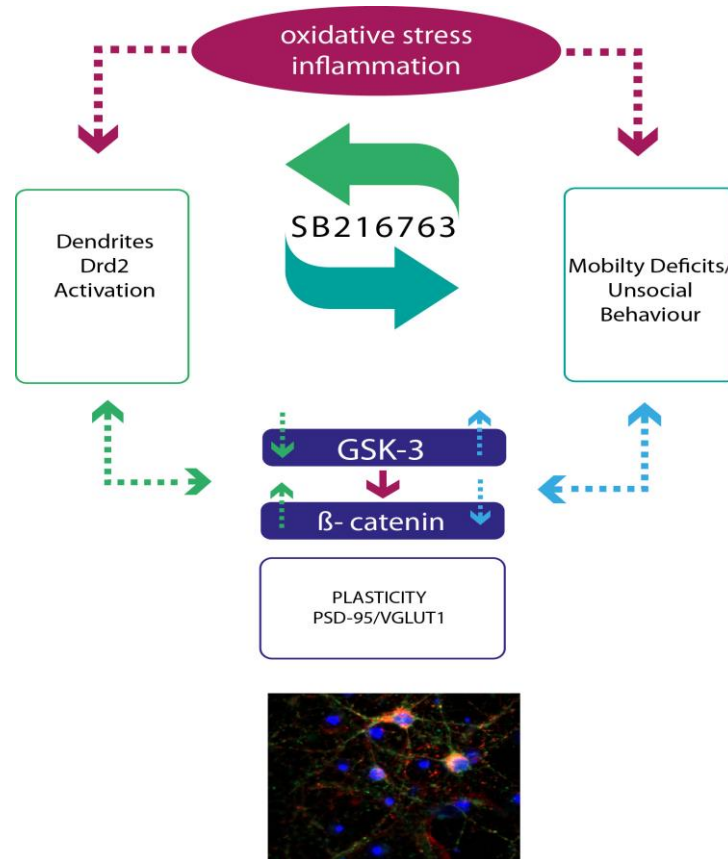


Figure 34. Cross talk between neuroinflammation, oxidative stress, GSK-3/β-catenin pathways and synaptic plasticity. Oxidative stress is recognized to influence neuroinflammation and GSK-3 activation is followed by phosphorylation and consequent degradation of β-catenin. However by blocking inflammation β-catenin is indirect able to activate DRD2 (based on (262)).

#### 5.3.1. Determination of possible toxic effect on Mecp2 KO mice during SB216763 treatment

Based on the literature three different doses of SB216763 inhibitor were used: 0,1; 0,5 and 1mg/kg/day. For each dose we use 5 mice. Vehicle Mecp2 KO animals displayed a steady increase in the severity of the RTT-like phenotype. The total score shows a tendency for the rescue of the RTT phenotype, being most detectable in the case of 0,5mg/kg/day SB216763 treatment. During the whole experiment none of the selected

doses induced a weight loss in the Mecp2 KO mice. Besides no negative effect on the life-span during the drug treatment in comparison with the vehicle Mecp2 Ko group was observed. The drug was well tolerated (Supplementary Figure 13 and 14).

For 0.5mg/kg/day dose we made a representative weekly average of the weights of all animals. Mecp2 KO mice treated with vehicle or inhibitor display same average weight. No toxicity was associated with SB216763 treatment. No difference in weight of animals between vehicle and SB216763 treated groups were obtained (Figure 35).

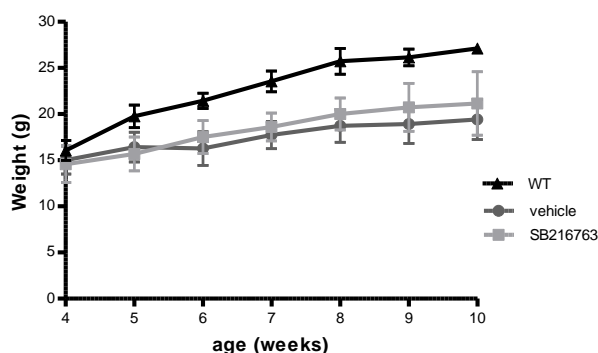


Figure 35 No effect on body weight was observed after the drug treatment in Mecp2 KO mice, however Mecp2 KO mice display reduced body weight compared with the WT animals (vehicle n=10, mice treated with SB216763 n=10).

### 5.3.2. Single and total symptoms score after SB216763 treatment

After the dose optimization experiment the symptom onset was evaluated in SB216763 Mecp2 KO mice. We measured score of mobility, tremor, breathing, gait, hindlimb clasp and general condition (Figure 36). The plots show the overall distribution of symptoms at 7, 8, 9, and 10 weeks of age. All vehicle and drug treated mice developed neurological symptoms. During each week of treatment the score values were calculated separately, then normalized with respect to the vehicle group using one-way ANOVA with Bonferoni's post hoc multiple comparison.

The scores show a significant improvement in mobility, tremor and breathing from 7 to 10 weeks of age in the treated group versus the vehicle control. Treatment with GSK-3 inhibitor improved mobility, tremor and breathing phenotype by an average of 50-60% respect to untreated KO mice, having also effect on older mice KO mice after the drug administration suffer less the tremor, and breathing irregularities. SB216763 treated mice at the vehicle "end point" are still in a good condition. The symptoms in treated

### Results Part 3

animals are less severe. Regarding the phenotypes of gait, hindlimb clamping or general condition symptom, a significant improvement was also observed but at less extent, and the trend became significant in older mice. If we plot the average of the six scored symptoms to create a total score, a significant phenotypic improvement is observed during the whole time of the treatment. SB216763 induced slower progression of the disease, and some of the treated mice did not develop any detectable symptoms until 8 weeks of age (Figure 37).

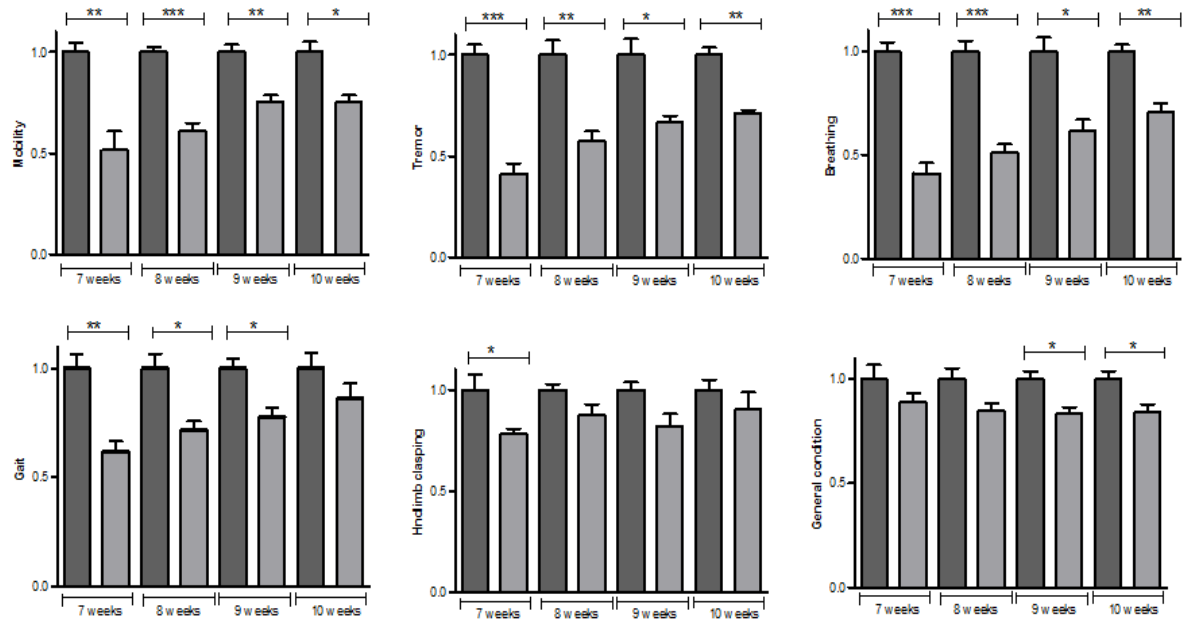


Figure 36. Treatment with SB216763 reduces symptoms in Mecp2 KO mice (vehicle n=25, mice treated with SB216763 n=25). A) Plot of average symptom scores representing mobility, tremor, breathing B) gait, hindlimb clamping and general condition scores normalized vs control group, \*p< 0,05; \*\* p< 0,01; \*\*\* p< 0,001.

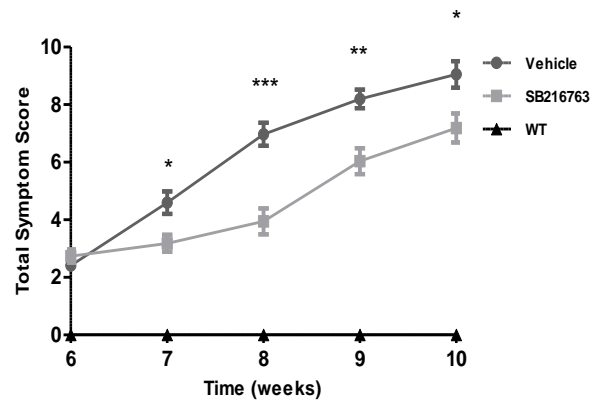


Figure 37. Treatment with GSK-3 inhibitor reduces symptoms in *Mecp2* KO mice. Representative plot of average symptom score showing phenotypic severity progression in *Mecp2* KO untreated mice and significant improvement in SB216763 treated group;  $p < 0,05$ ; \*\*  $p < 0,01$ ; \*\*\*  $p < 0,001$ .

### 5.3.3. Evaluation of the life span in *Mecp2* KO mice treated with SB216763

Given these positive results that SB216763 improved the score of *Mecp2* KO mice, we wondered whether GSK-3 inhibitor could affect life span of RTT KO mice. The mice treated with SB216763 displayed positive effect on the survival of KO mice. Figure 38 presents the average of life span of vehicle and treated group (Kaplan–Meier log-rank test). The vehicle group display the average life span of 70 days. In the SB216763 treated group the average life span is 91 days, meaning an improvement of 21 (\*\*  $p < 0,01$ ). Considering the whole population of *Mecp2* treated mice survival curve was even 30% longer when compared to the vehicle group. The administration is improving the general condition of animals. They do not suffer sudden weight loss what allow them to live longer.

Thus, the drug administration in *Mecp2* KO mice increases their well-being overall by diminishing Rett syndrome symptomatology.

## Results Part 3

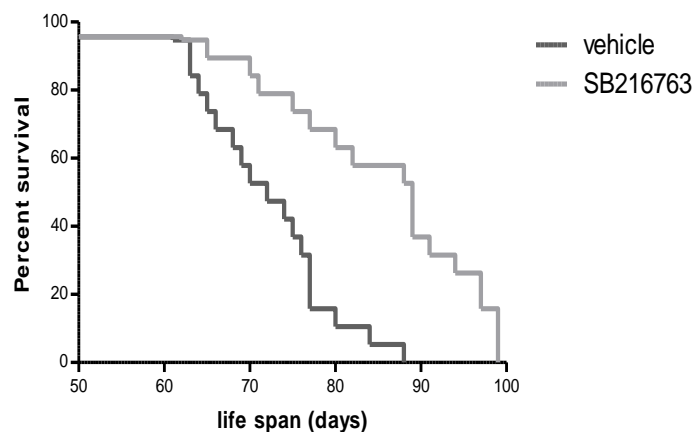


Figure 38. Treatment with SB216763 prolongs life span of the RTT animals. Treatment with GSK-3beta inhibitor prolongs survival in *Mecp2* KO mice (vehicle group 70 days; SB216763: 91 days; \*\* $p < 0.01$ ; vehicle 25 and mice treated with SB216763 with  $n=19$ ).

### 5.3.4. Assessment of mobility deficits in *Mecp2* KO mice after SB216763 treatment

GSK-3b heterozygous (+/-) show multiple neurobehavioural abnormalities including aggressive behaviours, increased anxiety, reduced movement, and poor memory processing (263).

To address in an unbiased manner whether SB216763 administration can be associated with an improvement in the motor impairments in the *Mecp2* KO mice, we followed the battery of the behaviour test previously described in Material and methods. A few behavioural tests were performed in order to validate the improvement after administration.

#### 5.3.4.1. Bar cross test

We undertook bar cross test, performed weekly. It was observed that the GSK inhibitor was able to improve test performance in comparison with the vehicle-treated group. Rett model mice receiving the drug regimen achieved the better scores, such as a shorter time to cross the bar and fewer number of slips. Figure 39 shows that besides

delayed time to cross the bar, Mecp2 KO vehicle animals display higher number of slips when compared to WT mice. However, the drug restored the mobility deficits. The observed effects were specific for SB216763 administration. Overall response to the drug treatment was even 60%, reflecting that Mecp2 KO drug-treated mice slipped away less than their vehicle, showing clear improvement. Mecp2 KO exhibited a marked tendency to slip off the bar, a sign of ataxia. KO treated mice failed significantly less and were able to maintain balance. Taking into account that Mecp2 KO mice instead of walking and maintain a stable upright posture, they displayed ventral recumbence it is worth to mention that drug administration was able to reduce the ventral recumbence problem.

At 8 weeks the treated group to cross the bar spends around 17 sec while the vehicle group spends around 25 sec. At 9 weeks of age, the vehicle group spends around 35 sec, and the SB216763 treated group spends 25 sec. Reduction in the number of slips was also significant at 7 and 8 weeks. At 7 weeks the reduction is around 30%, from the average of 10 slips in the vehicle mice, to average of 7 in the treated animals. At 8 weeks of age the improvement in the treated group is still about 30%, presenting 10 slips for treated group, and 13 for the vehicle animals.

At the 10 weeks of age 3 out of 10 vehicle KO mice were not able to complete the test, while KO treated mice present still significant improvement related to time to cross the bar, and the tendency to lower slips number. At the end of the experiment vehicle KO mice indicate rapid weight loss and sudden aggravation of symptoms lead to death.

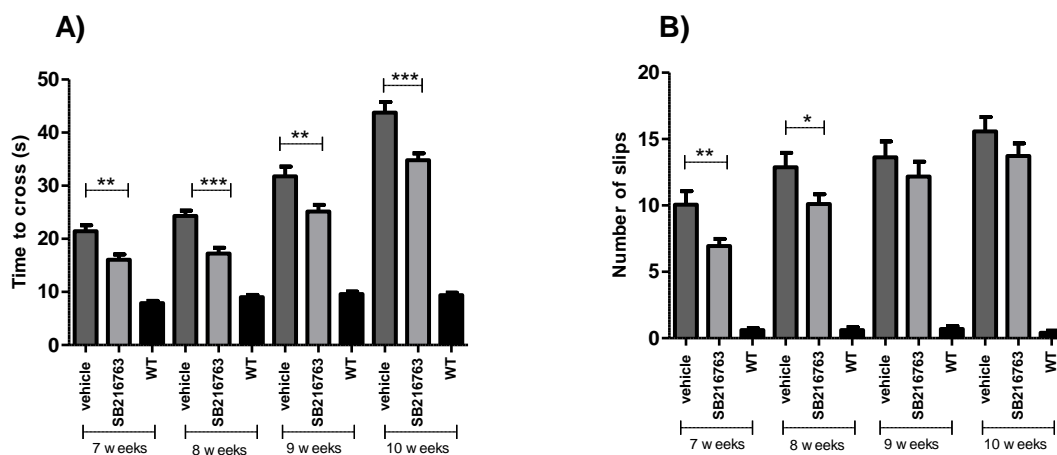


Figure 39. Treatment with SB216763 rescues locomotor deficits in Mecp2 KO mice. Bar cross test was carried out once per week; A) the time spent to cross the bar and B) number of slips were quantified from 7 to 10 weeks of age. Graphs represent the mean +/- SEM; n=10/ per group; p < 0,05; \*\* p < 0,01; \*\*\* p < 0,001.

## Results Part 3

### 5.3.4.2. Open field test

Motor function and anxiety were also evaluated using the well-established OPT. The performed OPT with SB216763 treatment has positive feedback. It suggests that present Rett phenotyping progress was improved after the drug administration. Replicable differences between the three analysed groups were found in several different aspects of open field behaviour. KO animals displaying restlessness compared to WT controls. Mecp2 KO untreated mice travelled shorter distances, performed more stops and spent less time in central area. More defecation bolouse, as an identification of anxious behaviour was detected in untreated KO mice, and this number was reduced after the drug treatment (Figure 40A). The SB216763 diminish the anxious behaviour increasing also the total rearing number when compared to KO vehicle group, reaching almost the level of WT animals, where the number was between 5 and 6 rearings / min (Figure 40B). The total number of crossing was similar in all studied groups indicating no significant changes (Figure 40C).

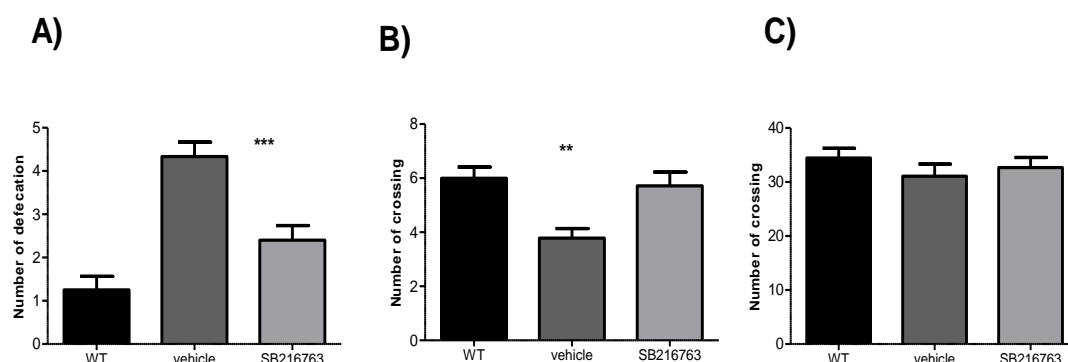


Figure 40. Improvement of progressive postnatal defects in locomotor and coordinated behaviours in RTT mice after SB216763 administration. A) The graphs show the behavioural performances in WT, Mecp2 KO vehicle and Mecp2 KO animals treated with SB216763 at 8 weeks of age. After SB216763 treatment the defecation bolouse is reduced suggesting the anxiety behaviour was reduced. B) OFT shows that the mean of rearings number is reduced in Mecp2 KO compared to WT, however after SB216763 treatment the recovery was observed (\*\*\*) C) The number of crossing between treated and untreated KO mice are similar in all tested groups. Graphs represent the mean +/- SEM; n=10/ per group.

### 5.3.4.3. Neophobia test

In addition to spontaneous movement, we also tested exploration and anxiety-related behaviour by assenting number of visited corners and rearing number. In neophobia

test obtained differences were clear between the KO and KO-treated group. We used a new cage each time for each single tested mouse. Number of visited corners was higher in SB216763 group and the number of rearing showed also a tendency to be improved after the drug administration. The number of visited corners was increased in the treated group mice, being around 10 for WT mice, 6 for Mecp2 KO vehicle, and 8 for KO-treated animals (Figure 41 A). In addition, KO mice exhibited higher number of rearings. The number for WT animal was 6 rearings per minute, KO untreated 2/min but for Mecp2 KO treated animals was about 4, suggesting approximately an improvement of 50% respectively to KO vehicle group (Figure 41B).

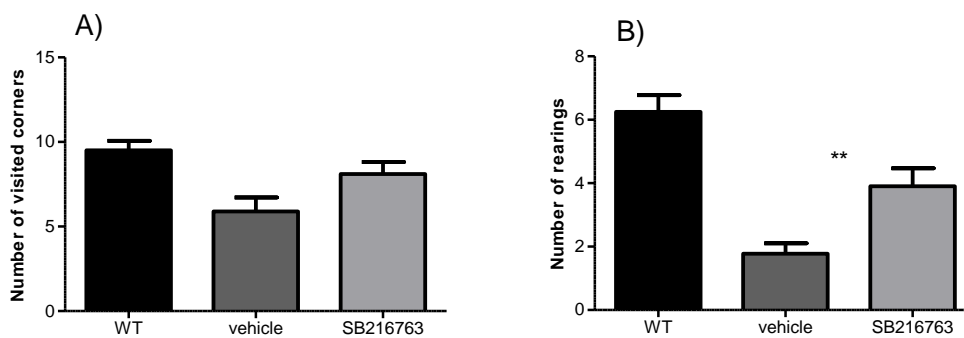


Figure 41. Exploratory and anxiety measurements obtained in the Neophobia corner test after SB216763 treatment. Bars showing sociability and social novelty preference in Mecp2 KO treated versus Mecp2 KO vehicle mice. SB216763 drug diminished neophobia in M ec p2 KO mice and showed visible tendency of improvement (A) in higher numbers of visited corners and performed B) higher rearings number (\*\*  $p < 0.01$ ). Mean  $\pm$  S.E.M.;  $n=10$ / per group.

#### 5.3.4.4. Wire grip test

Previously obtained data between WT and Mecp2 KO mice confirmed that 8 week-old Mecp2 mice display increased anxiety-like behaviours. Compared with WT mice as assessed by the elevated wire grip test, Mecp2 KO suffer impaired motor coordination, however with SB216763 treatment we can see some tendency to betterment.

SB216763 treated KO mice display significant difference interaction on forelimb grip performance. The number of crossed segments in SB216763 group was higher than in Mecp2 vehicle KO mice, reflecting in 11 crossed segments in WT mice, 4 in KO-untreated and 6 in SB216763 treated animals (Figure 42A). In treated group also problem to keep the wire during one minute of time is less detectable. The untreated Mecp2 KO can complete the test only with average of 60% respectively to the WT

### Results Part 3

littermates. However, after the drug administration results obtained in KO SB216763 treated mice are similar to WT group. The majority of treated-KO mice complete the whole test, keeping the wire during one minute of time (Figure 42B).

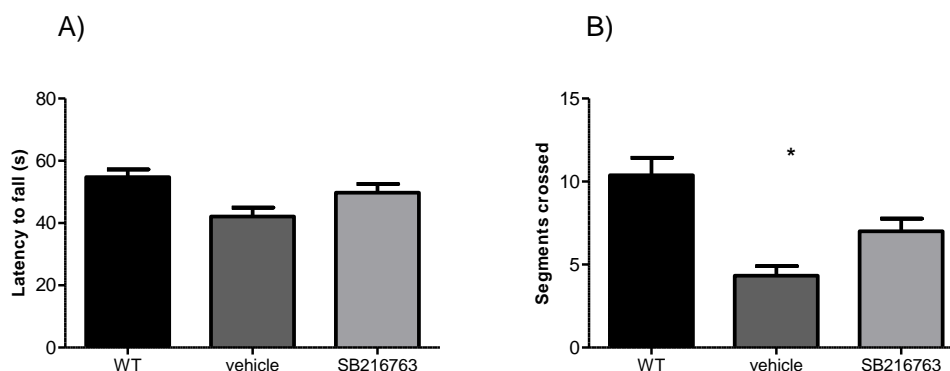


Figure 42. Treatment with SB216763 rescues locomotor deficits in Mecp2 KO mice. Grip strength test was carried out 8 weeks of age. Graphs represent the mean  $\pm$  SEM. A statistically significant difference was observed between the three groups. A) SB216763 treatment rescues the phenotype of Mecp2 KO animals according to number of segments crossed ( $*p < 0.05$ ) and B) represents a tendency of improvement related to the forelimb and hind limb (latency).

#### 5.3.4.5. Y-maze test

For further confirmation phenotype improvement after the GSK-3 inhibitor administration, Y-maze testing was carried out. A three-armed runway in the shape of the letter Y was used as previously described to measure exploratory behaviours in our mouse model. The tested mice were also at the 4 weeks post-treatment (8 weeks old). The data showed that the number of repetition is similar in all studied groups (Figure 43A). Higher rearing number in KO-treated group is a good indicator of exploratory behaviour. In our experiments even 20% of improvement was observed after the drug injections (Figure 43B). The ratio representing the number of entrances divided by the number of repetitions also displays a tendency to be ameliorated in KO-treated mice. That detects faster phenotype progression in control KO mice (Figure 43C). Higher number of entrance (Figure 43D) and reduced defecation bolouse (Figure 43E) confirm positive effect on anxious RTT phenotype after the drug administration. Besides, it was noticed that Mecp2 untreated KO mice displayed a repetitive selfgrooming. That is a long duration of the normal pattern of grooming of the entire body.

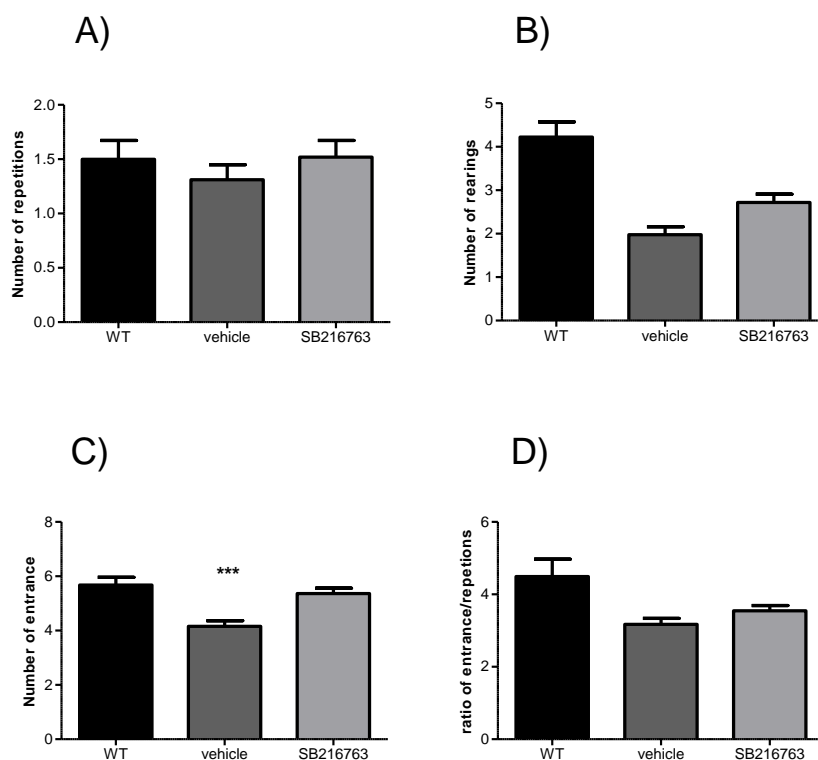


Figure 43. Exploratory and anxiety related measurement of the Y-maze test after the SB216763 treatment. Bars showing improvement in the number of repetition (A), rearing frequency (B) the ratio of entrance number entrances divided by number of repetitions (C) the number of entrance (D) and defecation bolouse (E). All parameters were improved in KO-treated group compared to vehicle group. Mean +/-S.E.M., n=10/ per group;\*\*\* p< 0,005

### 5.3.5. Levels of total and phosphorylated GSK-3 $\alpha$ and $\beta$ , $\beta$ -catenin before and after SB216763 treatment

Most functional studies of GSK-3 functions in neural development are based on pharmacological inhibitors. GSK-3 may also affect neuronal migration via regulation of  $\beta$ -catenin. It was already described that genetic manipulation of bcatenin in mice, either deletion or overexpression, leads to the disruption of brain and formation of spinal cord (264, 265).

GSK-3 may regulate neuronal migration during development by directing gene transcription and/or by rearranging the intracellular cytoskeleton. Results from  $\beta$ -catenin and active GSK-3 overexpression experiments suggest that both mechanisms may be important in neuronal migration. The role of GSK-3 and its clinical implication is essential. Defects in neuron migration are implicated in many neurodevelopmental

### Results Part 3

diseases (266). Moreover inhibition of GSK-3 was accompanied by marked upregulation of  $\beta$ -catenin (267).

We would like to investigate the link between GSK-3 $\alpha/\beta$  and  $\beta$ -catenin in WT, Mecp2 KO vehicle and KO mice treated with GSK-3 inhibitor. Levels of total and phosphorylated GSK-3 $\alpha$  and  $\beta$ ,  $\beta$ -catenin before and after SB216763 treatment were studied. 8 weeks of age WT littermates, Mecp2 treated and vehicle KO mice (4 weeks post treatment) were sacrificed to analyse the protein levels in Hippocampus region. The data was obtained by western blotting using appropriate Antibodies.

SB216763, does not affect the total level of GSK-3  $\alpha$  and  $\beta$ . Differences in levels of the GSKs are not statistically significant between any of the studied groups (Figure 44A). With regard to  $\beta$ -catenin a tendency was observed between WT and Mecp2 KO mice, with lower level in KO mice, and slight recovery after drug administration (Figure 44B). Then we measured the activity levels of GSK-3  $\alpha$  and  $\beta$ . Similar as in the rest of presented here experiment basal enzyme activity were analysed in hippocampal tissue from 8 weeks old KO and WT animals. In this region of brain the drug should be most effective. GSK-3 enzyme activity decreased after SB216763 treatment. Ph-GSK-3 $\alpha$  enzyme activity was significantly higher in KO mice but after administration of the selected inhibitor the level was similar to WT group, reaching 30% of decrease when compared to untreated Mecp2 KO mice. The same pattern was obtained for ph-GSK-3  $\beta$ , where SB216763 treated group reached 40% decrease of KO level (Figure 44C).

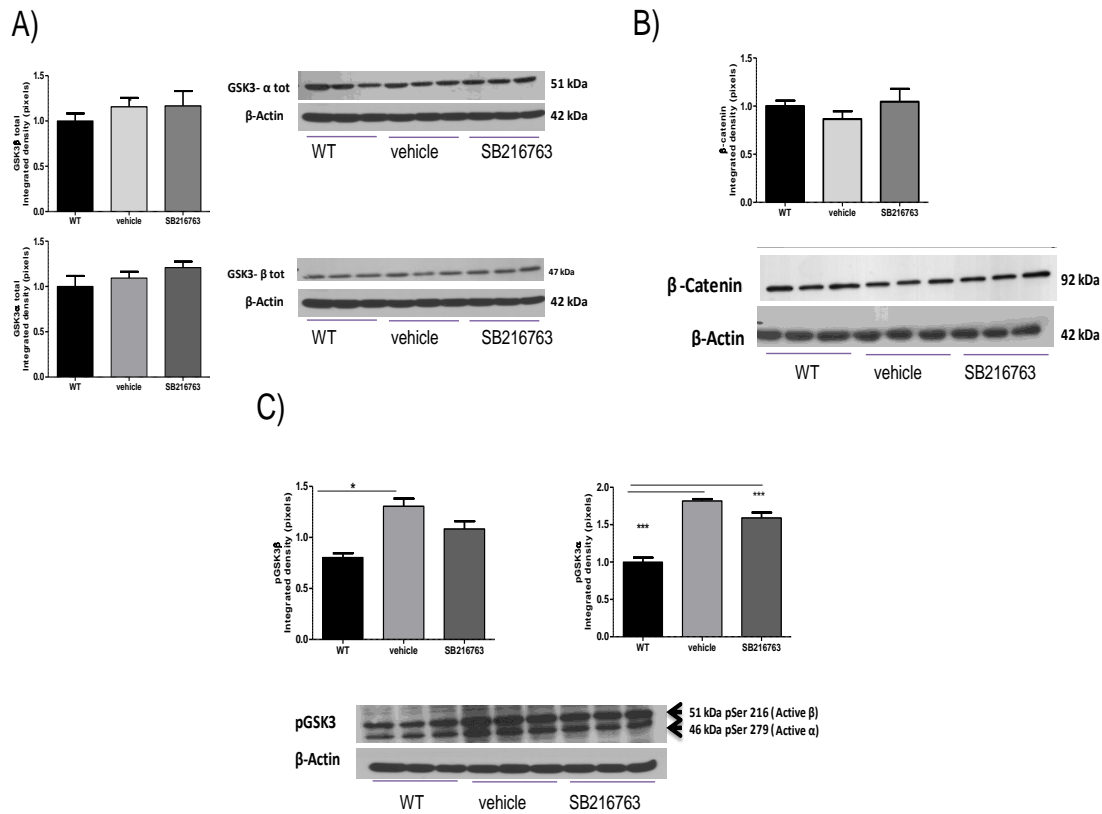


Figure 44. Characterization of total, ph GSK-3  $\alpha/\beta$  and  $\beta$ -catenin levels in hippocampus of Mecp2 KO mice after SB216763 treatment. A) Representative western blots of GSK-3  $\alpha$  (upper panel) and  $\beta$  (lower panel) and corresponding bands densities in three studied groups. B)  $\beta$ -catenin band densities and representative western blots corresponding to 3 groups. C) Western blotting of GSK-3  $\alpha$  and  $\beta$  enzymes activities analysed in WT and Mecp2 KO vehicle and treated animals. Values are mean  $\pm$  SEM,  $n=3$  each analysed group;  $p < 0,05$ ; \*\*  $p < 0,01$ ; \*\*\*  $p < 0,005$ .

### 5.3.6. Analysis of anti-inflammatory markers before and after SB216763 treatment - measurement of NF-kappaB activity

In 2008 it was described that pharmacological inhibition of GSK in primary cells reduces NF-kappaB activity (267). Intravenous (i.v.) injections of SB216763 inhibit inflammatory cytokine production in pulmonary alterations (inflammation and fibrosis). Pharmacological inhibition of GSK-3 in primary mouse hepatocytes reduced NF-kappaB activity (268). Since the brain of RTT is inflamed we were wondering how is the level of NF-kappaB in Mecp2 KO mice and if we can observed any changes after the GSK-3 inhibitor treatment.

Figure 45 shows representative western blot (Upper panel) of relative phosphorylation level of NF-kappaBp65 in WT and Mecp2 KO mice, with and without SB216763

### Results Part 3

administration. The level of NF-kappaBp65 is increased in Mecp2 KO mice relative to the WT mice. There is a slight but significant reduction in the level of NF-kappaBp65 after SB216763 treatment. Based on presented here western blot results we can conclude that the level of NF-kappaB in KO mice is even 50 % higher respectively to the WT, but after the administration the level can reach the WT baseline (lower panel).

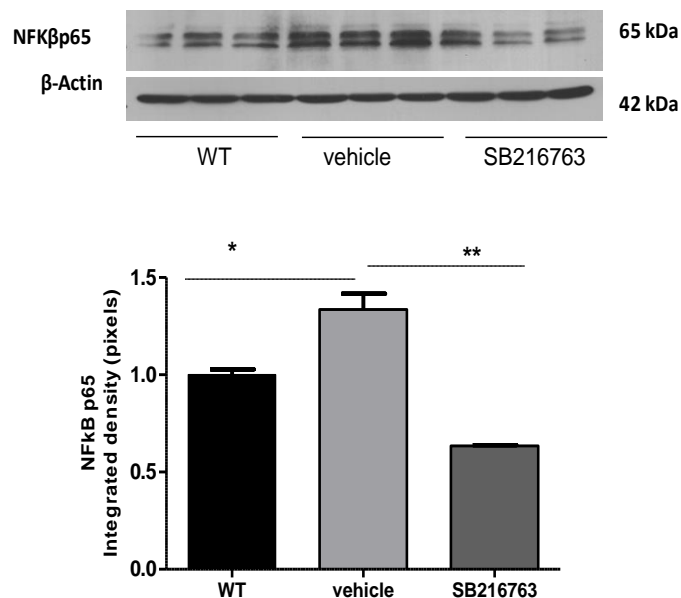


Figure 45. SB216763 treatment attenuated higher level of NF-kappaB in Mecp2 KO. Representative western blot shows the level of NF-kappaB p65 (NFKBp65) protein in hippocampal tissue from three experimental groups. β-actin was used as a loading control. Mean +/- SEM n=3 each group, p< 0,005; \*\* p< 0,01.

#### 5.3.7. Level of GSH in MeCP2 mice after administration of SB216763

In 2011 GSK-3 inhibition was suggested as an activator of antioxidant response, which prevented ROS production during neuronal ischemia (269). We first obtained dysregulated glutathione beam in Mecp2 KO mice. Next, it was interesting though to check the level of this ROS scavenger in mice treated with selected inhibitor of GSK-3. SB216763 administration rescued the level of GSx (Figure 46A). The level of GSH in Mecp2 KO mice treated with SB216763 when compared to vehicle mice was also higher in treated animals. GSSG level was lower in treated mice, what later on reflect in higher ratio of GSH/GSSG in treated mice (Figure 46B)

The decreased GSH and the increased GSSG in our RTT mice confirms the hypothesis that ROS generation process is accelerated in chronic inflammation of brain

tissue (Figure 20). However the drug treatment is able to recover the GSH level and also decrease the GSSG level. These results suggest a potential role of SB216763 in reduction of brain inflammation.

After drug administration at 8 and 10 weeks of age, the levels of GSH in Mecp2 KO mice SB216763-treated is increased when compared to the untreated Mecp2 KO mice, reaching a 50% of the GSH in WT mice (Figure 46B middle graph). These results could suggest that by targeting the GSK-3 pathway in the brain of RTT mice, oxidative stress is reduced and that the drug could have neuroprotective properties.

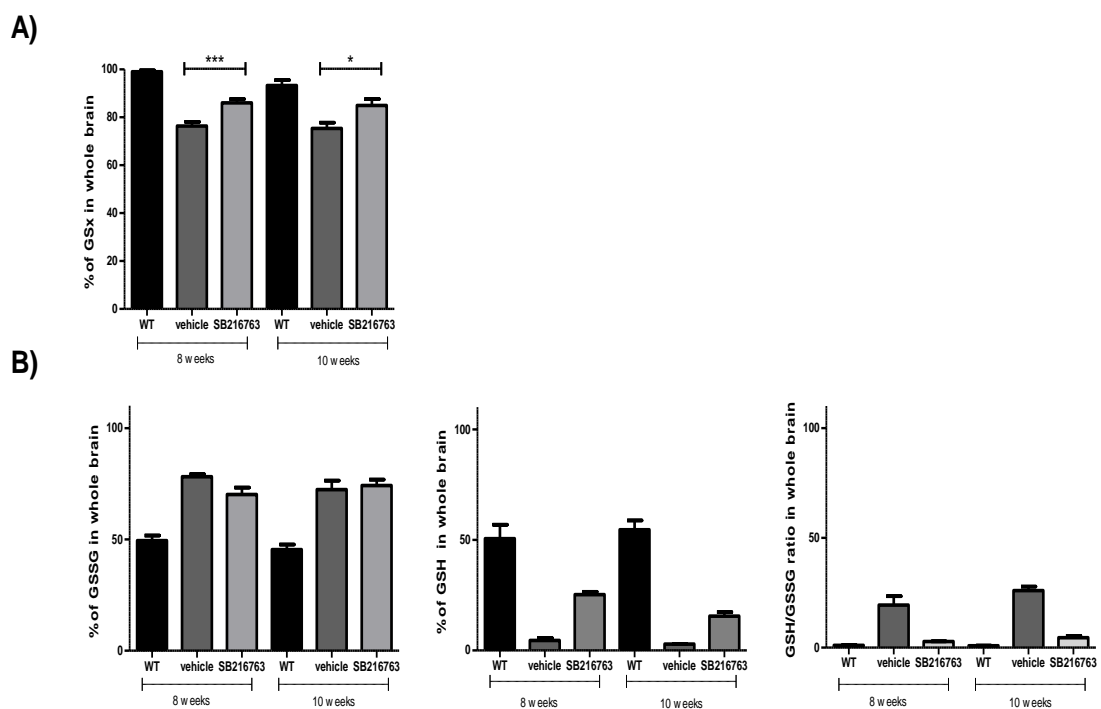


Figure 46. Levels of total (GSx), reduced (GSH), oxidized (GSSG), and GSH/GSSG ratio glutathione in Mecp2 KO animals after the SB216763 treatment. A) The levels of GSx at 8 and 10 weeks of age in KO treated group were significantly increased compared with KO vehicle mice. B) Higher level of GSSG and lower of GSH were detected in KO vehicle animals when compared to KO treated group. Calculated ratio of GSH vs GSSG glutathione was increased after administration of SB216763 in treated mice (at 8 and 10 weeks of age). All presented bars show the mean of two independent experiments +/- SEM (n=3 mice per group \* p< 0,05; \*\*\* p< 0,001).

## Results Part 3

### 5.3.8. Dendritic spine density in Mecp2 KO mice after SB216763 treatment

RTT displays lower spine density and GSK-3 influences dendritic development in an activity-dependent manner (270). It was interesting to evaluate dendrites condition in Mecp2 KO mice after the SB216763 injections.

We analysed the spine density in Mecp2 KO treated and untreated mice at 8 and 10 weeks of age. Analysis of total and mushroom spines were obtained as described with Neuronstudio software and the Sholl analysis algorithm (223).

As it is shown in figure 47 daily drug administration has provoked a significant difference in the number of total and mushroom types of spines at 8 weeks of age (Figure 47A). In KO treated mice total and mushroom number of spines are increased when compared to the vehicle group. In figure 38 it was shown that administrating the drug significantly prolong the life span. Following this observation we have also checked the number of spines at the end point of the experiment, when the vehicle group was about to die. Corresponding numbers of total and mushroom spines were calculated with 10 weeks old animals from all studied groups. In SB216763 treated mice group the total number of spines was still higher than in vehicle's mice. The mushroom type presents the growth trend in treated mice, but was not significant at the end point of the study (Figure 47B).

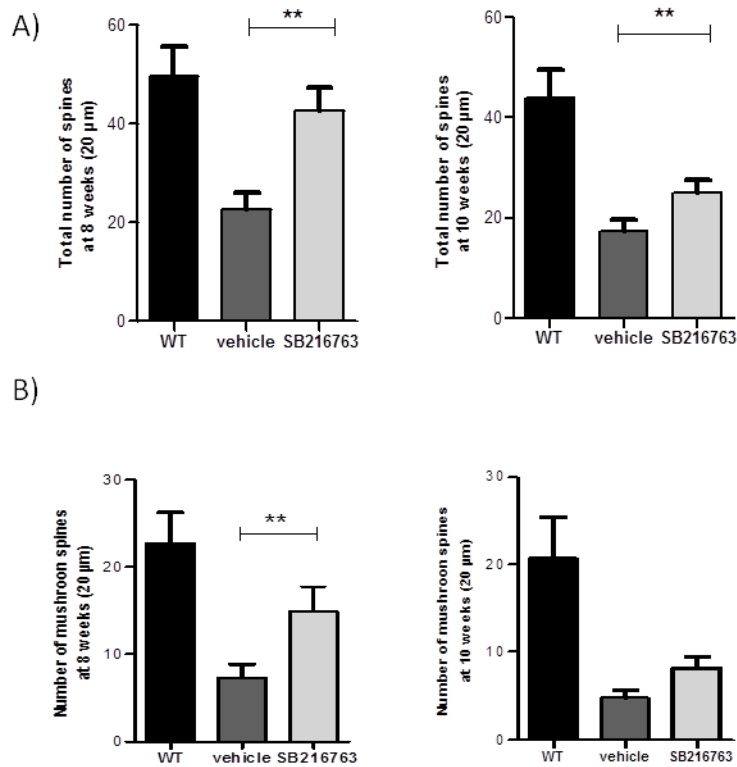


Figure 47. Changes in dendritic spine density in hippocampus region of Mecp2 KO mice after SB216763 treatment. Bars showing the spine density (mean $\pm$  SEM) in hippocampus region of Mecp2 deficient mice treated with SB216763 vs Mecp2 KO control animals at 4 weeks post-treatment (8 weeks of age) and 6 weeks post-treatment (10 weeks of age) with focus on total number of spines (A) and mushroom spines (B). Dendritic segments of 20  $\mu$ m were analysed for each group and the images were taken with Zeiss microscope 63 X 1.4 NA and processed with Neuron studio software. The bars represent the average of total count-spine in dendritic segments in three experimental groups;  $\pm$  SEM (n=3 mice per each in group, \*\*p<0.01 - the Sholl analysis).

### 5.3.9. Changes in levels of DRD2 dopamine receptors after SB216763 treatment

DRD2 receptor is involved in the spinogenesis process (182). We checked by quantitative real time-PCR whether DRD2 was activated after the treatment. RNA was isolated from hippocampus zone from WT, vehicle and GSK-3 inhibitor treated mice. The data showed that SB216763 administration increases the level of DRD2 receptor. RT-QPCR results showed an increase in the level of DRD2 receptor in the treatment group when compared to the vehicle control (Figure 48). The level of DRD2 in KO SB216763 treated mice reached the 40 % of WT mice. The drug administration

### Results Part 3

reflected a 20% improvement in the KO treated mice when compared to the vehicle mice.

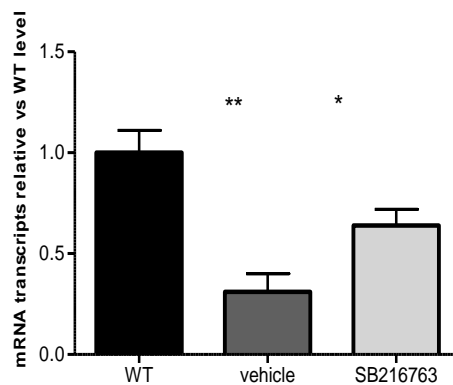


Figure 48. SB216763 treatment causes an increase in DRD2 level. All transcripts levels were determined using RT-qPCR (Applied Biosystem). The bars represent mean  $\pm$  SEM (\* $p$ <0,05 \*\* $p$ <0.01,  $n$ =3 each group).

#### 5.3.10. Preliminary studies on expression of PSD-95 and VGLUT1 in Mecp2 KO mice after SB216763 treatment

The precise mechanism underlying the involvement of Mecp2 in regulating morphological and functional aspects of synaptic signalling are yet to be identified. However, synaptic plasticity deficits are one of the most consistent findings and may provide important insights into RTT-like pathogenesis as well as serve as a target system for therapeutic interventions.

First we examined the cell distribution pattern of pre- and postsynaptic markers in WT vs Mecp2 KO mice. The difference between WT and KO groups obtained under confocal microscope are shown figure 18. The higher level of PSD-95 and VGLUT1 were detected in WT group based on *in vivo* studies. The confocal images at hippocampal region of WT, Mecp2 KO and Mecp2-SB216763 treated mice were performed (Figure 49A). The distribution pattern was clear. We confirmed the previous results of lower levels of PSD-95 and VGLUT1 in Mecp2 KO mice, however after SB216763 treatment the both markers were recovered, being significant in the case of PSD-95 and presenting a clear tendency in VGLUT1 staining (Figure 49B). Additional experiments need to be done in order to confirm this pattern of PSD-95 and VGLUT1 expression after the inhibitor treatment.

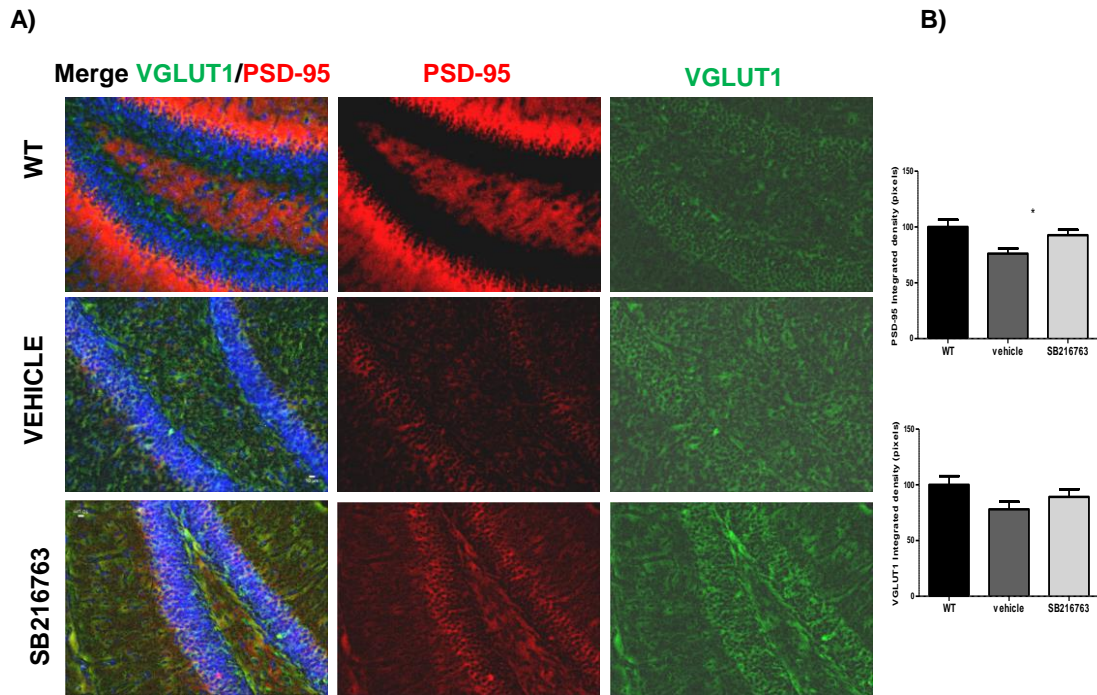


Figure 49. Determination of pre (PSD-95) and postsynaptic (VGLUT1) proteins expression in the hippocampal region of WT, symptomatic *Mecp2* KO mice after SB216763 administration. A) Representative pictures of areas in the hippocampal region under confocal microscope. Neurons were coimmunostained for PSD-95 (red), VGLUT1 (green), and DAPI counterstain (blue). The images were taken with Confocal microscope, Scale bar=20 $\mu$ m. B) Bars are representing positive cell density of PSD-95 and VGLUT1 markers in 3 studied group. All data are shown as a mean  $\pm$  SEM, n=3 mice each tested group; \*  $p < 0,05$ .

## Results Part 4

### 5.4. Part 4 Evaluation of selected classes of drugs targeting pathways and processes deregulated in Rett syndrome.

Despite the complex physiopathology of Rett syndrome, RTT mouse models have revealed essential information about the disease, most importantly the reversibility of its symptoms. This fact has stimulated the activity in exploring therapeutic approaches that are related to different pathways misregulated in Rett syndrome.

BDNF is one of the target for Rett. Different pharmacological, experimental strategies have been attempted to increase BDNF level in mouse model. We have also tried here one of the BDNF analogue, called copaxone. Copaxone (Glatiramer Acetate) is a Food Drug Administration (FDA) approved drug for Multiple Sclerosis which is known to increase BDNF levels. Copaxone; Glatimer Acetate was a gift from Teva Pharmaceutical Industries (Petah Tiqva, Israel). We follow our protocol. Drug was injected subcutaneously (s.b.), daily at the dose of 90mg/kg. In Supplementary Figure 1 we show that selected dose was well tolerated in Mecp2 KO mice, however did not display any significant improvement neither in total score nor in life span (Supplementary Figure 1, and Supplementary Figure 2 presenting score separately).

During the experiments, we would like to have a positive control in order to compare our improvement of the phenotype and/or life span with the drug that was already described as having positive feedback in Rett mice phenotype. For this reason we use cystamine. Unfortunately we could not repeat the improvement obtained and described before in Roux laboratory (179). A difficulty in the analysis of mouse models occurs, because frequently different tests are used to verify the severity of specific phenotypes, rendering difficult to compare different studies. Perhaps, a common severity score may help all researchers to take advantage of well described approaches and studies in different laboratories (Supplementary Figure 3 and 4).

Since in 2012 pharmacological interference with the glucocorticoid system was described as having influence on symptoms and lifespan in a mouse model of Rett syndrome (198). We have also tried one of the glucocorticoids drug-dexamethasone; 9-Fluoro-16 – Methylprednisolone. We first did the dose response experiment. Obtained by us results are presented in Supplementary Figure 5 and 6. Since the improvement was below 30% of almost all score categories, we did not follow the treatment for further analysis.

Bioamergic deficits had been initially observed in RTT mice (231). More recently a systematic investigation carried out in *Mecp2* KO mice confirmed a global alteration of monoamines in the medullar region in fully symptomatic mice (189). Our hypothesis was that selected by us dopamine modulators could contribute to irregular breathing pattern, or mobility symptoms fully described in Rett mice. We used Ropinirole (4-[2-(dipropylamino)ethyl]-2-indolinone monohydrochloride) and mix treatment of L-Dopa (L-3,4 Dihydroxyphenilalanina methyl ester hydrchloride, D1507) /DDCI (Benserazide, B7283) as already described in Results Part2. Obtained results of treatment with ropinirole are in Supplementary Figures 7 - 8. The global improvement of the score in *Mecp2* KO mice was average of 30%, being less efficient when compared to L-Dopa +Ddci treatment, which was dedicated to detailed studies.

Bromperidol was used as a modulator of serotonin (Supplementary Figure 9 and 10). Despite selected low doses of the drug, it was toxic for *Mecp2* KO mice indicating weight lose and shorter life span in treated animals group.

While there is wide consensus for a relevant role in *Mecp2* in development of GABAergic circuits (154), it was also important for us to check if using drugs targeting the GABA pathway we could improve the Rett phenotype or prolong the lifespan. Indeed, Gabapentin did not prolong the life span of animals but the score was even improved of 30 % when compared to untreated animals (Supplementary Figure11 and 12).

Trying to look for new pathway that could be involved in Rett disease we studied the GSK-3 pathway, obtaining good results by injection with SB216763, specific GSK-3 inhibitor (Described in results Part 3, Supplementary Figure13 and 14 selecting the optimal dose). TDZD8 treatment just confirmed us that targeting this pathway we are able to rescue some symptoms of the disease. However the TDZD8 was not that effective as SB216763 inhibitor. It improved the life span only of 12%, but the breathing score at 8-9 weeks of age was improved even untill 60% (Supplementary Figure 15 and 16).

Information about all used drugs and corresponding details to compound, dose or schedule of the administration are included in Table 12.

The improvement after the drugs treatment related to life span and phenotypic score (total and divided in 6 described before categories) is summarized separately for each drug in Table 13. Following the study protocol obtained before all treated mice where compared to *Mecp2* KO vehicle/placebo mice.

## Results Part 4

Antioxidant drugs are also good target for rescue the Rett phenotype. We used a few antioxidant drugs, however further analysis are required to confirm the new obtained data (Supplementary Figures 17 – 24). One of the most promising results were obtained with VDAC1 inhibitor (DIDS).

Epigenetics medicaments included histones deacetylase (HDAC) and DNA-demethylating inhibitors were tested in Mecp2 KO mice. DNA-demethylating drugs could be relevant for several neurodegenerative and neurodevelopmental diseases. Most of the current treatments have been done with HDACs. Histones are important nuclear proteins that bind DNA in the formation of nucleosomes and control transcription. Chromatin remodeling and transcription is regulated partly via histone acetylation, which is promoted by the opposing activities of histone acetyltransferases and HDACs. HDAC inhibitors affect histones similar as transcription factors that are influenced by acetylation (24). HDAC inhibitors can promote either transcription activation or suppression by relaxing DNA conformations. Because HDAC inhibitors induce growth arrest in cell proliferation models, HDAC inhibitors have also been used as anti-cancer drugs (271). Moreover, HDAC inhibition has been shown to be neuroprotective in mouse models of spinal muscular atrophy and Huntington's disease (272). Furthermore HDAC inhibitor is neuroprotective and corrects aberrant gene transcription also in Amyotrophic lateral sclerosis (ALS) mice and it has been recently shown to be safe and well tolerable in ALS patients while improving hypoacetylation. On the other hand, some of the HDACs inhibitors like Sodium phenylbutyrate (NaPB) suppress the production of ROS from microglia cells in response to various stimuli indicating its antioxidant activities (273).

Unfortunately none of selected epigenetic drugs was able to reduce the Rett phenotype or prolong the life span of KO mice (Supplementary Figures 25 – 33).

## Results Part 4

Name of dug (Synonyms)	Dose (MDT)	Adminis- tration	Manufacturer	LD 50 (literature)	Final dose	Schedule/ treatment frequency	Vehicle (dissolved in)
Copaxone; Glatimer Acetate	x	s.b.	Teva Pharmaceutica I Industries (Petah Tiqva, Israel)	x	90 mg/kg	every day	saline
Dexamethasone; 9 -Fluoro-16 - Methylprednisolone, Desamethasone	0,1; 0,5 and 1mg/kg/day	i.p.	D1756, Sigma	> 3.000 mg/kg	no improvement	every day	Saline +2% of EtOH
L-Dopa (L-3,4 Dihydroxyphenilalanina methyl ester hydrchloride /Ddci	x	i.p. 1st Ddci after 15 min L- Dopa	Sigma L-Dopa D1507; Ddci- Benserazide, B7283	200 L- Dopa and 50 Ddci mg/kg/day	30 L-Dopa and 12 Ddci mg/kg/day	every day	saline
Ropinirole (4-[2- (dipropylamino)ethyl]-2-indolinone monohydrochloride)	0,3, 1 and 3 mg/kg	i.p.	Ropinirol (gift from the bellvitge group)	x	1mg/lkg	every day	saline
Bromperidol (powder)	0,1; 1 and 10 mg/kg	i.p.	Fitzgerald 50RR11333	156mg/kg	none, too toxic	every day	10% of DMSO
Cysteamine	in agreement with Roux et al., 2012	drinking water	Sigma M6500	Borrell- Pages, M., et al., 2006	225 mg/kg	every day	drinking water
Gabapentin, Neurontin1- (Aminomethyl)-cyclohexaneacetic acid	1; 10 and 50 mg/kg	i.p.	Sigma G154	1000- 2000 mg/kg	1mg/kg	every 2 days	saline
3-(2,4-dichlorophenyl)-4-(1- methyl-1H-indol-3-yl)-1H-pyrrole- 2,5-dione, SB216763	0,1; 0,5 and 1mg/kg/day	i.p.	Selleckchem; No.S1075	25mg/kg	0,5mg/kg/ day	every day	20% of DMSO
TDZD8 (4-Benzyl-2-methyl-1,2,4- thiadiazolidine-3,5-dione)	0,1; 0,5 and 1mg/kg	i.p.	Sigma T8325	x	0,5mg/kg	every day	20% DMSO
Vitamins C (L-Threoascorbic acid) and Vitamin E (D- $\alpha$ -Tocopherol)	x	food	Sigma / SNIFF company	vit c 11,900 mg/kg	50 mg/kg/day of vitamins C&E	every day	food no extra dose of vitamins
The LiQsorb® Liposomal CoQ10	10; 400 and 1200 mg/kg/day	drinking water	Tishcon	more than 2500mg/kg	400 mg/kg/day	every day	water
Resveratrol	20 mg/kg	i.p.	Sigma R5010	400mg/kg	20 mg/kg	every day	8% etanol in 20% of Cyclodextrin (MQ water)
VDAC1 inhibitor (SIGMA D3514), DIDS 4,4'- Diisothiocyanatostilbene-2,2'- disulfonic acid disodium salt	x	i.p.	Sigma	x	25 mg/kg/day	every day	0.1 M KHCO <sub>3</sub>
AZA (VIDAZA)	0,1; 0,25 and 0.5 mg / kg	i.p.	A3656 Sigma	190 mg/kg	0,25 mg/kg	every 2 days	saline
SAHA ( suberoylanilide hydroxamic acid; Vorinostat)	x	i.p.	galchimia	> 400 mg/kg	50 mg/kg	every 2 days	10% DMSO
Sodium phenylbutyrate (NaPB), TriButyrate; 4-Phenylbutyric acid sodium salt; 4-phenylbutyrate	1; 10; 50; 100 and 300 mg/day	i.p.	Calbiochem	525 mg/kg	None, low improvement	every day	saline
Trichostatin A (TSA)	1 and 5 mg/kg	i.p.	Sigma T8552	50 mg/kg	None, low improvement	every day	10% DMSO
Entinostat	2.5; 5; 10 mg/kg	s.b.	BioVision MS- 275,SNDX-275	20 mg/kg	None, too toxic	every day	10% DMSO

Table 12. Summary of selected drugs used for *in vivo* studies in RTT mice model.

## Results Part 4

pathway	drugs	life span	total score	score					
				mobility	gait	hinlimb claspings	tremor	breathing	general condition
<b>BDNF</b>	Copaxone	x	33%	30%	0%	5%	50%	40%	75%
<b>Glucocorticoides</b>	Dexametasone	x	22%	35%	15%	10%	15%	50%	10%
<b>Dopamine</b>	L-DOPA+inhibidor Ddc	17%	48%	60%	30%	25%	70%	70%	30%
	Ropinirole	13%	32%	50%	15%	15%	40%	50%	20%
	L-Dopa + inhibidor DDC plus vitamins c and e	18%	48%	65%	30%	20%	60%	75	35
	L-DOPA	3%	20%	20%	20%	15%	25%	25%	15%
<b>Serotonin</b>	Bromperidol	x	X	X	X	X	X	X	X
<b>Glutamate</b>	Cysteamine	x	24%	X	X	X	X	X	X
<b>GABA</b>	Gabapentin	8%	41%	30%	20%	30%	60%	40%	25%
<b>GSK-3</b>	SB-216763	27%	34%	50%	40%	20%	60%	60%	20%
	TDZD8	12%	25%	40%	20%	25%	30%	60%	30%
<b>Oxidative stress</b>	Vitamic C+E	16%	32%	30%	25%	5%	30%	40%	20%
	CoQ10	25%	35%	35%	15%	10%	55%	50%	30%
	Resveratrol	5%	32%	50%	25%	20%	60%	40%	15%
	DIDS	4%	31%	50%	25%	10%	40%	50%	20%
<b>Epigenetic drugs</b>	5-Azacytidine	23%, but not reproducible	x	35%	45%	15%	25%	45%	20%
	SAHA	x	x	X	X	X	X	X	X
	Sodium phenylbutirate	x	17%	25%	10%	15%	35%	40%	5%
	TSA	x	17%	5%	10%	5%	35%	35%	15%
	Entinostat	14	35%	40%	20%	10%	70%	50%	50%

Table 13. Improvement of selected drug treatment in RTT mouse model related to life span, total and separated score respectively to vehicle treated groups.

## **Discussion**



### 5.1. Part 1

#### **Evaluation of molecular and behavioural tests to estimate therapeutic effects of pharmacological treatments in Mecp2 KO mice**

The studies in the thesis were aimed at discovering the pharmacological treatment in Mecp2 KO male mice. The drugs were tested in male model of RTT disease. The life span and the phenotype were analysed during the progression of the disease, with and without drug treatment.

Genetically modified Mecp2 mouse models have several symptoms like Rett patients. Before to start the application of the drugs to Mecp2 KO mice it was essential to confirm the genotype and phenotype of the colony that was established in IDIBELL animal's facility, Barcelona. The primers described by Guy et al., 2007 (67) were adopted for PCR experiments to confirm the Mecp2 KO genotype. The obtained results as expected have shown the evidence of all three groups: WT, Mecp2 KO and HZ mice.

RTT-like phenotype development serves as a feature of Mecp2 KO mice. On average the KO mice started to have symptoms at 5-6 weeks of age, and the severity increased during the time. After postnatal 9 week, symptoms aggravated rapidly and induced death at around 10 weeks of age, while their WT littermates scored 0, and survived till 24 months of age. The symptoms score was adopted from Guy et al (67), based on previous studies that described the sum symptoms score as a good indicator for categorizing Mecp2 KO animals. The data shown in this thesis also confirmed that the Mecp2 KO are substantially underweight from 4-5 weeks of age.

Based on presented results it can be also concluded that the mobility and gait disturbance consistently occurred earlier, followed by tremor and hindlimb claspings, and the last two to appear were abnormal general condition and irregular breathing. In RTT disorder, usually the clinical signs begin with hypotonia, microcephaly, and later develop into the respiratory abnormalities (53). Based on that, it is not surprising that the breathing or general condition scores may not be the most suitable indicators of the phenotype development. During the progression of the disease each symptom score showed huge variability (data not shown), however total symptom score clearly reflects the RTT phenotype progression with the time of the experiment. The general condition and tremor scores present great deviation while hindlimb claspings or mobility scores were similar. At the 10 weeks of age the number of scored Mecp2 KO mice was diminished, some of the animals died or were culled.

## Discussion Part 1

As we already know RTT mouse model provide potent resources for investigating the genotype-phenotype pathway. That is why I also examined the phenotype progression in the *Mecp2* KO mice. However the underlying alterations to neuronal network behaviour that lead to the clinical symptoms are still poorly understand.

In many studies it is already confirmed, that symptomatic *Mecp2* KO demonstrated progressive motor deficits. By using exploration and anxiety-related behaviour tests it is shown that *Mecp2* KO mice have a strong interaction genotype x age (189). The bar cross test has shown that during the time we can observe the progression in the mobility dysfunction. 8 weeks of age was selected as time to perform the rest of the tests. At this stage all the symptoms were present and the general conditions of mice were still acceptable for human reason to follow the experiment. *Mecp2* KO showed the reduced rearing frequency compared to WT and lower number of visited corners suggesting the neophobia behaviour (corner test). The data obtained in open field were similar in both groups, however it was marked tendency in *Mecp2* KO mice. They exhibit stiff and uncoordinated gait and tremor. In wire grip test the hind limb claspings disorders were noticed. The *Mecp2* KO animal was mostly not able to grip the wire during one minute, and if so no movement of animal was noticed. Anxiety parameters were next performed in Y-maze test. The ratio between the number of entrance divided by the number of repetitions was higher in WT mice. This data suggest more exploratory behaviour in WT group mice respectively indicate the anxiety of KO mice.

Similar like in other laboratories (53), also in animal facility of IDIBELL the symptoms of the *Mecp2* KO mice during the behaviour experiment were subsequently worsen and finally lead to a drastic weight loss and death at around 10 weeks of age. That is why some of animals reached humane endpoint before the end of experiments and therefore were excluded from analyses.

At the birth *Mecp2* KO mice do not present significant difference when compared to the WT in the level of bioamines, but noradrenaline content tends to be reduced (231) suggesting that progression of the irregular breathing phenotype could correlate with a degeneration of the noradrenaline neuromodulatory system. It was already suggested that deficits of noradrenaline in *Mecp2* KO mice could be related to deficits expression of Th and an its active form - pSer-40 (pTh) (153). Th and pTh are enzymes important in the synthesis of bioamines. These enzymes are critical for production of dopamine and noradrenaline and they often act as the rate-limiting step of catecholamine reaction. I used the Th and pTh as markers for noradrenergic neurons, and the results

show the evidence not only in the reduction of Th positive neurons, as was already published (157), but also in the reduction of pTh. The results of lower Th and pTh staining probably are corresponding with the respiratory phenotype and motor disabilities. It can also suggest that the neurons are less efficient to produce dopamine (156). At the birth Th expression in male *Mecp2* KO mice is at the level of WT animals, but the level is reduced at 8 week old animal (158), when the breathing and mobility anomalies occur. Previous data describe that by increasing levels of dopamine and noradrenaline *in vivo* (administration of noradrenaline reuptake inhibitor Desipramine; (156) the respiratory functions in *Mecp2* KO mice were improved. It also suggest that dopamine and/or noradrenaline may be direct affected by absence of *Mecp2* as a *Mecp2*-binding site was found in Th promoter exploring the possible regulation of Th by the *Mecp2* protein.

We presented here reduced levels of Th and pTh in *Mecp2* KO animal during the progression of the disease. By using these markers it is possible to monitor probable improvement after the drug treatment related either to breathing and mobility phenotype dysfunctions or level of bioamines; noradrenaline and dopamine included.

Functional knock out of *Mecp2* is characterized by both pre-synaptic and post-synaptic deficits in symptomatic *Mecp2* KO mice. Using the immunohistochemistry technique it was also confirmed that fact in this thesis. The intensity of both markers was lower in KO mice versus age-matched WT littermates. The results were obtained in brain tissues. By PSD-95 and VGLUT1 measurements is possible to assess the status of the synaptic development, which is dysregulated in Rett. PSD-95 is a key postsynaptic protein that is involved in synapse maturation and exerts a major influence on synaptic strength and plasticity, and VGLUT1 plays an important role in glutamate transport (274). One of the goals was to improve the synaptic stability/plasticity and glutamate transportation. It would be possible using specific drugs related to these pathways. The improvement of the drug could be then confirm by molecular studies of PSD-95 and VGLUT1 levels after selected drug administration.

OS in RTT has also a potential role that could explain genotype-phenotype correlation. Biochemical evidence of OS like excessive release of glutamate in *Mecp2* deficit microglia or reduced glutathione, are related to neurological symptom severity (142). RTT patients have also abnormal mitochondrial morphology detected in skeletal muscle, what is a consequence of defects in forelimb and hind limb measurements. It was already noticed, that symptomatic mice present lower level of total glutathione

## Discussion Part 1

(GSx). The obtained here data confirm that. Moreover the level of reduced glutathione (GSH) in KO mice is also reduced, while oxidized glutathione (GSSG) is higher versus age matched WT littermates. OS has many potential downstream therapeutic targets such a GABA neurotransmission, the IRAK1/NF-kappaB axis or catecholamine signaling. One idea was to try antioxidants drugs for RTT mice to regulate unbalanced OS path.

Many molecular changes that occur for example during epileptogenesis are not yet clarified and could be attributed to cell death, reorganization of neural networks, alteration in the release of neurotransmitters. Next performed test between WT and KO groups, based on the fact that the number of synapses has been reported reduced (173) was Golgi staining. This test was used in order to monitor spine density. Obtained by us results are showing that not only the total spine number in Mecp2 KO animals is lower, but also the mature spines, so called mushroom shape, are presenting the reduced number with respect to the WT group. BDNF regulation, glutamate or dopaminergic signaling improvement could be a promising strategy for reversing cognitive deficits in preclinical models of Rett disease, where as a positive feedback spine density should be restored. Selected drug administration could stimulate spine formation leading to an increase in the number of spines on these neurons.

To conclude, with the unique combinations of behavioural and molecular tests that distinguish WT and Mecp2 KO animals, it is possible to evaluate and compare the effects of drugs targeting different biological processes and pathways. Further analyses of the effects of the tested drugs which demonstrated initial efficacy in Mecp2 KO mice will focus on detailed studies of specific molecular pathways targeted by selected compounds.

### 5.2. Part 2

#### **Improvement of the Rett Syndrome phenotype in a *Mecp2* mouse model upon treatment with Levodopa and a Dopa Decarboxylase Inhibitor**

The lack of *Mecp2* protein results in catecholaminergic deficits in neurons located in the central and peripheral nervous system (158, 275) and levels of several biogenic amines, like dopamine or norepinephrine are reduced (Ide et al., 2005). To activate the dopaminergic pathway we did the combination of L-Dopa with Ddci treatment. From the previous experiments we know that L-Dopa treatment alone already can improve the motor ability in *Mecp2* KO mice (189). Based on my last results it can be concluded that the treatment with Ddci, that protects the conversion of L-Dopa to dopamine in periphery, is more efficient.

First, by daily monitoring the weight of each animal it was determined whether the administration of L-Dopa, Ddci or the combination L-Dopa + Ddci was toxic for the *Mecp2* KO mice. The *Mecp2* KO mice treated with vehicle (saline serum), L-Dopa, Ddci, or the combination L-DOPA + Ddci had similar weights, independent of the compound used. Moreover, at the time of sacrifice liver tissues were resected for pathological analysis. No toxicity was detected in any of the mice used in the different drug treatments confirming selected dose as being well tolerated for *Mecp2* KO mice.

*Mecp2* KO mice display the deficits in motor behaviour, neurosensorial processing, and physiological indexes (189, 232). To follow the score test, I demonstrated that mice treated with the combination of L-Dopa / Ddci showed an approximately 50% improvement of the symptoms score compared to vehicle *Mecp2* littermates, and an approximately 35% improvement vs L-Dopa treated group. Moreover, the impact of the drug on the life span of the KO mice is rather high, with the evidence of 20% increase, corresponding to significant enhancement of survival.

By administration with L-Dopa / Ddci we also assume to decrease the dopaminergic disturbances in the *Mecp2* KO mice, which is one of the reason why the motor symptoms in *Mecp2* KO treated mice could be reduced (bar cross test). SNpc, the main source of dopamine in the brain, is altered, participating in turn to the appearance of *in vivo* motor deficits. This improvement suggests that the DA nigrostriatal deficits also play a role in the locomotor abilities of the KO mice.

## Discussion Part 2

Since by injecting Ddci a higher amount of L-Dopa is crossing the BBB, we should be able to detect the higher level of dopamine in the brain tissue. In this regard, we found that the hippocampus of Mecp2 KO mice compared to control littermates showed significant lower levels of dopamine, what was expected. After L-Dopa/Ddci administration the level of dopamine rises. We observed the same pattern in caudate putamen, but not in frontal cortex.

Since in previous studies the dendritic spine pathologies in Mecp2 KO mice were described (133, 276), then we asked whether Mecp2 KO mice exhibited reduced deficits in dendritic spine after the drug administration. Spine density in hippocampus of Mecp2 KO mice with L-Dopa / Ddci treatment showed improvement in hippocampus region of Mecp2 deficient mice vs control animals with focus not only on the total number of spines but also on the more mature, mushroom type of spines. This is direct evidence that MeCP2 deficiency leads to immature synaptic function, reduced spine density and organization in a manner that can be partially rescued by L-Dopa / Ddci administration.

Most importantly, the increase in spinogenesis under the combined therapy regimen is associated with the enhanced expression of the DRD2 in the MB of the Rett mouse model. This is another advantage of the L-Dopa + Ddci treatment because DRD2 elicits extensive spine formation (182).

Next we analysed the Th-positive neurons. By administration of L-Dopa / Ddci the Th level in SNpc was increased. Deficit in active Th as is described before appears to aggravate the pathology at later stages (277). After L-Dopa / Ddci treatment not only the Th level is increased but also phosphorylation of Th is improved. Taking into account that Th phosphorylation is responsible for maintaining catecholamine levels in tissue, it is suggested that we improving here the metabolic pathway of biosynthesis of the biogenic amines. Described results support the idea of L-Dopa / Ddci treatment. The increased numbers of Th-expressing and pTh-expressing neurons leads to partial recovery of catecholamines and DA neurons deficits in the SNpc which are affected in the Mecp2 KO mouse.

We evaluated the improvement of L-Dopa / Ddci treatment on the phenotype with details related to motor/activity and the life span. In contrast to Mecp2-vehicle KO mice, the group with L-Dopa / Ddci treatment exhibited slower progression of the phenotype and prolonged the life span. We also found that the number of active dopaminergic neurons (Th and pTh) increased when L-Dopa / Ddci treatment was performed. Additionally, we have demonstrated a higher density in dendritic spine of

hippocampus region in the treated group of mice, supported by increased dopamine receptor level, which is involved in the spinogenesis process (182).

Although further studies are needed to explore these results, I believe that presented here data point a potential utility of L-Dopa / DdcI treatment for RTT disease. Such prospective therapies also have significant implications for other autism spectrum disorders and neurodevelopmental conditions that have similar phenotypes, genetic susceptibility, and underlying neurobiological mechanisms.

## Discussion Part 3

### 5.3. Part 3

#### **Part 3 Glycogen synthase kinase-3 inhibitor, SB216763, displays therapeutic potential in a mouse model of Rett syndrome**

This study provides the first *in vivo* evidence that GSK-3 pathway is involved in Rett syndrome.

The assessed results with SB216763 treatment indicate that GSK-3 signalling is very important in development of nervous system. Selected here drug treatment indicates GSK-3 pathway as being involved in the Rett syndrome disease. For the first time we presented here the relationship between Mecp2 KO mice model and levels of GSK-3, pGSK-3 or  $\beta$ -catenin in brain tissue. The total level of GSK-3  $\alpha$  and  $\beta$  are similar in Mecp2 KO mice compared to WT, but the active forms of the enzymes are upregulated. This dependence is changed after the SB216763 treatment. The level of active GSK-3  $\alpha$  and  $\beta$  in KO mice after the drug injections is lower, being comparable with this in WT mice. Besides, the level of  $\beta$ -catenin is slightly lower in untreated mice, what is displayed as a tendency of being higher after the injections. Our results implicate the GSK-3 inhibitor as being able to improve the clinical symptoms of the disease with consequences at the molecular and cellular levels in the brain of Mecp2 KO mouse.

Herein, it was presented that SB216763 inhibitor can improve Rett syndrome symptomatology in association with the stimulation of neuronal dendritic growth, supported also by higher level of DRD2-receptor after the drug administration. As it was already described, GSK-3 inhibition also parallels dendritic growth and maturation *in vivo* (270). In our study not only total but also specific mushroom spine density was significantly augmented in Mecp2 KO mice after the treatment. It may be suggested that by inhibition of GSK-3 in Rett mice we can induced *in vivo* dendritic cell development and maturation.

Moreover, a variety of molecules, including growth factors and DRD2, can signal through GSK-3/ $\beta$ -catenin signalling activation (262). It can be envisaged in plasticity observed after the SB216763 treatment. Lower level of pre and postsynaptic markers in Mecp2 KO mice seemed to be consistent with the symptom progression and severity. Our data report that after the treatment both markers present a higher level, what could explain slower symptom progression during the time and prolongation of life span. With selected low dose of SB216763 obtained effects were obvious not only in young animals, but also significant differences we noticed in older mice

Most importantly, the results confirmed our hypothesis that SB21673 treatment ameliorated the motor deficiency of the RTT mouse model. The obtained results from bar cross test, open field or Grip test support the assumption that reduced movement in Mecp2 KO mice is partly recover after the drug administration. In neophobia or Y-maze tests we could observed that not only mobility of the KO mice was improved but also the anxious behaviour or susceptibility to stress were reduced.

Overall, the reported findings herein are promising in this preclinical model of Rett syndrome. We confirmed here the advanced state of inflammation in Mecp2 KO mice, presenting higher activity level of NF-kappaB in brain of untreated mice respect to WT. After the SB216763 injections we can conclude decrease of inflammation in the brain of Mecp2 KO mice, reflecting in lower activity level of NF-kappaB.

Besides, treatment with SB216763 results in an increase of glutathione level in Mecp2 KO treated mice. It has been previously suggested that inhibition of GSK-3 has a capacity to undergo oxidative metabolism and has protective effects of neurons, counteracted ischemic neuronal death (269). We examined the effect of SB216763 treatment on antioxidant system that is affected in Rett syndrome disease. A higher level of GSH leads to the conclusion of antioxidant defence after the drug treatment. That reflects in upregulated GSH synthesis as a response to mild oxidative damage (278). Present data show that reduction of GSK-3 activity by small-molecules inhibitors activates a program generating antioxidant defence in inflamed brain of Rett mice.

Understanding the regulation of GSK-3 and its activity would be very important for potential recovery of RTT syndrome. Even relative small changes might have a large impact on development outcomes such as determination of neurons in the brain.

Our results expand the knowledge about GSK-3 in the context of Rett syndrome. The new data indicate that the selected inhibitor, SB216763, could be a potential treatment that partially could rescue Rett phenotype. The drug can be addressed to have neuroprotection properties via the improvement of synaptic plasticity, reduced oxidant and inflammation damage or rescue mobility dysfunctions.

Further analysis and experiments need to be done in order to confirm described here novelty for the Rett syndrome disease.

## Discussion Part 4

### 5.4. Part 4

#### Part 4 Evaluation of selected classes of drugs targeting pathways and processes deregulated in Rett syndrome.

##### discussion and open questions

To date, almost 15 years after the discovery of MECP2 gene as the main causative gene of RTT, many questions remain open. In particular, the molecular mechanism underlying the pathogenesis of this disease is already unclear. The generation of mouse models only partially elucidated the relationship between MECP2 gene and RTT pathology. May RTT symptoms be caused by a global alteration of chromatin structure or by deregulation of some specific genes? From several years, in fact, the gene-specific or global regulatory role of MeCP2 has been debated. The large number of available data suggests the importance of MeCP2 in global chromatin dynamics, in addition to the role as a gene-specific transcriptional regulator, the latter depending on specific and/or alternative cofactors.

Noteworthy, the mouse model that better recapitulate RTT phenotype is the *Mecp2* KO mouse, although RTT patients are heterozygous for MECP2 mutations. This implies that all studies carried out on this mouse model do not take account of X inactivation occurring in patients. Another open question is that RTT clinical signs regard almost exclusively nervous system defects, even if MeCP2 is ubiquitously expressed. Might this phenomenon depend on brain-specific molecular partners, neural-specific epigenetic and/or post-translational modifications?

To date, only subtle correlation between types of mutation and severity of phenotype has been found, due to extreme heterogeneity of the disorder and also because patients carrying the same mutation can manifest a different severity score. A confounding effect can derive from X chromosome skewing, but it is still possible that unknown modifier genes could play an important role. Moreover, also the spatio-temporal expression of the bona fide MeCP2 target gene, BDNF, in mouse models and RTT patients is still controversial. Furthermore, a difficulty in the analysis of several mouse models occurs, because frequently different tests are used to verify the severity of specific phenotypes, rendering difficult to compare different studies. Perhaps, a common severity score for all mice models may help researchers to take advantage of

different approaches. Finally, this overview suggests that further research is needed to clarify the pathophysiology of RTT and further analyses for treatments, such as include heterozygous mouse females in the preclinical assays. It would also help to use different types of Rett mouse models and test the same drugs over different labs. Once the results are robust enough through diverse labs, the drug could be ready to go for clinical assays.



## **Conclusions**



Based on the findings presented in this PhD thesis the following conclusions can be drawn:

### Part 1

We performed a comprehensive panel of experiments investigating the differences between *Mecp2* KO and WT littermate mice at the behavioural and molecular levels. This was further extended to evaluate the specific drug treatments efficacy.

### Part 2

Combined administration of Levodopa and a Dopa decarboxylase inhibitor in Rett syndrome mouse model was well tolerated, diminished Rett syndrome-associated symptoms and increased lifespan.

The use of L-Dopa + Ddci in the *Mecp2* KO mice induced dendritic growth mediated by dopaminergic neurons.

L-Dopa + Ddci-treated group exhibited higher Th and pTh expression and dopamine levels in comparison to the vehicle treated group.

### Part 3

The results presented here reveal an important role for the relationship between *Mecp2* and GSK-3 signaling in Rett syndrome disease

Inhibitor of GSK-3, SB216763, improved life span and reduced single and total symptoms scores, as well as motor deficiency in *Mecp2* KO mice.

Inhibition of GSK-3 is a possible strategy for stimulation of neuronal dendritic growth

Treatment with SB216763 decreased inflammation and strengthened antioxidant defense in the brain of *Mecp2*KO mice

## Conclusions

### Part 4

Treatment with copaxone, a BDNF analogue reflect rather low improvement in Mecp2 KO studied mice, displaying also very variable results between studied animals.

Previously described positive effect of cysteamine was not reproduced in our laboratory (Roux et al., 2012).

Treatment with dexamethasone, an example of glucocorticoids intervention display rather low improvement – approximately 20% when compared to untreated mice.

Ropinirole treatment confirmed that dopaminergic pathway is dysregulated in Rett. Both life span and the phenotype were improved. However, the efficiency was lower compared to L-dopa + Ddc treatment.

Injections of bromperidol, a serotonin modulator, were toxic for Mecp2 KO mice. Even though the selected doses were very low, they caused significant reduction of body weight in the KO treated group.

Gabapentin, one of GABA modulators, improved the phenotype, but not life span of Mecp2 KO animals, being more efficient with the low dose.

TDZD8 treatment confirmed previously described role of GSK-3 inhibition in Rett. Both life span and phenotype were improved. However, the efficacy was lower than after SB216763 treatment.

Antioxidants studied in this thesis displayed improvement of 30% in Rett syndrome phenotype. Some of selected drugs prolonged the life span by 25% when compared to the vehicle group. Treatments with antioxidants drugs might be worth for further evaluation.

Epigenetics drugs evaluated in this thesis, even though some of them were suggested to be relevant for Rett syndrome, did not show any specific improvement.

## References



## References

1. Berger, S. L., Kouzarides, T., Shiekhatar, R., and Shilatifard, A. An operational definition of epigenetics. *Genes Dev*, 23: 781-783, 2009.
2. Waddington, C. H. The epigenotype. 1942. *Int J Epidemiol*, 41: 10-13, 1942.
3. Chen, T. and Li, E. Establishment and maintenance of DNA methylation patterns in mammals. *Curr Top Microbiol Immunol*, 301: 179-201, 2006.
4. Fraga, M. F., Ballestar, E., Paz, M. F., Ropero, S., Setien, F., Ballestar, M. L., Heine-Suner, D., Cigudosa, J. C., Urioste, M., Benitez, J., Boix-Chornet, M., Sanchez-Aguilera, A., Ling, C., Carlsson, E., Poulsen, P., Vaag, A., Stephan, Z., Spector, T. D., Wu, Y. Z., Plass, C., and Esteller, M. Epigenetic differences arise during the lifetime of monozygotic twins. *Proc Natl Acad Sci U S A*, 102: 10604-10609, 2005.
5. Palini, S., De Stefani, S., Scala, V., Dusi, L., and Bulletti, C. Epigenetic regulatory mechanisms during preimplantation embryo development. *Ann N Y Acad Sci*, 1221: 54-60, 2011.
6. Tang, C. S. and Epstein, R. J. A structural split in the human genome. *PLoS One*, 2: e603, 2007.
7. Luger, K., Mader, A. W., Richmond, R. K., Sargent, D. F., and Richmond, T. J. Crystal structure of the nucleosome core particle at 2.8 Å resolution. *Nature*, 389: 251-260, 1997.
8. Sharma, S., Kelly, T. K., and Jones, P. A. Epigenetics in cancer. *Carcinogenesis*, 31: 27-36, 2010.
9. Straussman, R., Nejman, D., Roberts, D., Steinfeld, I., Blum, B., Benvenisty, N., Simon, I., Yakhini, Z., and Cedar, H. Developmental programming of CpG island methylation profiles in the human genome. *Nat Struct Mol Biol*, 16: 564-571, 2009.
10. Deaton, A. M. and Bird, A. CpG islands and the regulation of transcription. *Genes Dev*, 25: 1010-1022, 2011.
11. Tate, P. H. and Bird, A. P. Effects of DNA methylation on DNA-binding proteins and gene expression. *Curr Opin Genet Dev*, 3: 226-231, 1993.
12. Boyes, J. and Bird, A. DNA methylation inhibits transcription indirectly via a methyl-CpG binding protein. *Cell*, 64: 1123-1134, 1991.
13. Nan, X., Campoy, F. J., and Bird, A. MeCP2 is a transcriptional repressor with abundant binding sites in genomic chromatin. *Cell*, 88: 471-481, 1997.
14. Bestor, T. H. The DNA methyltransferases of mammals. *Hum Mol Genet*, 9: 2395-2402, 2000.
15. Bostick, M., Kim, J. K., Esteve, P. O., Clark, A., Pradhan, S., and Jacobsen, S. E. UHRF1 plays a role in maintaining DNA methylation in mammalian cells. *Science*, 317: 1760-1764, 2007.
16. Chen, T., Ueda, Y., Dodge, J. E., Wang, Z., and Li, E. Establishment and maintenance of genomic methylation patterns in mouse embryonic stem cells by Dnmt3a and Dnmt3b. *Mol Cell Biol*, 23: 5594-5605, 2003.
17. Razin, A. and Riggs, A. D. DNA methylation and gene function. *Science*, 210: 604-610, 1980.

## References

18. Fatemi, M. and Wade, P. A. MBD family proteins: reading the epigenetic code. *J Cell Sci*, 119: 3033-3037, 2006.
19. Lopez-Serra, L. and Esteller, M. Proteins that bind methylated DNA and human cancer: reading the wrong words. *Br J Cancer*, 98: 1881-1885, 2008.
20. Kouzarides, T. Chromatin modifications and their function. *Cell*, 128: 693-705, 2007.
21. Bernstein, B. E., Meissner, A., and Lander, E. S. The mammalian epigenome. *Cell*, 128: 669-681, 2007.
22. Agger, K., Christensen, J., Cloos, P. A., and Helin, K. The emerging functions of histone demethylases. *Curr Opin Genet Dev*, 18: 159-168, 2008.
23. Al-Mahdawi, S., Pinto, R. M., Ismail, O., Varshney, D., Lymperi, S., Sandi, C., Trabzuni, D., and Pook, M. The Friedreich ataxia GAA repeat expansion mutation induces comparable epigenetic changes in human and transgenic mouse brain and heart tissues. *Hum Mol Genet*, 17: 735-746, 2008.
24. Camelo, S., Iglesias, A. H., Hwang, D., Due, B., Ryu, H., Smith, K., Gray, S. G., Imitola, J., Duran, G., Assaf, B., Langley, B., Khoury, S. J., Stephanopoulos, G., De Girolami, U., Ratan, R. R., Ferrante, R. J., and Dangond, F. Transcriptional therapy with the histone deacetylase inhibitor trichostatin A ameliorates experimental autoimmune encephalomyelitis. *J Neuroimmunol*, 164: 10-21, 2005.
25. Gondcaille, C., Depreter, M., Fourcade, S., Lecca, M. R., Leclercq, S., Martin, P. G., Pineau, T., Cadepond, F., ElEtr, M., Bertrand, N., Beley, A., Duclos, S., De Craemer, D., Roels, F., Savary, S., and Bugaut, M. Phenylbutyrate up-regulates the adrenoleukodystrophy-related gene as a nonclassical peroxisome proliferator. *J Cell Biol*, 169: 93-104, 2005.
26. Azevedo, F. A., Carvalho, L. R., Grinberg, L. T., Farfel, J. M., Ferretti, R. E., Leite, R. E., Jacob Filho, W., Lent, R., and Herculano-Houzel, S. Equal numbers of neuronal and nonneuronal cells make the human brain an isometrically scaled-up primate brain. *J Comp Neurol*, 513: 532-541, 2009.
27. Xin, Y., Chanrion, B., Liu, M. M., Galfalvy, H., Costa, R., Ilievski, B., Rosoklija, G., Arango, V., Dwork, A. J., Mann, J. J., Tycko, B., and Haghghi, F. Genome-wide divergence of DNA methylation marks in cerebral and cerebellar cortices. *PLoS One*, 5: e11357, 2010.
28. Johnson, M. B., Kawasawa, Y. I., Mason, C. E., Krsnik, Z., Coppola, G., Bogdanovic, D., Geschwind, D. H., Mane, S. M., State, M. W., and Sestan, N. Functional and evolutionary insights into human brain development through global transcriptome analysis. *Neuron*, 62: 494-509, 2009.
29. Yeo, G., Holste, D., Kreiman, G., and Burge, C. B. Variation in alternative splicing across human tissues. *Genome Biol*, 5: R74, 2004.
30. Cao, X., Yeo, G., Muotri, A. R., Kuwabara, T., and Gage, F. H. Noncoding RNAs in the mammalian central nervous system. *Annu Rev Neurosci*, 29: 77-103, 2006.
31. Feng, J., Chang, H., Li, E., and Fan, G. Dynamic expression of de novo DNA methyltransferases Dnmt3a and Dnmt3b in the central nervous system. *J Neurosci Res*, 79: 734-746, 2005.
32. Sanchez-Mut, J. V., Huertas, D., and Esteller, M. Aberrant epigenetic landscape in intellectual disability. *Prog Brain Res*, 197: 53-71, 2012.

## References

33. Guo, J. U., Su, Y., Zhong, C., Ming, G. L., and Song, H. Hydroxylation of 5-methylcytosine by TET1 promotes active DNA demethylation in the adult brain. *Cell*, 145: 423-434, 2011.
34. Lein, E. S., Hawrylycz, M. J., Ao, N., Ayres, M., Bensinger, A., Bernard, A., Boe, A. F., Boguski, M. S., Brockway, K. S., Byrnes, E. J., Chen, L., Chen, L., Chen, T. M., Chin, M. C., Chong, J., Crook, B. E., Czaplinska, A., Dang, C. N., Datta, S., Dee, N. R., Desaki, A. L., Desta, T., Diep, E., Dolbeare, T. A., Donelan, M. J., Dong, H. W., Dougherty, J. G., Duncan, B. J., Ebbert, A. J., Eichele, G., Estin, L. K., Faber, C., Facer, B. A., Fields, R., Fischer, S. R., Fliss, T. P., Frensley, C., Gates, S. N., Glattfelder, K. J., Halverson, K. R., Hart, M. R., Hohmann, J. G., Howell, M. P., Jeung, D. P., Johnson, R. A., Karr, P. T., Kawal, R., Kidney, J. M., Knapik, R. H., Kuan, C. L., Lake, J. H., Laramie, A. R., Larsen, K. D., Lau, C., Lemon, T. A., Liang, A. J., Liu, Y., Luong, L. T., Michaels, J., Morgan, J. J., Morgan, R. J., Mortrud, M. T., Mosqueda, N. F., Ng, L. L., Ng, R., Orta, G. J., Overly, C. C., Pak, T. H., Parry, S. E., Pathak, S. D., Pearson, O. C., Puchalski, R. B., Riley, Z. L., Rockett, H. R., Rowland, S. A., Royall, J. J., Ruiz, M. J., Sarno, N. R., Schaffnit, K., Shapovalova, N. V., Sivisay, T., Slaughterbeck, C. R., Smith, S. C., Smith, K. A., Smith, B. I., Sodt, A. J., Stewart, N. N., Stumpf, K. R., Sunkin, S. M., Sutram, M., Tam, A., Teemer, C. D., Thaller, C., Thompson, C. L., Varnam, L. R., Visel, A., Whitlock, R. M., Wohnoutka, P. E., Wolkey, C. K., Wong, V. Y., Wood, M., Yaylaoglu, M. B., Young, R. C., Youngstrom, B. L., Yuan, X. F., Zhang, B., Zwingman, T. A. and Jones, A. R. Genome-wide atlas of gene expression in the adult mouse brain. *Nature*, 445: 168-176, 2007.
35. Jin, S. G., Wu, X., Li, A. X., and Pfeifer, G. P. Genomic mapping of 5-hydroxymethylcytosine in the human brain. *Nucleic Acids Res*, 39: 5015-5024, 2011.
36. Feng, J., Zhou, Y., Campbell, S. L., Le, T., Li, E., Sweatt, J. D., Silva, A. J., and Fan, G. Dnmt1 and Dnmt3a maintain DNA methylation and regulate synaptic function in adult forebrain neurons. *Nat Neurosci*, 13: 423-430, 2010.
37. Klein, C. J., Botuyan, M. V., Wu, Y., Ward, C. J., Nicholson, G. A., Hammans, S., Hojo, K., Yamanishi, H., Karpf, A. R., Wallace, D. C., Simon, M., Lander, C., Boardman, L. A., Cunningham, J. M., Smith, G. E., Litchy, W. J., Boes, B., Atkinson, E. J., Middha, S., PJ, B. D., Parisi, J. E., Mer, G., Smith, D. I., and Dyck, P. J. Mutations in DNMT1 cause hereditary sensory neuropathy with dementia and hearing loss. *Nat Genet*, 43: 595-600, 2011.
38. Wu, H., Coskun, V., Tao, J., Xie, W., Ge, W., Yoshikawa, K., Li, E., Zhang, Y., and Sun, Y. E. Dnmt3a-dependent nonpromoter DNA methylation facilitates transcription of neurogenic genes. *Science*, 329: 444-448, 2010.
39. Ma, D. K., Jang, M. H., Guo, J. U., Kitabatake, Y., Chang, M. L., Pow-Anpongkul, N., Flavell, R. A., Lu, B., Ming, G. L., and Song, H. Neuronal activity-induced Gadd45b promotes epigenetic DNA demethylation and adult neurogenesis. *Science*, 323: 1074-1077, 2009.
40. Miller, C. A., Gavin, C. F., White, J. A., Parrish, R. R., Honasoge, A., Yancey, C. R., Rivera, I. M., Rubio, M. D., Rumbaugh, G., and Sweatt, J. D. Cortical DNA methylation maintains remote memory. *Nat Neurosci*, 13: 664-666, 2010.
41. Levenson, J. M., O'Riordan, K. J., Brown, K. D., Trinh, M. A., Molfese, D. L., and Sweatt, J. D. Regulation of histone acetylation during memory formation in the hippocampus. *J Biol Chem*, 279: 40545-40559, 2004.
42. Guan, J. S., Haggarty, S. J., Giacometti, E., Dannenberg, J. H., Joseph, N., Gao, J., Nieland, T. J., Zhou, Y., Wang, X., Mazitschek, R., Bradner, J. E., DePinho, R. A., Jaenisch, R., and Tsai, L. H. HDAC2 negatively regulates memory formation and synaptic plasticity. *Nature*, 459: 55-60, 2009.

## References

43. Alarcon, J. M., Malleret, G., Touzani, K., Vronskaya, S., Ishii, S., Kandel, E. R., and Barco, A. Chromatin acetylation, memory, and LTP are impaired in CBP<sup>+/-</sup> mice: a model for the cognitive deficit in Rubinstein-Taybi syndrome and its amelioration. *Neuron*, 42: 947-959, 2004.
44. Urdinguio, R. G., Sanchez-Mut, J. V., and Esteller, M. Epigenetic mechanisms in neurological diseases: genes, syndromes, and therapies. *Lancet Neurol*, 8: 1056-1072, 2009.
45. Rett, A. On a unusual brain atrophy syndrome in hyperammonemia in childhood. *Wien Med Wochenschr*, 116: 723-726, 1966.
46. Hagberg, B., Aicardi, J., Dias, K., and Ramos, O. A progressive syndrome of autism, dementia, ataxia, and loss of purposeful hand use in girls: Rett's syndrome: report of 35 cases. *Ann Neurol*, 14: 471-479, 1983.
47. Amir, R. E., Van den Veyver, I. B., Wan, M., Tran, C. Q., Francke, U., and Zoghbi, H. Y. Rett syndrome is caused by mutations in X-linked MECP2, encoding methyl-CpG-binding protein 2. *Nat Genet*, 23: 185-188, 1999.
48. Lewis, J. D., Meehan, R. R., Henzel, W. J., Maurer-Fogy, I., Jeppesen, P., Klein, F., and Bird, A. Purification, sequence, and cellular localization of a novel chromosomal protein that binds to methylated DNA. *Cell*, 69: 905-914, 1992.
49. Quaderi, N. A., Meehan, R. R., Tate, P. H., Cross, S. H., Bird, A. P., Chatterjee, A., Herman, G. E., and Brown, S. D. Genetic and physical mapping of a gene encoding a methyl CpG binding protein, *Mecp2*, to the mouse X chromosome. *Genomics*, 22: 648-651, 1994.
50. Chahrour, M., Jung, S. Y., Shaw, C., Zhou, X., Wong, S. T., Qin, J., and Zoghbi, H. Y. MeCP2, a key contributor to neurological disease, activates and represses transcription. *Science*, 320: 1224-1229, 2008.
51. Klose, R. J. and Bird, A. P. MeCP2 behaves as an elongated monomer that does not stably associate with the Sin3a chromatin remodeling complex. *J Biol Chem*, 279: 46490-46496, 2004.
52. Skene, P. J., Illingworth, R. S., Webb, S., Kerr, A. R., James, K. D., Turner, D. J., Andrews, R., and Bird, A. P. Neuronal MeCP2 is expressed at near histone-octamer levels and globally alters the chromatin state. *Mol Cell*, 37: 457-468, 2010.
53. Chahrour, M. and Zoghbi, H. Y. The story of Rett syndrome: from clinic to neurobiology. *Neuron*, 56: 422-437, 2007.
54. Hagberg, B. Clinical manifestations and stages of Rett syndrome. *Ment Retard Dev Disabil Res Rev*, 8: 61-65, 2002.
55. Trevathan, E. and Naidu, S. The clinical recognition and differential diagnosis of Rett syndrome. *J Child Neurol*, 3 Suppl: S6-16, 1988.
56. Huppke, P., KOhler, K., Brockmann, K., Stettner, G. M., and Gartner, J. Treatment of epilepsy in Rett syndrome. *Eur J Paediatr Neurol*, 11: 10-16, 2007.
57. Steffenburg, U., Hagberg, G., and Hagberg, B. Epilepsy in a representative series of Rett syndrome. *Acta Paediatr*, 90: 34-39, 2001.
58. Krajnc, N., Zupancic, N., and Orazem, J. Epilepsy treatment in Rett syndrome. *J Child Neurol*, 26: 1429-1433, 2011.

## References

59. Hendrich, B. and Bird, A. Identification and characterization of a family of mammalian methyl-CpG binding proteins. *Mol Cell Biol*, 18: 6538-6547, 1998.
60. Braunschweig, D., Simcox, T., Samaco, R. C., and LaSalle, J. M. X-Chromosome inactivation ratios affect WTMeCP2 expression within mosaic Rett syndrome and *MeCP2*<sup>-/+</sup> mouse brain. *Hum Mol Genet*, 13: 1275-1286, 2004.
61. LaSalle, J. M., Goldstine, J., Balmer, D., and Greco, C. M. Quantitative localization of heterogeneous methyl-CpG-binding protein 2 (MeCP2) expression phenotypes in normal and Rett syndrome brain by laser scanning cytometry. *Hum Mol Genet*, 10: 1729-1740, 2001.
62. Shahbazian, M. D., Antalffy, B., Armstrong, D. L., and Zoghbi, H. Y. Insight into Rett syndrome: MeCP2 levels display tissue- and cell-specific differences and correlate with neuronal maturation. *Hum Mol Genet*, 11: 115-124, 2002.
63. Shahbazian, M. D. and Zoghbi, H. Y. Rett syndrome and MeCP2: linking epigenetics and neuronal function. *Am J Hum Genet*, 71: 1259-1272, 2002.
64. Kishi, N. and Macklis, J. D. MECP2 is progressively expressed in post-migratory neurons and is involved in neuronal maturation rather than cell fate decisions. *Mol Cell Neurosci*, 27: 306-321, 2004.
65. Knudsen, G. P., Neilson, T. C., Pedersen, J., Kerr, A., Schwartz, M., Hulten, M., Bailey, M. E., and Orstavik, K. H. Increased skewing of X chromosome inactivation in Rett syndrome patients and their mothers. *Eur J Hum Genet*, 14: 1189-1194, 2006.
66. Schanen, N. C., Dahle, E. J., Capozzoli, F., Holm, V. A., Zoghbi, H. Y., and Francke, U. A new Rett syndrome family consistent with X-linked inheritance expands the X chromosome exclusion map. *Am J Hum Genet*, 61: 634-641, 1997.
67. Guy, J., Gan, J., Selfridge, J., Cobb, S., and Bird, A. Reversal of neurological defects in a mouse model of Rett syndrome. *Science*, 315: 1143-1147, 2007.
68. Horike, S. How the methyl-CpG binding protein-related epigenetic disease turns on the genes that produce its symptoms. *Tanpakushitsu Kakusan KOs*, 50: 978-984, 2005.
69. Li, Y., Wang, H., Muffat, J., Cheng, A. W., Orlando, D. A., Loven, J., Kwok, S. M., Feldman, D. A., Bateup, H. S., Gao, Q., Hockemeyer, D., Mitalipova, M., Lewis, C. A., Vander Heiden, M. G., Sur, M., Young, R. A., and Jaenisch, R. Global transcriptional and translational repression in human-embryonic-stem-cell-derived Rett syndrome neurons. *Cell Stem Cell*, 13: 446-458, 2013.
70. Alvarez-Saavedra, M., Antoun, G., Yanagiya, A., Oliva-Hernandez, R., Cornejo-Palma, D., Perez-Iratxeta, C., Sonenberg, N., and Cheng, H. Y. miRNA-132 orchestrates chromatin remodeling and translational control of the circadian clock. *Hum Mol Genet*, 20: 731-751, 2011.
71. D'Esposito, M., Quaderi, N. A., Ciccociola, A., Bruni, P., Esposito, T., D'Urso, M., and Brown, S. D. Isolation, physical mapping, and northern analysis of the X-linked human gene encoding methyl CpG-binding protein, MECP2. *Mamm Genome*, 7: 533-535, 1996.
72. Kudo, S. Methyl-CpG-binding protein MeCP2 represses Sp1-activated transcription of the human leuKOsialin gene when the promoter is methylated. *Mol Cell Biol*, 18: 5492-5499, 1998.
73. Jones, D. P., Carlson, J. L., Samiec, P. S., Sternberg, P., Jr., Mody, V. C., Jr., Reed, R. L., and Brown, L. A. Glutathione measurement in human plasma. Evaluation of sample

## References

collection, storage and derivatization conditions for analysis of dansyl derivatives by HPLC. *Clin Chim Acta*, 275: 175-184, 1998.

74. Kriaucionis, S. and Bird, A. The major form of MeCP2 has a novel N-terminus generated by alternative splicing. *Nucleic Acids Res*, 32: 1818-1823, 2004.

75. Nan, X., Ng, H. H., Johnson, C. A., Laherty, C. D., Turner, B. M., Eisenman, R. N., and Bird, A. Transcriptional repression by the methyl-CpG-binding protein MeCP2 involves a histone deacetylase complex. *Nature*, 393: 386-389, 1998.

76. Zachariah, R. M. and Rastegar, M. Linking epigenetics to human disease and Rett syndrome: the emerging novel and challenging concepts in MeCP2 research. *Neural Plast*, 2012: 415825, 2012.

77. Matijevic, T., Knezevic, J., Slavica, M., and Pavelic, J. Rett syndrome: from the gene to the disease. *Eur Neurol*, 61: 3-10, 2009.

78. Chadwick, L. H. and Wade, P. A. MeCP2 in Rett syndrome: transcriptional repressor or chromatin architectural protein? *Curr Opin Genet Dev*, 17: 121-125, 2007.

79. Ben-Shachar, S., Chahrour, M., Thaller, C., Shaw, C. A., and Zoghbi, H. Y. Mouse models of MeCP2 disorders share gene expression changes in the cerebellum and hypothalamus. *Hum Mol Genet*, 18: 2431-2442, 2009.

80. Martinowich, K., Hattori, D., Wu, H., Fouse, S., He, F., Hu, Y., Fan, G., and Sun, Y. E. DNA methylation-related chromatin remodeling in activity-dependent BDNF gene regulation. *Science*, 302: 890-893, 2003.

81. Guy, J., Cheval, H., Selfridge, J., and Bird, A. The role of MeCP2 in the brain. *Annu Rev Cell Dev Biol*, 27: 631-652, 2011.

82. Petazzi, P., Sandoval, J., Szczesna, K., Jorge, O. C., Roa, L., Sayols, S., Gomez, A., Huertas, D., and Esteller, M. Dysregulation of the long non-coding RNA transcriptome in a Rett syndrome mouse model. *RNA Biol*, 10: 1197-1203, 2013.

83. Bienvenu, T. and Chelly, J. Molecular genetics of Rett syndrome: when DNA methylation goes unrecognized. *Nat Rev Genet*, 7: 415-426, 2006.

84. Cohen, S., Gabel, H. W., Hemberg, M., Hutchinson, A. N., Sadacca, L. A., Ebert, D. H., Harmin, D. A., Greenberg, R. S., Verdine, V. K., Zhou, Z., Wetsel, W. C., West, A. E., and Greenberg, M. E. Genome-wide activity-dependent MeCP2 phosphorylation regulates nervous system development and function. *Neuron*, 72: 72-85, 2011.

85. Ballas, N., Lioy, D. T., Grunseich, C., and Mandel, G. Non-cell autonomous influence of MeCP2-deficient glia on neuronal dendritic morphology. *Nat Neurosci*, 12: 311-317, 2009.

86. Maezawa, I. and Jin, L. W. Rett syndrome microglia damage dendrites and synapses by the elevated release of glutamate. *J Neurosci*, 30: 5346-5356, 2009.

87. Maezawa, I., Swanberg, S., Harvey, D., LaSalle, J. M., and Jin, L. W. Rett syndrome astrocytes are abnormal and spread MeCP2 deficiency through gap junctions. *J Neurosci*, 29: 5051-5061, 2009.

88. Baker, S. A., Chen, L., Wilkins, A. D., Yu, P., Lichtarge, O., and Zoghbi, H. Y. An AT-hook domain in MeCP2 determines the clinical course of Rett syndrome and related disorders. *Cell*, 152: 984-996, 2013.

## References

89. Klose, R. J., Sarraf, S. A., Schmiedeberg, L., McDermott, S. M., Stancheva, I., and Bird, A. P. DNA binding selectivity of MeCP2 due to a requirement for A/T sequences adjacent to methyl-CpG. *Mol Cell*, 19: 667-678, 2005.
90. Nan, X., Hou, J., Maclean, A., Nasir, J., Lafuente, M. J., Shu, X., Kriaucionis, S., and Bird, A. Interaction between chromatin proteins MECP2 and ATRX is disrupted by mutations that cause inherited mental retardation. *Proc Natl Acad Sci U S A*, 104: 2709-2714, 2007.
91. Chen, R. Z., Akbarian, S., Tudor, M., and Jaenisch, R. Deficiency of methyl-CpG binding protein-2 in CNS neurons results in a Rett-like phenotype in mice. *Nat Genet*, 27: 327-331, 2001.
92. Ghosh, R. P., Horowitz-Scherer, R. A., Nikitina, T., ShlyakhtenKO, L. S., and Woodcock, C. L. MeCP2 binds cooperatively to its substrate and competes with histone H1 for chromatin binding sites. *Mol Cell Biol*, 30: 4656-4670, 2010.
93. Stancheva, I., Collins, A. L., Van den Veyver, I. B., Zoghbi, H., and Meehan, R. R. A mutant form of MeCP2 protein associated with human Rett syndrome cannot be displaced from methylated DNA by notch in *Xenopus* embryos. *Mol Cell*, 12: 425-435, 2003.
94. Agarwal, N., Hardt, T., Brero, A., Nowak, D., Rothbauer, U., Becker, A., Leonhardt, H., and Cardoso, M. C. MeCP2 interacts with HP1 and modulates its heterochromatin association during myogenic differentiation. *Nucleic Acids Res*, 35: 5402-5408, 2007.
95. Harikrishnan, K. N., Chow, M. Z., Baker, E. K., Pal, S., Bassal, S., Brasacchio, D., Wang, L., Craig, J. M., Jones, P. L., Sif, S., and El-Osta, A. Brahma links the SWI/SNF chromatin-remodeling complex with MeCP2-dependent transcriptional silencing. *Nat Genet*, 37: 254-264, 2005.
96. Kernohan, K. D., Jiang, Y., Tremblay, D. C., Bonvissuto, A. C., Eubanks, J. H., Mann, M. R., and Berube, N. G. ATRX partners with cohesin and MeCP2 and contributes to developmental silencing of imprinted genes in the brain. *Dev Cell*, 18: 191-202, 2010.
97. Fuks, F., Hurd, P. J., Wolf, D., Nan, X., Bird, A. P., and Kouzarides, T. The methyl-CpG-binding protein MeCP2 links DNA methylation to histone methylation. *J Biol Chem*, 278: 4035-4040, 2003.
98. Wan, M., Zhao, K., Lee, S. S., and Francke, U. MECP2 truncating mutations cause histone H4 hyperacetylation in Rett syndrome. *Hum Mol Genet*, 10: 1085-1092, 2001.
99. Balmer, D., Arredondo, J., Samaco, R. C., and LaSalle, J. M. MECP2 mutations in Rett syndrome adversely affect lymphocyte growth, but do not affect imprinted gene expression in blood or brain. *Hum Genet*, 110: 545-552, 2002.
100. Kaufmann, W. E., Johnston, M. V., and Blue, M. E. MeCP2 expression and function during brain development: implications for Rett syndrome's pathogenesis and clinical evolution. *Brain Dev*, 27 Suppl 1: S77-S87, 2005.
101. Urdinguio, R. G., Lopez-Serra, L., Lopez-Nieva, P., Alaminos, M., Diaz-Uriarte, R., Fernandez, A. F., and Esteller, M. Mecp2-null mice provide new neuronal targets for Rett syndrome. *PLoS One*, 3: e3669, 2008.
102. Urdinguio, R. G., Fernandez, A. F., Lopez-Nieva, P., Rossi, S., Huertas, D., Kulis, M., Liu, C. G., Croce, C. M., Calin, G. A., and Esteller, M. Disrupted microRNA expression caused by Mecp2 loss in a mouse model of Rett syndrome. *Epigenetics*, 5: 656-663, 2010.

## References

103. Ballestar, E., Ropero, S., Alaminos, M., Armstrong, J., Setien, F., Agrelo, R., Fraga, M. F., Herranz, M., Avila, S., Pineda, M., Monros, E., and Esteller, M. The impact of MECP2 mutations in the expression patterns of Rett syndrome patients. *Hum Genet*, 116: 91-104, 2005.
104. Makedonski, K., Abuhatzira, L., Kaufman, Y., Razin, A., and Shemer, R. MeCP2 deficiency in Rett syndrome causes epigenetic aberrations at the PWS/AS imprinting center that affects UBE3A expression. *Hum Mol Genet*, 14: 1049-1058, 2005.
105. Samaco, R. C., Hogart, A., and LaSalle, J. M. Epigenetic overlap in autism-spectrum neurodevelopmental disorders: MECP2 deficiency causes reduced expression of UBE3A and GABRB3. *Hum Mol Genet*, 14: 483-492, 2005.
106. Nuber, U. A., Kriaucionis, S., Roloff, T. C., Guy, J., Selfridge, J., Steinhoff, C., Schulz, R., LipKowitz, B., Ropers, H. H., Holmes, M. C., and Bird, A. Up-regulation of glucocorticoid-regulated genes in a mouse model of Rett syndrome. *Hum Mol Genet*, 14: 2247-2256, 2005.
107. Peddada, S., Yasui, D. H., and LaSalle, J. M. Inhibitors of differentiation (ID1, ID2, ID3 and ID4) genes are neuronal targets of MeCP2 that are elevated in Rett syndrome. *Hum Mol Genet*, 15: 2003-2014, 2006.
108. McGill, B. E., Bundle, S. F., Yaylaoglu, M. B., Carson, J. P., Thaller, C., and Zoghbi, H. Y. Enhanced anxiety and stress-induced corticosterone release are associated with increased *Crh* expression in a mouse model of Rett syndrome. *Proc Natl Acad Sci U S A*, 103: 18267-18272, 2006.
109. Itoh, M., Ide, S., Takashima, S., Kudo, S., Nomura, Y., Segawa, M., Kubota, T., Mori, H., Tanaka, S., Horie, H., Tanabe, Y., and Goto, Y. Methyl CpG-binding protein 2 (a mutation of which causes Rett syndrome) directly regulates insulin-like growth factor binding protein 3 in mouse and human brains. *J Neuropathol Exp Neurol*, 66: 117-123, 2007.
110. Deng, V., Matagne, V., Banine, F., Frerking, M., Ohliger, P., Budden, S., Pevsner, J., Dissen, G. A., Sherman, L. S., and Ojeda, S. R. FXYD1 is an MeCP2 target gene overexpressed in the brains of Rett syndrome patients and *Mecp2*-null mice. *Hum Mol Genet*, 16: 640-650, 2007.
111. Jordan, C., Li, H. H., Kwan, H. C., and Francke, U. Cerebellar gene expression profiles of mouse models for Rett syndrome reveal novel MeCP2 targets. *BMC Med Genet*, 8: 36, 2007.
112. Yasui, D. H., Peddada, S., Bieda, M. C., Vallerio, R. O., Hogart, A., Nagarajan, R. P., Thatcher, K. N., Farnham, P. J., and LaSalle, J. M. Integrated epigenomic analyses of neuronal MeCP2 reveal a role for long-range interaction with active genes. *Proc Natl Acad Sci U S A*, 104: 19416-19421, 2007.
113. Neul, J. L., Kaufmann, W. E., Glaze, D. G., Christodoulou, J., Clarke, A. J., Bahi-Buisson, N., Leonard, H., Bailey, M. E., Schanen, N. C., Zappella, M., Renieri, A., Huppke, P., and Percy, A. K. Rett syndrome: revised diagnostic criteria and nomenclature. *Ann Neurol*, 68: 944-950, 2010.
114. Bahi-Buisson, N., Nectoux, J., Rosas-Vargas, H., Milh, M., Boddaert, N., Girard, B., Cances, C., Ville, D., Afenjar, A., Rio, M., Heron, D., N'Guyen Morel, M. A., Arzimanoglou, A., Philippe, C., Jonveaux, P., Chelly, J., and Bienvu, T. Key clinical features to identify girls with CDKL5 mutations. *Brain*, 131: 2647-2661, 2008.
115. Ariani, F., Hayek, G., Rondinella, D., Artuso, R., Mencarelli, M. A., Spanhol-Rosseto, A., Pollazzon, M., Buoni, S., Spiga, O., Ricciardi, S., Meloni, I., Longo, I., Mari, F., Broccoli, V.,

## References

- Zappella, M., and Renieri, A. FOXP1 is responsible for the congenital variant of Rett syndrome. *Am J Hum Genet*, 83: 89-93, 2008.
116. Kilstrup-Nielsen, C., Rusconi, L., La Montanara, P., Ciceri, D., Bergo, A., Bedogni, F., and Landsberger, N. What we know and would like to know about CDKL5 and its involvement in epileptic encephalopathy. *Neural Plast*, 2012: 728267, 2012.
117. Fehr, S., Wilson, M., Downs, J., Williams, S., Murgia, A., Sartori, S., Vecchi, M., Ho, G., Polli, R., Psoni, S., Bao, X., de Klerk, N., Leonard, H., and Christodoulou, J. The CDKL5 disorder is an independent clinical entity associated with early-onset encephalopathy. *Eur J Hum Genet*, 21: 266-273, 2013.
118. Tao, J., Van Esch, H., Hagedorn-Greiwe, M., Hoffmann, K., Moser, B., Raynaud, M., Sperner, J., Fryns, J. P., Schwinger, E., Gecz, J., Ropers, H. H., and Kalscheuer, V. M. Mutations in the X-linked cyclin-dependent kinase-like 5 (CDKL5/STK9) gene are associated with severe neurodevelopmental retardation. *Am J Hum Genet*, 75: 1149-1154, 2004.
119. Kortum, F., Das, S., Flindt, M., Morris-Rosendahl, D. J., Stefanova, I., Goldstein, A., Horn, D., Klopocki, E., Kluger, G., Martin, P., Rauch, A., Roumer, A., Saitta, S., Walsh, L. E., Wiczorek, D., Uyanik, G., Kutsche, K., and Dobyns, W. B. The core FOXP1 syndrome phenotype consists of postnatal microcephaly, severe mental retardation, absent language, dyskinesia, and corpus callosum hypogenesis. *J Med Genet*, 48: 396-406, 2011.
120. Armstrong, D. D. Neuropathology of Rett syndrome. *J Child Neurol*, 20: 747-753, 2005.
121. Reiss, A. L., Faruque, F., Naidu, S., Abrams, M., Beaty, T., Bryan, R. N., and Moser, H. Neuroanatomy of Rett syndrome: a volumetric imaging study. *Ann Neurol*, 34: 227-234, 1993.
122. Wenk, G. L. Rett syndrome: neurobiological changes underlying specific symptoms. *Prog Neurobiol*, 51: 383-391, 1997.
123. Wenk, G. L. and Mobley, S. L. Choline acetyltransferase activity and vesamicol binding in Rett syndrome and in rats with nucleus basalis lesions. *Neuroscience*, 73: 79-84, 1996.
124. Brucke, T., Sofic, E., Killian, W., Rett, A., and Riederer, P. Reduced concentrations and increased metabolism of biogenic amines in a single case of Rett-syndrome: a postmortem brain study. *J Neural Transm*, 68: 315-324, 1987.
125. Lekman, A., Witt-Engerstrom, I., Gottfries, J., Hagberg, B. A., Percy, A. K., and Svennerholm, L. Rett syndrome: biogenic amines and metabolites in postmortem brain. *Pediatr Neurol*, 5: 357-362, 1989.
126. Zoghbi, H. Y., Percy, A. K., Glaze, D. G., Butler, I. J., and Riccardi, V. M. Reduction of biogenic amine levels in the Rett syndrome. *N Engl J Med*, 313: 921-924, 1985.
127. Segawa, M. and Nomura, Y. The pathophysiology of the Rett syndrome from the standpoint of polysomnography. *Brain Dev*, 12: 55-60, 1990.
128. Segawa, M. and Nomura, Y. Polysomnography in the Rett syndrome. *Brain Dev*, 14 Suppl: S46-54, 1992.
129. Hamberger, A., Gillberg, C., Palm, A., and Hagberg, B. Elevated CSF glutamate in Rett syndrome. *Neuropediatrics*, 23: 212-213, 1992.
130. Lappalainen, R. and RiiKOnen, R. S. High levels of cerebrospinal fluid glutamate in Rett syndrome. *Pediatr Neurol*, 15: 213-216, 1996.

## References

131. Lappalainen, R., Lindholm, D., and RiiKOnen, R. Low levels of nerve groWTh factor in cerebrospinal fluid of children with Rett syndrome. *J Child Neurol*, 11: 296-300, 1996.
132. Riikonen, R. and Vanhala, R. Levels of cerebrospinal fluid nerve-groWTh factor differ in infantile autism and Rett syndrome. *Dev Med Child Neurol*, 41: 148-152, 1999.
133. Chapleau, C. A., Calfa, G. D., Lane, M. C., Albertson, A. J., Larimore, J. L., Kudo, S., Armstrong, D. L., Percy, A. K., and Pozzo-Miller, L. Dendritic spine pathologies in hippocampal pyramidal neurons from Rett syndrome brain and after expression of Rett-associated MECP2 mutations. *Neurobiol Dis*, 35: 219-233, 2009.
134. Fukuda, T., Itoh, M., Ichikawa, T., Washiyama, K., and Goto, Y. Delayed maturation of neuronal architecture and synaptogenesis in cerebral cortex of *Mecp2*-deficient mice. *J Neuropathol Exp Neurol*, 64: 537-544, 2005.
135. Timmusk, T., Palm, K., Metsis, M., Reintam, T., Paalme, V., Saarma, M., and Persson, H. Multiple promoters direct tissue-specific expression of the rat BDNF gene. *Neuron*, 10: 475-489, 1993.
136. Aid, T., Kazantseva, A., Piirsoo, M., Palm, K., and Timmusk, T. Mouse and rat BDNF gene structure and expression revisited. *J Neurosci Res*, 85: 525-535, 2007.
137. Tao, X., Finkbeiner, S., Arnold, D. B., Shaywitz, A. J., and Greenberg, M. E. Ca<sup>2+</sup> influx regulates BDNF transcription by a CREB family transcription factor-dependent mechanism. *Neuron*, 20: 709-726, 1998.
138. Dani, V. S., Chang, Q., Maffei, A., Turrigiano, G. G., Jaenisch, R., and Nelson, S. B. Reduced cortical activity due to a shift in the balance between excitation and inhibition in a mouse model of Rett syndrome. *Proc Natl Acad Sci U S A*, 102: 12560-12565, 2005.
139. Ogier, M., Wang, H., Hong, E., Wang, Q., Greenberg, M. E., and Katz, D. M. BDNF expression and respiratory function improve after ampakine treatment in a mouse model of Rett syndrome. *J Neurosci*, 27: 10912-10917, 2007.
140. de Kloet, C. S., Vermetten, E., Geuze, E., Kavelaars, A., Heijnen, C. J., and Westenberg, H. G. Assessment of HPA-axis function in posttraumatic stress disorder: pharmacological and non-pharmacological challenge tests, a review. *J Psychiatr Res*, 40: 550-567, 2006.
141. Champagne, D. L., Bagot, R. C., van Hasselt, F., Ramakers, G., Meaney, M. J., de Kloet, E. R., Joels, M., and Krugers, H. Maternal care and hippocampal plasticity: evidence for experience-dependent structural plasticity, altered synaptic functioning, and differential responsiveness to glucocorticoids and stress. *J Neurosci*, 28: 6037-6045, 2008.
142. Sofic, E., Riederer, P., Killian, W., and Rett, A. Reduced concentrations of ascorbic acid and glutathione in a single case of Rett syndrome: a postmortem brain study. *Brain Dev*, 9: 529-531, 1987.
143. Squillaro, T., Alessio, N., Cipollaro, M., Melone, M. A., Hayek, G., Renieri, A., Giordano, A., and Galderisi, U. Reduced expression of MECP2 affects cell commitment and maintenance in neurons by triggering senescence: new perspective for Rett syndrome. *Mol Biol Cell*, 23: 1435-1445, 2012.
144. Valinluck, V., Tsai, H. H., Rogstad, D. K., Burdzy, A., Bird, A., and Sowers, L. C. Oxidative damage to methyl-CpG sequences inhibits the binding of the methyl-CpG binding

## References

- domain (MBD) of methyl-CpG binding protein 2 (MeCP2). *Nucleic Acids Res*, 32: 4100-4108, 2004.
145. De Felice, C., Signorini, C., Leoncini, S., Pecorelli, A., Durand, T., Valacchi, G., Ciccoli, L., and Hayek, J. The role of oxidative stress in Rett syndrome: an overview. *Ann N Y Acad Sci*, 1259: 121-135, 2012.
146. Sticozzi, C., Belmonte, G., Pecorelli, A., Cervellati, F., Leoncini, S., Signorini, C., Ciccoli, L., De Felice, C., Hayek, J., and Valacchi, G. Scavenger receptor B1 post-translational modifications in Rett syndrome. *FEBS Lett*, 587: 2199-2204, 2013.
147. Grosser, E., Hirt, U., Janc, O. A., Menzfeld, C., Fischer, M., Kempkes, B., Vogelgesang, S., Manzke, T. U., Opitz, L., Salinas-Riester, G., and Muller, M. Oxidative burden and mitochondrial dysfunction in a mouse model of Rett syndrome. *Neurobiol Dis*, 48: 102-114, 2012.
148. De Felice, C., Ciccoli, L., Leoncini, S., Signorini, C., Rossi, M., Vannuccini, L., Guazzi, G., Latini, G., Comporti, M., Valacchi, G., and Hayek, J. Systemic oxidative stress in classic Rett syndrome. *Free Radic Biol Med*, 47: 440-448, 2009.
149. Cossart, R., Bernard, C., and Ben-Ari, Y. Multiple facets of GABAergic neurons and synapses: multiple fates of GABA signalling in epilepsies. *Trends Neurosci*, 28: 108-115, 2005.
150. Lewis, D. A., Curley, A. A., Glausier, J. R., and Volk, D. W. Cortical parvalbumin interneurons and cognitive dysfunction in schizophrenia. *Trends Neurosci*, 35: 57-67, 2012.
151. Maliszewska-Cyna, E., Bawa, D., and Eubanks, J. H. Diminished prevalence but preserved synaptic distribution of N-methyl-D-aspartate receptor subunits in the methyl CpG binding protein 2 (MeCP2)-null mouse brain. *Neuroscience*, 168: 624-632, 2010.
152. Chao, H. T., Zoghbi, H. Y., and Rosenmund, C. MeCP2 controls excitatory synaptic strength by regulating glutamatergic synapse number. *Neuron*, 56: 58-65, 2007.
153. Zhang, Z. W., Zak, J. D., and Liu, H. MeCP2 is required for normal development of GABAergic circuits in the thalamus. *J Neurophysiol*, 103: 2470-2481, 2010.
154. Chao, H. T., Chen, H., Samaco, R. C., Xue, M., Chahrour, M., Yoo, J., Neul, J. L., Gong, S., Lu, H. C., Heintz, N., Ekker, M., Rubenstein, J. L., Noebels, J. L., Rosenmund, C., and Zoghbi, H. Y. Dysfunction in GABA signalling mediates autism-like stereotypies and Rett syndrome phenotypes. *Nature*, 468: 263-269, 2010.
155. Okado, N., Narita, M., and Narita, N. A biogenic amine-synapse mechanism for mental retardation and developmental disabilities. *Brain Dev*, 23 Suppl 1: S11-15, 2001.
156. Roux, J. C., Dura, E., Moncla, A., Mancini, J., and Villard, L. Treatment with desipramine improves breathing and survival in a mouse model for Rett syndrome. *Eur J Neurosci*, 25: 1915-1922, 2007.
157. Roux, J. C. and Villard, L. Biogenic amines in Rett syndrome: the usual suspects. *Behav Genet*, 40: 59-75, 2010.
158. Viemari, J. C., Roux, J. C., Tryba, A. K., Saywell, V., Burnet, H., Pena, F., Zanella, S., Bevengut, M., Barthelemy-Requin, M., Herzing, L. B., Moncla, A., Mancini, J., Ramirez, J. M., Villard, L., and Hilaire, G. Mecp2 deficiency disrupts norepinephrine and respiratory systems in mice. *J Neurosci*, 25: 11521-11530, 2005.

## References

159. Nielsen, J. B., Bertelsen, A., and Lou, H. C. Low CSF HVA levels in the Rett syndrome: a reflection of restricted synapse formation? *Brain Dev*, 14 Suppl: S63-65, 1992.
160. Guy, J., Hendrich, B., Holmes, M., Martin, J. E., and Bird, A. A mouse *Mecp2*-null mutation causes neurological symptoms that mimic Rett syndrome. *Nat Genet*, 27: 322-326, 2001.
161. Shahbazian, M., Young, J., Yuva-Paylor, L., Spencer, C., Antalffy, B., Noebels, J., Armstrong, D., Paylor, R., and Zoghbi, H. Mice with truncated MeCP2 recapitulate many Rett syndrome features and display hyperacetylation of histone H3. *Neuron*, 35: 243-254, 2002.
162. Moretti, P., Levenson, J. M., Battaglia, F., Atkinson, R., Teague, R., Antalffy, B., Armstrong, D., Arancio, O., Sweatt, J. D., and Zoghbi, H. Y. Learning and memory and synaptic plasticity are impaired in a mouse model of Rett syndrome. *J Neurosci*, 26: 319-327, 2006.
163. Collins, A. L., Levenson, J. M., Vilaythong, A. P., Richman, R., Armstrong, D. L., Noebels, J. L., David Sweatt, J., and Zoghbi, H. Y. Mild overexpression of MeCP2 causes a progressive neurological disorder in mice. *Hum Mol Genet*, 13: 2679-2689, 2004.
164. Luikenhuis, S., Giacometti, E., Beard, C. F., and Jaenisch, R. Expression of MeCP2 in postmitotic neurons rescues Rett syndrome in mice. *Proc Natl Acad Sci U S A*, 101: 6033-6038, 2004.
165. Van Esch, H. MECP2 Duplication Syndrome. *Mol Syndromol*, 2: 128-136, 2012.
166. Samaco, R. C., Fryer, J. D., Ren, J., Fyffe, S., Chao, H. T., Sun, Y., Greer, J. J., Zoghbi, H. Y., and Neul, J. L. A partial loss of function allele of methyl-CpG-binding protein 2 predicts a human neurodevelopmental syndrome. *Hum Mol Genet*, 17: 1718-1727, 2008.
167. Pelka, G. J., Watson, C. M., Radziewicz, T., Hayward, M., Lahooti, H., Christodoulou, J., and Tam, P. P. *Mecp2* deficiency is associated with learning and cognitive deficits and altered gene activity in the hippocampal region of mice. *Brain*, 129: 887-898, 2006.
168. Fyffe, S. L., Neul, J. L., Samaco, R. C., Chao, H. T., Ben-Shachar, S., Moretti, P., McGill, B. E., Goulding, E. H., Sullivan, E., Tecott, L. H., and Zoghbi, H. Y. Deletion of *Mecp2* in *Sim1*-expressing neurons reveals a critical role for MeCP2 in feeding behaviour, aggression, and the response to stress. *Neuron*, 59: 947-958, 2008.
169. Samaco, R. C., Mandel-Brehm, C., Chao, H. T., Ward, C. S., Fyffe-Maricich, S. L., Ren, J., Hyland, K., Thaller, C., Maricich, S. M., Humphreys, P., Greer, J. J., Percy, A., Glaze, D. G., Zoghbi, H. Y., and Neul, J. L. Loss of MeCP2 in aminergic neurons causes cell-autonomous defects in neurotransmitter synthesis and specific behavioural abnormalities. *Proc Natl Acad Sci U S A*, 106: 21966-21971, 2009.
170. Gemelli, T., Berton, O., Nelson, E. D., Perrotti, L. I., Jaenisch, R., and Monteggia, L. M. Postnatal loss of methyl-CpG binding protein 2 in the forebrain is sufficient to mediate behavioural aspects of Rett syndrome in mice. *Biol Psychiatry*, 59: 468-476, 2006.
171. Stearns, N. A., Schaeviz, L. R., Bowling, H., Nag, N., Berger, U. V., and Berger-Sweeney, J. Behavioural and anatomical abnormalities in *Mecp2* mutant mice: a model for Rett syndrome. *Neuroscience*, 146: 907-921, 2007.
172. Matarazzo, V., Cohen, D., Palmer, A. M., Simpson, P. J., Khokhar, B., Pan, S. J., and Ronnett, G. V. The transcriptional repressor *Mecp2* regulates terminal neuronal differentiation. *Mol Cell Neurosci*, 27: 44-58, 2004.

## References

173. Smrt, R. D., Eaves-Egenes, J., Barkho, B. Z., Santistevan, N. J., Zhao, C., Aimone, J. B., Gage, F. H., and Zhao, X. *Mecp2* deficiency leads to delayed maturation and altered gene expression in hippocampal neurons. *Neurobiol Dis*, 27: 77-89, 2007.
174. Belichenko, N. P., Belichenko, P. V., and Mobley, W. C. Evidence for both neuronal cell autonomous and nonautonomous effects of methyl-CpG-binding protein 2 in the cerebral cortex of female mice with *Mecp2* mutation. *Neurobiol Dis*, 34: 71-77, 2009.
175. Tropea, D., Giacometti, E., Wilson, N. R., Beard, C., McCurry, C., Fu, D. D., Flannery, R., Jaenisch, R., and Sur, M. Partial reversal of Rett Syndrome-like symptoms in MeCP2 mutant mice. *Proc Natl Acad Sci U S A*, 106: 2029-2034, 2009.
176. McGraw, C. M., Samaco, R. C., and Zoghbi, H. Y. Adult neural function requires MeCP2. *Science*, 333: 186, 2011.
177. Schmid, D. A., Yang, T., Ogier, M., Adams, I., Mirakhur, Y., Wang, Q., Massa, S. M., Longo, F. M., and Katz, D. M. A TrkB small molecule partial agonist rescues TrkB phosphorylation deficits and improves respiratory function in a mouse model of Rett syndrome. *J Neurosci*, 32: 1803-1810, 2012.
178. Deogracias, R., Yazdani, M., Dekkers, M. P., Guy, J., Ionescu, M. C., Vogt, K. E., and Barde, Y. A. Fingolimod, a sphingosine-1 phosphate receptor modulator, increases BDNF levels and improves symptoms of a mouse model of Rett syndrome. *Proc Natl Acad Sci U S A*, 109: 14230-14235, 2012.
179. Roux, J. C., Zala, D., Panayotis, N., Borges-Correia, A., Saudou, F., and Villard, L. [Unexpected link between Huntington disease and Rett syndrome]. *Med Sci (Paris)*, 28: 44-46, 2012.
180. Abdala, A. P., Dutschmann, M., Bissonnette, J. M., and Paton, J. F. Correction of respiratory disorders in a mouse model of Rett syndrome. *Proc Natl Acad Sci U S A*, 107: 18208-18213, 2010.
181. De Filippis, B., Nativio, P., Fabbri, A., Ricceri, L., Adriani, W., Lacivita, E., Leopoldo, M., Passarelli, F., Fuso, A., and Laviola, G. Pharmacological Stimulation of the Brain Serotonin Receptor 7 as a Novel Therapeutic Approach for Rett Syndrome. *Neuropsychopharmacology*, 2014.
182. Fasano, C., Bourque, M. J., Lapointe, G., Leo, D., Thibault, D., Haber, M., Kortleven, C., Desgroseillers, L., Murai, K. K., and Trudeau, L. E. Dopamine facilitates dendritic spine formation by cultured striatal medium spiny neurons through both D1 and D2 dopamine receptors. *Neuropharmacology*, 67: 432-443, 2013.
183. Kitt, C. A. and Wilcox, B. J. Preliminary evidence for neurodegenerative changes in the substantia nigra of Rett syndrome. *Neuropediatrics*, 26: 114-118, 1995.
184. Jellinger, K., Armstrong, D., Zoghbi, H. Y., and Percy, A. K. Neuropathology of Rett syndrome. *Acta Neuropathol*, 76: 142-158, 1988.
185. Jellinger, K. A. Rett Syndrome -- an update. *J Neural Transm*, 110: 681-701, 2003.
186. Blandini, F., Nappi, G., Tassorelli, C., and Martignoni, E. Functional changes of the basal ganglia circuitry in Parkinson's disease. *Prog Neurobiol*, 62: 63-88, 2000.
187. Jenner, P. Functional models of Parkinson's disease: a valuable tool in the development of novel therapies. *Ann Neurol*, 64 Suppl 2: S16-29, 2008.

## References

188. Nguyen, M. V., Du, F., Felice, C. A., Shan, X., Nigam, A., Mandel, G., Robinson, J. K., and Ballas, N. MeCP2 is critical for maintaining mature neuronal networks and global brain anatomy during late stages of postnatal brain development and in the mature adult brain. *J Neurosci*, 32: 10021-10034, 2012.
189. Panayotis, N., Pratte, M., Borges-Correia, A., Ghata, A., Villard, L., and Roux, J. C. Morphological and functional alterations in the substantia nigra pars compacta of the *Mecp2*-null mouse. *Neurobiol Dis*, 41: 385-397, 2011.
190. Zanella, S., Mebarek, S., Lajard, A. M., Picard, N., Dutschmann, M., and Hilaire, G. Oral treatment with desipramine improves breathing and life span in Rett syndrome mouse model. *Respir Physiol Neurobiol*, 160: 116-121, 2008.
191. Riederer, P., Weiser, M., Wichart, I., Schmidt, B., Killian, W., and Rett, A. Preliminary brain autopsy findings in prodromic Rett syndrome. *Am J Med Genet Suppl*, 1: 305-315, 1986.
192. Wenk, G. L., Naidu, S., Casanova, M. F., Kitt, C. A., and Moser, H. Altered neurochemical markers in Rett's syndrome. *Neurology*, 41: 1753-1756, 1991.
193. Doppler, E., Rockenstein, E., Ubhi, K., Inglis, C., Mante, M., Adame, A., Crews, L., Hitzl, M., Moessler, H., and Masliah, E. Neurotrophic effects of Cerebrolysin in the *Mecp2*(308/Y) transgenic model of Rett syndrome. *Acta Neuropathol*, 116: 425-437, 2008.
194. Nag, N. and Berger-Sweeney, J. E. Postnatal dietary choline supplementation alters behaviour in a mouse model of Rett syndrome. *Neurobiol Dis*, 26: 473-480, 2007.
195. Ricceri, L., De Filippis, B., Fusco, A., and Laviola, G. Cholinergic hypofunction in *MeCP2*-308 mice: beneficial neurobehavioural effects of neonatal choline supplementation. *Behav Brain Res*, 221: 623-629, 2011.
196. Schaevitz, L. R., Moriuchi, J. M., Nag, N., Mellot, T. J., and Berger-Sweeney, J. Cognitive and social functions and *groWTh* factors in a mouse model of Rett syndrome. *Physiol Behav*, 100: 255-263, 2010.
197. Weng, S. M., McLeod, F., Bailey, M. E., and Cobb, S. R. Synaptic plasticity deficits in an experimental model of rett syndrome: long-term potentiation saturation and its pharmacological reversal. *Neuroscience*, 180: 314-321, 2011.
198. Braun, S., Kottwitz, D., and Nuber, U. A. Pharmacological interference with the glucocorticoid system influences symptoms and lifespan in a mouse model of Rett syndrome. *Hum Mol Genet*, 21: 1673-1680, 2012.
199. De Filippis, B., Ricceri, L., Fusco, A., and Laviola, G. Neonatal exposure to low dose corticosterone persistently modulates hippocampal mineralocorticoid receptor expression and improves locomotor/exploratory behaviour in a mouse model of Rett syndrome. *Neuropharmacology*, 68: 174-183, 2012.
200. De Filippis, B., Fabbri, A., Simone, D., Canese, R., Ricceri, L., Malchiodi-Albedi, F., Laviola, G., and Fiorentini, C. Modulation of RhoGTPases improves the behavioural phenotype and reverses astrocytic deficits in a mouse model of Rett syndrome. *Neuropsychopharmacology*, 37: 1152-1163, 2012.
201. Panighini, A., Duranti, E., Santini, F., Maffei, M., Pizzorusso, T., Funel, N., Taddei, S., Bernardini, N., Ippolito, C., Viridis, A., and Costa, M. Vascular dysfunction in a mouse model of rett syndrome and effects of curcumin treatment. *PLoS One*, 8: e64863, 2013.

## References

202. Buchovecky, C. M., Turley, S. D., Brown, H. M., Kyle, S. M., McDonald, J. G., Liu, B., Pieper, A. A., Huang, W., Katz, D. M., Russell, D. W., Shendure, J., and Justice, M. J. A suppressor screen in *Mecp2* mutant mice implicates cholesterol metabolism in Rett syndrome. *Nat Genet*, 45: 1013-1020, 2013.
203. Brendel, C., Belakhov, V., Werner, H., Wegener, E., Gartner, J., Nudelman, I., Baasov, T., and Huppke, P. Readthrough of nonsense mutations in Rett syndrome: evaluation of novel aminoglycosides and generation of a new mouse model. *J Mol Med (Berl)*, 89: 389-398, 2011.
204. Kondo, M., Gray, L. J., Pelka, G. J., Christodoulou, J., Tam, P. P., and Hannan, A. J. Environmental enrichment ameliorates a motor coordination deficit in a mouse model of Rett syndrome--*Mecp2* gene dosage effects and BDNF expression. *Eur J Neurosci*, 27: 3342-3350, 2008.
205. Lonetti, G., Angelucci, A., Morando, L., Boggio, E. M., Giustetto, M., and Pizzorusso, T. Early environmental enrichment moderates the behavioural and synaptic phenotype of *Mecp2* KO mice. *Biol Psychiatry*, 67: 657-665, 2010.
206. Nag, N., Moriuchi, J. M., Peitzman, C. G., Ward, B. C., Kolodny, N. H., and Berger-Sweeney, J. E. Environmental enrichment alters locomotor behaviour and ventricular volume in *Mecp2* 1lox mice. *Behav Brain Res*, 196: 44-48, 2009.
207. Gadalla, K. K., Bailey, M. E., Spike, R. C., Ross, P. D., Woodard, K. T., Kalburgi, S. N., Bachaboina, L., Deng, J. V., West, A. E., Samulski, R. J., Gray, S. J., and Cobb, S. R. Improved survival and reduced phenotypic severity following AAV9/MECP2 gene transfer to neonatal and juvenile male *Mecp2* knockOut mice. *Mol Ther*, 21: 18-30, 2013.
208. Garg, S. K., Liroy, D. T., Cheval, H., McGann, J. C., Bissonnette, J. M., Murtha, M. J., Foust, K. D., Kaspar, B. K., Bird, A., and Mandel, G. Systemic delivery of MeCP2 rescues behavioural and cellular deficits in female mouse models of Rett syndrome. *J Neurosci*, 33: 13612-13620, 2013.
209. Derecki, N. C., Cronk, J. C., Lu, Z., Xu, E., Abbott, S. B., Guyenet, P. G., and Kipnis, J. Wild-type microglia arrest pathology in a mouse model of Rett syndrome. *Nature*, 484: 105-109, 2012.
210. Johnson, R. A., Lam, M., Punzo, A. M., Li, H., Lin, B. R., Ye, K., Mitchell, G. S., and Chang, Q. 7,8-dihydroxyflavone exhibits therapeutic efficacy in a mouse model of Rett syndrome. *J Appl Physiol*, 112: 704-710, 2012.
211. Ellaway, C., Williams, K., Leonard, H., Higgins, G., Wilcken, B., and Christodoulou, J. Rett syndrome: randomized controlled trial of L-carnitine. *J Child Neurol*, 14: 162-167, 1999.
212. Ellaway, C. J., Peat, J., Williams, K., Leonard, H., and Christodoulou, J. Medium-term open label trial of L-carnitine in Rett syndrome. *Brain Dev*, 23 Suppl 1: S85-89, 2001.
213. De Felice, C., Signorini, C., Durand, T., Ciccoli, L., Leoncini, S., D'Esposito, M., Filosa, S., Oger, C., Guy, A., Bultel-Ponce, V., Galano, J. M., Pecorelli, A., De Felice, L., Valacchi, G., and Hayek, J. Partial rescue of Rett syndrome by omega-3 polyunsaturated fatty acids (PUFAs) oil. *Genes Nutr*, 7: 447-458, 2012.
214. Zappella, M., Genazzani, A., Facchinetti, F., and Hayek, G. Bromocriptine in the Rett syndrome. *Brain Dev*, 12: 221-225, 1990.
215. Nielsen, J. B., Lou, H. C., and Andresen, J. Biochemical and clinical effects of tyrosine and tryptophan in the Rett syndrome. *Brain Dev*, 12: 143-147, 1990.

## References

216. Gorbachevskaya, N., Bashina, V., Gratchev, V., and Iznak, A. Cerebrolysin therapy in Rett syndrome: clinical and EEG mapping study. *Brain Dev*, 23 Suppl 1: S90-93, 2001.
217. Glaze, D. G., Percy, A. K., Motil, K. J., Lane, J. B., Isaacs, J. S., Schultz, R. J., Barrish, J. O., Neul, J. L., O'Brien, W. E., and Smith, E. O. A study of the treatment of Rett syndrome with folate and betaine. *J Child Neurol*, 24: 551-556, 2009.
218. Freilinger, M., Dunkler, D., Lanator, I., Item, C. B., Muhl, A., Fowler, B., and Bodamer, O. A. Effects of creatine supplementation in Rett syndrome: a randomized, placebo-controlled trial. *J Dev Behav Pediatr*, 32: 454-460, 2011.
219. Hagebeuk, E. E., KOelman, J. H., Duran, M., Abeling, N. G., Vyth, A., and Poll-The, B. T. Clinical and electroencephalographic effects of folinic acid treatment in Rett syndrome patients. *J Child Neurol*, 26: 718-723, 2011.
220. Hagebeuk, E. E., Duran, M., KOelman, J. H., Abeling, N. G., Vyth, A., and Poll-The, B. T. Folinic acid supplementation in Rett syndrome patients does not influence the course of the disease: a randomized study. *J Child Neurol*, 27: 304-309, 2012.
221. Miralves, J., Magdeleine, E., and Joly, E. Design of an improved set of oligonucleotide primers for genotyping MeCP2tm1.1Bird KO mice by PCR. *Mol Neurodegener*, 2: 16, 2007.
222. Towbin, H., Staehelin, T., and Gordon, J. Electrophoretic transfer of proteins from polyacrylamide gels to nitrocellulose sheets: procedure and some applications. 1979. *Biotechnology*, 24: 145-149, 1992.
223. Rodriguez, A., Ehlenberger, D. B., Dickstein, D. L., Hof, P. R., and Wearne, S. L. Automated three-dimensional detection and shape classification of dendritic spines from fluorescence microscopy images. *PLoS One*, 3: e1997, 2008.
224. Rodriguez, A., Ehlenberger, D. B., Hof, P. R., and Wearne, S. L. Rayburst sampling, an algorithm for automated three-dimensional shape analysis from laser scanning microscopy images. *Nat Protoc*, 1: 2152-2161, 2006.
225. Sholl, D. A. Dendritic organization in the neurons of the visual and motor cortices of the cat. *J Anat*, 87: 387-406, 1953.
226. Choleris, E., Thomas, A. W., Kavaliers, M., and Prato, F. S. A detailed ethological analysis of the mouse open field test: effects of diazepam, chlordiazepoxide and an extremely low frequency pulsed magnetic field. *Neurosci Biobehav Rev*, 25: 235-260, 2001.
227. De Filippis, B., Ricceri, L., and Laviola, G. Early postnatal behavioural changes in the Mecp2-308 truncation mouse model of Rett syndrome. *Genes Brain Behav*, 9: 213-223, 2010.
228. Katz, D. M., Berger-Sweeney, J. E., Eubanks, J. H., Justice, M. J., Neul, J. L., Pozzo-Miller, L., Blue, M. E., Christian, D., Crawley, J. N., Giustetto, M., Guy, J., Howell, C. J., Kron, M., Nelson, S. B., Samaco, R. C., Schaevitz, L. R., St Hillaire-Clarke, C., Young, J. L., Zoghbi, H. Y., and Mamounas, L. A. Preclinical research in Rett syndrome: setting the foundation for translational success. *Dis Model Mech*, 5: 733-745, 2012.
229. Kilkenny, C., Browne, W. J., Cuthill, I. C., Emerson, M., and Altman, D. G. Improving bioscience research reporting: The ARRIVE guidelines for reporting animal research. *J Pharmacol Pharmacother*, 1: 94-99, 2010.
230. Ferrer, I., Kapfhammer, J. P., Hindelang, C., Kemp, S., Troffer-Charlier, N., Broccoli, V., Callyzot, N., Mooyer, P., Selhorst, J., Vreken, P., Wanders, R. J., Mandel, J. L., and Pujol, A.

## References

- Inactivation of the peroxisomal ABCDRD2 transporter in the mouse leads to late-onset ataxia involving mitochondria, Golgi and endoplasmic reticulum damage. *Hum Mol Genet*, 14: 3565-3577, 2005.
231. Ide, S., Itoh, M., and Goto, Y. Defect in normal developmental increase of the brain biogenic amine concentrations in the *mecp2*-null mouse. *Neurosci Lett*, 386: 14-17, 2005.
232. Santos, M., Silva-Fernandes, A., Oliveira, P., Sousa, N., and Maciel, P. Evidence for abnormal early development in a mouse model of Rett syndrome. *Genes Brain Behav*, 6: 277-286, 2007.
233. Taneja, P., Ogier, M., Brooks-Harris, G., Schmid, D. A., Katz, D. M., and Nelson, S. B. Pathophysiology of locus ceruleus neurons in a mouse model of Rett syndrome. *J Neurosci*, 29: 12187-12195, 2009.
234. Gu, M., Owen, A. D., Toffa, S. E., Cooper, J. M., Dexter, D. T., Jenner, P., Marsden, C. D., and Schapira, A. H. Mitochondrial function, GSH and iron in neurodegeneration and Lewy body diseases. *J Neurol Sci*, 158: 24-29, 1998.
235. Pearce, R. K., Owen, A., Daniel, S., Jenner, P., and Marsden, C. D. Alterations in the distribution of glutathione in the substantia nigra in Parkinson's disease. *J Neural Transm*, 104: 661-677, 1997.
236. Mena, M. A., Davila, V., and Sulzer, D. Neurotrophic effects of L-DOPA in postnatal MB dopamine neuron/cortical astrocyte cocultures. *J Neurochem*, 69: 1398-1408, 1997.
237. Wang, I. T., Reyes, A. R., and Zhou, Z. Neuronal morphology in MeCP2 mouse models is intrinsically variable and depends on age, cell type, and *Mecp2* mutation. *Neurobiol Dis*, 58: 3-12, 2013.
238. Loupe, P. S., Bredemeier, J. D., Schroeder, S. R., and Tessel, R. E. Dopamine reuptake inhibitor GBR-12909 induction of aberrant behaviours in animal models of dopamine dysfunction. *Int J Dev Neurosci*, 20: 323-333, 2002.
239. Elian, M. and Rudolf, N. D. EEG and respiration in Rett syndrome. *Acta Neurol Scand*, 83: 123-128, 1991.
240. Kerr, A. M. A review of the respiratory disorder in the Rett syndrome. *Brain Dev*, 14 Suppl: S43-45, 1992.
241. Viemari, J. C., Bevegut, M., Burnet, H., Coulon, P., Pequignot, J. M., Tiveron, M. C., and Hilaire, G. *Phox2a* gene, A6 neurons, and noradrenaline are essential for development of normal respiratory rhythm in mice. *J Neurosci*, 24: 928-937, 2004.
242. Gantz, S. C., Ford, C. P., Neve, K. A., and Williams, J. T. Loss of *Mecp2* in substantia nigra dopamine neurons compromises the nigrostriatal pathway. *J Neurosci*, 31: 12629-12637, 2011.
243. Mena, M. A., Casarejos, M. J., Solano, R. M., and de Yébenes, J. G. Half a century of L-DOPA. *Curr Top Med Chem*, 9: 880-893, 2009.
244. Han, S. K., Mytilineou, C., and Cohen, G. L-DOPA up-regulates glutathione and protects mesencephalic cultures against oxidative stress. *J Neurochem*, 66: 501-510, 1996.
245. Chinta, S. J. and Andersen, J. K. Dopaminergic neurons. *Int J Biochem Cell Biol*, 37: 942-946, 2005.

## References

246. Bauman, M. L., Kemper, T. L., and Arin, D. M. Pervasive neuroanatomic abnormalities of the brain in three cases of Rett's syndrome. *Neurology*, 45: 1581-1586, 1995.
247. Armstrong, D., Dunn, J. K., Antalffy, B., and Trivedi, R. Selective dendritic alterations in the cortex of Rett syndrome. *J Neuropathol Exp Neurol*, 54: 195-201, 1995.
248. Fiala, J. C., Spacek, J., and Harris, K. M. Dendritic spine pathology: cause or consequence of neurological disorders? *Brain Res Brain Res Rev*, 39: 29-54, 2002.
249. Molinoff, P. B. and Axelrod, J. Biochemistry of catecholamines. *Annu Rev Biochem*, 40: 465-500, 1971.
250. Kumer, S. C. and Vrana, K. E. Intricate regulation of Th activity and gene expression. *J Neurochem*, 67: 443-462, 1996.
251. Mena, M. A., Davila, V., Bogaluvsky, J., and Sulzer, D. A synergistic neurotrophic response to l-dihydroxyphenylalanine and nerve growth factor. *Mol Pharmacol*, 54: 678-686, 1998.
252. Doble, B. W. and Woodgett, J. R. GSK-3: tricks of the trade for a multi-tasking kinase. *J Cell Sci*, 116: 1175-1186, 2003.
253. Mukai, F., Ishiguro, K., Sano, Y., and Fujita, S. C. Alternative splicing isoform of tau protein kinase I/glycogen synthase kinase 3beta. *J Neurochem*, 81: 1073-1083, 2002.
254. Prickaerts, J., Moechars, D., Cryns, K., Lenaerts, I., van Craenendonck, H., Goris, I., Daneels, G., Bouwknecht, J. A., and Steckler, T. Transgenic mice overexpressing glycogen synthase kinase 3beta: a putative model of hyperactivity and mania. *J Neurosci*, 26: 9022-9029, 2006.
255. Beaulieu, J. M., Sotnikova, T. D., Yao, W. D., Kockeritz, L., Woodgett, J. R., Gainetdinov, R. R., and Caron, M. G. Lithium antagonizes dopamine-dependent behaviours mediated by an AKT/glycogen synthase kinase 3 signaling cascade. *Proc Natl Acad Sci U S A*, 101: 5099-5104, 2004.
256. Hooper, C., Markevich, V., Plattner, F., Killick, R., Schofield, E., Engel, T., Hernandez, F., Anderton, B., Rosenblum, K., Bliss, T., Cooke, S. F., Avila, J., Lucas, J. J., Giese, K. P., Stephenson, J., and Lovestone, S. Glycogen synthase kinase-3 inhibition is integral to long-term potentiation. *Eur J Neurosci*, 25: 81-86, 2007.
257. Zhu, L. Q., Wang, S. H., Liu, D., Yin, Y. Y., Tian, Q., Wang, X. C., Wang, Q., Chen, J. G., and Wang, J. Z. Activation of glycogen synthase kinase-3 inhibits long-term potentiation with synapse-associated impairments. *J Neurosci*, 27: 12211-12220, 2007.
258. Hall, A. C., Brennan, A., Goold, R. G., Cleverley, K., Lucas, F. R., Gordon-Weeks, P. R., and Salinas, P. C. Valproate regulates GSK-3-mediated axonal remodeling and synapsin I clustering in developing neurons. *Mol Cell Neurosci*, 20: 257-270, 2002.
259. Zhu, L. Q., Liu, D., Hu, J., Cheng, J., Wang, S. H., Wang, Q., Wang, F., Chen, J. G., and Wang, J. Z. GSK-3 beta inhibits presynaptic vesicle exocytosis by phosphorylating P/Q-type calcium channel and interrupting SNARE complex formation. *J Neurosci*, 30: 3624-3633, 2010.
260. Peineau, S., Bradley, C., Taghibiglou, C., Doherty, A., Bortolotto, Z. A., Wang, Y. T., and Collingridge, G. L. The role of GSK-3 in synaptic plasticity. *Br J Pharmacol*, 153 Suppl 1: S428-437, 2008.

## References

261. Portis, S., Giunta, B., Obregon, D., and Tan, J. The role of glycogen synthase kinase-3 signaling in neurodevelopment and fragile X syndrome. *Int J Physiol Pathophysiol Pharmacol*, 4: 140-148, 2012.
262. L'Episcopo, F., Tirolo, C., Testa, N., Caniglia, S., Morale, M. C., Deleidi, M., Serapide, M. F., Pluchino, S., and Marchetti, B. Plasticity of subventricular zone neuroprogenitors in MPTP (1-methyl-4-phenyl-1,2,3,6-tetrahydropyridine) mouse model of Parkinson's disease involves cross talk between inflammatory and Wnt/beta-catenin signaling pathways: functional consequences for neuroprotection and repair. *J Neurosci*, 32: 2062-2085, 2012.
263. Kimura, T., Yamashita, S., Nakao, S., Park, J. M., Murayama, M., Mizoroki, T., Yoshiike, Y., Sahara, N., and Takashima, A. GSK-3beta is required for memory reconsolidation in adult brain. *PLoS One*, 3: e3540, 2008.
264. Chenn, A. and Walsh, C. A. Increased neuronal production, enlarged forebrains and cytoarchitectural distortions in beta-catenin overexpressing transgenic mice. *Cereb Cortex*, 13: 599-606, 2003.
265. Zechner, D., Fujita, Y., Hulsken, J., Muller, T., Walther, I., Taketo, M. M., Crenshaw, E. B., 3rd, Birchmeier, W., and Birchmeier, C. beta-Catenin signals regulate cell growth and the balance between progenitor cell expansion and differentiation in the nervous system. *Dev Biol*, 258: 406-418, 2003.
266. Kim, W. Y. and Snider, W. D. Functions of GSK-3 Signaling in Development of the Nervous System. *Front Mol Neurosci*, 4: 44, 2011.
267. Gotschel, F., Kern, C., Lang, S., Sparna, T., Markmann, C., Schwager, J., McNelly, S., von Weizsacker, F., Laufer, S., Hecht, A., and Merfort, I. Inhibition of GSK-3 differentially modulates NF-kappaB, CREB, AP-1 and beta-catenin signaling in hepatocytes, but fails to promote TNF-alpha-induced apoptosis. *Exp Cell Res*, 314: 1351-1366, 2008.
268. Gurrieri, C., Piazza, F., Gnoato, M., Montini, B., Biasutto, L., Gattazzo, C., Brunetta, E., Cabrelle, A., Cinetto, F., Niero, R., Facco, M., Garbisa, S., Calabrese, F., Semenzato, G., and Agostini, C. 3-(2,4-dichlorophenyl)-4-(1-methyl-1H-indol-3-yl)-1H-pyrrole-2,5-dione (SB216763), a glycogen synthase kinase-3 inhibitor, displays therapeutic properties in a mouse model of pulmonary inflammation and fibrosis. *J Pharmacol Exp Ther*, 332: 785-794, 2010.
269. Valerio, A., Bertolotti, P., Delbarba, A., Perego, C., Dossena, M., Ragni, M., Spano, P., Carruba, M. O., De Simoni, M. G., and Nisoli, E. Glycogen synthase kinase-3 inhibition reduces ischemic cerebral damage, restores impaired mitochondrial biogenesis and prevents ROS production. *J Neurochem*, 116: 1148-1159, 2011.
270. Rui Y, Myers KR, Yu K, Wise A, De Blas AL, Hartzell HC, Zheng JQ. Activity-dependent regulation of dendritic growth and maintenance by glycogen synthase kinase 3β. *Nat Commun*, 4: 2628, 2013
271. Vigushin, D. M. and Coombes, R. C. Histone deacetylase inhibitors in cancer treatment. *Anticancer Drugs*, 13: 1-13, 2002.
272. Chang, J. G., Hsieh-Li, H. M., Jong, Y. J., Wang, N. M., Tsai, C. H., and Li, H. Treatment of spinal muscular atrophy by sodium butyrate. *Proc Natl Acad Sci U S A*, 98: 9808-9813, 2001.
273. Roy, A., Ghosh, A., Jana, A., Liu, X., Brahmachari, S., Gendelman, H. E., and Pahan, K. Sodium phenylbutyrate controls neuroinflammatory and antioxidant activities and protects dopaminergic neurons in mouse models of Parkinson's disease. *PLoS One*, 7: e38113, 2012.

## References

274. El-Husseini, A. E., Schnell, E., Chetkovich, D. M., Nicoll, R. A., and Brecht, D. S. PSD-95 involvement in maturation of excitatory synapses. *Science*, 290: 1364-1368, 2000.
275. Wang, H., Chan, S. A., Ogier, M., Hellard, D., Wang, Q., Smith, C., and Katz, D. M. Dysregulation of BDNF expression and neurosecretory function in *Mecp2* KO mice. *J Neurosci*, 26: 10911-10915, 2006.
276. Stuss, D. P., Boyd, J. D., Levin, D. B., and Delaney, K. R. MeCP2 mutation results in compartment-specific reductions in dendritic branching and spine density in layer 5 motor cortical neurons of YFP-H mice. *PLoS One*, 7: e31896, 2012.
277. Dunkley, P. R., Bobrovskaya, L., Graham, M. E., von Nagy-Felsobuki, E. I., and Dickson, P. W. Th phosphorylation: regulation and consequences. *J Neurochem*, 91: 1025-1043, 2004.
278. Mytilineou, C., Walker, R. H., JnoBaptiste, R., and Olanow, C. W. Levodopa is toxic to dopamine neurons in an in vitro but not an in vivo model of oxidative stress. *J Pharmacol Exp Ther*, 304: 792-800, 2003.

## **Publication list**



## Publication list

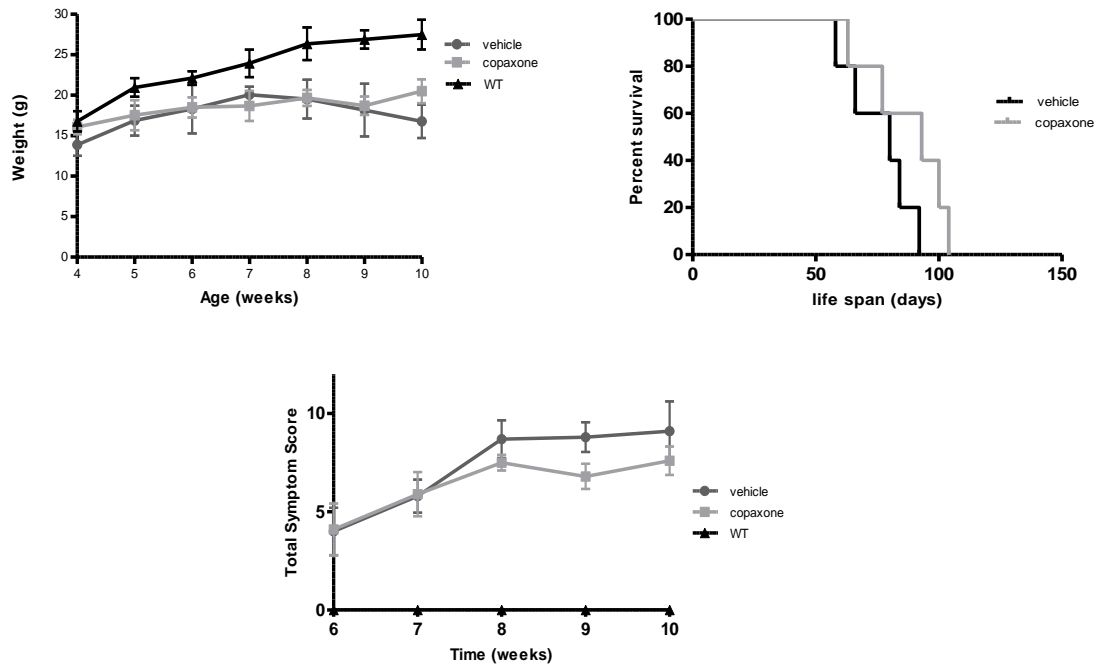
- Glycogen synthase kinase-3 inhibitor, SB216763, displays therapeutic potential in a mouse model of Rett syndrome (Manuscript in preparation) **Karolina Szczesna**, Olga de la Caridad, Paolo Petazzi, Laura Roa, Mauricio A. Saez, Mario L ucariello, Dori Huertas, Manel Esteller
- MECP2 in circadian rhythms. (Manuscript in preparation) Alexia Martinez de Paz, Jose Sanchez-Mut, Mauricio Saez, Paolo Petazzi, **Karolina Szczesna**, Dori Huertas, Juan Ausio, Manel Esteller
- Complexity of Interdependent Epigenetic Signals in Skin Cancer Initiation (KS and JS contributed equally to this work; Manuscript in preparation) **Karolina Szczesna**, Juan Sandoval, Balaji Rajashekar Meelis Kull, Vijayachitra Modhukur, Jaak Vilo, Dori Huertas, Manel Esteller
- Understanding chromatin diseases: molecular mechanisms and treatment. The DISCHROM Multi-ITN Consortium (Review in preparation) **Karolina Szczesna**, Dori Huertas, Manel Esteller
- Mutations in JMJD1C Are Involved in Autism Spectrum Disorders, Intellectual Disability and Rett Syndrome (Journal of Neuroscience, Manuscript under consideration) Mauricio Saez, Juana Fernandez-Rodriguez, Catia Moutinho, Jose Sanchez-Mut, Antonio Gomez, Paolo Petazzi, **Karolina Szczesna**, Olga de la Caridad, Dori Huertas, Adriana Lopez-Doriga, Montserrat Mila, Luis Perez-Jurado, Judith Armstrong, Mercedes Pineda, Conxi Lazaro, and Manel Esteller
- Improvement of the Rett Syndrome Phenotype in a Mecp2 Mouse Model Upon Treatment with Levodopa and a Dopa Decarboxylase Inhibitor. *Neuropsychopharmacology*. 2014 Jun 11 [Epub ahead of print]. **Szczesna K**, de la Caridad O, Petazzi P, Soler M, Roa L, Saez MA, Fourcade S, Pujol A, Artuch-Iriberry R, Molero-Luis M, Vidal A, Huertas D, Esteller M.
- A DERL3-associated defect in the degradation of SLC2A1 mediates the Warburg effect. *Nat Commun*. 2014 Apr 3 Lopez-Serra P, Marcilla M, Villanueva A, Ramos-Fernandez A, Palau A, Leal L, Wahi JE, Setien-Baranda F, **Szczesna K**, Moutinho C, Martinez-Cardus A, Heyn H, Sandoval J, Puertas S, Vidal A, Sanjuan X, Martinez-Balibrea E, Viñals F, Perales JC, Bramsem JB, Ørntoft TF, Andersen CL, Tabernero J, McDermott U, Boxer MB, Vander Heiden MG, Albar JP, Esteller M.
- Dysregulation of the long non-coding RNA transcriptome in a Rett syndrome mouse model. *RNA Biol*. 2013 Apr 17;10(7). Petazzi P, Sandoval J, **Szczesna K**, Jorge OC, Roa L, Sayols S, Gomez A, Huertas D, Esteller M.
- Whole-genome bisulfite DNA sequencing of a DNMT3B mutant patient. *Epigenetics* 2012;7(6):542-50. Heyn H, Vidal E, Sayols S, Sanchez-Mut JV, Moran S, Medina I, Sandoval J, Simó-Riudalbas L, **Szczesna K**, Huertas D, Gatto S, Matarazzo MR, Dopazo J, Esteller



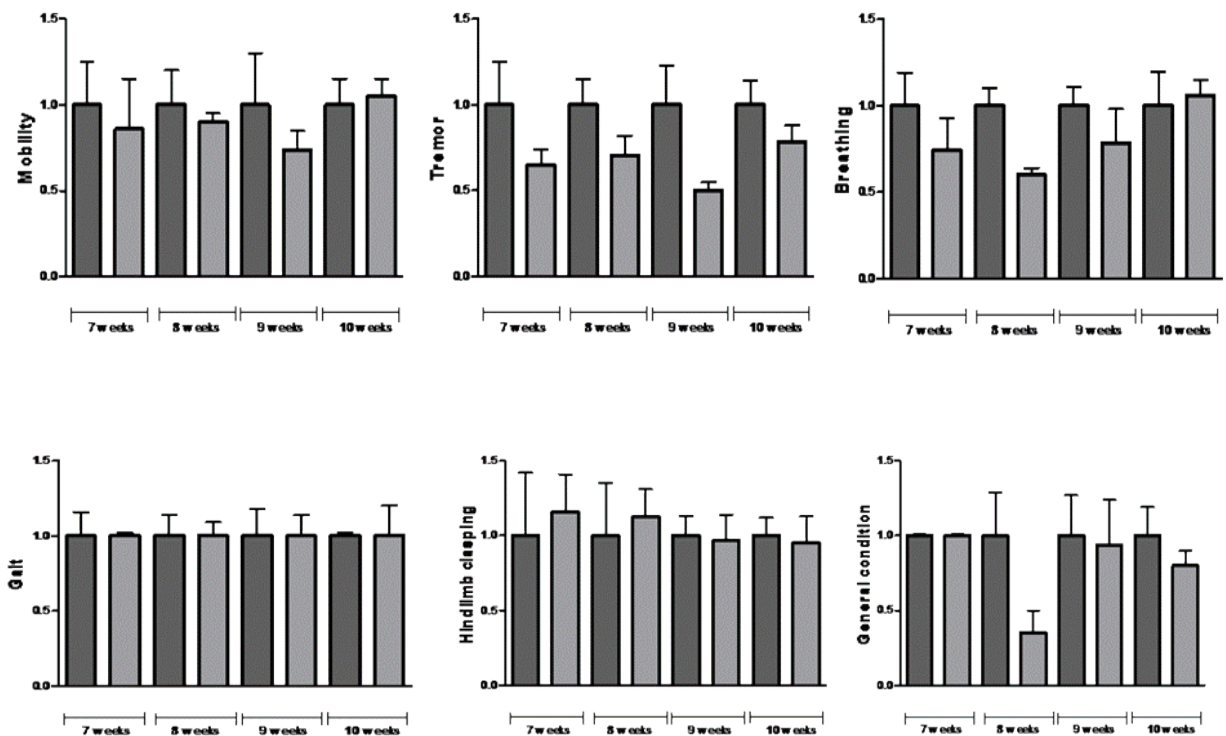
## **Annex 1**



## 1) BDNF-targeting treatments - Copaxone



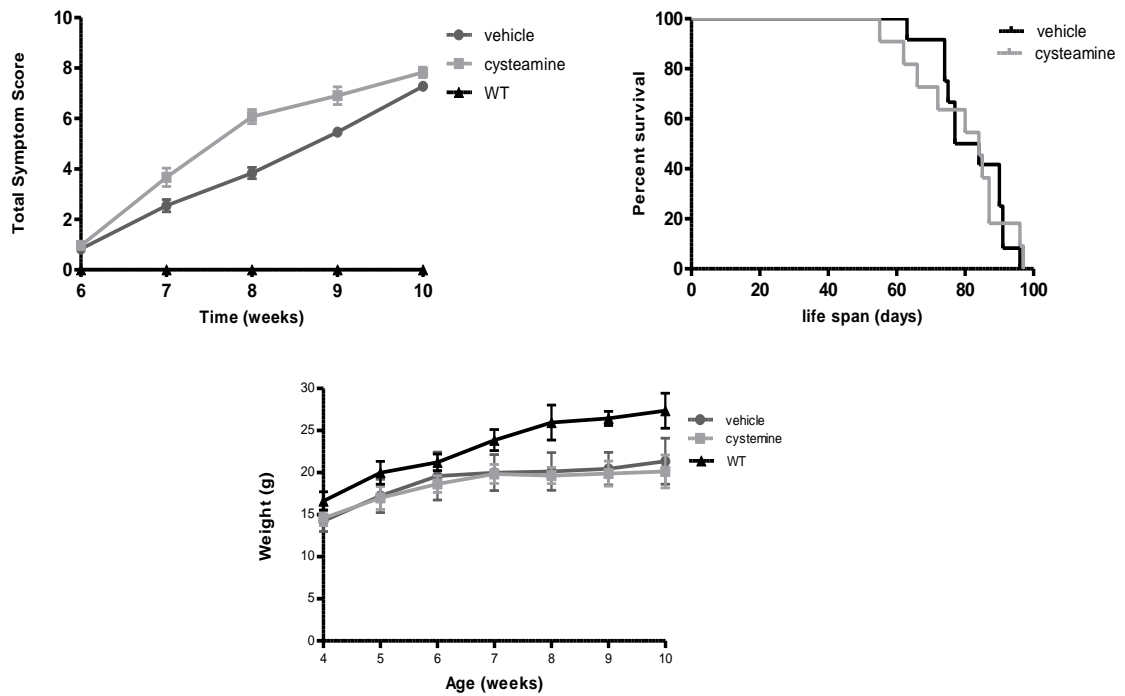
Supplementary Figure 1. No effect of MeCP2 deletion on body weight was observed after the drug treatment. Copaxone did not affect survival of *MeCP2* KO mice and total symptom score was also not affected.



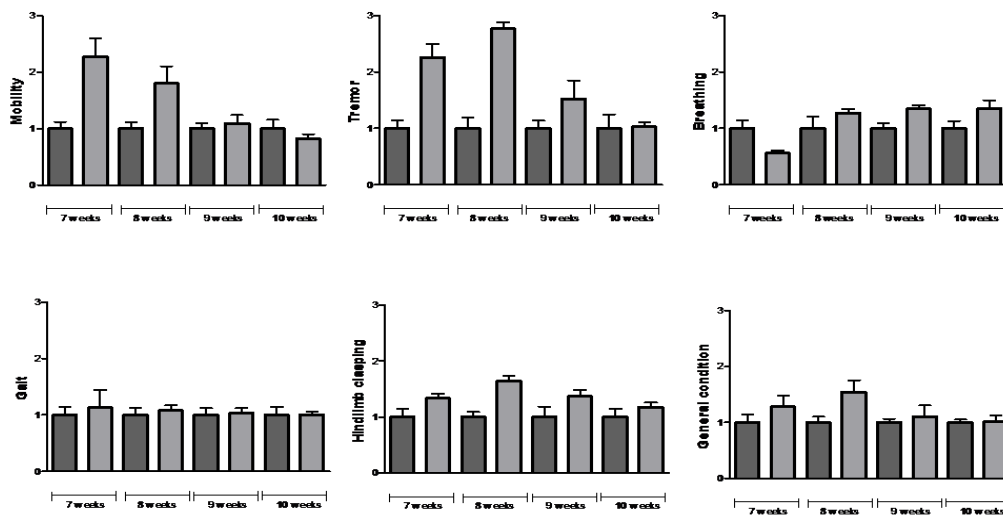
Supplementary Figure 2. No significant improvement was detected after the copaxone treatment. Plot of average symptom scores representing mobility, tremor, breathing, gait, hindlimb clasping and general condition normalized versus control group.

## Annex 1

### 2) BDNF-targeting treatments - Cysteamine

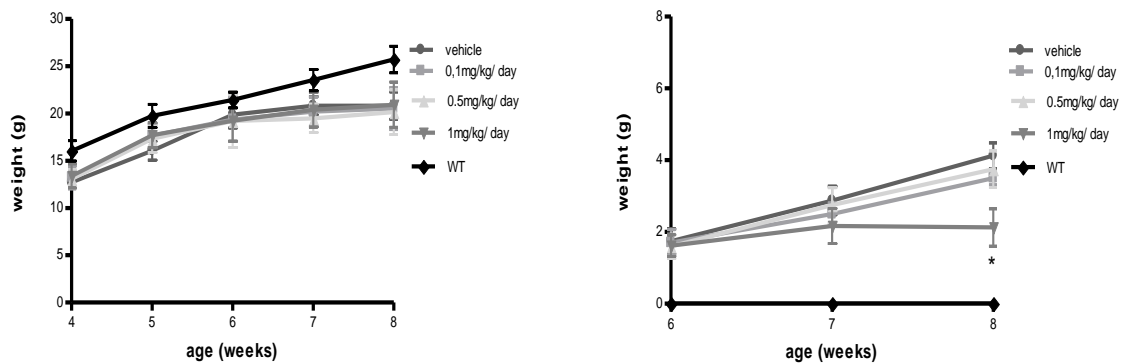


Supplementary Figure 3. No effect of MeCP2 deletion on body weight was observed after the drug treatment. Treatment of cysteamine did not improve total symptom score and did not prolong survival of *Mecp2* KO mice.

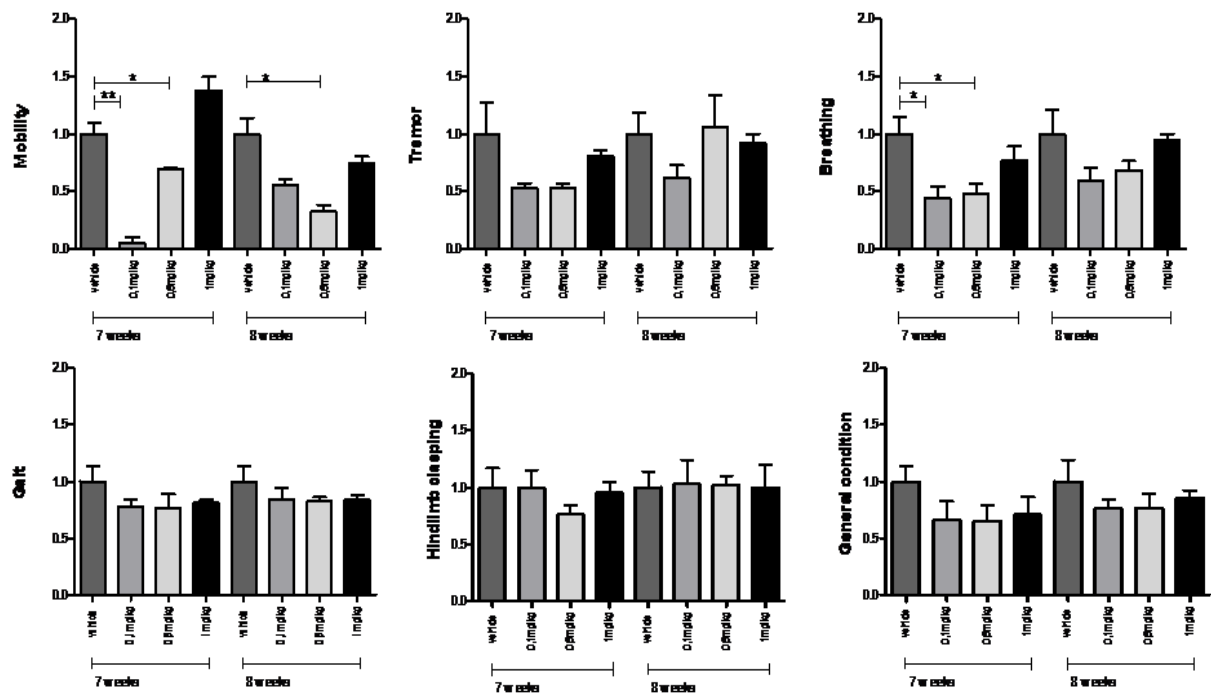


Supplementary Figure 4. Plot of average symptom scores after cysteamine treatment representing mobility, tremor, breathing gait, hindlimb clasp and general condition normalized versus control group.

## 3) Treatments modulating the glucocorticoid hormone system – dexamethasone



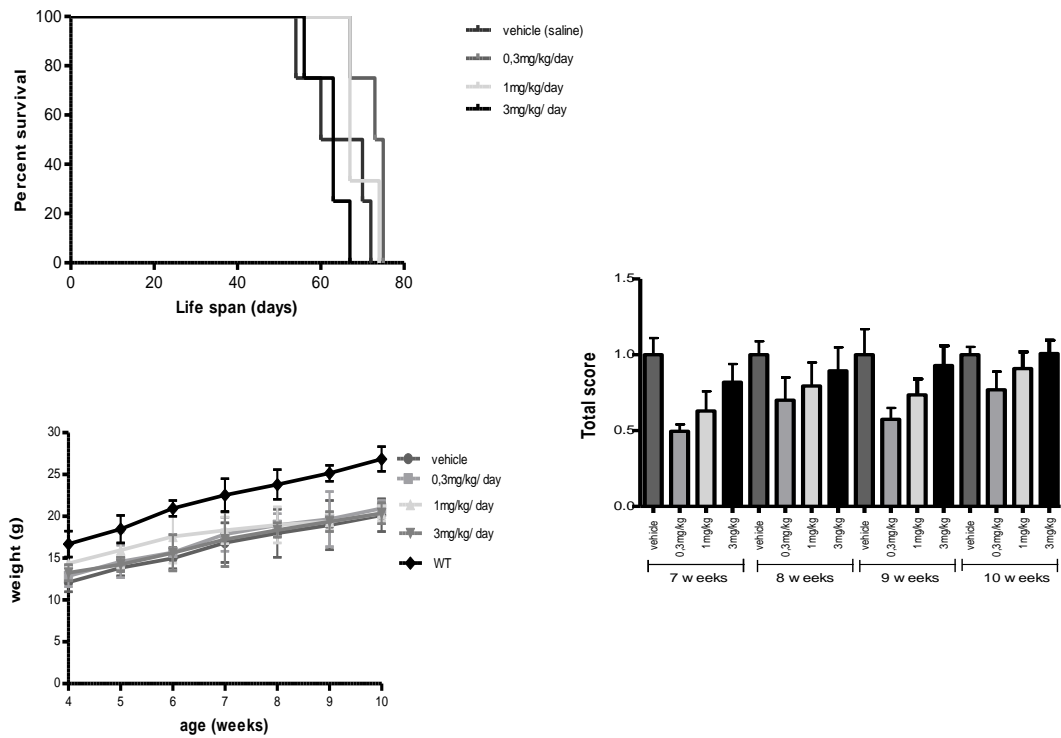
Supplementary Figure 5. No effect of MeCP2 deletion on body weight was observed after the drug treatment. Dexamethasone affect total symptom score.



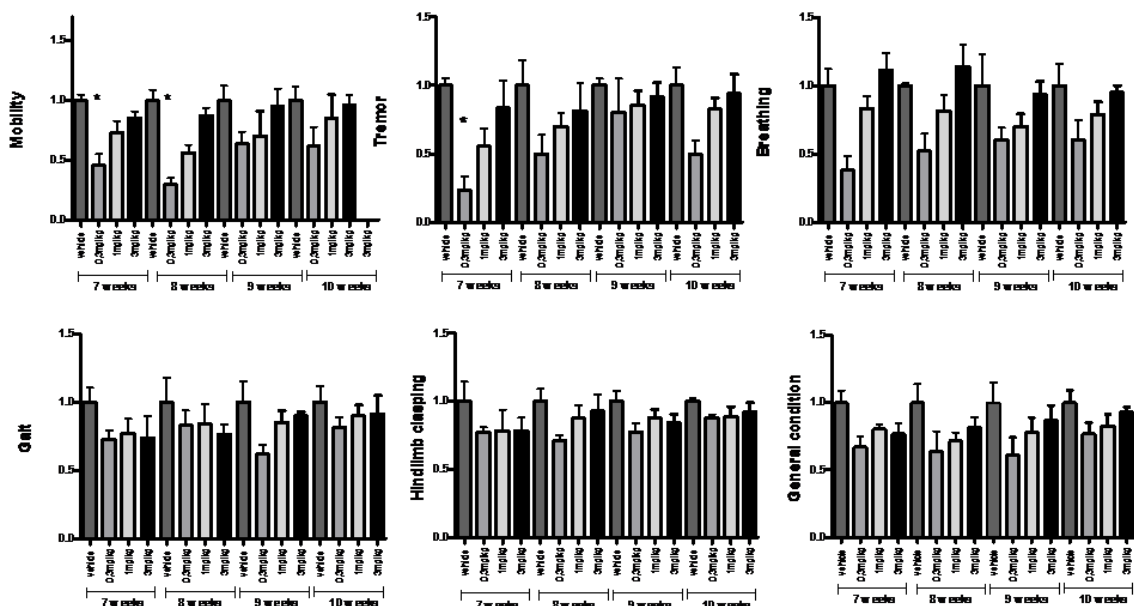
Supplementary Figure 6. Significant improvement was detected after the dexamethasone treatment regarding to mobility and breathing score. Plot of average symptom scores representing mobility, tremor, breathing gait, hindlimb clamping and general condition normalized versus control group. (vehicle n=5, mice treated with dexamethasone n=5/each dose).

## Annex 1

### 4) Treatments targeting bioamines – ropinirole

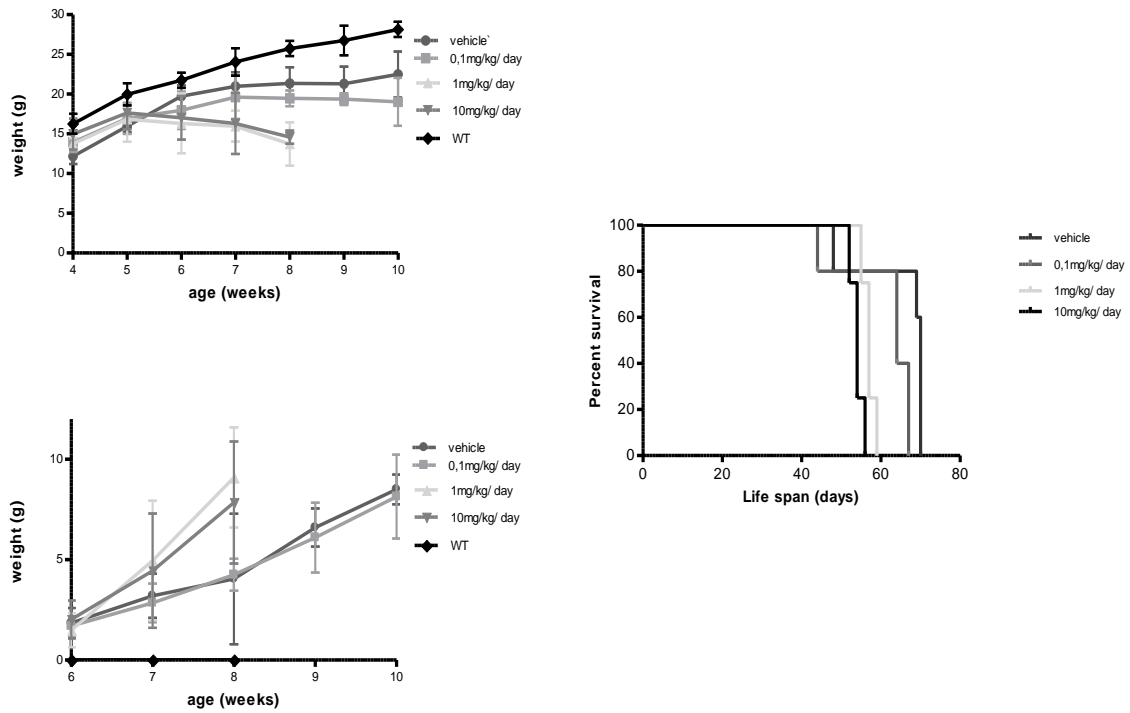


Supplementary Figure 7. No effect of MeCP2 deletion on body weight was observed after the drug treatment. Treatment of ropinirole improved total symptom score and but does not prolong survival of *Mecp2* KO mice.

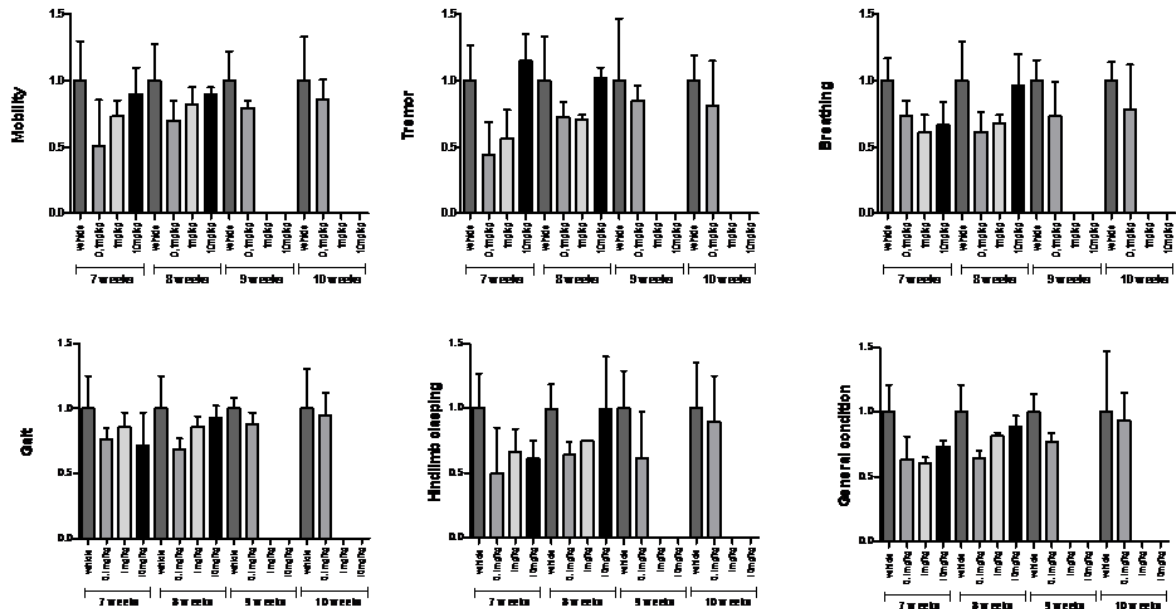


Supplementary Figure 8. Plot of average symptom scores after ropinirole treatment representing mobility, tremor, breathing gait, hindlimb clasping and general condition normalized versus control group.

5) Treatments targeting bioamines – bromperidol



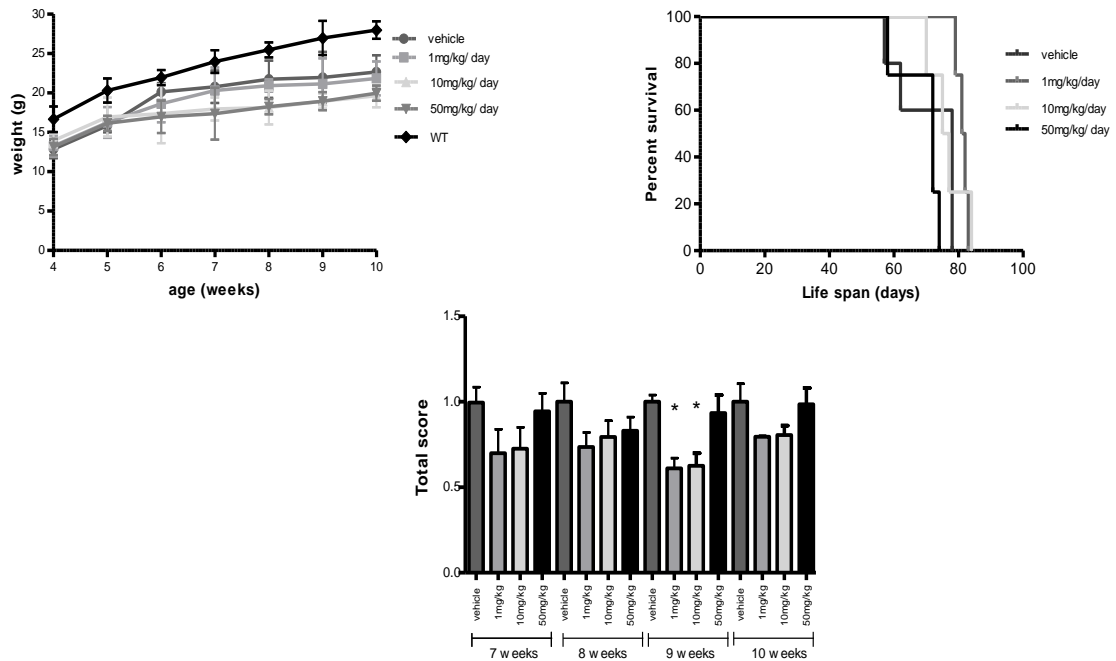
Supplementary Figure 9. Deletion on body weight in Mecp2 KO mice was observed after the high dose of drug treatment. Treatment of bromperidol does not improve significantly neither total symptom score nor life span of Mecp2 KO animals.



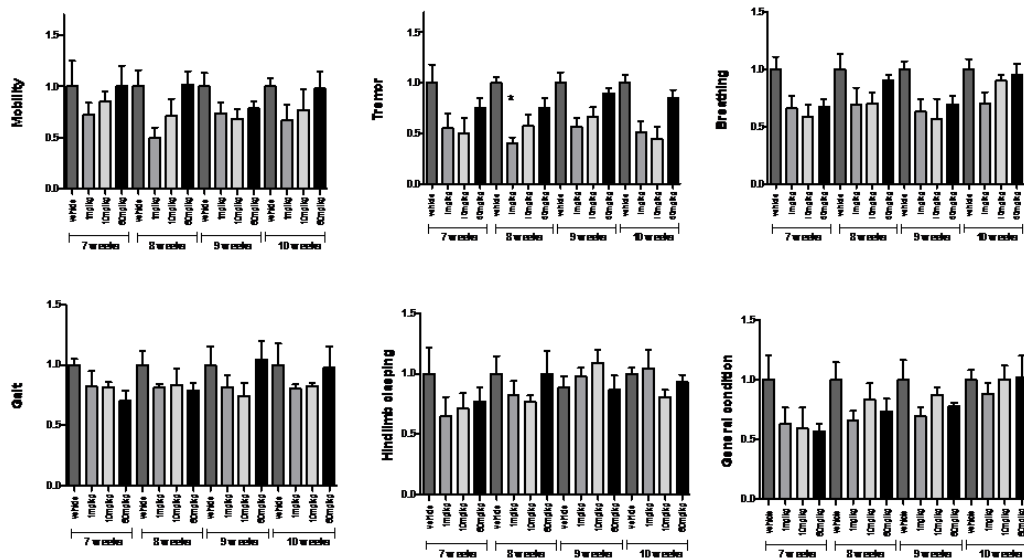
Supplementary Figure 10. Plot of average symptom scores after bromperidol treatment representing mobility, tremor, breathing gait, hindlimb clasping and general condition normalized versus control group.

## Annex 1

### 6) GABA targeting treatments - Gabapentin

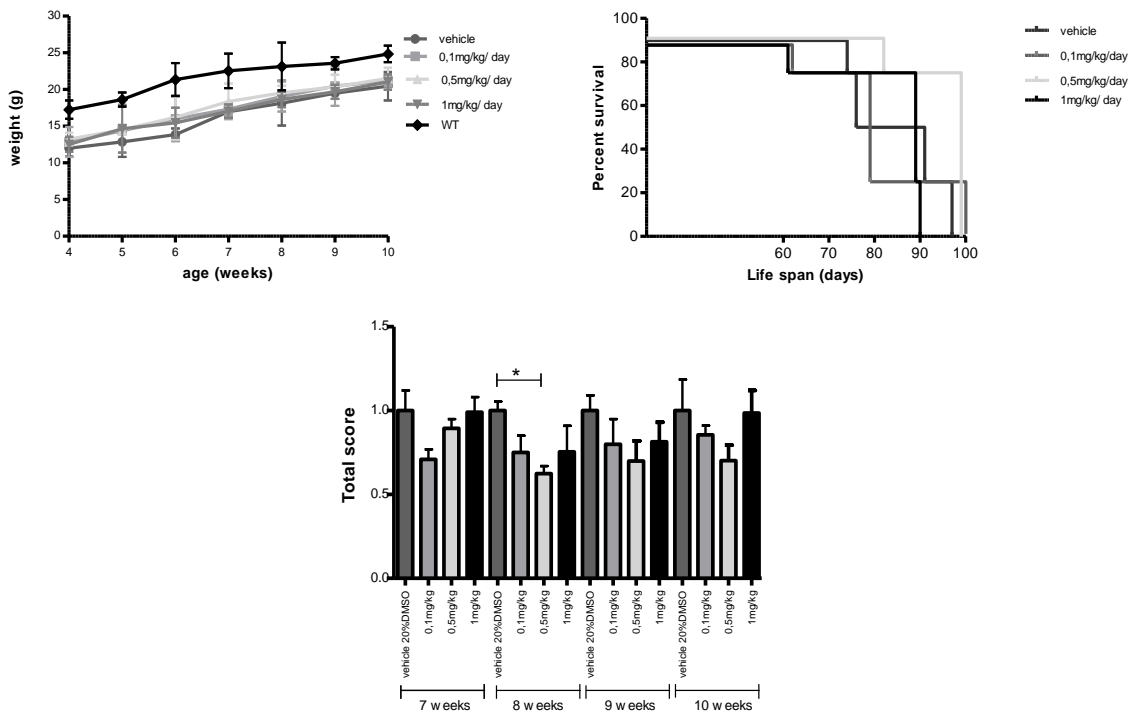


Supplementary Figure 11. No effect of MeCP2 deletion on body weight was observed after the drug treatment. Treatment of gabapentin improves total symptom score prolongs survival of Mecp2 KO mice.

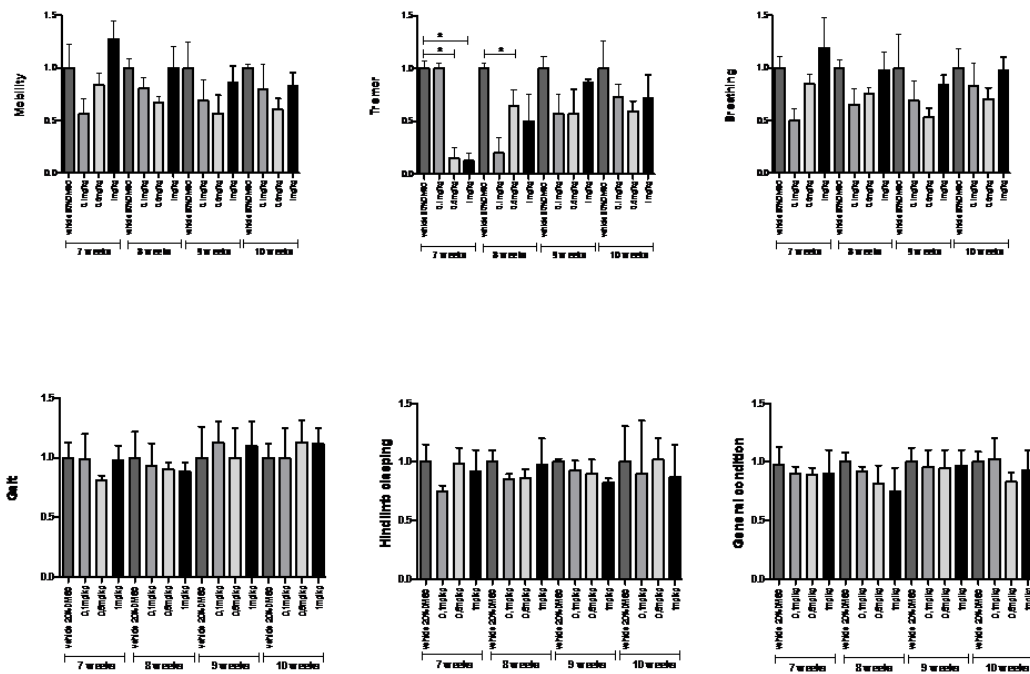


Supplementary Figure 12. Plot of average symptom scores after gabapentin treatment representing mobility, tremor, breathing gait, hindlimb clasping and general condition normalized versus control group.

7) GSK-3B inhibitor treatments – SB216763



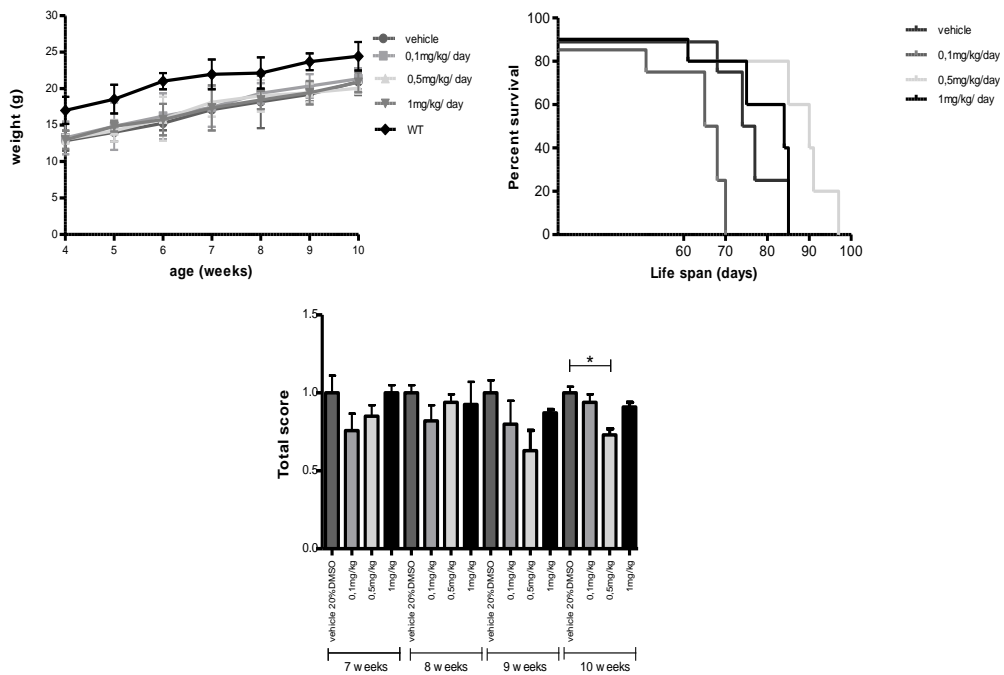
Supplementary Figure 13. No effect of MeCP2 deletion on body weight was observed after the drug treatment. Treatment of low dose of SB216763 significant prolongs survival of *Mecp2* KO mice and improves total symptom score.



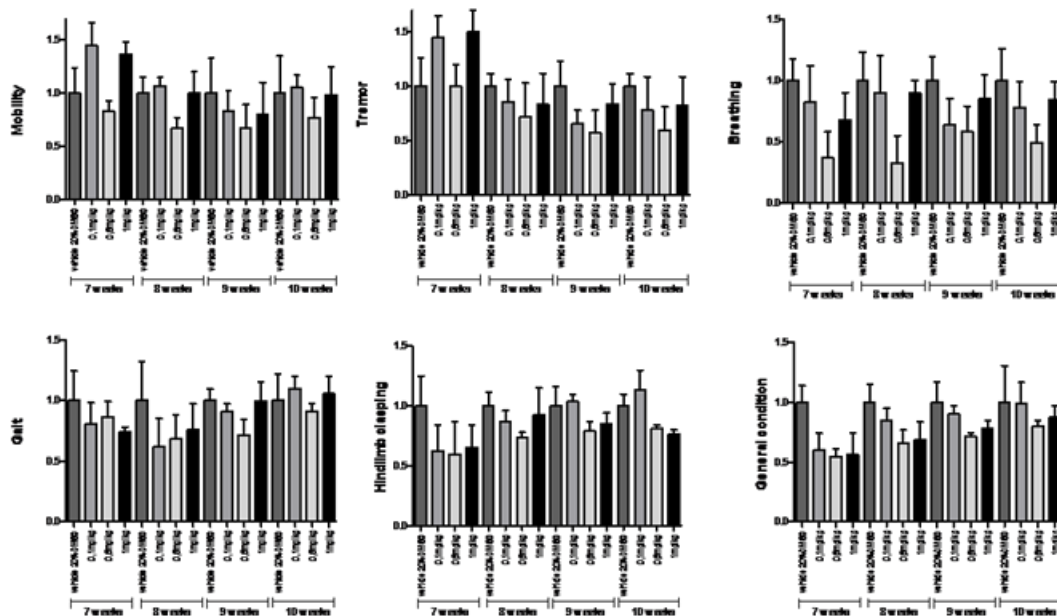
Supplementary Figure 14. Plot of average symptom scores after SB216763 treatment representing mobility, tremor, breathing gait, hindlimb clasping and general condition normalized versus control group.

# Annex 1

## 8) GSK-3B inhibitor treatments – TDZD8

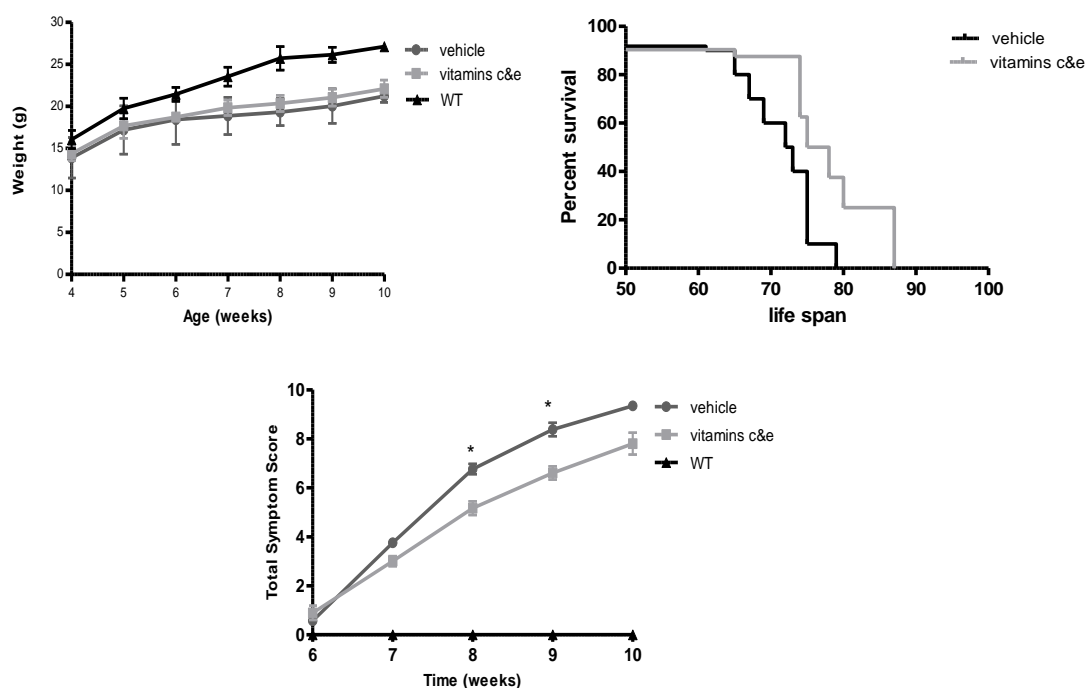


Supplementary Figure 15. No effect of MeCP2 deletion on body weight was observed after the drug treatment. Treatment of low dose of TDZD8 significant prolongs survival of *Mecp2* KO mice and improves total symptom score.

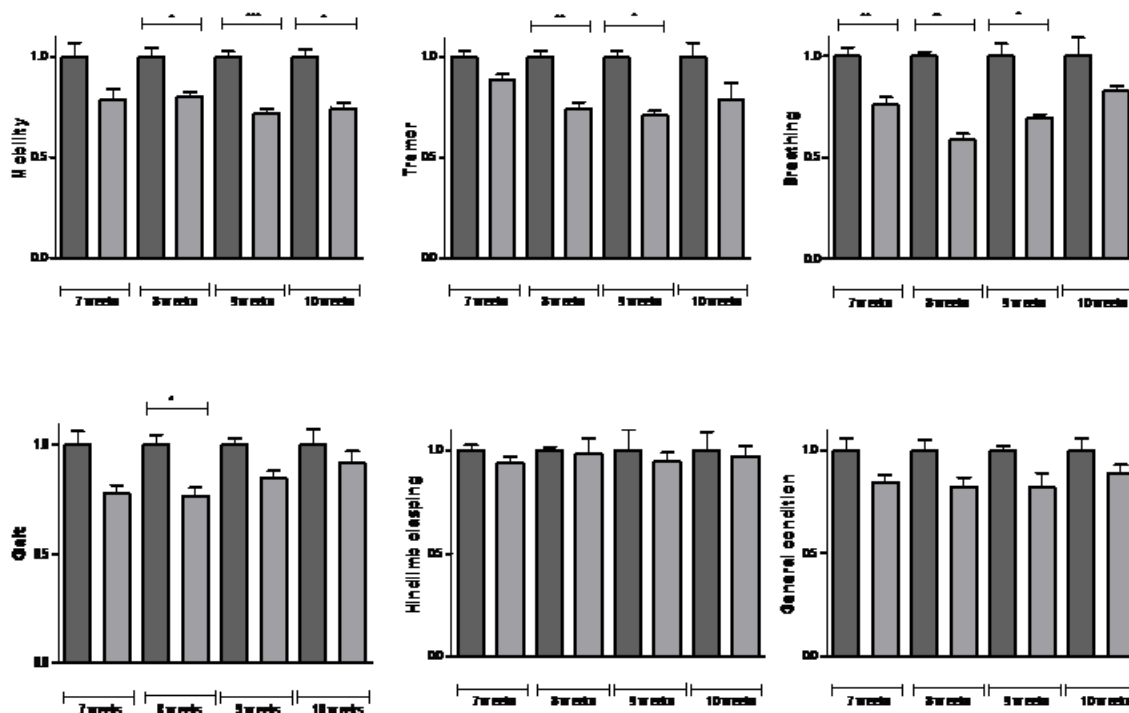


Supplementary Figure 16. Plot of average symptom scores after TDZD8 treatment representing mobility, tremor, breathing gait, hindlimb clasp and general condition normalized versus control group.

## 9) Oxidative damage and related drugs treatments – vitamins C and E

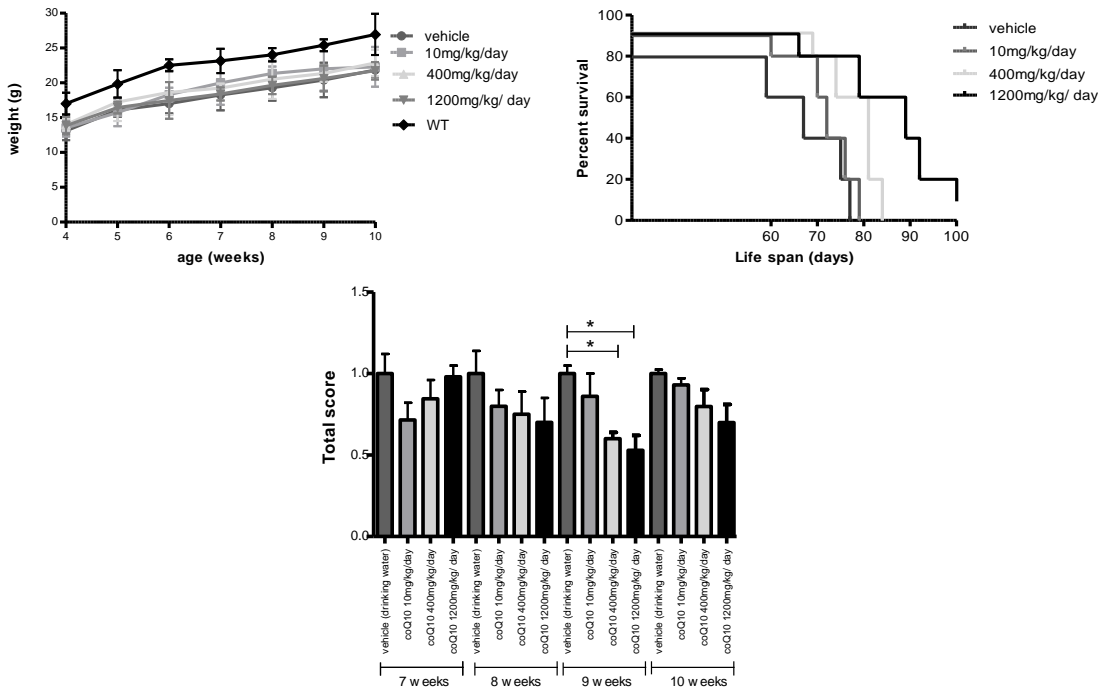


Supplementary Figure 17. No effect of MeCP2 deletion on body weight was observed after the drug treatment. Treatment of vitamins c and e prolongs survival of Mecp2 KO mice and improves total symptom score.

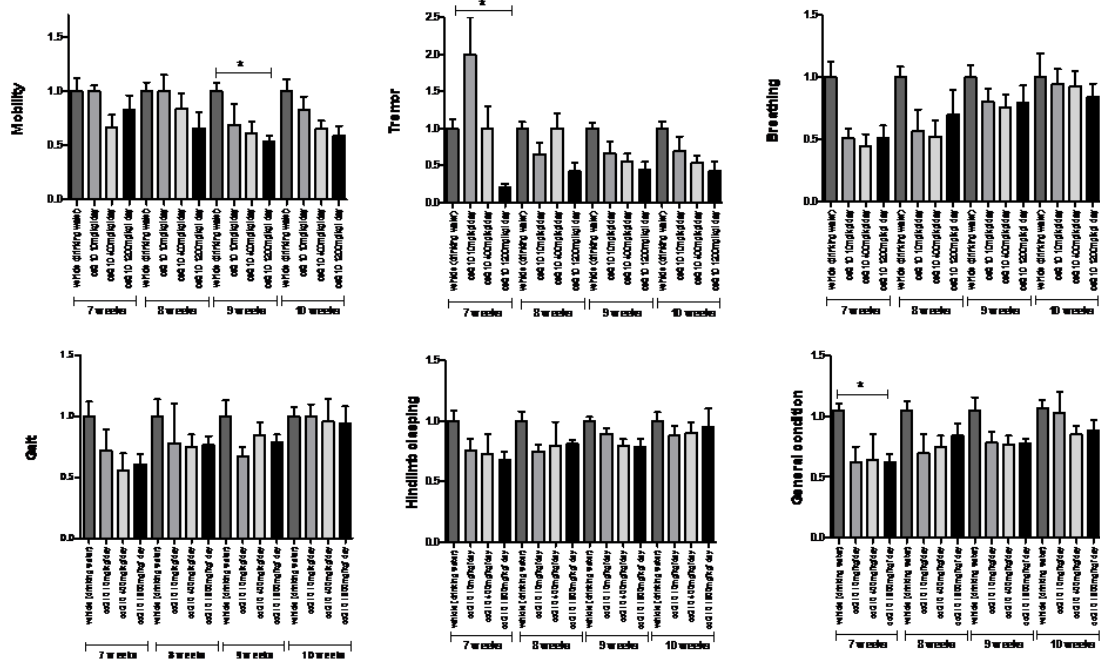


Supplementary Figure 18. Significant improvement was detected after the vitamins treatment regarding to mobility and breathing score. Plot of average symptom scores representing mobility, tremor, breathing gait, hindlimb clasping and general condition normalized versus control group.

10) Oxidative damage and related drugs treatments – CoQ10

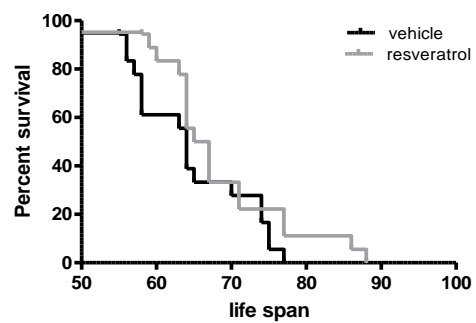
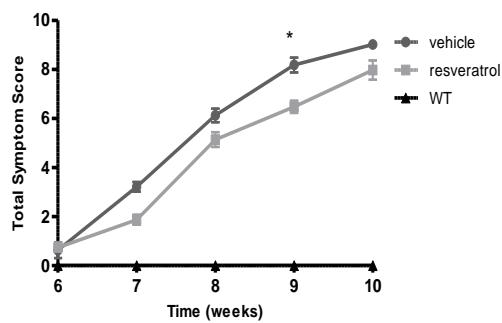
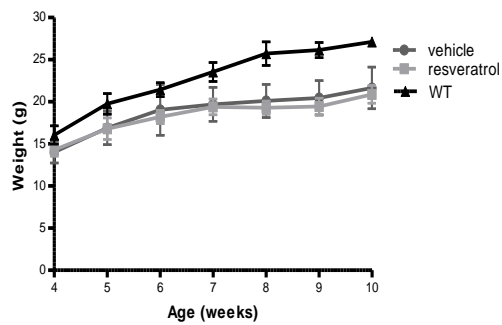


Supplementary Figure 19. No effect of MeCP2 deletion on body weight was observed after the drug treatment. Treatment of CoQ10 prolongs survival of Mecp2 KO mice and improves total symptom score.

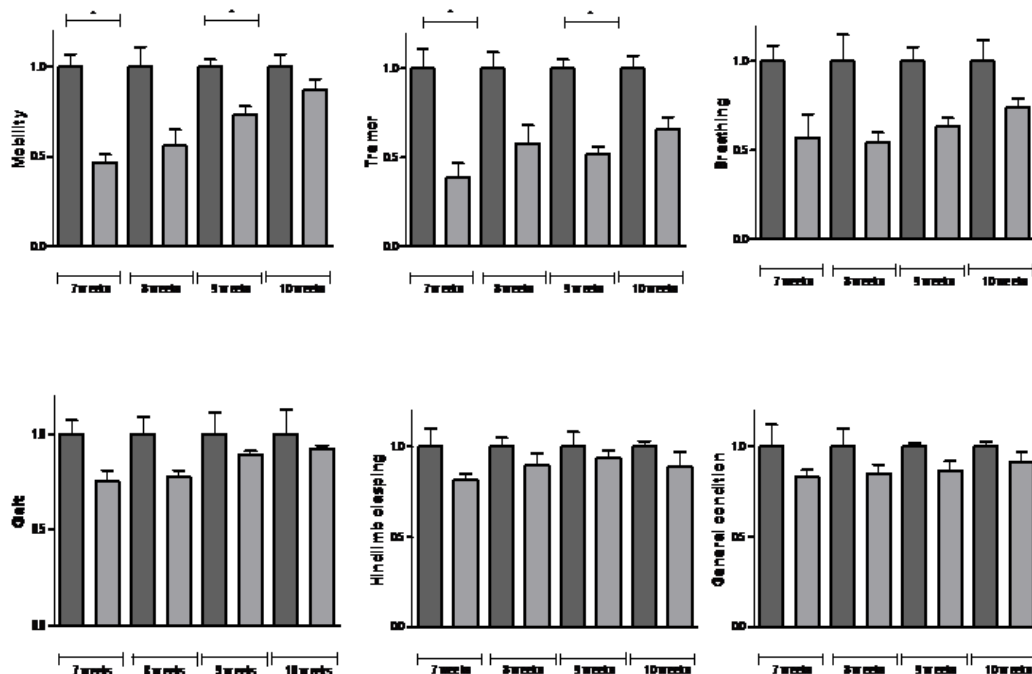


Supplementary Figure 20. Significant improvement was detected after the CoQ10 treatment regarding to mobility and tremor score. Plot of average symptom scores representing mobility, tremor, breathing gait, hindlimb clasp and general condition normalized versus control group

## 11) Oxidative damage and related drugs treatments – resveratrol



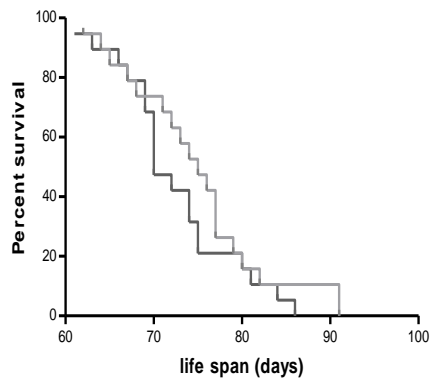
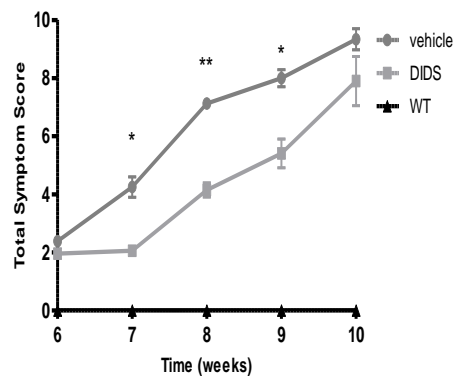
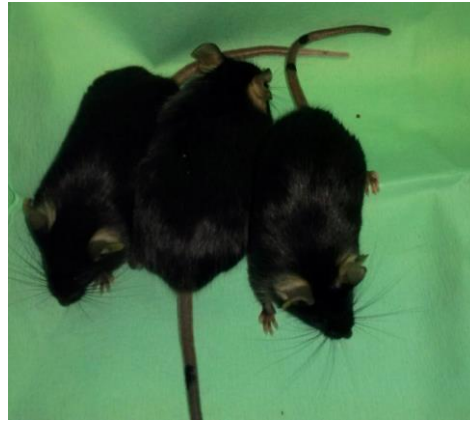
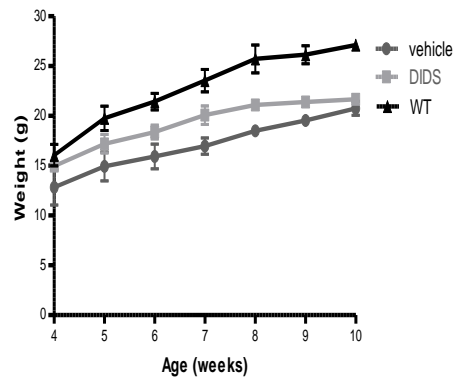
Supplementary Figure 21. No effect of MeCP2 deletion on body weight was observed after the drug treatment. Treatment of resveratrol did not prolong survival of Mecp2 KO mice but improves total symptom score.



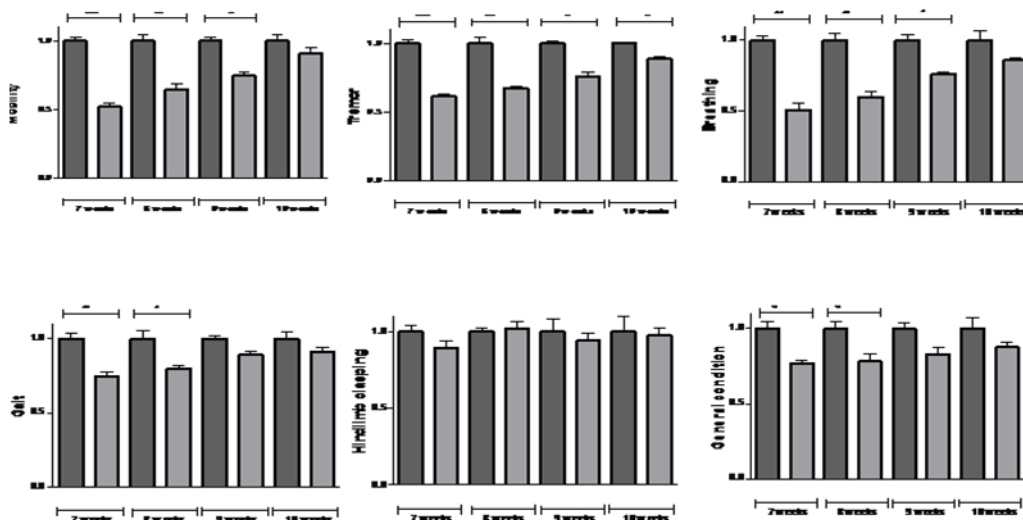
Supplementary Figure 22. Significant improvement was detected after the resveratrol treatment regarding to mobility and tremor score. Plot of average symptom scores representing mobility, tremor, breathing gait, hindlimb clasping and general condition normalized versus control group.

## Annex 1

### 12) Oxidative damage and related drugs treatments – DIDS (VDAC1 inhibitor)

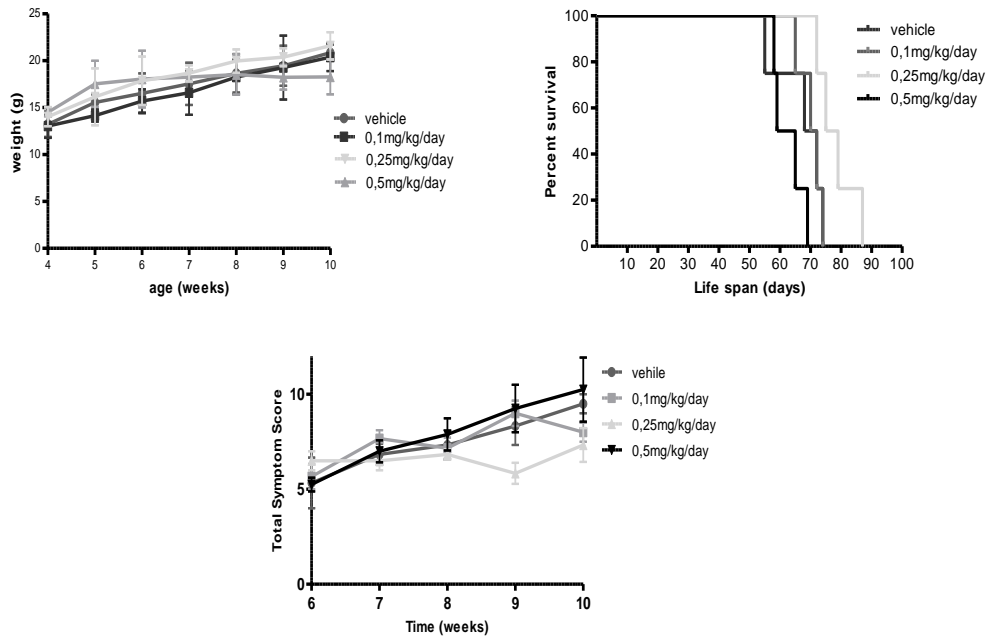


Supplementary Figure 23. No effect of MeCP2 deletion on body weight was observed after the drug treatment. Treatment of DIDS improves total symptom score but it did not prolong survival of Mecp2 KO mice.

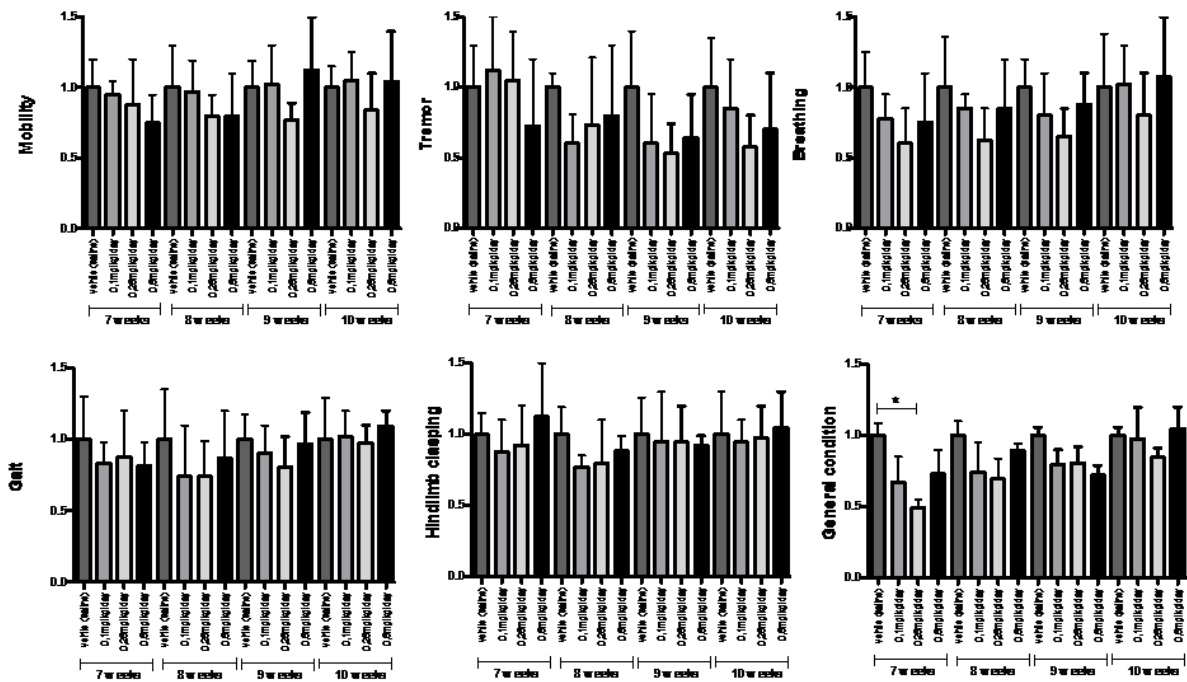


Supplementary Figure 24. Significant improvement was detected after the DIDS treatment. Plot of average symptom scores representing mobility, tremor, breathing gait, hindlimb clasping and general condition normalized versus control group.

13) Treatments targeting epigenetic modifications – DNMTs inhibitors – AZA (VIDAZA)



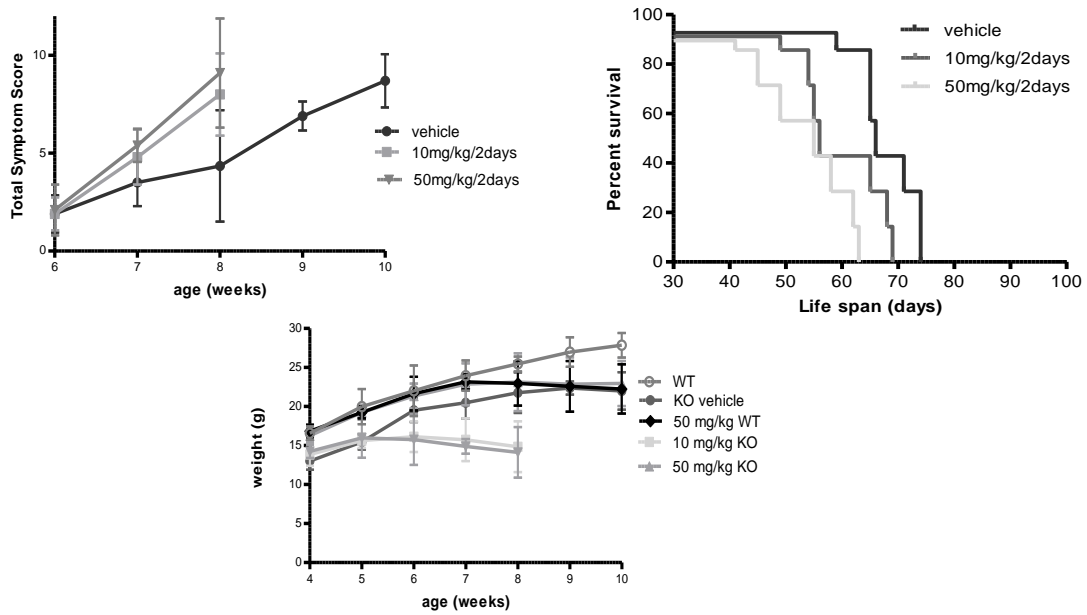
Supplementary Figure 25. No effect of MeCP2 deletion on body weight was observed after the drug treatment. Treatment of AZA improved total symptom score and depends on the dose prolongs survival of Mecp2 KO mice.



Supplementary Figure 26. Plot of average symptom scores after AZA treatment representing mobility, tremor, breathing gait, hindlimb clasping and general condition normalized versus control group.

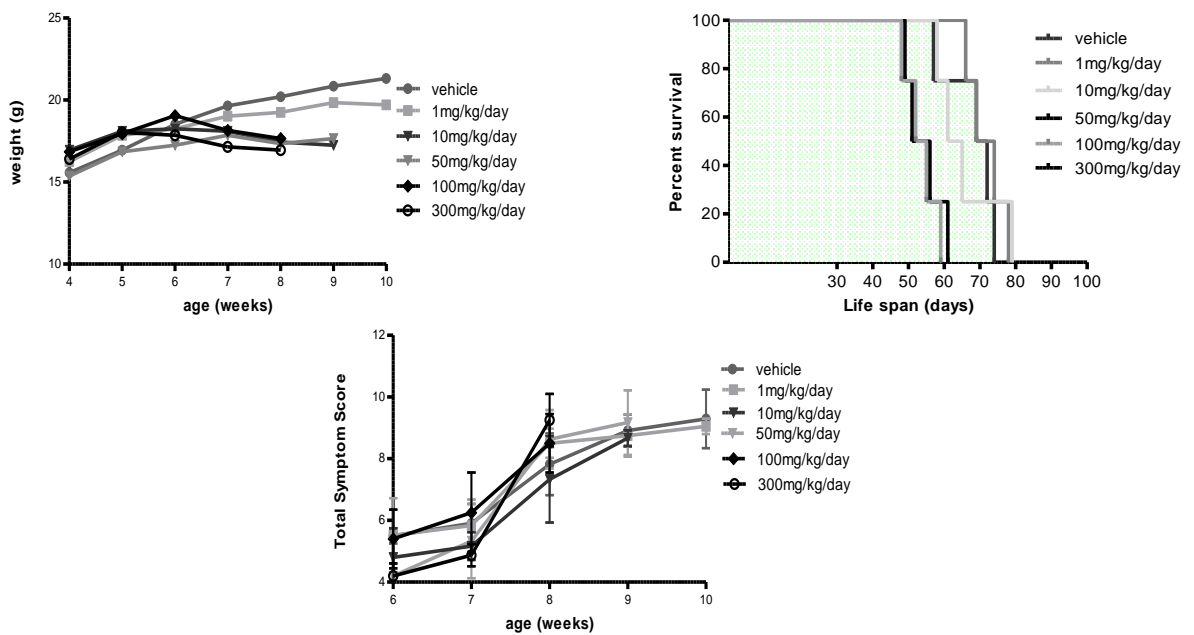
## Annex 1

### 14) Treatments targeting epigenetic modifications – HDACs inhibitors – SAHA (Vorinostat)

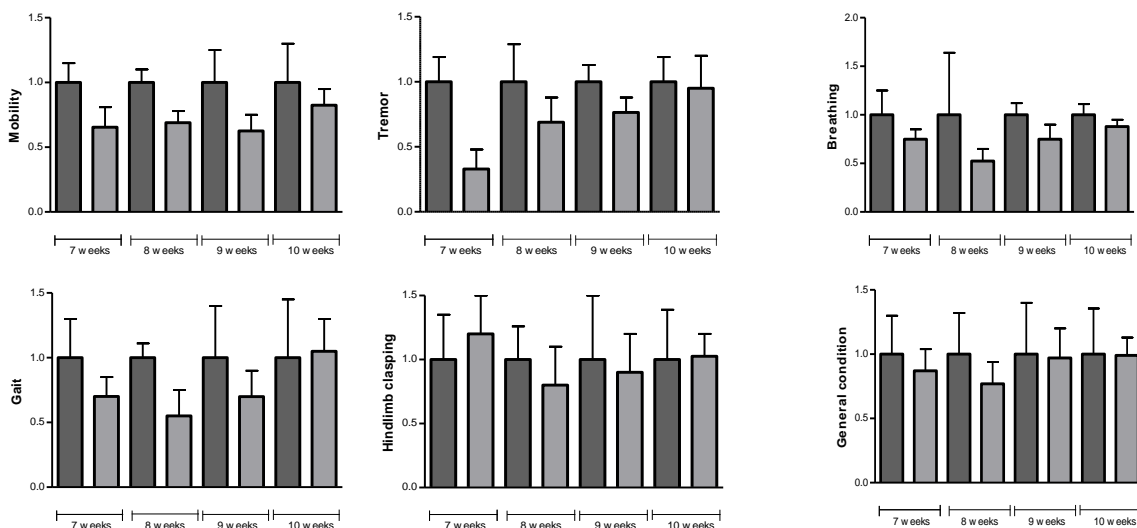


Supplementary Figure 27. Deletion on body weight in Mecp2 KO mice was observed after the drug treatment. Treatment of SAHA does not improve total symptom score and present high toxicity shortening survival of Mecp2 KO mice.

15) Treatments targeting epigenetic modifications – HDACs inhibitors – sodium phenylbutyrate (NaPB)



Supplementary Figure 28. Deletion on body weight in Mecp2 KO mice was observed after the drug treatment. Treatment of NaPB does not improve total symptom score and present high toxicity shortening survival of Mecp2 KO mice. Therapeutic window in the case of NaPB 1mg/kg/day.

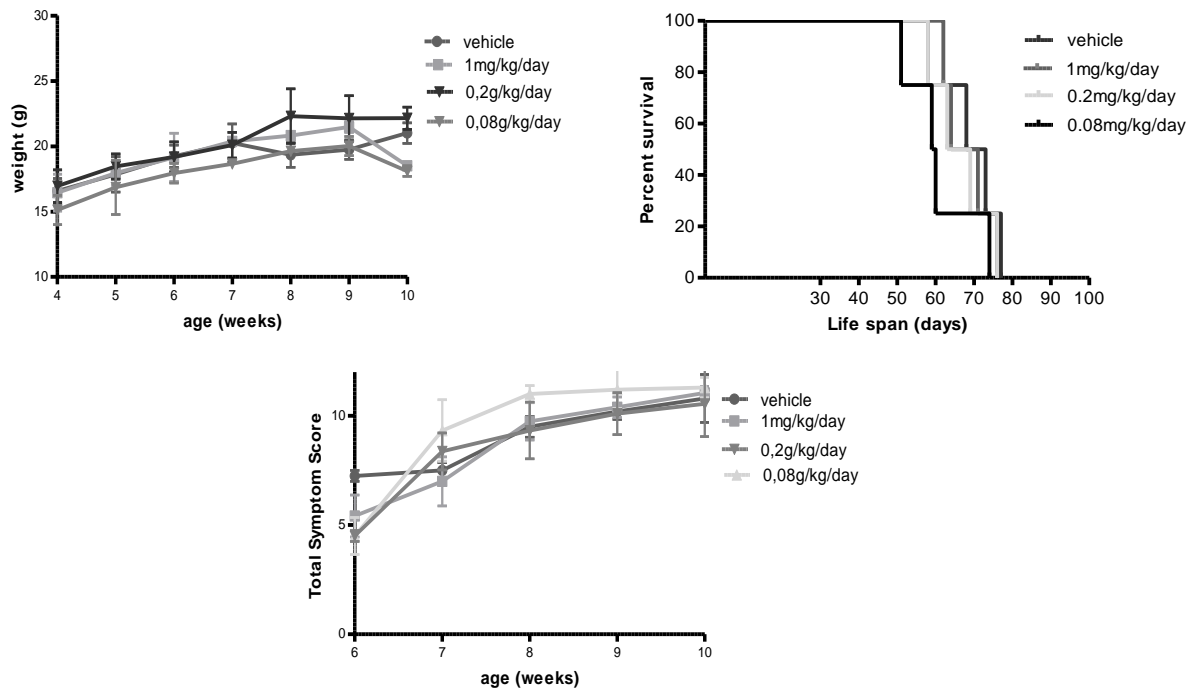


Supplementary Figure 29. Plot of average symptom scores after NaPB 1mg/kg/day treatment representing mobility, breathing and tremor normalized versus control group.

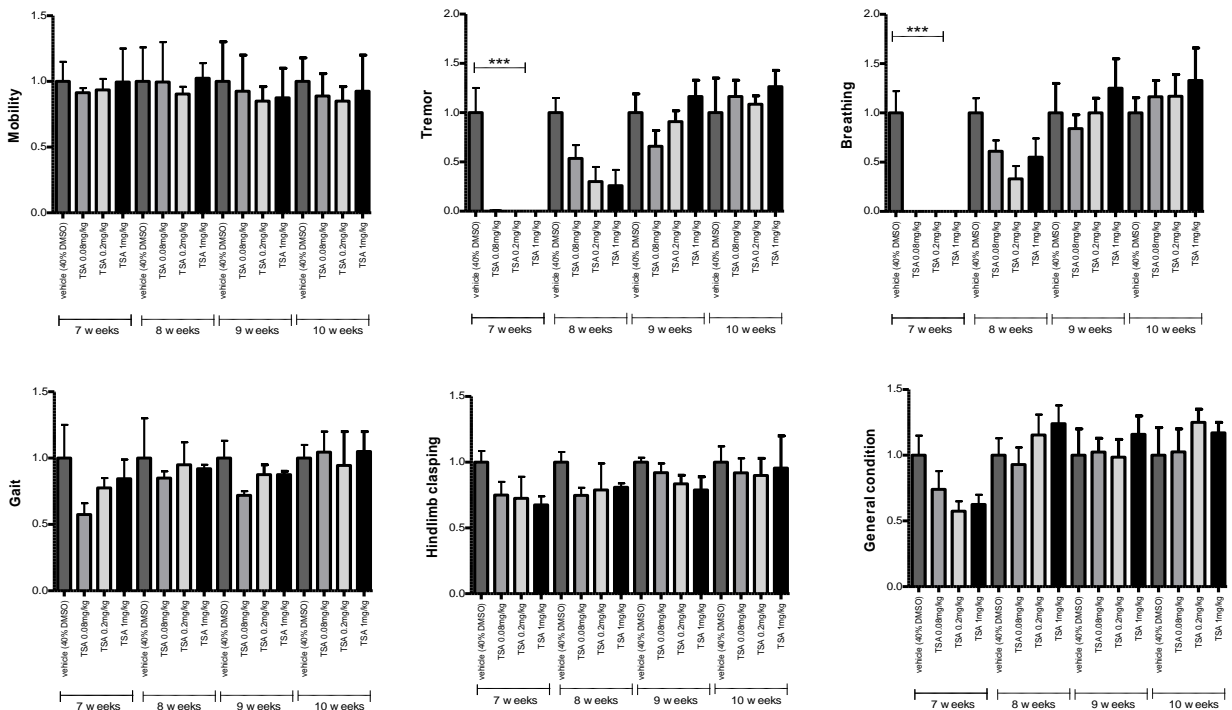
# Annex 1

## 16) Treatments targeting epigenetic modifications – HDACs inhibitors – trichostatin

### A (TSA)

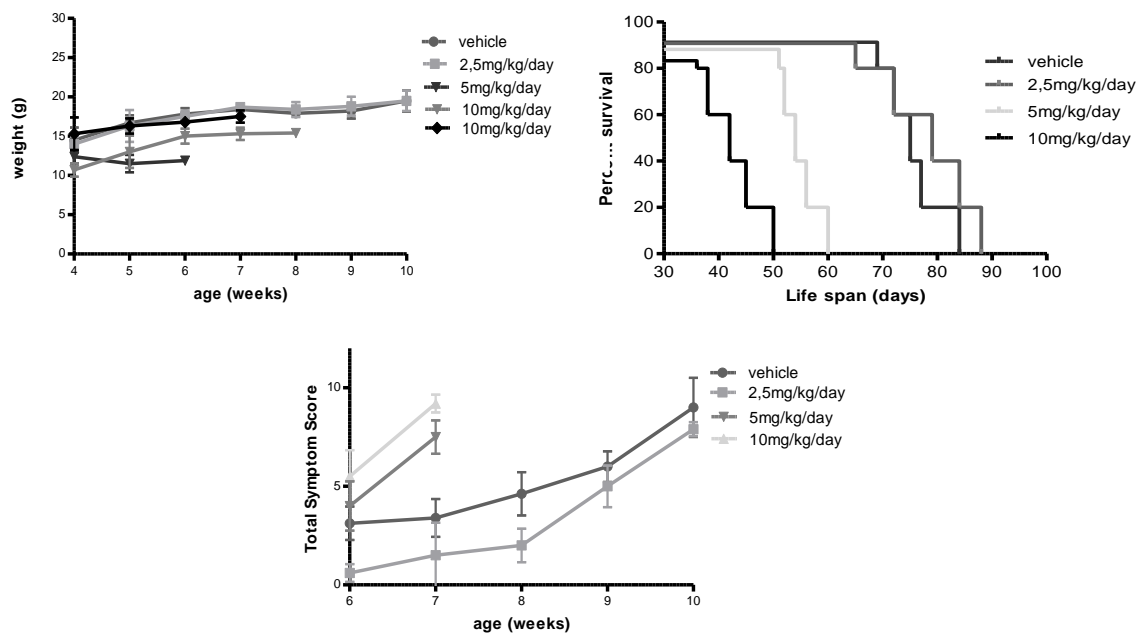


Supplementary Figure 30. No deletion on body weight in *Mesp2* KO mice was observed after the drug treatment. Treatment of TSA does not improve neither total symptom score nor life span of *Mesp2* KO animals.

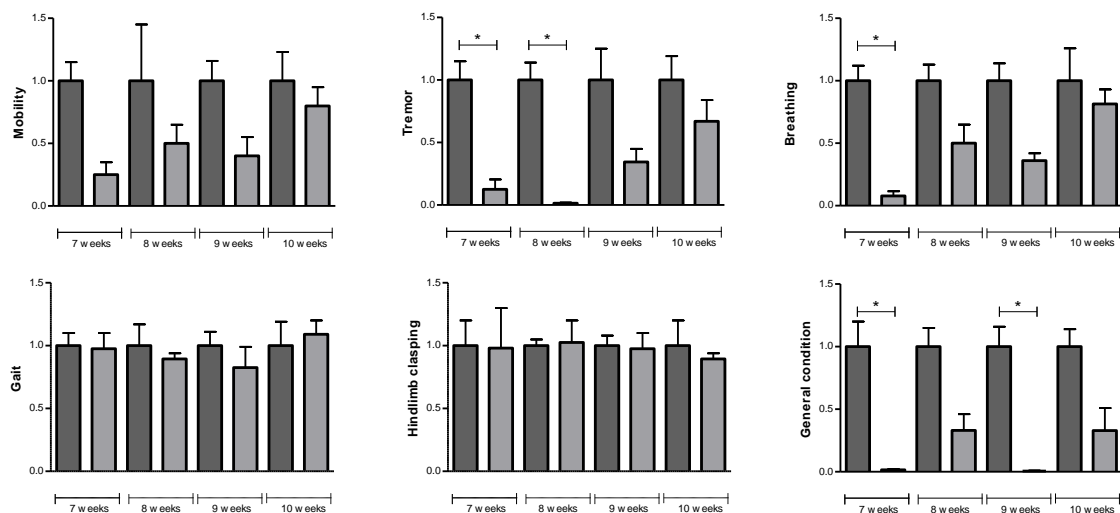


Supplementary Figure 31. Plot of average symptom scores after TSA treatment representing general condition, breathing, tremor and mobility normalized versus control group.

17) Treatments targeting epigenetic modifications – HDACs inhibitors – entinostat (MS-275)



Supplementary Figure 32. Deletion on body weight in Mecp2 KO mice was observed after the high dose of drug treatment. Treatment of MS-275 does not improve neither total symptom score nor life span of Mecp2 KO animals.



Supplementary Figure 33. Plot of average symptom scores after MS-275 2,5mg/kg/day treatment representing mobility, breathing, tremor and general condition normalized versus control group.



**Contrary to the expectation  
that science will reveal one single clear answer,  
more often than not scientists have to be satisfied  
with several answers  
and even more question as a result.**



# Improvement of the Rett Syndrome Phenotype in a *Mecp2* Mouse Model Upon Treatment with Levodopa and a Dopa-Decarboxylase Inhibitor

Karolina Szczesna<sup>1</sup>, Olga de la Caridad<sup>1</sup>, Paolo Petazzi<sup>1</sup>, Marta Soler<sup>1</sup>, Laura Roa<sup>1</sup>, Mauricio A Saez<sup>1</sup>, Stéphane Fourcade<sup>2,3,4</sup>, Aurora Pujol<sup>2,3,4,5</sup>, Rafael Artuch-Iriberrí<sup>4,6</sup>, Marta Molero-Luis<sup>4,6</sup>, August Vidal<sup>7</sup>, Dori Huertas<sup>\*1</sup> and Manel Esteller<sup>\*1,5,8</sup>

<sup>1</sup>Cancer Epigenetics and Biology Program (PEBC), Bellvitge Biomedical Research Institute (IDIBELL), Barcelona, Spain; <sup>2</sup>Neurometabolic Diseases Laboratory, Bellvitge Biomedical Research Institute (IDIBELL), Barcelona, Spain; <sup>3</sup>Institute of Neuropathology, University of Barcelona, Barcelona, Spain; <sup>4</sup>Center for Biomedical Research on Rare Diseases (CIBERER), ISCIII, Madrid, Spain; <sup>5</sup>Institució Catalana de Recerca i Estudis Avançats (ICREA), Barcelona, Spain; <sup>6</sup>Neurometabolic Unit, Hospital Sant Joan de Déu, Barcelona, Spain; <sup>7</sup>Department of Pathology, Bellvitge University Hospital, Bellvitge Biomedical Research Institute (IDIBELL), Barcelona, Spain; <sup>8</sup>Department of Physiological Sciences II, School of Medicine, University of Barcelona, Barcelona, Spain

Rett Syndrome is a neurodevelopmental autism spectrum disorder caused by mutations in the gene coding for methyl CpG-binding protein (MeCP2). The disease is characterized by abnormal motor, respiratory, cognitive impairment, and autistic-like behaviors. No effective treatment of the disorder is available. *Mecp2* knockout mice have a range of physiological and neurological abnormalities that resemble the human syndrome and can be used as a model to interrogate new therapies. Herein, we show that the combined administration of Levodopa and a Dopa-decarboxylase inhibitor in RTT mouse models is well tolerated, diminishes RTT-associated symptoms, and increases life span. The amelioration of RTT symptomatology is particularly significant in those features controlled by the dopaminergic pathway in the nigrostriatum, such as mobility, tremor, and breathing. Most important, the improvement of the RTT phenotype upon use of the combined treatment is reflected at the cellular level by the development of neuronal dendritic growth. However, much work is required to extend the duration of the benefit of the described preclinical treatment.

*Neuropsychopharmacology* advance online publication, 9 July 2014; doi:10.1038/npp.2014.136

## INTRODUCTION

Mutations in the X-linked *MECP2* gene are the primary cause of Rett syndrome (RTT; OMIM no. 312750), a neurodevelopmental autism spectrum disorder with delayed onset that affects 1 in 10 000 girls (Amir *et al*, 1999). Mutations most frequently occur sporadically, and familial cases are rare. Patients with RTT appear to develop normally up to 6–18 months of age. The clinical features of RTT include small hands and feet, and a decelerated rate of head growth (Neul and Zoghbi, 2004). RTT patients show abnormal neuronal morphology but not neuronal death (Armstrong, 1995), which implies that RTT is a neurodevelopmental, rather than a neurodegenerative disorder. MeCP2 is widely expressed, but it is most abundant in

neurons of the mature nervous system (Kishi and Macklis, 2004).

The brain and cerebrospinal fluid analyses performed in RTT patients showed reduced levels of dopamine (Riderer *et al*, 1986; Lekman *et al*, 1989; Wenk *et al*, 1991). A low frequency of dopamine 2 receptors (D2R) in the brain of an RTT girl have been described (Chiron *et al*, 1993), and subsequently concluded as being a possible cause for low numbers of spines (Fasano *et al*, 2013). Neuropathology also revealed a reduction in the number of neurons in the substantia nigra (Kitt and Wilcox, 1995), and a reduction in tyrosine hydroxylase (Th) immunoreactivity (Jellinger *et al*, 1988). An abnormal thinning of dendrites within the substantia nigra in RTT girls was also described (Jellinger, 2003). An alteration of dopaminergic metabolism may also be involved in the abnormal motor movements and late motor deterioration that are observed in the classic form of RTT (FitzGerald *et al*, 1990).

The symptoms of RTT are caused by a neuronal MeCP2 deficiency, and expression of MeCP2 in postmitotic neurons rescues RTT in mice (Luikenhuis *et al*, 2004). The mouse model we studied harbors a deletion of *Mecp2* exons 3 and 4, which encode the methyl-binding domain and the

\*Correspondence: Dr D Huertas or Dr M Esteller, Cancer Epigenetics and Biology Program (PEBC), Bellvitge Biomedical Research Institute (IDIBELL), 3rd Floor, Hospital Duran i Reynals, Avenue Gran Via 199-203, L'Hospitalet, Barcelona 08908, Catalonia, Spain, Tel: +34 932607253, Fax: +34 932607140, E-mail: dhuertas@idibell.cat or mesteller@idibell.cat Received 3 February 2014; revised 28 May 2014; accepted 2 June 2014; accepted article preview online 11 June 2014

transcription repression domain, respectively (Guy *et al*, 2001). As previously described not only in RTT patients but also in RTT model mice, the levels of norepinephrine and dopamine are reduced (Ide *et al*, 2005) and Th-expressing neurons are deficient (Viemari *et al*, 2005). A deficiency in the midbrain (MB) of catecholaminergic metabolism in *Mecp2* knockout (KO) mice has also been described (Samaco *et al*, 2009). The MB dopaminergic (mDA) area substantia nigra pars compacta (SNpc) regulates the production of motor strategies (Blandini *et al*, 2000), and dopaminergic deficit is also the cause of motor deficits in Parkinson disease (Jenner, 2008). In this regard, the mature dendritic arbors of pyramidal neurons are severely retracted, and dendritic spine density is markedly reduced in *Mecp2* KO mice (Nguyen *et al*, 2012). Most importantly, it has already been demonstrated that a conditional loss of *Mecp2* in brain areas induces motor impairments and dopaminergic deficits in the SNpc of *Mecp2* KO mice. Most strikingly, when L-Dopa treatment is implemented, the behavioral effects of *Mecp2* KO are improved (Panayotis *et al*, 2011).

Following the dopaminergic deficiency in RTT described above, and the usual combination of L-Dopa with a dopa-decarboxylase inhibitor (Ddci) to prevent the conversion of levodopa into dopamine in the peripheral circulation (Olanow *et al*, 2001) and to provide an efficient dopaminergic stimulation therapy in Parkinsonism and related disorders (Mena *et al*, 2009), we wondered whether the same type of dual approach could help ameliorate the clinicopathological features of the *Mecp2* null mouse. We observed that the combined administration of L-Dopa and the Ddci benserazide was able to improve the mobility, tremor, and breathing phenotype of the *Mecp2* KO mice in association with an increase in dopaminergic activity and dendritic spine density.

## MATERIALS AND METHODS

### Animals

Experiments were performed on the B6.129P2(c)-*Mecp2*<sup>tm1</sup>+1Bird mouse model for RTT (Guy *et al*, 2001). The exact strain used was C57BL/6J and it was maintained by backcrossing with C57BL/6J purchased from The Jackson Laboratory. Both pre-symptomatic and symptomatic mice were analyzed at different developmental stages. A total of 157 littermate male mice were used in the study divided in five groups: *Mecp2* wild-type (WT;  $n = 30$ ), *Mecp2*-/*y* vehicle-treated ( $n = 39$ ), *Mecp2*-/*y* Ddci-treated ( $n = 15$ ), *Mecp2*-/*y* L-Dopa-treated ( $n = 30$ ), and *Mecp2*-/*y* L-Dopa + Ddci-treated ( $n = 43$ ). Animals used for the experiments were all males and ranged in age from 4 to 10 weeks. All mice procedures and experiments were approved by the Ethics Committee for Animal Experiments of the IDIBELL Centre, under the guidelines set out under Spanish animal welfare laws. For the pharmacological treatments, treated and untreated (vehicle) mice were studied. *Mecp2*-deficient treated and untreated mice were compared with their respective WT littermates. The *Mecp2* -/*y* (null male) and WT (male) mice were subjected to immunohistochemistry, neurochemical analysis, and western blot studies at 24, 55, and 70 postnatal days. For the pharmacological treatments, *Mecp2* KO mice received

for 6 weeks a once-a-day dose of intraperitoneal Ddci (12 mg/kg/day, Benserazide, B7283; Sigma-Aldrich) in saline vehicle, L-Dopa (30 mg/kg/day, Sigma-Aldrich; D1507) or L-Dopa + Ddci. In the L-Dopa + Ddci group, the Ddci drug was injected 15 min before L-Dopa administration.

### Score Test

The score was based on that previously adopted in the study of the *Mecp2* null mouse model (Guy *et al*, 2001; Guy *et al*, 2007). The treatment started when animals were 4 weeks old. At that time, it was still not possible to observe characteristic symptoms of this model. Every day, mice were weighed in order to apply the appropriate dose of the injection. Every 2 days (the starting point being the first day of treatment), neurological defects in an *MeCP2* mouse model were scored (blind to genotype and treatment; twice a week, at the same time of day), focusing on mobility, gait, hindlimb claspings, tremor, breathing, and general condition. Each of the six symptoms was scored from 0 to 2; 0 corresponds to the symptom being absent or the same as in the WT animal, 1 where the symptom was present, and 2 when the symptom was severe. In detail:

(A) Mobility: the mouse is observed when placed on bench, then when handled gently. 0 = As WT. 1 = Reduced movement when compared with WT: extended freezing period when first placed on bench and longer periods spent immobile. 2 = No spontaneous movement when placed on the bench; mouse can move in response to a gentle prod or a food pellet placed nearby.

(B) Gait: 0 = As WT. 1 = Hind legs are spread wider than WT when walking or running with reduced pelvic elevation, resulting in a 'waddling' gait. 2 = More severe abnormalities: tremor when feet are lifted, walks backward or 'bunny hops' by lifting both rear feet at once.

(C) Hindlimb claspings: mouse observed when suspended by holding base of the tail. 0 = Legs splayed outward. 1 = Hindlimbs are drawn toward each other (without touching) or one leg is drawn into the body. 2 = Both legs are pulled in tightly, either touching each other or touching the body.

(D) Tremor: mouse observed while standing on the flat palm of the hand. 0 = No tremor. 1 = Intermittent mild tremor. 2 = Continuous tremor or intermittent violent tremor.

(E) Breathing: movement of flanks observed while animal is standing still. 0 = Normal breathing. 1 = Periods of regular breathing interspersed with short periods of more rapid breathing or with pauses in breathing. 2 = Very irregular breathing—gaspings or panting.

(F) General condition: mouse observed for indicators of general well-being such as coat condition, eyes, and body stance. 0 = Clean shiny coat, clear eyes, and normal stance. 1 = Eyes dull, coat dull/ungroomed, and somewhat hunched stance. 2 = Eyes crusted or narrowed, piloerection, and hunched posture.

If at any point an animal scored 2 out of 2 for the last three criteria, or if the animal lost 20% of its body weight during the experiment, it was killed. Inter-rater reliability for each qualitative parameter was assessed using a Cohen's Kappa statistic (Kappa) that controls for chance agreement between two raters (study rater and an experienced rater), with a value of 1 indicating perfect agreement, and

performed for all the individuals. All the parameters show Kappa > 0.7 and associated *p*-value < 0.05. For the measure of Cohen's Kappa statistics was used using irr package (Gamer *et al*, 2012) under R statistical software (R Core Team, 2013). The two observers scored in a blind fashion manner in relation to the MeCP2 genotype, drug treatment, and age of the animal.

The bar cross test, as previously described (Ferrer *et al*, 2005; Lopez-Erauskin *et al*, 2011), was also carried out. In brief, it was done using a 100-cm-long and 2-cm-wide wooden bar that was wide enough for mice to stand on with their hind feet hanging over the edge, such that any slight lateral misstep would result in a slip. The bar was raised 50 cm above the bench surface so that animals did not jump off and would not be injured upon falling from the bar. The mice were placed at one end of the bar and were expected to cross to the other end. To eliminate the novelty of the task as a source of slips, all animals underwent three trials on the bar the day before and at the beginning of the testing session. In an experimental session, the numbers of hindlimb lateral slips and falls from the bar were counted in three consecutive trials. If an animal fell, it was placed back on the bar at the point from which it had fallen, and was allowed to complete the task.

### Western Blot

For western blotting, animals were killed 4 weeks after the first treatment (at 8 weeks of age), and the MB area with the dopaminergic region was rapidly removed from the brain and cut with a Rodent Brain Slicer matrix (Zivic Instruments; 2 mm sections). Next, the protein extract was obtained with lysis buffer (20 mM Tris-HCl, pH 7.5, 150 mM NaCl, 2 mM EGTA, 0.1% Triton X-100, and complete protease inhibitor and phosphatase inhibitor cocktail tablet from Sigma and Roche) sonicated and denatured for 10 min at 95 °C. Protein concentrations were determined using the BCA (Pierce BCA Protein Assay kit). An amount of 25 µg of each protein sample was separated on a 10% SDS-polyacrylamide gel by sodium dodecyl sulfate electrophoresis, and transferred onto a PVDF membrane (Immobilon-P, Millipore) by liquid electroblotting (Mini Trans-Blot Cell, Bio-Rad) for 1 h at 100 V. The membrane was blocked in 5% nonfat dry milk in TBS 0.1% Tween 20 for 1 h at room temperature (RT). Primary antibody specific to Th (Millipore) was used at a dilution of 1:1000, overnight (ON) at 4 °C. After extensive washing, the membrane was incubated with secondary antibody peroxidase-conjugate for 1 h at RT. Finally, the specific reaction was detected with a chemiluminescence reagent kit (Supersignal West Pico chemiluminescent, Thermo Scientific). Digital images were processed with a GS-800 Calibrated Densitometer (Bio-Rad). Bands were quantified with Bio-Rad Quantity One software. In all cases, images correspond to the results of one representative experiment out of three. The level of Th was normalized with an antibody to actin, used as a loading control.

### Immunofluorescence Analysis

Mice were deeply anesthetized with dolethal (Vetoquinol), perfused transcardially with NaCl (0.9%) followed by

buffered 4% paraformaldehyde in saline-phosphate buffer, pH 7.5. Brains were post-fixed ON in the same solution, subsequently dehydrated in 30% sucrose until the contents reached the bottom of the tube. All brains were dissected into 2 mm coronal sections (Rodent Brain Slicer matrix, Zivic Instruments) and cryoprotected in OCT, then stored at -80 °C. Sections of 25 µm were cut from the MB region with SNpc using a cryostat (Microm Microtech). The brain regions were identified using AGEA Allen Brain Atlas Mouse. All the immunostaining steps were carried out free-floating in solution. The staining protocol followed was based on previous detailed descriptions (Roux *et al*, 2007; Dura *et al*, 2008). All tissues were permeabilized and blocked with 0.2% of Triton X-100, 20% goat serum/PBS for 1 h at RT, and incubated with the appropriate primary antibodies (1:1000 mouse Th and 1:1000 rabbit phospho-Th; MS X Th, Millipore; and Phospho-Th, Cell Signaling) in 0.2% Triton X-100, 2% goat serum/PBS ON at 4 °C. Anti-mouse Alexa 488/anti-rabbit Alexa 555 were used as secondary antibodies. DAPI (4,6-diamino-2-phenolindol dihydrochloride) counterstaining was performed on all sections, in order to visualize the nucleus, and coverslips were mounted in Mowiol (Calbiochem) after staining. The double-labeled images were acquired using a Leica TCS SP5 Spectral Confocal microscope (Leica, Milton Keynes, UK; magnification: HCX PL APO lambda blue × 63 oil, numerical aperture (NA): 1.4, and 1024 × 1024 resolution; Acquisition Software: Leica Application suite Advanced Fluorescence, version 2.6.0.7266). Z project and Tile were carried out in order to achieve complete staining with both antibodies. Densitometric analysis of the staining level was performed on 8-bit images using ImageJ Fiji vs 1.47 software (<http://rsb.info.nih.gov>). The integrated density was calculated as the sum of the pixel values in a region of interest. We obtained pictures from different slices in the same region and then calculated the average of the successive impaired sections for each animal in each experimental group (total five).

### Golgi Staining

Golgi staining was done to study the neuronal morphologies (FD Rapid GolgiStain Kit, FD Neurotechnologies). Animals were anesthetized as described above. Brains were extracted and all protocols were performed according to the manufacturer's instructions. Three brains from each of the treated groups were dissected into 2-mm coronal pieces (Rodent Brain Slicer matrix, Zivic Instruments), mounted in freezing medium (TFM, Triangle Biomedical) and stored at -80 °C. Sections of 80-100 µm were cut using a cryostat and mounted on gelatin-coated microscope slides with solution C. We proceeded with the staining protocols by following the instructions included in the manual. Between 10 and 15 neurons of the hippocampus zone were analyzed from two animals from each group. Images of dendritic spines were acquired with a Zeiss Axio Observer Z1 with an Apotome microscope (magnification: Plan-APOCHROMAT; × 63 oil Dic NA. 1.4; Acquisition Software: ZEN 2011), and reconstructed in three dimensions using the NeuronStudio software for image processing to enable higher identification and to improve the quality of the spine analysis (Rodriguez *et al*, 2006; Rodriguez *et al*, 2008). Dendritic

spines were counted by Sholl analysis over a length of 20  $\mu\text{m}$  with concentric circles of 10  $\mu\text{m}$  (Sholl, 1953).

### RNA Isolation from MB and Real-Time qPCR Analysis

For total RNA preparation, the tissue was resuspended in TriZol (Life Technologies), purified with chloroform and precipitated with isopropanol, then washed with ethanol, and dissolved in sterile water. cDNA synthesis was performed with 1  $\mu\text{g}$  total RNA and random hexamers primers using the superscript KIT (Life Technologies). Aliquots (1  $\mu\text{l}$ ) of diluted cDNA (1:4) were amplified by the SYBR Green PCR Master Mix (Life Technologies) in a final volume of 10  $\mu\text{l}$ . Real-time PCRs were performed in triplicate on an Applied Biosystems 7900HT Fast Real-Time PCR system. All primer pairs were designed with Primer 3 software and validated by gel electrophoresis to amplify specific single products. All data were normalized with respect to an endogenous control: PPIA or RPL38. Relative mRNA levels were calculated using qBASE plus software (Biogazelle). PCR cycles were divided into initial denaturation at 95  $^{\circ}\text{C}$  for 5 min, followed by 40 cycles of 95  $^{\circ}\text{C}$ , for 30 s, 60  $^{\circ}\text{C}$  for 30 s, and 72  $^{\circ}\text{C}$  for 30 s. The following primers were used: *Drd1* (forward 5'-ATGGCTCCTAACACTTCTACCA-3'; reverse 5'-GGGTATTCCCTAAGAGAGTGGAC-3'), *Drd2* (forward 5'-TGGATCCACTGAACCTGTCC-3'; reverse 5'-TTGTAGTGGGGCCTGTCTG-3'), *PPIA* (forward 5'-CAAATGCTGGACCAAACACAA-3'; reverse 5'-GTTTCATGCCTTCTTTCACCTT-3'), *RPL38* (forward 5'-AGGATGCCAAGTCTGTCAAGA-3'; reverse 5'-TCCTTGCTGTGATAACCAGGG-3').

### Dopamine Assay

For the determination of dopamine levels in brain regions, the Mouse Dopamine Elisa Kit was used (Blue Gene, cat. no. E03D0043, Shanghai, China). In brief, mice were killed at 8 weeks and the studied brain regions were dissected and snap-frozen. Samples were weighed and homogenized in presence of saline solution (20  $\mu\text{l}/\text{mg}$  tissue). The resulting suspension was then sonicated and centrifuged to remove insoluble material. The samples were diluted and assayed according to the manufacturer's protocol. The final dopamine concentration for each sample was normalized with the respective total protein amount.

### Glutathione Assay Kit

For the determination of total glutathione (GSx), reduced glutathione (GSH), and oxidized (GSSG) a Glutathione Assay Kit (Bio Vision, cat. no. K264-100 kit; Milpitas, California) was used. At 8 weeks of age, the mice were killed, and the brain was rapidly removed. Brain tissues were washed in 0.9% NaCl solution and homogenized on ice with 100  $\mu\text{l}$  ice-cold Glutathione Assay Buffer for 40 mg of tissue. 60  $\mu\text{l}$  of each homogenate was placed into a tube containing 20  $\mu\text{l}$  of cold perchloric Acid (PCA) and vortexed several seconds to achieve a uniform emulsion. Next, the samples were centrifuged and the supernatant (containing GSH) was collected. Ice-cold KOH (20  $\mu\text{l}$ ) was added to 40  $\mu\text{l}$  of PCA preserved samples to precipitate the PCA and neutralize the samples. In order to detect the GSH, we add assay buffer, until 90  $\mu\text{l}$  final volume. To obtain the GSx,

70  $\mu\text{l}$  of assay buffer was added to 10  $\mu\text{l}$  of each sample with 10  $\mu\text{l}$  of Reducing Agent Mix to convert GSSG to GSH. To get the results of GSSG, to the 60  $\mu\text{l}$  of assay buffer and 10  $\mu\text{l}$  of sample, 10  $\mu\text{l}$  of GSH Quencher was added to quench GSH. After 10 min of RT incubation, 10  $\mu\text{l}$  of Reducing Agent Mix was added to destroy the excess GSH Quencher and convert GSSG to GSH. After 10 min of RT incubation, 10  $\mu\text{l}$  of o-phthalaldehyde probe was added to all samples. Next, all samples were incubated at RT in the dark for at least 30 min. The fluorescence was read at Ex/Em = 340/420 nm

### Statistical Analysis

The data obtained from WT and KO animals in the initial experiments were compared using Student's unpaired *t*-test. Score data, bar cross, immunofluorescence, qPCR analysis, Golgi staining, and western blot experiments in the different treatments groups were compared by one-way analysis of variance (ANOVA) with Tukey's or Bonferroni's Multiple Comparison *post hoc* test for intergroup comparisons. All results were analyzed using GraphPad 5.04 Prism software. Life span data were plotted as Kaplan–Meier survival curves. Results were considered significant for values of  $*p < 0.05$ ,  $**p < 0.01$ , or  $***p < 0.001$ . Data are presented as the mean and SEM.

## RESULTS

### The Combined L-Dopa + Ddci Treatment of *Mecp2* Null Mice is Well Tolerated, Diminishes RTT-Associated Symptoms, and Increases Life span

RTT patients and *Mecp2* KO mice manifest a progressive postnatal neurological phenotype (Guy *et al*, 2001; Chahrour and Zoghbi, 2007). *Mecp2* KO mice are apparently normal until 4 weeks of age and then begin to suffer cognitive and motor dysfunctions. The progression of symptoms in the *Mecp2* KO male mice leads to rapid weight loss and death at  $\sim 10$  weeks of age in comparison with WT animals (Guy *et al*, 2001). To test the effect of the L-Dopa + Ddci combination on the symptomatology of RTT mice, we treated the animals daily over 6 weeks. We used a once-a-day dose of intraperitoneal Ddci, L-Dopa or L-Dopa + Ddci. In the L-Dopa + Ddci group, the Ddci drug was injected 15 min before L-Dopa administration. The used doses are those that have proven efficient in mice models of Parkinson's disease (Chartoff *et al*, 2001; Santini *et al* 2009). Every 2 days, we scored the neurological recovery of the *MeCP2* model mice as previously described (Guy *et al*, 2007). We started the treatments when the animals were 4 weeks old because by 6 weeks of age it is already possible to observe some of the characteristic symptoms of the *Mecp2* KO model, that is, reduced mobility, retraction of the legs, tremor, irregular breathing, and difficulties with walking. First, we determined whether the administration of L-Dopa, Ddci, or the combination L-Dopa + Ddci was toxic for the *Mecp2* KO mice by daily monitoring the weight of each animal. The *Mecp2* KO mice treated with either the vehicle (saline serum), L-Dopa, Ddci, or the combination L-DOPA + Ddci showed had similar weights, independent of the compound used (Figure 1a). At the time of killing,

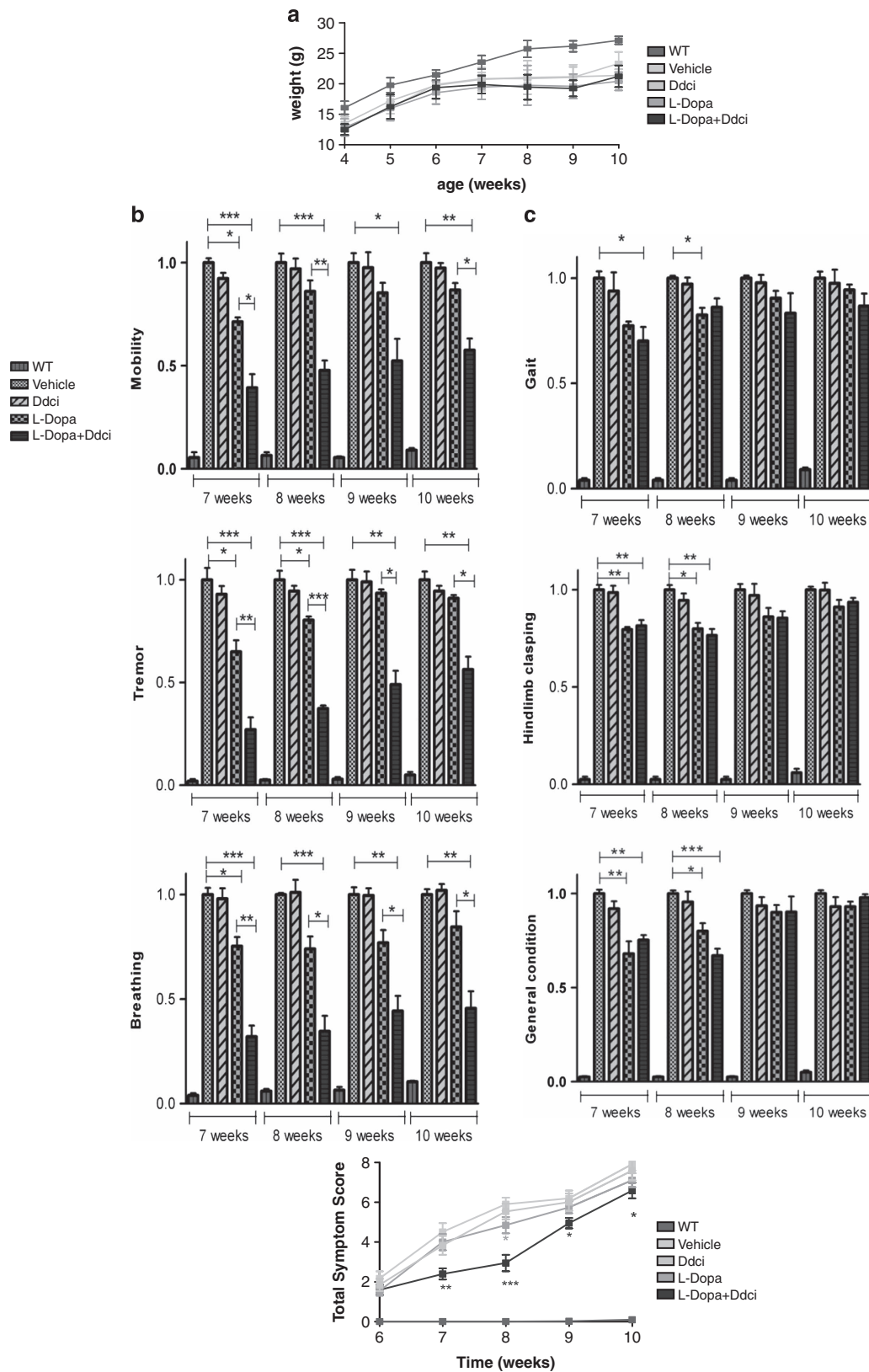


**Figure 1** Effect of L-Dopa and L-Dopa + Ddci (dopa-decarboxylase inhibitor) treatments on the *Mecp2* null phenotype. The number of animals used in each experiment was 30 for wild-type (WT) control, 37 for vehicle, 40 for L-Dopa + Ddci, 30 for L-Dopa, and 15 for Ddci. (a) Measurement of mice body weight during treatment. No effect on body weight was observed after the treatments in the *Mecp2* KO mice. (b) Plots showing 'Score Test' (Guy *et al.*, 2001) improvement upon L-Dopa + Ddci treatment related to mobility, tremor, and breathing. (c) Plots showing 'Score Test' (Guy *et al.*, 2001) improvement related to gait, hindlimb clasping, and general conditions that are less affected by the treatments. (d) Plot of total average symptom scores showing 'Score Test' (Guy *et al.*, 2001) improvement in *Mecp2* KO-treated mice upon L-Dopa + Ddci treatment. For the described pairwise comparisons, a Tukey HSD *post hoc* test was performed after the one-way analysis of variance. \* $p < 0.05$ , \*\* $p < 0.01$ , and \*\*\* $p < 0.001$ .

liver tissues were resected for pathological analysis, and no toxicity was detected in any of the mice used in the different drug treatments (Supplementary Figure 1). Finally, we have studied possible neurotoxicity by measuring oxidative stress in the brain of these animals. The ratio of reduced (GSH) vs oxidized (GSSG) GSH shows that the *Mecp2* KO mice undergoes a significant oxidative stress in comparison with the WT littermate mice (Supplementary Figure 1), and that the L-Dopa + Ddci treatment significantly reduces oxidative stress in the brain of these animals (Supplementary Figure 1).

We next analyzed the effect of the L-Dopa + Ddci combined treatment in the *Mecp2* KO mice on the clinicopathological phenotype of this RTT model. We measured score mobility, tremor, breathing, gait, hindlimb claspings, and general condition (Guy *et al*, 2001; Guy *et al*, 2007) (Figure 1b and c). The plots show the overall distribution of symptoms at 7, 8, 9, and 10 weeks of age, and compare the scores of the vehicle, L-Dopa, Ddci, and L-Dopa + Ddci-treated groups. During each week of treatment, the 'Score Test' values (Guy *et al*, 2001) were separately calculated, then normalized with respect to the vehicle group using one-way ANOVA with Bonferroni's *post hoc* multiple comparison. We confirmed the existence of a significant improvement in mobility, tremor, and breathing from 7 to 10 weeks of age in the vehicle vs L-Dopa group as has been previously described (Panayotis *et al*, 2011), but remarkably the improvement in the symptoms was significantly greater in the L-Dopa + Ddci-treated group,  $p < 0.001$  (Figure 1b). There was no difference between vehicle and Ddci alone (Figure 1b). Treatment with L-Dopa + Ddci improved the mobility, tremor, and breathing phenotype by an average of 50%, having less effect on older mice. Regarding the phenotypes of gait, hindlimb claspings or general condition symptom, a significant improvement was observed with both L-Dopa and L-Dopa + Ddci treatments in younger mice (7–8 weeks) that became a non-significant trend in older mice (9–10 weeks; Figure 1c). If we plot the average of the eight scored symptoms to create

a total score (Guy *et al*, 2001), a significant phenotypic improvement is observed in the L-Dopa + Ddci-treated group (Figure 1d). We further determined the possible restoration of the motor impairments in the *Mecp2* null mice upon administration of L-Dopa + Ddci therapy by using the bar cross test (Ferrer *et al*, 2005; Lopez-Erauskin *et al*, 2011). We observed that L-Dopa alone was able to improve test performance in comparison with the vehicle-treated group, but the Rett model mice receiving the combined L-Dopa + Ddci regimen achieved the best scores, such as a shorter time to cross the bar (Figure 2a) and fewer slips (Figure 2b). Illustrative movies of the bar cross test in the WT animal and in the *Mecp2* null mice treated with the vehicle or the L-Dopa + Ddci combination are included in Supplementary Material. Overall for the tests used, the efficacy of the studied combination was particularly evident in the first weeks when there may be a window for therapeutic opportunities. Most importantly, the observed improvement in the disease-linked features was also associated with an increased life span of the male *Mecp2* null mice that received the L-Dopa + Ddci combination therapy ( $p < 0.001$ , Kaplan–Meier log-rank test; Figure 2e).

Thus, the combined administration of L-Dopa + Ddci in *Mecp2*-deficient mice increases their well-being overall by diminishing RTT symptomatology, particularly those features controlled by the dopaminergic pathway in the nigrostriatum, such as mobility, tremor, and breathing.

### The use of L-Dopa + Ddci in the *Mecp2* Null Mice Induces Dendritic Growth Mediated by Dopaminergic Neurons

Beyond the amelioration of the RTT clinical phenotype described above, we wondered whether the L-Dopa + Ddci treatment was also associated with an improvement in the pathological cellular and tissular changes observed in the brain of *Mecp2* null mice. Morphological studies in postmortem brain samples from RTT individuals exhibited a characteristic neuropathology that included decreased

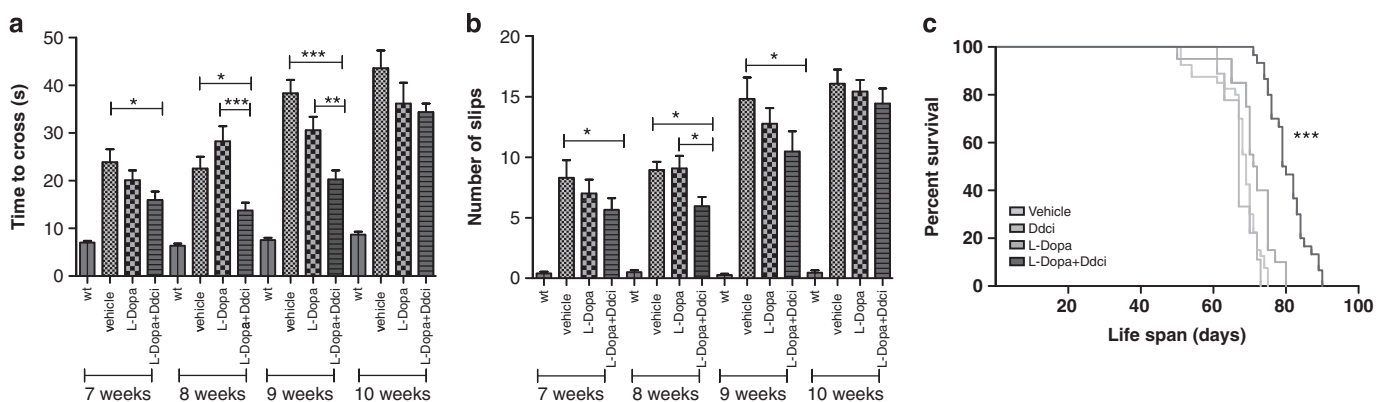


**Figure 2** Treatment with L-Dopa + Ddci (dopa-decarboxylase inhibitor) reduces motor deficits and prolongs survival in *Mecp2* knockout (KO) mice. Twenty animals were used for each treatment group in a and b. (a) Combination treatment of L-Dopa + Ddci rescues locomotor deficits in *Mecp2* KO mice. The bar cross test was carried out weekly; the time spent to cross the bar, and (b) number of slips were quantified from 7 to 10 weeks of age. Graphs illustrate the mean and SEM of two independent experiments. For the described pairwise comparisons, a Tukey HSD *post hoc* test was performed after the one-way analysis of variance. \* $p < 0.05$ , \*\* $p < 0.01$ , and \*\*\* $p < 0.001$ . (c) Treatment with L-Dopa + Ddci prolongs survival in *Mecp2* KO mice (vehicle group  $68.9 \pm 3.08$  days; L-Dopa  $71 \pm 3.4$  days; and L-Dopa + Ddci:  $80.5 \pm 4.4$  days; \*\*\* $p < 0.001$ ; for all graphs: vehicle  $n = 30$ , mice treated with L-Dopa + Ddci  $n = 30$ , and mice treated with L-Dopa alone with  $n = 10$ , Ddci group  $n = 10$ ).

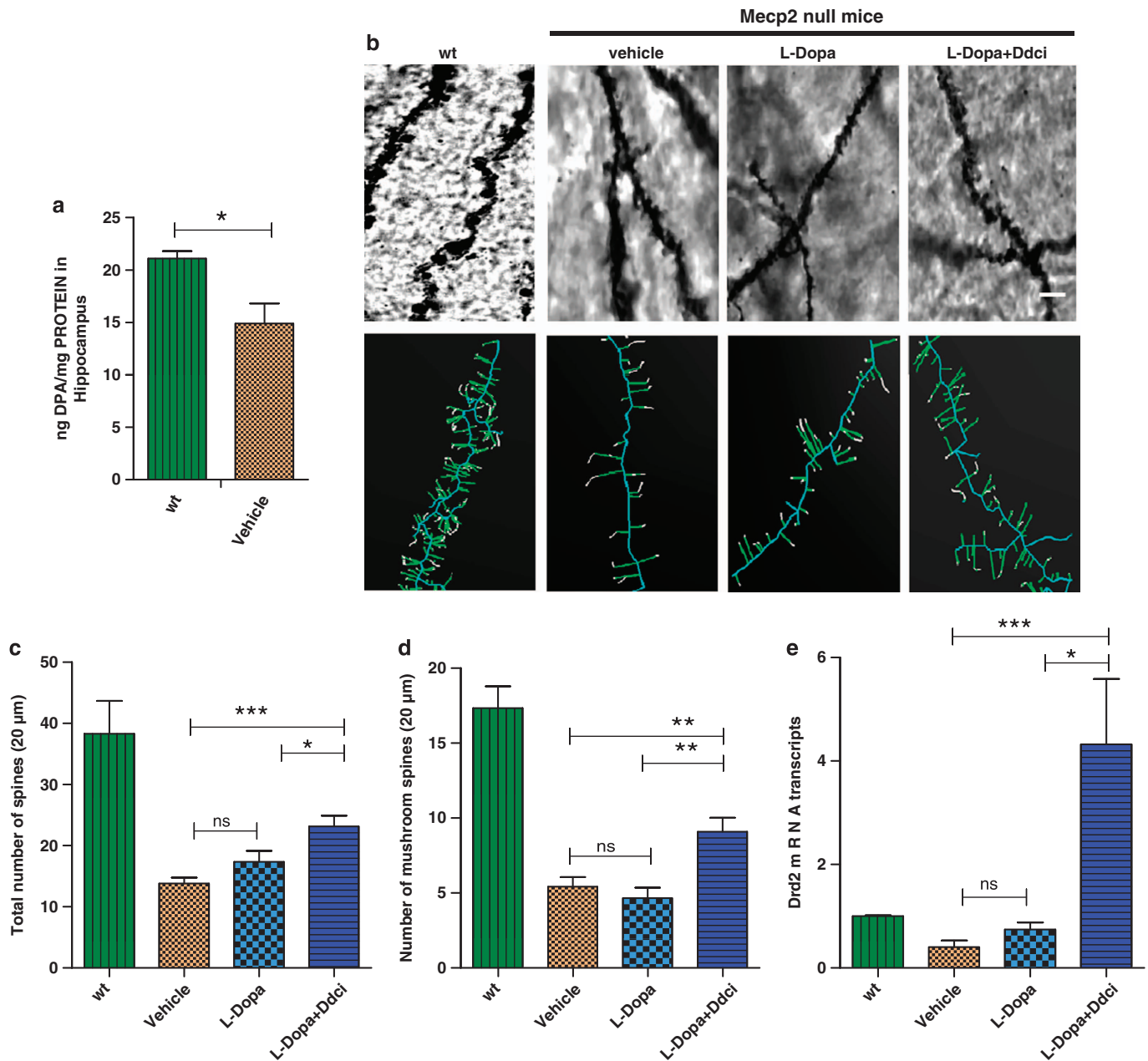


**Figure 3** Determination of neuronal dendritic growth in the *Mecp2* null mice upon L-Dopa + Ddci (dopa-decarboxylase inhibitor) treatment. (a) Dopamine concentration normalized with the respective total protein amount in hippocampus of wild-type (WT) and *Mecp2* null mice. (b) Spine density in hippocampus of WT and *Mecp2* null mice with or without treatment acquired with a Zeiss wide-field microscope,  $\times 63$  magnification, 1.4 numerical aperture. (Below) Bars showing the spine density (mean and SEM) in the hippocampus region of *Mecp2*-deficient mice vs WT, and treated with L-Dopa + Ddci or L-Dopa alone, at 4 weeks post treatment (8 weeks of age), focusing on the total number of spines (c) and mushroom spines (d). Dendritic segments of 20  $\mu$ m were analyzed for each group, and images were obtained with a Zeiss microscope,  $\times 63$  magnification, and processed with NeuronStudio software. The bars illustrate the average total count of spines in dendritic segments in the four experimental groups (Sholl analysis). (e) L-Dopa + Ddci treatment causes an increase in dopamine 2 receptor (D2R) levels. All transcript levels were determined using qRT-PCR (Applied Biosystem). The values (mean and SEM) are the ratio with respect to WT, which is assigned a value of 1 (line) \* $p < 0.05$ , \*\* $p < 0.01$ . For the described pairwise comparisons, a Tukey HSD *post hoc* test was performed after the one-way analysis of variance. \* $p < 0.05$ , \*\* $p < 0.01$ , and \*\*\* $p < 0.001$ .

neuronal size and increased neuronal density in the cerebral cortex, hypothalamus and the hippocampal formation (Bauman *et al*, 1995), and decreased dendritic growth in pyramidal neurons of the subiculum and frontal and motor cortices (Armstrong *et al*, 1995). The quantitative analyses of dendritic spine density in postmortem brain tissue from

RTT individuals also revealed that hippocampal CA1 pyramidal neurons have lower spine density than age-matched female control individuals (Chapleau *et al*, 2009). In the *Mecp2* KO mice, CA1 pyramidal neurons showed lower dendritic spine density than those from WT littermates (Chapleau *et al*, 2012). These observations are

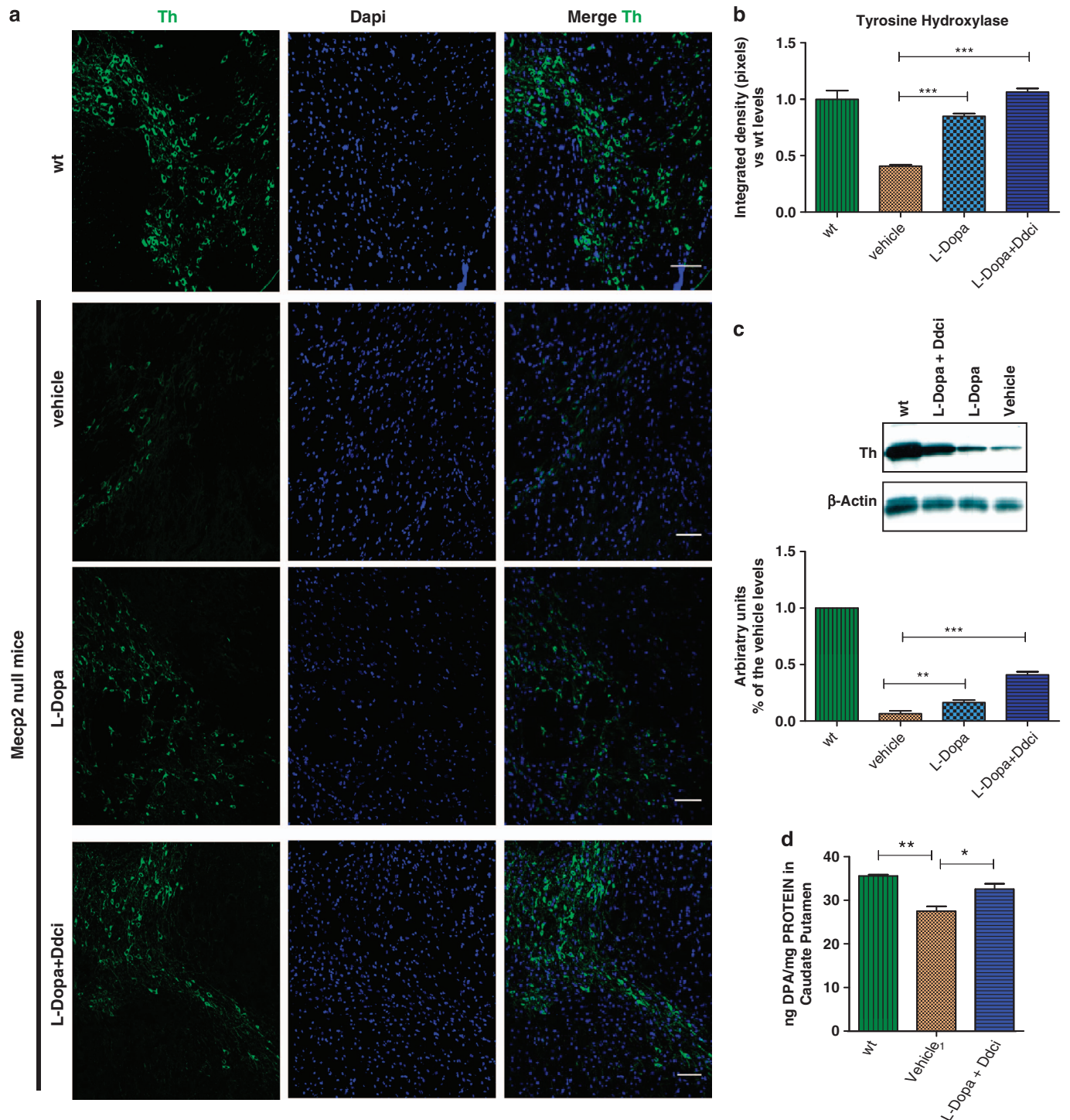


**Figure 4** Determination of tyrosine hydroxylase (Th) expression in the *Mecp2* null mice upon different treatments. (a) Representative immunostaining of coronal brain sections from Substantia nigra pars compacta (SNpc). Midbrain dopaminergic neurons were coimmunostained for Th (green) and DAPI (4,6-diamino-2-phenolindol dihydrochloride) counterstain (blue). Scale bars, 100  $\mu$ m. (b) Quantification of Th-positive staining in all aforementioned experimental groups. Bars represent the integrated density (ImageJ Fiji vs. 1.47) of the picture obtained with a SP55 confocal microscope,  $\times$  63 objective. An increase in Th levels in *Mecp2*-deficient mice treated with L-Dopa and L-Dopa + Ddci is observed. (c) Representative western blot showing the levels of Th proteins in midbrain from four experimental groups. Actin was used as a loading control. (d) Dopamine concentration normalized with the respective total protein amount in caudate putamen of wild-type (WT) and *Mecp2* null mice treated with vehicle or L-Dopa + Ddci (dopa-decarboxylase inhibitor). All animals were analyzed 4 weeks post treatment (8 weeks old),  $n = 10$  per group. One-way analysis of variance (ANOVA) and a *post hoc* test were used for statistical comparison. For the described pairwise comparisons, a Tukey HSD *post hoc* test was performed after the one-way ANOVA. \* $p < 0.05$ , \*\* $p < 0.01$ , and \*\*\* $p < 0.001$ .

particularly important in our model because Dopamine facilitates dendritic spine formation, and the improvement of the symptomatology in the studied *Mecp2* null mouse model upon L-Dopa + Ddci use could be in part explained by the stimulation of neuronal dendritic growth. In this regard, we found that the hippocampus of *Mecp2* KO mice compared with control littermates showed significant lower levels of dopamine (Figure 3a). Because most of the abnormalities in morphology, density of dendritic spines, and reduction of synaptic activity in RTT occur in the hippocampus region (Fiala et al, 2002; Dani et al, 2005; Chang et al, 2006; Chao et al, 2007), we evaluated the dendrite status in this region in the differently treated *Mecp2* null mice.

Using Golgi staining (Figure 3b) and NeuronStudio software and the Sholl analysis algorithm (Rodriguez et al, 2008), we found that the RTT mice treated with the L-Dopa + Ddci combination showed a significant increase in the number of spines in comparison with vehicle-treated animals (Figure 3c). Further refinement of the analyses by counting mushroom spine density, as an example of the more mature type of spines (Chapleau et al, 2009), also showed a significant increase of this class of spines in the *Mecp2* null mice that received the L-Dopa + Ddci treatment (Figure 3d). Most importantly, the increase in spinogenesis under the combined therapy regimen is associated with the enhanced expression of the Dopamine 2 Receptor (D2R) in the MB of the Rett mouse model (Figure 3e), with an additional beneficial amplification effect for the L-Dopa + Ddci treatment because D2R elicits extensive spine formation (Fasano et al, 2013). The role of Dopamine in reverting *Mecp2* null mice features is also highlighted by the study of the expression levels of Th, the rate-limiting enzyme of dopamine synthesis, which works by catalyzing the hydroxylation of tyrosine to L-Dopa (Molinoff and Axelrod, 1971). The *Mecp2* null mice exhibit low levels of Th expression in comparison with the WT group, assessed by immunofluorescence staining in MB (Figure 4a and b), and we observed a recovery of physiological levels of Th in the L-Dopa + Ddci-treated group. These results are consistent with the increase of Th-expressing neurons observed upon L-Dopa in Parkinson disease patients (Porrit et al, 2000), animal models of Parkinson disease (Betarbet et al, 1997; Tandé et al, 2006; Espadas et al, 2012) and, most importantly, in the studied RTT mouse model (Panayotis et al, 2011; Kao et al, 2013). Herein, the addition of Ddci to the L-Dopa treatment further enhance Th expression (Figure 4a and b). Western blot analyses confirmed the upregulation of Th in the *Mecp2* null group that received the combined treatment (Figure 4c). Furthermore, the L-Dopa + Ddci-treated group significantly recovered dopamine levels in comparison with the vehicle-treated group (Figure 4d). Thus, the formation of new spines induced by an activation of dopaminergic neurons is a likely mechanism that explains the observed improvement of the RTT phenotype upon the combined administration of L-Dopa + Ddci.

## DISCUSSION

Overall, our results indicate that the use of strategies similar to those used in the therapy of Parkinson disease could also

be useful for treating RTT. Herein, we show that the combination of L-Dopa and the peripherally acting amino-acid decarboxylase inhibitor benserazide, a commonly used therapeutic regimen in Parkinson diseases in the formulation known as Madopar, can improve RTT symptomatology in association with the stimulation of neuronal dendritic growth. These results link with the dopaminergic defects observed in RTT, such as the well-known reduction in levels of dopamine in the brain and cerebrospinal fluid analyses (Riederer et al, 1986; Lekman et al, 1989; Wenk et al, 1991), a low D2R content (Chiron et al, 1993), and reduced Th immunoreactivity (Jellinger et al, 1988). In the RTT mouse models, the dopamine levels are also reduced (Ide et al, 2005) and there is a deficiency of Th-expressing neurons (Viemari et al, 2005). This dopamine-associated impairment is associated, as in our study, with an abnormal thinning of dendrites (Jellinger, 2003), and dendritic spine density is also significantly diminished in *Mecp2* KO mice (Nguyen et al, 2012). Most importantly, the results extend the original observation that L-Dopa treatment ameliorated the motor deficiency of the RTT mouse model (Panayotis et al, 2011) to formally prove that the addition of the Ddci is able to further improve the clinical symptoms of the disease with consequences at the molecular and cellular levels in the brains of these animals. In comparison with the pioneering study of Panayotis et al (2011), we used a higher dose of L-Dopa, an intraperitoneal injection instead of an oral administration, and the effects were more obvious in younger ages. Importantly, both studies support that a targeting of the dopamine pathway improves the Rett phenotype in the described mice model. However, a caution note should also be included because we observed that the improvement of the phenotype diminished with the duration of the treatment and our survival curves did not extend beyond 90 days.

To our knowledge, the biomedical literature only features a single case of a Rett patient who has received L-Dopa, but the authors did not study its effect on the patient's mobility, tremor, and breathing (Nomura et al, 1997). However, we know that the combination of L-Dopa and another Ddci (carbidopa) is able to improve the symptomatology of Th-deficient patients (Segawa syndrome, OMIM 606407) (Ludecke et al, 1995; Dionisi-Vici et al, 2000). These results are very interesting because we confirmed the diminished expression of Th in the RTT mouse model (Panayotis et al, 2011; Kao et al, 2013) and because the Segawa syndrome features some clinical overlap with RTT, being a progressive neurodevelopmental disorder with onset during the first year of life, Parkinsonian features and respiratory distress (Ludecke et al, 1995; Brautigam et al, 1999).

Overall, the findings reported herein are promising to overcome the dopaminergic defects observed in this preclinical model of RTT, but much effort will be required to extend the duration of the benefits of the described treatments or to analyze its effect in female mice in future studies of this devastating disorder.

## FUNDING AND DISCLOSURE

The authors declare no conflict of interest.

## ACKNOWLEDGEMENTS

This study was supported by the European Community's Seventh Framework Program (FP7/2007–2013), under grant agreement PITN-GA-2012-316758– EPITRAIN project and PITN-GA-2009-238242—DISCHROM; ERC grant agreement 268626—EPINORC project; the E-RARE EuroRETT network (PI071327) and the CIBER on Rare Diseases (CIBERER) from the Carlos III Health Institute; the Fondation Lejeune (France); MINECO projects SAF2011-22803, CSD2006-00049; the Cellex Foundation; the Botín Foundation; the Catalan Association for Rett Syndrome; and the Health and Science Departments of the Catalan Government (Generalitat de Catalunya) projects AGAUR 2009SGR1315 and 2009SGR85. KS and PP are EPITRAIN Research Fellows; SF is a Miguel Servet Researcher (CP11/00080); and ME and AP are ICREA Research Professors.

## REFERENCES

- Amir RE, Van den Veyver IB, Wan M, Tran CQ, Francke U, Zoghbi HY (1999). Rett syndrome is caused by mutations in X-linked MECP2, encoding methyl-CpG-binding protein 2. *Nat Genet* 23: 185–188.
- Armstrong D, Dunn JK, Antalffy B, Trivedi R (1995). Selective dendritic alterations in the cortex of Rett syndrome. *J Neuropathol Exp Neurol* 54: 195–201.
- Armstrong D (1995). The neuropathology of Rett syndrome—overview 1994. *Neuropediatrics* 26: 100–104.
- Bauman ML, Kemper TL, Arin DM (1995). Pervasive neuroanatomic abnormalities of the brain in three cases of Rett's syndrome. *Neurology* 45: 1581–1586.
- Betarbet R, Turner R, Chockkan V, DeLong MR, Allers KA, Walters J et al (1997). Dopaminergic neurons intrinsic to the primate striatum. *J Neurosci* 17: 6761–6768.
- Blandini F, Nappi G, Tassorelli C, Martignoni E (2000). Functional changes of the basal ganglia circuitry in Parkinson's disease. *Prog Neurobiol* 62: 63–88.
- Brautigam C, Steenbergen-Spanjers GC, Hoffmann GF, Dionisi-Vici C, van den Heuvel LP, Smeitink JA et al (1999). Biochemical and molecular genetic characteristics of the severe form of tyrosine hydroxylase deficiency. *Clin Chem* 45: 2073–2078.
- Chahrouh M, Zoghbi HY (2007). The story of Rett syndrome: from clinic to neurobiology. *Neuron* 56: 422–437.
- Chang Q, Khare G, Dani V, Nelson S, Jaenisch R (2006). The disease progression of Mecp2 mutant mice is affected by the level of BDNF expression. *Neuron* 49: 341–348.
- Chao HT, Zoghbi HY, Rosenmund C (2007). MeCP2 controls excitatory synaptic strength by regulating glutamatergic synapse number. *Neuron* 56: 58–65.
- Chapleau CA, Boggio EM, Calfa G, Percy AK, Giustetto M, Pozzo-Miller L (2012). Hippocampal CA1 pyramidal neurons of Mecp2 mutant mice show a dendritic spine phenotype only in the presymptomatic stage. *Neural Plast*, published online 30 July 2012, doi:10.1155/2012/976164.
- Chapleau CA, Calfa GD, Lane MC, Albertson AJ, Larimore JL, Kudo S et al (2009). Dendritic spine pathologies in hippocampal pyramidal neurons from Rett syndrome brain and after expression of Rett-associated MECP2 mutations. *Neurobiol Dis* 35: 219–233.
- Chartoff EH, Marck BT, Matsumoto AM, Dorsa DM, Palmiter RD (2001). Induction of stereotypy in dopamine-deficient mice requires striatal D1 receptor activation. *Proc Natl Acad Sci USA* 98: 10451–10456.
- Chiron C, Bulteau C, Loc'h C, Raynaud C, Garreau B, Syrota A et al (1993). Dopaminergic D2 receptor SPECT imaging in Rett syndrome: increase of specific binding in striatum. *J Nucl Med* 34: 1717–1721.
- Dani VS, Chang Q, Maffei A, Turrigiano GG, Jaenisch R, Nelson SB (2005). Reduced cortical activity due to a shift in the balance between excitation and inhibition in a mouse model of Rett syndrome. *Proc Natl Acad Sci USA* 102: 12560–12565.
- Dionisi-Vici C, Hoffmann GF, Leuzzi V, Hoffken H, Brautigam C, Rizzo C et al (2000). Tyrosine hydroxylase deficiency with severe clinical course: clinical and biochemical investigations and optimization of therapy. *J Pediatr* 136: 560–562.
- Dura E, Villard L, Roux JC (2008). Expression of methyl CpG binding protein 2 (Mecp2) during the postnatal development of the mouse brainstem. *Brain Res* 1236: 176–184.
- Espadas I, Darmopil S, Vergano-Vera E, Ortiz O, Oliva I, Vicario-Abejon C et al (2012). L-DOPA-induced increase in TH-immunoreactive striatal neurons in parkinsonian mice: insights into regulation and function. *Neurobiol Dis* 48: 271–281.
- Fasano C, Bourque MJ, Lapointe G, Leo D, Thibault D, Haber M et al (2013). Dopamine facilitates dendritic spine formation by cultured striatal medium spiny neurons through both D1 and D2 dopamine receptors. *Neuropharmacology* 67: 432–443.
- Ferrer I, Kapfhammer JP, Hindelang C, Kemp S, Troffer-Charlier N, Broccoli V et al (2005). Inactivation of the peroxisomal ABCD2 transporter in the mouse leads to late-onset ataxia involving mitochondria, Golgi and endoplasmic reticulum damage. *Hum Mol Genet* 14: 3565–3577.
- Fiala JC, Spacek J, Harris KM (2002). Dendritic spine pathology: cause or consequence of neurological disorders? *Brain Res Rev* 39: 29–54.
- FitzGerald PM, Jankovic J, Glaze DG, Schultz R, Percy AK (1990). Extrapyramidal involvement in Rett's syndrome. *Neurology* 40: 293–295.
- Gamer M, Lemon J, Fellows I, Singh P (2012). irr: Various Coefficients of Interrater Reliability and Agreement. R package version 0.84.
- Guy J, Gan J, Selfridge J, Cobb S, Bird A (2007). Reversal of neurological defects in a mouse model of Rett syndrome. *Science* 315: 1143–1147.
- Guy J, Hendrich B, Holmes M, Martin JE, Bird A (2001). A mouse Mecp2-null mutation causes neurological symptoms that mimic Rett syndrome. *Nat Genet* 27: 322–326.
- Ide S, Itoh M, Goto Y (2005). Defect in normal developmental increase of the brain biogenic amine concentrations in the mec2-null mouse. *Neurosci Lett* 386: 14–17.
- Jellinger K, Armstrong D, Zoghbi HY, Percy AK (1988). Neuropathology of Rett syndrome. *Acta Neuropathol* 76: 142–158.
- Jellinger KA (2003). Rett Syndrome – an update. *J Neural Transm* 110: 681–701.
- Jenner P (2008). Functional models of Parkinson's disease: a valuable tool in the development of novel therapies. *Ann Neurol* 64(Suppl 2): S16–S29.
- Kao FC, Su SH, Carlson GC, Liao W (2013). MeCP2-mediated alterations of striatal features accompany psychomotor deficits in a mouse model of Rett syndrome. *Brain Struct Funct* (e-pub ahead of print 12 November 2013).
- Kishi N, Macklis JD (2004). MECP2 is progressively expressed in post-migratory neurons and is involved in neuronal maturation rather than cell fate decisions. *Mol Cell Neurosci* 27: 306–321.
- Kitt CA, Wilcox BJ (1995). Preliminary evidence for neurodegenerative changes in the substantia nigra of Rett syndrome. *Neuropediatrics* 26: 114–118.
- Lekman A, Witt-Engerstrom I, Gottfries J, Hagberg BA, Percy AK, Svennerholm L (1989). Rett syndrome: biogenic amines and metabolites in postmortem brain. *Pediatr Neurol* 5: 357–362.
- Lopez-Erauskin J, Fourcade S, Galino J, Ruiz M, Schluter A, Naudi A et al (2011). Antioxidants halt axonal degeneration in a mouse model of X-adrenoleukodystrophy. *Ann Neurol* 70: 84–92.
- Ludecke B, Dworniczak B, Bartholome K (1995). A point mutation in the tyrosine hydroxylase gene associated with Segawa's syndrome. *Hum Genet* 95: 123–125.

- Luikenhuis S, Giacometti E, Beard CF, Jaenisch R (2004). Expression of MeCP2 in postmitotic neurons rescues Rett syndrome in mice. *Proc Natl Acad Sci USA* **101**: 6033–6038.
- Mena MA, Casarejos MJ, Solano RM, de Yébenes JG (2009). Half a century of L-DOPA. *Curr Top Med Chem* **9**: 880–893.
- Molinoff PB, Axelrod J (1971). Biochemistry of catecholamines. *Annu Rev Biochem* **40**: 465–500.
- Neul JL, Zoghbi HY (2004). Rett syndrome: a prototypical neurodevelopmental disorder. *Neuroscientist* **10**: 118–128.
- Nguyen MV, Du F, Felice CA, Shan X, Nigam A, Mandel G et al (2012). MeCP2 is critical for maintaining mature neuronal networks and global brain anatomy during late stages of postnatal brain development and in the mature adult brain. *J Neurosci* **32**: 10021–10034.
- Nomura Y, Kimura K, Arai H, Segawa M (1997). Involvement of the autonomic nervous system in the pathophysiology of Rett syndrome. *Eur Child Adolesc Psychiatry* **6**: 42–46.
- Olanow CW, Watts RL, Koller WC (2001). An algorithm (decision tree) for the management of Parkinson's disease (2001): treatment guidelines. *Neurology* **56**(Suppl 5): S1–S88.
- Panayotis N, Pratte M, Borges-Correia A, Ghata A, Villard L, Roux JC (2011). Morphological and functional alterations in the substantia nigra pars compacta of the Mecp2-null mouse. *Neurobiol Dis* **41**: 385–397.
- Porritt MJ, Batchelor PE, Hughes AJ, Kalnins R, Donnan GA, Howells DW (2000). New dopaminergic neurons in Parkinson's disease striatum. *Lancet* **356**: 44–45.
- R Core Team (2013). *R: A Language and Environment for Statistical Computing*. R Foundation for Statistical Computing, Vienna, Austria. ISBN 3-900051-07-0, <http://www.R-project.org/>.
- Riederer P, Weiser M, Wichart I, Schmidt B, Killian W, Rett A (1986). Preliminary brain autopsy findings in prodromal Rett syndrome. *Am J Med Genet Suppl* **1**: 305–315.
- Rodriguez A, Ehlenberger DB, Dickstein DL, Hof PR, Wearne SL (2008). Automated three-dimensional detection and shape classification of dendritic spines from fluorescence microscopy images. *PLoS ONE* **3**: e1997.
- Rodriguez A, Ehlenberger DB, Hof PR, Wearne SL (2006). Rayburst sampling, an algorithm for automated three-dimensional shape analysis from laser scanning microscopy images. *Nat Protoc* **1**: 2152–2161.
- Roux JC, Dura E, Moncla A, Mancini J, Villard L (2007). Treatment with desipramine improves breathing and survival in a mouse model for Rett syndrome. *Eur J Neurosci* **25**: 1915–1922.
- Samaco RC, Mandel-Brehm C, Chao HT, Ward CS, Fyffe-Maricich SL, Ren J et al (2009). Loss of MeCP2 in aminergic neurons causes cell-autonomous defects in neurotransmitter synthesis and specific behavioral abnormalities. *Proc Natl Acad Sci USA* **106**: 21966–21971.
- Santini E, Alcacer C, Cacciatore S, Heiman M, Hervé D, Greengard P et al (2009). L-DOPA activates ERK signaling and phosphorylates histone H3 in the striatonigral medium spiny neurons of hemiparkinsonian mice. *J Neurochem* **108**: 621–633.
- Sholl DA (1953). Dendritic organization in the neurons of the visual and motor cortices of the cat. *J Anat* **87**: 387–406.
- Tandé D, Höglinger G, Debeir T, Freundlieb N, Hirsch EC, François C (2006). New striatal dopamine neurons in MPTP-treated macaques result from a phenotypic shift and not neurogenesis. *Brain* **129**: 1194–1200.
- Viemari JC, Roux JC, Tryba AK, Saywell V, Burnet H, Pena F et al (2005). Mecp2 deficiency disrupts norepinephrine and respiratory systems in mice. *J Neurosci* **25**: 11521–11530.
- Wenk GL, Naidu S, Casanova MF, Kitt CA, Moser H (1991). Altered neurochemical markers in Rett's syndrome. *Neurology* **41**: 1753–1756.



This work is licensed under a Creative Commons Attribution-NonCommercial-NoDerivs 3.0 Unported License. To view a copy of this license, visit <http://creativecommons.org/licenses/by-nc-nd/3.0/>

Supplementary Information accompanies the paper on the Neuropsychopharmacology website (<http://www.nature.com/npp>)

